ULTRAVIOLET DISINFECTION KINETICS FOR POTABLE WATER PRODUCTION

by

STEVE A AMOS

School of Chemical Engineering
The University of Adelaide

A thesis submitted for examination for the degree of
Master of Engineering Science

November 2007

This work contains no material which has been accepted for the award of any other degrees or diploma in any university or other tertiary institution and, to the best of my knowledge and belief, contains no material previously published or written by another person, except where due reference has been made in the text.

I give consent to this copy of my thesis, when deposited in the University Library, being available for loan and photocopying.

Mr Steven A Amos: ....

Date: 6/11/2008

SUMMARY

Irradiation with ultraviolet (UV) light is used for the disinfection of bacterial contaminants in the production of potable water, and in the treatment of selected wastewaters. However, efficacy of UV disinfection is limited by the combined effect of suspended solids concentration and UV absorbance. Limited published UV disinfection data are available that account for the combined effects of UV dose, suspended solids concentration and UV absorbance. This present lack of a rigorous quantitative understanding of the kinetics of UV disinfection limits process optimisation and wider application of UV treatment. The development and validation of an adequate model to describe UV disinfection kinetics presented in this thesis can therefore be justified by an increased confidence of reliability of design for UV disinfection.

Using the published data of Nguyen (1999), four established model forms were assessed to account for the combined effect of suspended solids and/or soluble UV absorbing compounds, and UV dose on the efficacy of disinfection. The four model forms were: a log-linear form, Davey Linear-Arrhenius (DL-A), Square-Root (or Ratkowsky-Belehradek) and a general n^{th} order Polynomial (*n*OP) form that was limited to a third order. Criteria for assessment of an adequate predictive model were established including: accuracy of predicted against observed values, *percent variance accounted for (%V)*, and; appraisal of residuals. The DL-A model was shown to best fit the data for UV disinfection of *Escherichia coli* (ATCC 25922); followed by the *n*OP, log-linear and Square-Root forms. However, the DL-A form must be used in conjunction with a first-order chemical reaction equation, and was shown to predict poorly at high experimental values of UV dose ($>$ 40,000 $\mu Ws\ cm^{-2}$). The DL-A model was not amenable to extrapolation beyond the observed UV dose range.

To overcome the shortcomings of the Davey Linear-Arrhenius model synthesis of two new, non-linear model forms was undertaken. The two models were a modified exponentially damped polynomial (EDP_m) and a form based on the Weibull probability distribution. The EDP_m model has three terms: a rate coefficient (k), a damping coefficient (λ), and; a breakpoint dose ($[dose]_B$). The rate coefficient governs the initial rate of disinfection prior to the onset of tailing, whilst the breakpoint is the UV dose that indicates the onset of tailing. The damping coefficient controls curvature in the survivor curve. The Weibull model has just two terms: a dimensionless scale parameter (β_0), and; a shape parameter (β_1). The scale parameter represents the level of disinfection in the tail of the survivor curve (as $\log_{10} N/N_0$), whilst the shape parameter governs the degree of curvature of the survivor data.

Each model was assessed against the independent and published UV disinfection data of Nelson (2000) for treatment of faecal coliforms in a range of waste stabilisation pond effluents. Both models were found to be well suited to account for tailing in these UV

disinfection data. Overall, the EDP_m model gave a better fit to the data than the Weibull model form.

To rigorously validate the suitability of the new EDP_m and Weibull models a series of experimental trials were designed and carried out in a small-scale pilot UV disinfection unit. These trials included data determined specifically at low values of UV dose (<10,000 μWs cm^{-2}) to fill the gap in the experimental data of Nguyen (1999).

The experimental trials were carried out using a commercially available, UV disinfection unit (LC5™ from Ultraviolet Technology of Australasia Pty Ltd). Purified water contaminated with *Escherichia coli* (ATCC 25922) with a range of feed water flow rates (1 to 4 L min^{-1}) was used. *E. coli* was selected because it is found in sewage, or water contaminated with faecal material, and is used as an indicator for the presence of enteric pathogens. *E. coli* should not be present in potable water. The hydrodynamics of water flow within the disinfection unit were established using digital video photography of dye trace studies with Methylene Blue. Nominal UV dose (2,700 to 44,200 μWs cm^{-2}) was controlled by manipulating the flow rate of feed water through the UV disinfection unit (i.e. residence time), or by varying the exposed length of the control volume of the disinfection unit. The transmittance of the feed water (at 254 nm) was adjusted by the addition of either a soluble UV absorbing agent (International Roast™ instant coffee powder; 0.001 to 0.07 g L^{-1}), or by addition of suspended matter as diatomaceous earth (Celite 503™; 0.1 to 0.7 g L^{-1}, with a median particle size of 23 μm).

The absorbing agent (instant coffee), when in a comparable concentration, was found to produce a greater reduction in water transmission than the suspended material (Celite 503™). It therefore contributed to a greater reduction in the initial rate of disinfection. Neither agent was found to produce a systematic reduction in the observed efficacy of disinfection however. Experimental results highlight that in the absence of soluble absorbing agents, or suspended solids, the initial rate of disinfection is higher when fewer viable bacteria are initially present.

Both the new EDP_m and Weibull forms gave a good fit to the experimental data. The EDP_m better fitted the data on the basis of residual sum-of-squares (0.03 to 2.13 for EDP_m *cf.* 0.16 to 4.37 for the Weibull form). These models are both of a form suitable for practical use in modelling UV disinfection data.

Results of this research highlight the impact of water quality, as influenced by the combined effect of UV dose, suspended solids concentration and UV absorbance, on small-scale UV disinfection for potable water production. Importantly, results show that the concentration of soluble UV absorbing agents and suspended solids are not in themselves sufficient criteria on which to base assessment of efficacy of UV disinfection.

ACKNOWLEDGMENTS

I would like to express my appreciation to the many people who provided assistance during the course of this investigation. In particular, I am grateful to the following:

from the School of Chemical Engineering, University of Adelaide;

Dr. K. R. (Ken) Davey, my principal supervisor, for his guidance, encouragement and many fruitful discussions,
Technical officers, Mr. Brian Mulcahy and Mr. Peter Kay for their skilled assistance in constructing apparatus,
Mr. Ben Daughtry for his valuable assistance with experimental data analyses, and
Ms. Felicity Lloyd for her time and effort in performing particle-size analyses,

from the School of Molecular Biosciences, University of Adelaide;

Dr. Connor Thomas, my co-supervisor, for his guidance, valuable discussion and helpful matter-of-fact advice on the microbiological aspects of the project,

from Ultraviolet Technology of Australasia Pty. Ltd. (UVTA);

Mr. Tony Gardner, Managing Director UVTA, for generously supplying the UV disinfection unit, and helpful discussion throughout the course of the research.

I hope that the results of my efforts justify the expectations and confidence of the people concerned, and the interest, help, and encouragement of my family, friends and colleagues.

TABLE OF CONTENTS

CHAPTER 1: INTRODUCTION

The distinction between *disinfection*[1] and *sterilisation* is often not understood. Disinfection refers to rendering harmless contaminating and *pathogenic* micro-organisms. Sterilisation is the destruction of all living matter. A working definition for both however is an agreed reduction in the number of viable contaminants.

Disinfection is widely used to treat municipal and industrial wastewater effluents and in the production of *potable* water. In recent years *ultraviolet* (UV) irradiation has been seen as an alternative to chemical disinfectants. UV disinfection provides an alternate means to disinfect not only for potable water production but also in wastewater treatment.

UV disinfection employs a narrow range of ultraviolet light, namely, wavelengths from 250 – 260 nm, to inactivate viable contaminant micro-organisms. The mechanism of UV disinfection is based on causing irreparable damage to cellular DNA. Specifically, germicidal UV irradiation at 254 nm causes dimerization of adjacent thymine monomers on the same strand of DNA. This prevents normal DNA transcription and replication, effectively resulting in inactivation (equivalent to death) of the cell (Block 1983; Nguyen 1999; Cano and Colome 1986).

UV is effective in the inactivation of both bacterial and viral contaminants. Other advantages of UV disinfection include that it:

- is non-intrusive
- does not require the addition of chemicals – this contrasts with widespread chlorination (UV can be used however in combination with oxidants for destruction of organic compounds)
- importantly, for potable water production, produces no noticeable adverse odour or taste (Kiely 1998)
- has a low energy and minimal space requirement compared to traditional disinfection (Nguyen 1999).

[1] *see* Appendix A for a definition of some important terms used throughout this research.

UV disinfection is used in the:

- food and beverage industry for production of potable water and process water treatment
- production of high purity water for the pharmaceutical and electronic industries
- aquaculture industry both in the treatment of growth media and in disinfection of water used in shellfish *depuration*.

An essential step to optimisation of UV disinfection efficacy is the synthesis and validation of an adequate mathematical model (Davey, Hall and Thomas 1995). Of particular interest is the modelling of the combined effect of UV dose and suspended solids concentration. In combination these two factors are known qualitatively to significantly influence UV efficacy. Extensive UV experimental data has been accumulated within The University of Adelaide's *Food Research Group* (FRG) where Nguyen (1999) proposed a model to include the effect of UV dose on the rate coefficient for disinfection. Additional analyses of these disinfection data for treatment of *Escherichia coli* highlighted however that the disinfection rate coefficient exhibited dependence on both UV dose and suspended solids concentration, that is, a combined effect. The predictive model form of Nguyen (1999) is therefore not adequate.

There is therefore the need for the synthesis and validation of an adequate quantitative and predictive model for the combined effect of UV dose and suspended solids concentration on disinfection kinetics of contaminant bacteria. The acquisition of a robust model for the kinetics of UV disinfection can be justified by increased confidence in reliability of process design. In the longer term, this is a necessary prerequisite for process optimisation. Against this background a study of UV disinfection for potable water production has been undertaken and the results are presented in this thesis.

1.1 Research Aims

The principal aims of this research are to:

- Evaluate the potential of existing model forms for predicting the efficacy of UV disinfection as affected by combined UV dose and concentration of suspended solids – using independent published data and through establishing rigorous criteria for fit of a predictive model
- Synthesise new, or extend existing, models to overcome any shortcomings highlighted in predictive capability
- Carry out experimental studies to determine adequate robust UV disinfection data on a selected bacterium
- Validate the model(s) of choice against these data.

The bacterium and pilot UV disinfection unit are chosen with a view to applying the findings to realistic problems related to UV disinfection for potable water production.

1.2 Outline of thesis

A logical and stepwise approach is adopted as a research strategy.

Chapter 2 presents a critical review of the relevant literature. The process and water quality factors that influence UV disinfection are highlighted and relevant published predictive models are assessed.

Chapter 3 presents a careful evaluation of four established and widely used model forms for potential prediction of the rate coefficient for disinfection, against accumulated UV disinfection data for the combined effect of UV dose and suspended solids concentration on disinfection kinetics of *Escherichia coli*. This bacterium is used as an indicator for the prescence of enteric pathogens – and is found in sewage and water contaminated with faecal waste. It should not be present in potable water. The four established model forms are the: log-linear, Davey Linear-Arrhenius (DL-A), Square-Root (or Ratkowky-Belehradek), and general n^{th} order polynomial form (*n*OP).

Criteria for the test of an adequate model are established and defined. These include: the accuracy of prediction against observed data, *percent variance accounted for (%V)*, and; careful analyses of plots of residuals.

The DL-A model is shown to best fit the criteria established for test of an adequate predictive model. However, a major shortcoming is highlighted in the DL-A model. This is the failure, when coupled with a first-order chemical reaction equation, to adequately predict disinfection at high values of UV dose (> 40,000 $\mu Ws\ cm^{-2}$). The need for a new, alternative model form is underscored.

Chapter 4 outlines the synthesis of two new, non-linear model forms for prediction of UV disinfection data as effected by combined UV dose, suspended solids concentration and UV absorbance. The model forms are initially validated against the published but limited UV disinfection data of Nelson (2000) for treatment of a range of waste stabilisation pond effluents.

To rigorously validate the suitability of the new predictive models, experimental trials were carried out using a pilot UV disinfection unit to generate robust data. The design and experimental details of these studies are presented in Chapter 5. An outline of digital photographic analyses and dye trace studies used to establish the hydrodynamics of water flow in the pilot disinfection unit are presented.

In Chapter 6 the experimental results are presented and extensively analysed. UV disinfection kinetics are discussed together with the the effects of process and water quality parameters. The suitability of the new mathematical models are assessed.

Chapter 7 presents conclusions arising from this research – together with recommendations for further work.

All notation used is listed at the back of this thesis, and the more important terms used throughout are defined in Appendix A. Where possible SI units are used. A number of publications arising from this research are listed in Appendix B. To aid transparency of this research, detailed calculations and raw experimental data are presented in appropriate appendices.

CHAPTER 2: LITERATURE REVIEW

2.1 Introduction

The disinfection of water and wastewaters by (UV) ultraviolet irradiation has developed rapidly over the last twenty years or so – although the micro-biocidal effect of solar UV irradiation has been known for some 120 years. Initially, Downes and Blount (1877) attributed the germicidal effect of sunlight to the presence of short-wave UV radiation (USEPA 1986; Severin and Suidan 1985; Meulemans 1987).

It had been known that the efficacy of UV radiation as a disinfectant is highly dependent on the wavelength of the radiation (Giese and Darby 2000; Wang *et al.* 2005). Early studies narrowed the optimum wavelength to a range of 250 to 266 nm (Severin and Suidan 1985). Subsequently, sensitivity to UV light was found to be species dependent, and later to be strain variable within a species (Severin and Suidan 1985). Maximum irreparable damage to cells caused by exposure to UV irradiation has been suggested to occur at 265 nm (Crandall 1986; Nguyen 1999; Meulemans 1987). This is schematically illustrated in Figure 2.1 below.

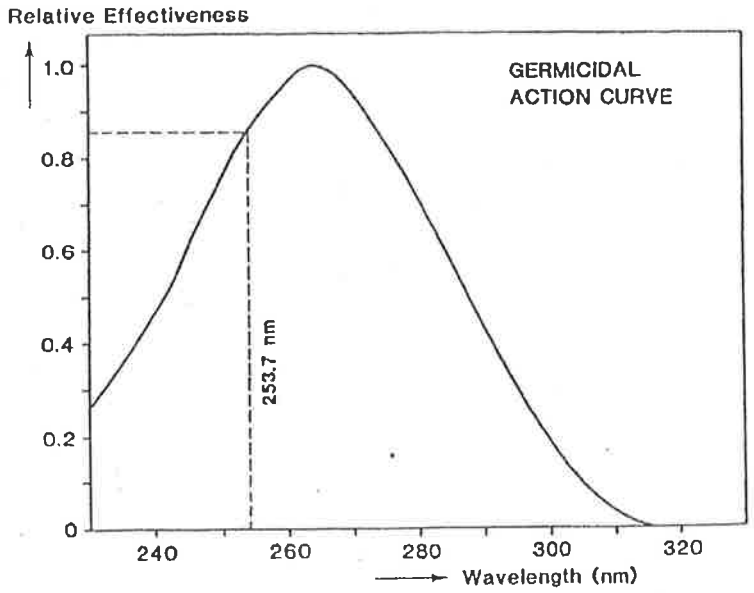

Figure 2.1 Germicidal effectiveness versus wavelength (*from* Meulemans 1987)

However some micro-organisms are more sensitive to different wavelengths. For example, nematodes, worm eggs and tobacco mosaic virus are more sensitive to UV at 220 nm (USEPA 1996).

Disinfection by UV irradiation is a physical process as opposed to a chemical process. A drawback with chemical processes is persistence of chemical residuals, and possibly disinfection by-products, within the treated water. UV is advantageous in that toxic compounds, such as those produced by chlorination, can be avoided. A potential disadvantage is that no residual disinfectant is retained in the distribution system to suppress microbial regrowth. Importantly, for potable water production, UV disinfection produces no noticeable adverse odour or taste problems that often arise with chlorination (Kiely 1998; Nguyen 1999).

The mechanism through which UV irradiation is thought to inactivate the viable bacterial cell is by irreparable damage to the cellular DNA. Germicidal UV irradiation at 254 nm causes dimerization of adjacent thymine monomers on the same strand of DNA. This prevents normal DNA transcription and replication, effectively resulting in inactivation of the bacterial cell (Block 1983; Nguyen 1999; Cano and Colome 1986). Since optimum absorbance by nucleic acids is at approximately 254 nm (Qasim 1999; USEPA 1986), this is the primary wavelength delivered by most UV disinfection technology (Harm 1980; USEPA 1986; Meulemans 1987).

2.2 UV disinfection design principles

The principles used in the design of a UV disinfection reactor are those that apply to the design of a continuous flow reactor in which the relevant reaction is the UV inactivation of contaminating micro-organisms. The main operating parameter is the UV dose. The UV dose distribution is influenced by hydrodynamics of water flow, soluble UV absorbing agents, and; suspended solids levels.

2.2.1 Sources of UV radiation

Since its development by Hewitt in 1901 (USEPA 1986; Severin and Suidan 1985; Harm 1980; Meulemans 1987), the mercury vapour lamp has been established as the main source of UV radiation. The UV radiation is generated by striking an electric arc through mercury

vapour. Discharge of the energy generated by excitation of the mercury vapour results in the emission of UV light (USEPA 1986; Meulemans 1987). The most widely used lamp is the low-pressure mercury lamp (USEPA 1986; Qasim 1999). This is generally recognised as the most effective and efficient source of UV radiation (Qasim 1999). The main reason low-pressure lamps are used is that about 85 percent of the UV output is in the form of monochromatic UV light at a wavelength of near 254 nm (Qasim 1999; Nguyen 1999; USEPA 1986; Meulemans 1987). About 7 to 10 percent of emitted light is at a wavelength of 185 nm (Nguyen 1999). However large numbers of lamps currently in use employ a lamp envelope that has a low transmittance at 185 nm (USEPA 1986).

Medium pressure vapour lamps emit light across a broad range of the visible and ultraviolet portions of the electromagnetic spectrum. The medium pressure vapour lamp is used primarily for treatment of wastewaters and water contaminated with organic compounds. Medium pressure UV disinfection systems also provide a much greater treatment capacity (~ 25 times greater) than low pressure systems due to their greater output intensity (Nguyen 1999; Meulemans 1987). The radiation output from the medium-pressure vapour arc is more widely spread over the spectral range as is illustrated in Figure 2.2.

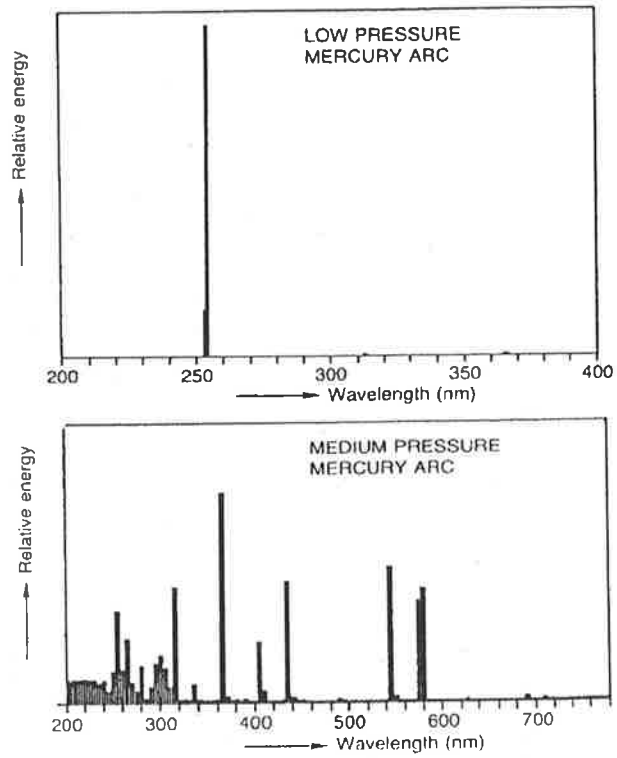

Figure 2.2 Emission spectra for low and high pressure mercury vapour lamps (*from* Meulemans 1987)

High pressure vapour lamps also emit over a broad spectral range. Consequently, both the medium and high-pressure mercury vapour lamps are used more often in the advanced oxidation processes, involving the destructive treatment of organic compounds (USEPA 1990). The amount of both radiated light and self-absorption of the UV radiation increases with increasing vapour pressure (Nguyen 1999).

The lower the mercury vapour pressure, the greater the intensity of the mercury resonance line at 253.7 nm (USEPA 1986). In multiple lamp configurations (since lamps transmit little of the light from adjacent lamps) excessively close lamps can result in reduced efficiency (Qualls and Johnson 1985; Qualls, Dorfman and Johnson 1989; USEPA 1986).

2.2.2 Mechanism of UV induced damage

UV energy emitted from a source is transferred to the micro-organism, and is absorbed by cellular material. This cellular material comprises primarily protein and nucleic acids (Harm 1980; USEPA 1986; Brock and Madigan 1991). The fundamental premise of UV disinfection is that the radiation must be absorbed by the micro-organisms such that the energy can have a damaging effect (Qasim 1999; USEPA 1986). When the cellular DNA absorbs sufficient UV irradiation, it induces a structural change that prevents replication of the micro-organism (Cano and Colome 1986; Brock and Madigan 1991).

In the 1960's, intrastrand thymine dimer formation in cellular DNA was found to be the underlying mechanism behind UV disinfection (Severin and Suidan 1985). Cellular proteins and nucleic acids are colourless, but are very absorptive of UV radiation from 200 to 300 nm (USEPA 1986; Wang *et al.* 2005), with the optimum absorbance of nucleic acids around 254 nm (Qasim 1999). Although numerous mechanisms exist by which UV irradiation induces photochemical changes, in DNA the most dominant is the dimerization of two adjacent pyrimidine molecules on the same polynucleotide strand (Harm 1980; USEPA 1986).

Consequently, DNA is the primary target of UV disinfection. Dimerization of adjacent thymine monomers is illustrated schematically in Figure 2.3. Formation of many thymine dimers along a single DNA strand makes replication very difficult (USEPA 1986; Brock and Madigan 1991).

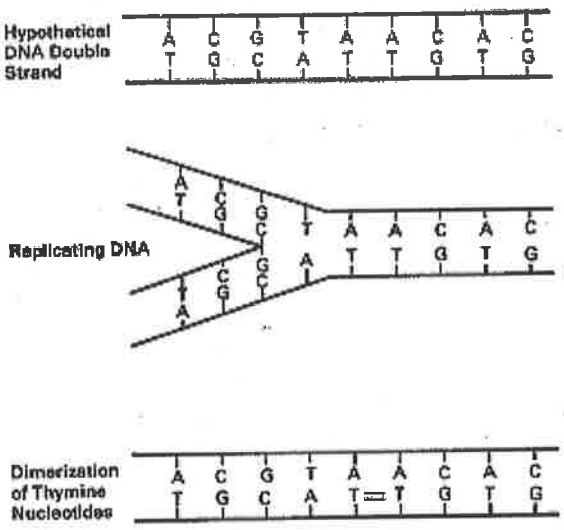

Figure 2.3 Example of UV induced damage to DNA (*from* USEPA 1986)

The absorption spectrum of nucleic acids has been found to be very similar to the relative germicidal effectiveness of UV radiation as a function of wavelength. Figure 2.4 presents the relative percent absorption for a solution of RNA compared to relative germicidal effectiveness. The similarity between the two supports the notion that the main mechanism of UV induced damage is by photochemical alteration to nucleic acid within the target cell (USEPA 1986).

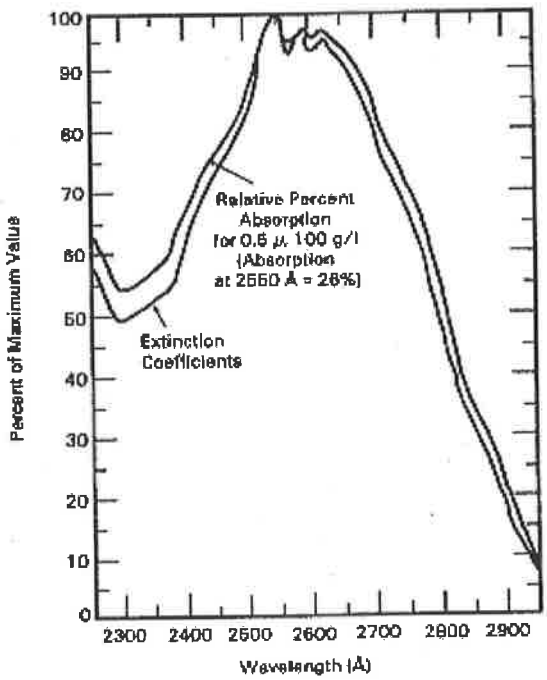

Figure 2.4 Relative abiotic effect of UV on *E. coli* compared to relative absorption of ribose nucleic acid (*from* USEPA 1986)

2.2.3 Cell repair to UV damage

Many cells can repair and thereby reverse the damaging effects of UV radiation (Severin and Suidan 1985; Baron and Bourbigot 1996; Hengesbach *et al.* 1993). UV induced damage to DNA can be repaired by both light-dependent (photoreactivation) and light-independent (dark repair) mechanisms (Nebot Sanz *et al.* 2007; Bohrerova and Linden 2007; Harm 1980).

Photoreactivation is the phenomenon whereby inactivated microorganisms regain activity through repair of pyrimidine dimers in the DNA under near UV and visible light exposure ranging from 310 to 480 nm (Nebot Sanz *et al.* 2007). Repair is initiated via the enzyme photolyase, and can proceed without excision of the damaged DNA. The mechanism of light activated repair is illustrated in Figure 2.5, which schematically illustrates enzymatic removal, followed by replication and replacement of the damaged DNA.

Dark repair can occur without exposure to light, and involves enzymatic excision of dimers from the damaged DNA. Bacteria are known to use at least three dark-activated repair mechanisms, with all mechanisms regulated by expression of the *rec*A gene. The *rec*A gene product is a multifunctional protein involved in both DNA repair and the coordination of cell division (Jungfer, Schwartz and Obst 2007).

Photoreactivation is widely regarded as the more effective and more rapid repair mechanism, and is particularly significant in disinfection of wastewater where exposure to sunlight following UV treatment may occur (Bohrerova and Linden 2007; Nebot Sanz *et al.* 2007). The rate and extent of photoreactivation has been shown to vary greatly for a variety of different species and strains of waterborne bacteria (Harm, 1980). Viruses generally do not have the ability to repair UV induced damage except when in a host cell which has the ability to repair (USEPA 1986; Qasim 1999).

Both lamp intensity and spectral output have also been shown to significantly affect the rate and extent of photoreactivation (Bohrerova and Linden 2007). Medium pressure UV lamps produce a broad spectral output which damage further biological molecules in addition to DNA, whereas low pressure lamps typically emit a single germicidal wavelength only affecting DNA (Nebot Sanz *et al.* 2007). Reactivation following treatment from medium pressure lamps is more difficult as a result.

2.2.4 UV disinfection of potable water and wastewater effluent

The use of ultraviolet light to disinfect drinking (i.e. potable) water in the United States dates back to 1916 (USEPA 1996). More than 30 large-scale UV disinfection facilities had either been built or planned for construction in the United States by the mid 1980's (Qualls and Johnson 1985). The United States Environmental Protection Authority (USEPA) initially described UV irradiation as a "potentially desirable alternative" for wastewater disinfection when compared to more widely used chemical disinfectants (USEPA 1986). UV disinfection has also been used successfully in Austria since the 1960's (Sommer and Cabaj 1993). Huff and coworkers showed that UV disinfection would be viable in treating ship-board potable water supplies, utilising a dose range of between 4,000 and 11,000 $\mu Ws\ cm^{-2}$ (as cited in USEPA 1986). Taghipour (2004) determined UV doses of 3,500 $\mu Ws\ cm^{-2}$ and 6,200 $\mu Ws\ cm^{-2}$ to be required for a $\log_{10}$ reduction of *E. coli* in primary and secondary effluents respectively.

UV disinfection continues to find most use in the disinfection of secondary wastewater effluents, especially in new water treatment facilities (Nguyen 1999; USEPA 1986). Advancements in reactor design, equipment reliability and improvements in process control are continuing to increase the popularity of UV disinfection systems.

Several drawbacks exist with UV irradiation equipment that can be gleaned from the literature (Qasim 1999; Severin and Suidan 1985; USEPA 1985). These include:

- short-circuiting of contaminated water through the UV unit (affects residence time distribution and UV unit performance)
- shielding of micro-organisms to UV damage by suspended solids
- repair of UV damage that can occur after treatment with some micro-organisms
- lack of a chemical residual retained in the treated water.

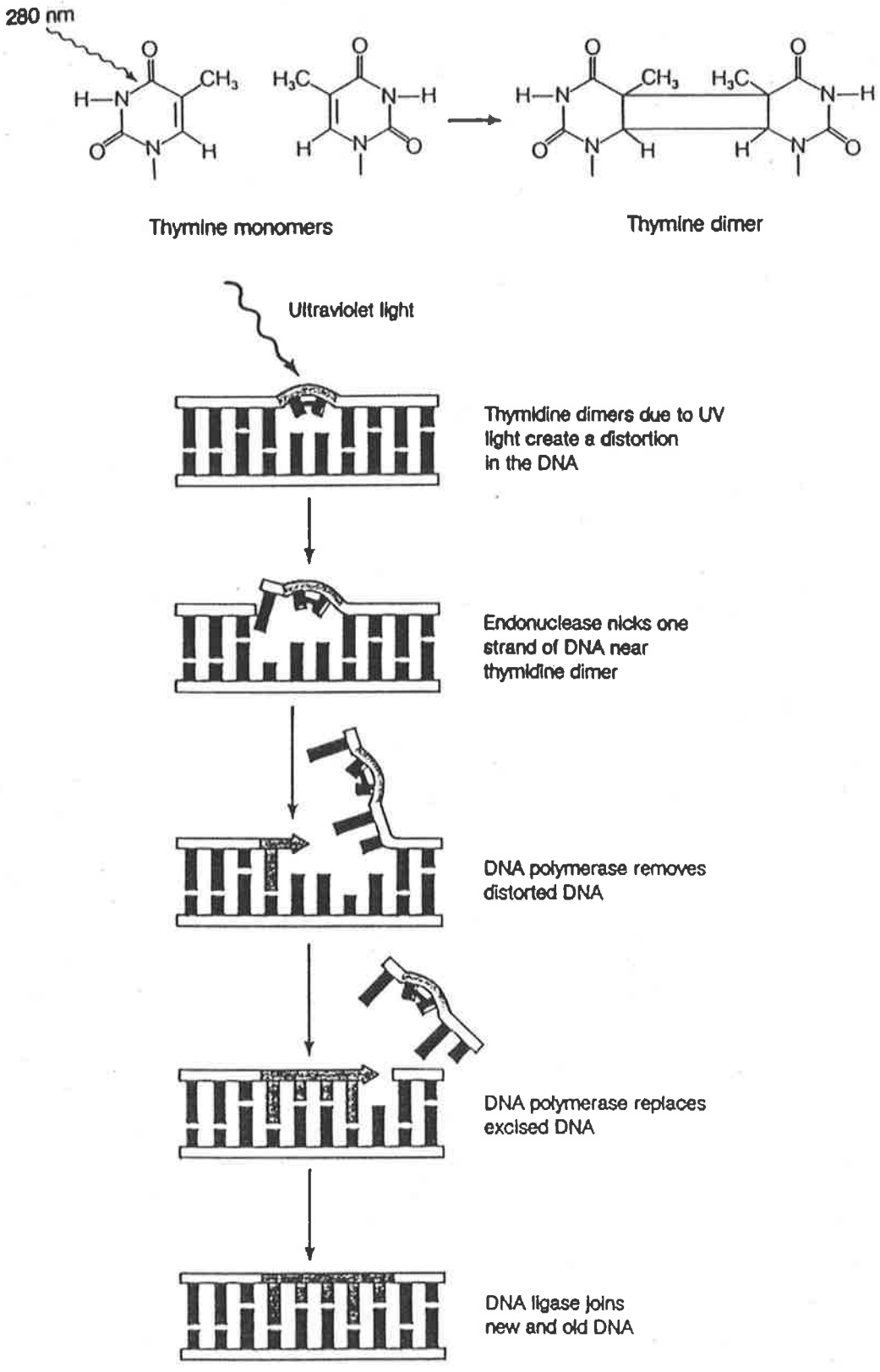

Figure 2.5 Thymine dimers distort the DNA molecule and prevent DNA replication and transcription (*after* Cano and Colome 1986)

Despite these pitfalls, possibly the overriding problem associated with UV disinfection technology is the fact that, in general, UV dose cannot be measured reliably and accurately within the reactor control volume. This results mainly from lack of knowledge of UV intensity with respect to position within the reactor (and to a lesser extent due to complex hydrodynamics often arising from multiple lamp arrays). A significant operational problem associated with UV disinfection is fouling of the lamp surface. Fouling materials are efficient absorbers of UV radiation and diminish the performance of the radiation based process (Lin, Johnston and Blatchley 1999; USEPA 1986; Severin and Suidan 1985).

Likewise, it has been postulated (USEPA 1996; Nguyen 1999) that repair mechanisms may limit the viability of UV radiation as a disinfectant. The practical solution is to apply sufficient UV dose such that repair will not occur following exposure to UV.

2.3 UV disinfection in combination with oxidants

Combination of UV disinfection with oxidising agents, such as hydrogen peroxide or ozone, is known to improve the efficacy of UV disinfection (Nguyen 1999; Crandall 1986; Bayliss and Waites 1979; Carnimeo *et al.* 1995; Murphy, Payne and Gagnon 2008). The main principle behind UV/oxidation technologies is the photolytic action of UV irradiation on a variety of oxidisers, ultimately producing highly reactive hydroxyl radicals. The sequence of reactions is (Nguyen 1999):

$$H_2O_2 + UV \rightarrow 2OH^{\bullet} \quad (2.1)$$

or

$$O_3 + UV + H_2O \rightarrow H_2O_2 + O_2 \quad (2.2)$$

$$H_2O_2 + UV \rightarrow 2OH^{\bullet} \quad (2.3)$$

or

$$2O_3 + H_2O_2 \rightarrow 2OH^{\bullet} + 3O_2 \quad (2.4)$$

Crandall (1986) used a combined UV/H_2O_2 process to control contaminant bacteria in hot water spas. The recommended level for hydrogen peroxide in spas and pools is 20 ppm as a minimum, with an ideal level of 30 – 40 ppm to ensure the safety of bathers. Hydrogen peroxide is generally used to control odour and prevent growth in the collection system. Carnimeo *et al.* (1995) found no repair to occur when the combined UV/H_2O_2 treatment is used, with a reduction in survivors observed with increasing duration of storage.

Murphy, Payne and Gagnon (2008) investigated the effects of chlorine, chlorine dioxide and monochloramine alone; and each in combination with UV treatment, on persistence of *E. coli* in water treatment effluent. Generally, UV treated systems in combination with chlorine, chlorine dioxide or monochloramine achieved greater levels of disinfection than in the presence of chemical disinfectants alone.

Bayliss and Waites (1979) reported UV irradiation and hydrogen peroxide to act synergistically to kill spores of *Bacillus subtilis* 706 when used together – but not when in succession. The presence of hydrogen peroxide produced a 2,000-fold increase in the rate of inactivation of *B. subtilis* spores compared to the use of UV irradiation alone. Bayliss and Waites (1979) also found a disinfection of 99.99% (4-$\log_{10}$ reductions) resulted with a 30 s exposure to UV of spores of six strains of *Bacillus* and *Clostridium* in the presence of hydrogen peroxide at 0.01 g mL^{-1}. Sobotka (1992) reported that when combined with hydrogen peroxide or ozone, the effectiveness of UV irradiation was found to increase 400-fold when used for inactivation of bacterial toxins.

UV irradiation catalyses ozone reduction into the hydroxyl radical and super-oxide ion, and promotes the production of free organic radicals (USEPA 1986; Nguyen 1999). Combined UV/ozonation is therefore found to be a superior treatment (to each separate treatment) in the removal of organics from water. Jones *et al.* (1985) found mineralisation of these organics was resisted when exposed to both low dosages of UV radiation and ozone in combination. Conversely, a six hour exposure to both ozone and UV resulted in a 20 % mineralisation of organic carbon from treated water. Jung, Oh and Kang (2008) found the UV dose required to achieve a 3-$\log_{10}$ reduction in *B. subtilis* spores to reduce from 43,500 μWs cm^{-2} in the absence of ozone, to 34,000 μWs cm^{-2} when exposed to ozone at 0.54 mg L^{-1} min. Further, when UV treatment preceded ozone exposure, the combined inactivation was equivalent to the sum of inactivations by each treatment alone. When ozonation preceded UV exposure, the efficacy of the combined treatment greatly increased due to photolytic decomposition of ozone leading to formation of hydroxyl radicals. Venosa *et al.* (1984) also found that sequential application of ozone-UV or UV-ozone was more economical than either UV or ozone alone (Severin and Suidan 1985). However, in comparison to chlorine and ozone, UV does not cause corrosion in water systems (Sobotka 1993).

2.4 Inactivation of pathogens by UV irradiation

The relationship described in much of the literature between UV dose and survival of micro-organisms shows a more rapid reduction of viable numbers to be expected at high UV dose (Nguyen 1999; Severin and Suidan 1985; USEPA 1996; Qasim 1999). It is believed that when micro-organisms are subjected to UV light a constant fraction of the number present are inactivated in each time increment (Crandall 1986; Kohler 1965; Qasim 1999; Harm 1980). That is, the kinetics of UV disinfection are widely assumed (Nguyen *et al.* 1998; Qasim 1999; Loge *et al.* 1996) to be of the form of a first-order chemical reaction with respect to UV dose. Mathematically, this classical log-linear model form is represented as:

$$\ln\frac{N}{N_0} = -kIt = -k[dose] \tag{2.5}$$

where: N_0 = number of viable micro-organisms initially present; N = number of micro-organisms surviving after t seconds of treatment; t = time of exposure to UV (s); I = the intensity of UV radiation ($\mu W\ cm^{-2}$); [*dose*] = the dose of UV light received ($\mu Ws\ cm^{-2}$); k = the disinfection rate coefficient ($\mu W^{-1}\ s^{-1}\ cm^2$).

Equation (2.5) represents idealised conditions – deviation from the first-order model often occurs in practice however (Qasim 1999; Nguyen 1999). The reader should carefully note that Equation (2.5) cannot be extrapolated to zero micro-organisms for increasing UV dose.

Figure 2.6 illustrates a typical UV survival curve. Experiments with mixed culture have shown that as the UV dose is increased, the efficiency of disinfection also increases, but in reduced proportion (Qasim 1999). This phenomenon is known as *tailing*[1](Cerf 1977; Qasim 1999), and is often attributed to the presence of particulate matter. However, tailing is known to also occur in the absence of particulate matter (Nguyen *et al.* 1998; Nguyen 1999). In general, the steep slope and logarithmic nature of the dose-survival curve causes the first flow fractions (low residence time hence low dose) to contribute most to average survival (Qualls, Dorfman and Johnson 1989).

[1] *see* Cerf 1977 for a seminal paper on tailing and other non-linear survival of thermally treated bacteria.

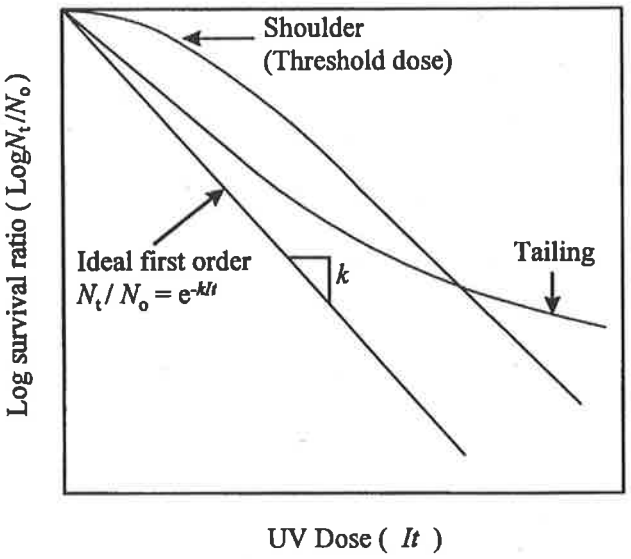

Figure 2.6 Illustration of the UV model and the interfering effects (*from* Qasim 1999)

Application of a sufficient dose of UV irradiation causes efficient inactivation of vegetative and sporus bacteria, viruses, and other pathogenic micro-organisms. Viruses are much more resistant to UV radiation than are bacteria (USEPA 1986; Nguyen 1999). Chang *et al.* (1985) reported the sensitivity to be from most to least sensitive (Dizer *et al.* 1993), namely:

E. coli > coliform organisms > polio virus type I > spores of *B. subtilis*

UV irradiation is also capable of disinfecting water contaminated with protozoa and algae; however these are increasingly resistant when compared to the micro-organisms mentioned above. Typically, UV doses for the provision of drinking water, range from 16,000 to 40,000 μWs cm^{-2}. Table 2.1 shows the levels of sensitivity of various micro-organisms when irradiated with a UV dose of 20,000 μWs cm^{-2}. *Escherichia coli* is seen to be one of the most readily inactivated micro-organisms, displaying a 6-log_{10} reduction in viable cells following treatment.

Table 2.1 Percent inactivation of different individually dispersed organisms when exposed to a UV dose of 20,000 μWs cm^{-2} (*adapted* from Cairns 1995)

Micro-organism	% Inactivation	$\log_{10} N/N_0$
Bacillus anthracis	99.9964	-3.6×10^{-5}
Clostridium tetani	97.8456	-2.2×10^{-2}
Corynebacterium diptheria	99.9999	-1.0×10^{-6}
Escherichia coli	99.9999	-1.0×10^{-6}
Legionella pneumophilia	99.9999	-1.0×10^{-6}
Mycobacterium tuberculosis	99.9536	-4.6×10^{-4}
Pseudomonas aeruginosa	99.9769	-2.3×10^{-4}
Salmonella paratyphi	99.9999	-1.0×10^{-6}
Shigella dysentriae	99.9999	-1.0×10^{-6}
Streptococcus faecalis	99.9972	-2.8×10^{-5}
Vibrio cholera	99.9162	-8.4×10^{-4}
Influenza virus	99.9997	-3.0×10^{-6}
Poliovirus	99.7846	-2.2×10^{-3}
Rotovirus (Reovirus)	98.3014	-1.7×10^{-2}
Saccharomyces cerevisiae	99.8179	-1.8×10^{-3}

Historically, disinfection data has shown (with few exceptions) that the order of ultraviolet light disinfection resistance is as follows (USEPA 1996), namely:

bacteria < viruses < bacterial spores < protozoan cysts and oocysts

Table 2.2 shows UV dose requirements for inhibition and destruction of a range of bacteria, yeast types and mould spores. It can be gleaned that a 3-$\log_{10}$ reduction in *B. subtilis* spores requires an approximate three-fold increase in dose compared to an equivalent reduction of *Escherichia coli.*

Table 2.2 Dose required (at 253.7 nm) to inhibit colony formation in 90 percent of the micro-organisms and for complete destruction (> 99.9 %) (*adapted from* USEPA 1996)

Micro-organism	(mWs cm^{-2})	
	90 %	> 99.9 %
Bacillus anthraces	4.52	8.7
B. megaterium spp. (veg)	1.3	2.5
B. megaterium spp. (spores)	2.73	5.2
B. paratyphosus	3.2	6.1
B. subtilis	5.8	11.0
B. subtilis (spores)	11.6	22.0
Corynebacterium diphtheria	3.37	6.5
Dysentry bacilli	2.2	4.2
Eberthella typos	2.14	4.1
Escherichia coli	3.0	6.6
Micrococcus candidus	6.05	12.3
Micrococcus sphaeroides	10.0	15.4
Nelsseria catarrhalis	4.4	8.5
Phytomonas tumafaclens	4.4	8.5
Proteus vulgaris	3.0	6.6
Pseudomonas aeruginosa	5.5	10.5
Pseudomonas fluorescens	3.5	6.6
S. enteritidis	4.0	7.6
S. typhimurium	8.0	15.2
Sarcina lutea	19.7	26.4
Serratia marcescens	2.42	6.16
Shigella paradysenteriae	1.68	3.4
Spirillum rubrum	4.4	6.16
Staphylococcus albus	1.84	5.72
Staphylococcus aureus	2.6	6.6

Table 2.2 *Continued*

Micro-organism	(mWs cm^{-2})	
	90 %	> 99.9 %
Streptococcus hemolyticus	2.16	5.5
Streptococcus lactis	6.15	8.8
Streptococcus viridans	2.0	3.8
Yeast		
Saccharomyces ellipsoideus	6.0	13.2
Saccharomyces spp.	8.0	17.6
Saccharomyces cerevisiae	6.0	13.2
Brewer's yeast	3.3	6.6
Baker's yeast	3.9	8.8
Common yeast cake	6.0	13.2
Mould spores		
Penicillium rogueforti	13.0	26.4
Penicillium expansum	13.0	22.0
Penicillium digitatum	44.0	88.0
Aspergillus glaucus	44.0	88.0
Aspergillus flavus	60.0	99.0
Aspergillus niger	132.0	330.0
Rhisopus nigricans	110.0	220.0
Mucor racemosus A	17.0	35.2
Mucor racemosus B	17.0	35.2
Oospora lactis	5.0	11.0

2.5 Effect of some process factors on the efficacy of UV disinfection

Factors that influence UV efficacy can be divided into three groups (Nguyen 1999; USEPA 1986):

- Physio-chemical properties of the water (e.g. pH, turbidity, dissolved organic and inorganics, type of microbial contaminants, particulate nature, colour and metal ions)
- UV reactor operating parameters including UV dosage, intensity gradient, and residence time distribution
- Maintenance requirements.

The characteristics of the water to be UV treated play a significant role in determining the efficacy of UV disinfection (Qasim 1999; Severin and Suidan 1985; Janex *et al.* 1998). Because the fundamental premise of UV disinfection is that radiation must be absorbed by

the micro-organisms, material in the water which absorbs UV irradiation, or shield micro-organisms from its influence, would be expected to influence disinfection (Severin and Suidan 1985; Meulemans 1987; Kiely 1988; Qasim 1999). In particular, suspended solids and soluble material that absorb UV light reduce the efficacy of UV irradiation (Parker and Darby 1995; Emerick *et al.* 1999; Emerick *et al.* 2000).

Various physical, chemical and biological components in the water will absorb ultraviolet energy. This absorption causes an attenuation of energy with increasing depth, reducing the available energy for absorption by micro-organisms (USEPA 1986; USEPA 1992). This UV absorbance is characteristic of the particulate and dissolved matter present, and is expressed as absorption of energy per unit depth. This is measured as absorbance (cm^{-1}). The absorbance is related to the % Transmittance of the water as measured by a UV spectrophotometer, given by:

$$\text{absorbance} = 2 - \log_{10}(\%\ \text{Transmittance}) \tag{2.6}$$

In design, an absorbance coefficient (δ) is used in most cases to express UV absorbance, and is directly related to the absorbance (cm^{-1}) as follows:

$$\delta = 2.3 \times (\text{absorbance}) \tag{2.7}$$

The UV absorbance coefficient is known to be a key parameter for design, control and monitoring of UV disinfection processes. Typically for wastewater treatment, the UV absorbance coefficient (δ) ranges from 0.2 to 0.3 cm^{-1} (USEPA 1986). Previous studies (Ho and Bohm 1981; Severin 1980; USEPA 1981; Petrasek *et al.* 1980; USEPA 1986) have suggested that UV transmission is a good parameter for correlating water quality to expected UV effectiveness.

Specific organic and inorganic compounds absorb germicidal UV at 253.7 nm. The absorbance coefficient (δ) affects the UV intensity in the reactor and has an impact on the sizing of the system and the lamp configuration. The single beam photometric method for measuring the UV absorbance of the liquid is the simplest procedure (USEPA 1986). It assumes that light not passing through the liquid (i.e. not received by the detector) is

absorbed. This is not necessarily true however (Qualls and Johnson 1983; 1985). If the liquid contains a substantial proportion of particulates, some of the UV light will be scattered, and still available within the liquid (USEPA 1986; Qasim 1999). Consequently, this method for measuring absorbance of the liquid overestimates the true absorbance.

Para-hydroxybenzoic acid (PHB) is one of a number of chemicals that have been reported by researchers to alter the transmission of waters to be tested (Whitby and Palmateer 1993). Instant coffee is another. This was used in the research of Nguyen (1999), Nguyen *et al.* (1998) and Davey *et al.* (1995).

2.5.1 Suspended solids

Optimum UV efficacy is obtained with waters of low turbidity. The presence of suspended solids has been qualitatively shown (Qasim 1999; Nguyen *et al.* 1998, Tchobanoglous *et al.* 1999; Taghipour 2004; Cantwell and Hofmann 2008; Hu *et al.* 2007) to produce tailing in survivor data. The effect of suspended solids on UV disinfection is three-fold (Severin and Suidan 1985):

- *Clumping* of micro-organisms skew the kinetic response due to the method by which survival is measured. (i.e. the Standard Plate Count Method)
- Micro-organisms that either clump together or are adsorbed to the surface of particulate matter are shielded in part from the effect of UV irradiation (not dissimilar to situations encountered with alternative disinfectants)
- UV light is scattered by particulates.

Suspended solids reduce efficacy of UV disinfection not only by absorbing and scattering UV radiation, but also by offering a physical barrier, or shielding micro-organisms from exposure to UV light (Nguyen 1999; Qasim 1999; Nelson 2000). The efficacy of UV disinfection decreases significantly with increasing concentration of suspended solids (Qualls and Johnson 1983, 1985; Qualls, Dorfman and Johnson 1989).

Yip and Konasewich (1972) showed that both suspended solids and soluble chemical compounds decrease UV transmittance. Qualls and Johnson (1983) found the key limitation to disinfecting to a level of 3 to 4-$\log_{10}$ reductions was the result of clumps

exceeding 70 μm in diameter[2]. Templeton, Andrews and Hofmann (2005) reported that shielding of coliforms during UV disinfection of wastewater is provided by particles as small as 10 μm, whereas particles smaller than 2 μm are large enough to protect viruses from UV light. Tailing phenomena are generally attributed to occlusion (or shadowing) of micro-organisms by suspended solids (Qasim 1999; Nguyen 1999; Loge *et al.* 1996; Whitby and Palmateer 1993; Tchobanoglous *et al.* 1999). The level of survivors observed in the tail is considered to be the "particulate" bacterial density – which in turn is a function of either suspended solids or turbidity (Nelson 2000; Loge *et al.* 1996; Darby *et al.* 1999; Taghipour 2004). Filtration prior to UV treatment can improve UV efficacy.

Kelly (1961) reported the efficacy of UV disinfection of seawater used in an oyster depuration (i.e. cleaning) process. The study showed that a 3-$\log_{10}$ reduction could be achieved using a UV dose of 57,600 μWs cm^{-2}, with initial bacterial densities ranging from 10^3 to 10^4 MPN per 100 millilitres, for values of turbidity ranging up to 20 JTU[3] (USEPA 1986). Similarly, Qualls, Flynn and Johnson (1983) found that occluded coliforms are a major factor in limiting disinfection to 3 to 4-$\log_{10}$ reductions. Oliver and Carey (1976) and Qualls and Johnson (1983) found that when sonication was used as a pretreatment to UV, disinfection efficacy increased significantly.

Singer and Nash (1977) reported tailing in survival kinetics with increasing UV dose, and found that a base level of coliforms would be present in the effluent following UV treatment. This was attributed to both water short-circuiting in the UV reactor and the presence of suspended solids. The effluent was found to be consistently disinfected to a level less than 200 MPN per 100 millilitres if the suspended solids concentration remained below 22 mg L^{-1} (USEPA 1986).

Petrasek *et al.* (1980) conducted a feasibility study to achieve reductions to less than 200 MPN per 100 millilitres in treated wastewater. These researchers illustrated the importance of the UV absorbance coefficient measured at 253.7 nm – but found this was not affected significantly by suspended solids or turbidity (USEPA 1986).

---

[2] This would just be visible to the naked eye.

[3] JTU = Jackson Turbidity Unit – measure of turbidity comparable to a Nephelometric Turbidity Unit (NTU).

Qualls, Flynn and Johnson (1983) and Scheible (1986) suggest that suspended or colloidal particles will not absorb a significant amount of UV light, and will scatter it back to the water (USEPA 1986). Therefore, absorbance measurements used for the purposes of design must account for scattered light.

The effects of suspended solids on full-scale UV disinfection efficacy have been widely studied (Petrasek *et al.* 1980; Severin 1980; Ho and Bohm 1981; Qualls, Flynn and Johnson 1983). Whitby and Palmateer (1993) studied a full-scale UV disinfection facility with different levels of returned activated sludge solids. On semi-log axes, a linear relationship between the suspended solids concentration and the number of surviving faecal coliforms was observed, meaning that an increase in suspended solids concentration results in a logarithmic increase in the number of coliforms remaining following treatment. This has also been reported by Scheible (1986), and other workers (USEPA 1986; Qasim 1999). Petrasek *et al.* (1980) however could not identify any relationship between the number of surviving faecal coliforms and suspended solids concentration – with suspended solids in the range of 5 to 50 mg L^{-1} and turbidity from 0.5 to 12 NTU. It has been recommended that the suspended solids concentration of wastewater be kept below 20 mg L^{-1} to ensure effective UV treatment (USEPA 1986; Qasim 1999).

Ho and Bohm (1981) postulated larger particles may be more effective in protecting bacteria from UV radiation. However, the effect of particle size has not been studied extensively (USEPA 1986). Oliver and Cosgrove (1975) postulated that although suspended solids concentration is important, the main controlling factor is likely the size distribution of the suspended solids in the effluent. Cantwell and Hofmann (2008) examined the potential for naturally occurring particles to protect indigenous coliforms against UV disinfection for a range of surface waters. A limit to disinfection of 2.5-$\log_{10}$ reductions was observed in the unfiltered effluent for a dose of 20,000 μWs cm^{-2}, which was increased to 3.4-$\log_{10}$ reductions when effluent was filtered through an 11 μm nylon filter. Chu *et al.* (2007) noted that the efficiency of UV disinfection was influenced both by particle size (distribution) and concentration, and that the virucidal efficacy of UV disinfection was adversely affected by the presence of faecal coliforms. Figure 2.7 shows schematically the reduction in disinfection efficacy attributed to the presence of particulate matter.

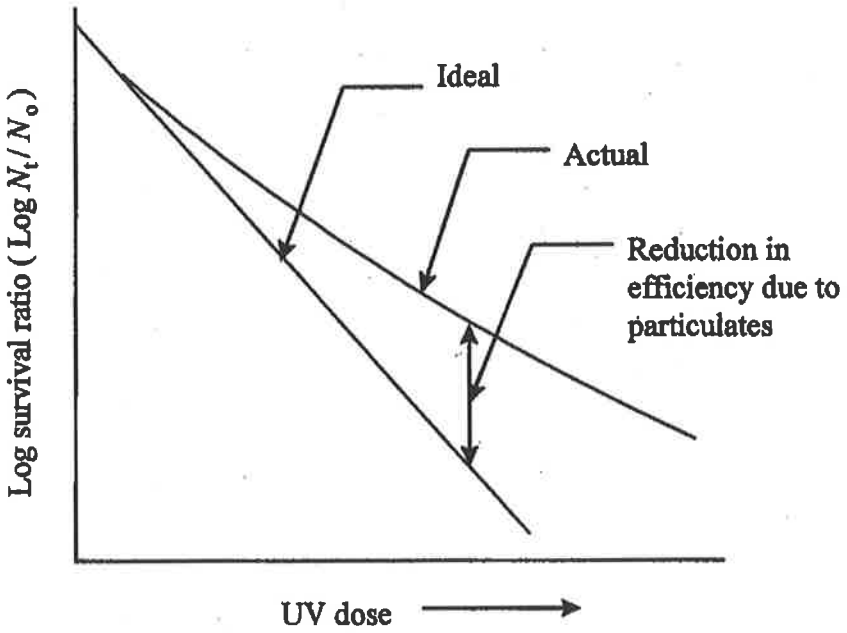

Figure 2.7 Effect of suspended solids on UV disinfection (*from* USEPA 1986)

2.5.2 Intensity profile

One of the major problems associated with UV disinfection is the difficulty in measuring accurately the intensity distribution within the disinfection control volume (USEPA 1986; Lin and Blatchley 2001; Severin and Suidan 1985; Qasim 1999; Suidan and Severin 1986). The intensity gradient is required in order to determine the dose distribution within the reactor.

The problem is magnified in wastewater treatment where complex reactor geometries and multiple lamp configurations make prediction of the UV intensity even more difficult (Janex *et al.* 1998; Lin and Blatchley 2001; Suidan and Severin 1986). The high UV absorbance typical of wastewaters also gives rise to much steeper intensity gradients (energy absorbed per unit area) within the reactor than are typically observed for potable water production (USEPA 1986). To date there are three main methods used for determination of UV intensity:

- Point-source summation
- Bioassay determination
- Chemical actinometry.

2.5.2.1 Point-source summation

Jacob and Dranoff (1970) first developed the point-source summation technique, that was subsequently first applied by Qualls and Johnson (1983) (USEPA 1986; Tchobanoglous *et al.* 1996). The UV lamp is represented as a finite series of point-sources that emit energy radially. The intensity at a particular point in the reactor is then the sum of the intensity contributions from all point-sources. This model also accounts for intensity attenuation within the reactor. The two main mechanisms of UV attenuation are dissipation and absorption.

The dissipation mechanism involves dilution of UV energy with increasing depth through the liquid. As the area over which UV energy is projected area increases with distance from the source (i.e. lamp), the energy per unit area (or intensity) decreases. For a sphere, the surface area over which UV energy is projected is used to determine the intensity (I):

$$I = \frac{S}{4\pi R^2} \tag{2.8}$$

where I = light intensity at distance R (cm) from lamp (μW cm^{-2}) and S = output of UV energy from the UV lamp (μW).

The absorptive attenuation of UV energy relates to the properties of the medium through which the UV energy is passing, and in the case of water will be affected by suspended solids and UV absorbing compounds. Beer's Law (Harm 1980, USEPA 1986) describes the attenuation as:

$$I = I_0 \, exp\,[-\delta R] \tag{2.9}$$

where I_0 = intensity of UV radiation at lamp surface (μW cm^{-2}) and δ = absorbance coefficient (cm^{-1}). Combining Equations (2.8) and (2.9) and rearranging yields:

$$I = \frac{S}{4\pi R^2} exp\,[-\delta R] \tag{2.10}$$

Equation (2.10) describes the intensity at a given distance from a single point-source of energy – and forms the basis for the point-source summation method. The assumptions made are that the receiving micro-organisms are spherical, and that energy from each

point-source is received perpendicular to a surface. Also, that the absorptive properties of the liquid are independent of UV intensity. This model neglects reflection, refraction, diffusion and diffraction of UV light however. The intensity at any point is then represented as the sum of intensities from all point-source contributions, given by:

$$I(R,z_0) = \sum_{n=1}^{n=N_L} \frac{S/N_L}{4\pi(R^2 + z_n{}^2)} .exp[-\delta(R^2 + z_n{}^2)^{0.5}] \qquad (2.11)$$

where N_L = the number of point-source elements in the lamp. The value of z_n is:

$$z_n = z_0 - L(n/N_L) \qquad (2.12)$$

where L is the length of the lamp. A schematic of the lamp is shown in Figure 2.8, where it can be seen that the lamp is divided into a series of N_L point-source elements.

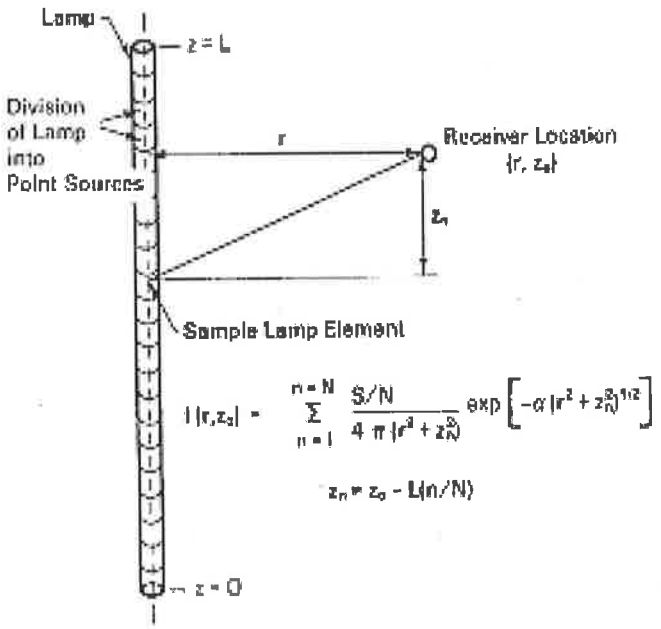

Figure 2.8 Schematic of lamp geometry for point source summation of intensity (*from* USEPA 1986)

Point source-summation becomes much more complex with complex reactor geometries and multiple lamp banks. This necessitates computational methods for solution (Janex *et al.* 1998; Lin and Blatchley 2001; USEPA 1986).

2.5.2.2 Bioassay determination

Qualls and Johnson (1983) proposed a bioassay approach for estimation of intensity distributions within a UV disinfection reactor (USEPA 1986). The first step of this involved determination of a dose-survival curve for a pure culture of *B. subtillis* spores. This was done by exposing the spores to a known and measurable intensity of UV light at a wavelength of 253.7 nm. The dose was then varied by controlling exposure time to generate a standard dose-survival response. The *B. subtillis* spores were injected into a UV disinfection system. By comparing the log-survival of numbers of spores treated by the disinfection system with the standardised dose-survival curve, the dose delivered by the disinfection unit can be reliably determined (Cabaj, Sommer and Schoenen 1996; Leuker 1999; Qualls and Johnson 1983).

This same technique can be used in a dynamic system with a non-reactive tracer to determine the residence time distribution characteristics of the disinfection reactor. By accounting for the hydrodynamics in this way, Qualls and Johnson (1983; 1985) demonstrated that it was possible to implicitly solve for the average intensity within the reactor. Estimates of intensity by the point-source summation method have been shown to compare favourably with intensity estimates made using bioassay determination (USEPA 1986).

The bioassay technique has been suggested as the only available technique to directly compare the performance of different commercial disinfection units, and; also provides a means by which to detect poor mixing across intensity gradients (Qualls and Johnson 1985). However, the bioassay technique requires refinement – particularly in regard to standardisation of methods and procedures (Crandall 1986).

2.5.2.3 Chemical actinometry

Photochemical actinometry utilises the concept of changes in oxidation states of particular ions as induced by energy supplied by UV irradiation (USEPA 1986). The extent of transition from one ion to another is compared with a known degree of transition and dosage obtained from static testing (Crandall 1986). In this way, the similarities between actinometry and the bioassay technique are clear. Bioassays performed on the residence time distribution (RTD) encountered during UV disinfection provide a useful means of highlighting the significance of the initial fractions of the RTD, and are also useful as a

diagnostic tool to test mixing across velocity gradients (Qualls, Dorfmann and Johnson 1989; Qualls and Johnson 1985).

2.5.3 Residence time distribution (RTD)

The prediction of the efficacy of large-scale UV reactors for wastewater disinfection remains inaccurate (Janex *et al.* 1998; Lin and Blatchley 2001; USEPA 1986). This is largely due to a lack of knowledge of the nature of the hydrodynamics for continuous UV disinfection processes.

Evaluation of a specific UV disinfection unit is dependent upon knowledge of the nature of the hydrodynamics within the control volume of the reactor. An analysis of the residence time distribution (RTD) is often employed to evaluate both system performance and design capacity (USEPA 1986; Janex *et al.* 1998). The residence time governs the delivered UV dose, and therefore efficacy of disinfection. Typically, tracer studies are conducted using either a dye, or salt-solution, coupled with a measuring device at a point downstream of the reactor volume. Spectrophotometric analyses may be used in the case of a coloured dye, and conductivity measurements are made in the case of a salt tracer.

A wide range of performance (i.e. efficacy) indices can be derived from a knowledge of the residence time distribution, and can be used to evaluate disinfection reactor performance (Thampi and Sorber 1987). For example, the Morrill dispersion index is defined as the ratio of times required for 90% and 10% of the tracer to pass through the reactor respectively. A suggested design goal for disinfection reactors is a value less than two (USEPA 1986). Performance indices give measures of: effective reactor volume, extent of dispersion, and evidence of short-circuiting. However, simple tracer studies are not adequate to provide a complete understanding of the mixing regimes under conditions of rapid reactions as are the case in UV disinfection (Darby, Snider and Tchobanoglous 1993).

Radial turbulence is also important in UV disinfection reactors (Cortelyou 1954; Lin and Blatchley 2001; Janex *et al.* 1998; USEPA 1986), particularly when a non-uniform intensity distribution exists within the reactor. Radial turbulence ensures each element of water in the reaction volume is exposed to the same nominal UV intensity – greatly simplifying subsequent analysis (Qasim 1999; Janex *et al.* 1998; Qualls and Johnson

1985). However, some axial dispersion will be associated with induced radial dispersion (turbulence) yielding a dispersive or non-ideal plug flow reactor (Qasim 1999). Coupling of the intensity and residence time distributions yields a spatial distribution of UV dose within the reactor volume. The development of a UV dose distribution is often considered a necessary step towards process optimisation. A knowledge of it will provide improved insight into the nature of UV disinfection reactor design.

2.6 UV disinfection unit design

Most commercial UV disinfection units are relatively simple, and are all similar in design (Nguyen 1999; Qasim 1999; USEPA 1986). They comprise a reaction volume in which the wastewater is disinfected, which either contains or is surrounded by an array of UV lamps. The capacity of a UV disinfection reactor depends critically upon the flow rate of water, level of suspended solids, the absorbance of the effluent to be treated, and the target level of disinfection (Qasim 1999; USEPA 1986; Nguyen 1999). Common elements to UV disinfection systems used for wastewater treatment include (Nguyen 1999; Qasim 1999):

- an integrator to record lamp usage
- an indicator for lamp failure
- a UV intensity monitor to prevent under-dosing
- a temperature sensor to monitor lamp surface temperature
- a water flow sensor and controller to prevent under-dosing and excessive heating of lamps which may result if the flow of water becomes stagnant.

UV unit design is based on three main objectives (USEPA 1986; Qasim 1999).

First, maximum use should be made of the UV lamp power. This suggests minimizing the absorbance of the water to be disinfected, as well as any dead-volume in the reactor. Ineffective use of the reactor volume results in reduced treatment capacity and increased power requirements.

Second, the UV disinfection unit should be a plug-flow reactor with radial turbulence encouraged. This is particularly important where a non-uniform intensity field exists, ensuring a uniform nominal UV dose is delivered.

Third, head-loss should also be minimised. Head-loss is a governing factor in UV reactor design (Qasim 1999; USEPA 1986). However, some losses will be incurred by promoting radial turbulence.

UV reactors are of two basic types: contact and non-contact reactors.

Contact reactors comprise those in which the UV lamps are submerged in the wastewater to be treated. The lamps are enclosed in quartz sleeves which are transparent to UV light and are slightly larger in diameter than the lamps. The sleeves prevent excessive cooling of the lamp surface, which would lead to a reduced lamp output. The lamps are often arranged in either staggered or uniform banks or arrays. Staggering of the lamps encourages turbulent flow conditions, such that plug flow can be more closely approached (USEPA 1986; Qasim 1999).

Non-contact reactors are generally characterized by those in which water is carried though a series of transparent tubes (of either Teflon® or another fluorinated polymer) (USEPA 1986; Qasim 1999; Thampi and Sorber 1987). The UV lamps are placed outside and parallel to the tubes, or are inserted as a removable rack (either vertically or horizontally) between the flow tubes (Qasim 1999; USEPA 1986). Alternatively, a lamp-array may be suspended above an open channel through which the water flows. The lamps do not come in direct contact with the wastewater, and the reactors are termed non-contact. In non-contact systems, such as the tubular arrays, it is possible to maintain the lamps at their optimal wall-temperature by controlling the temperature of the ambient air surrounding the lamps (USEPA 1986).

Frequently, the Teflon tubing or quartz sleeves become fouled through contact with the wastewater. Fouling reduces the transmission of radiation to the wastewater, and results in a reduced nominal UV intensity available for disinfection (Lin, Johnston and Blatchley 1999; Qasim 1999; Severin and Suidan 1985; USEPA 1986). Consequently, periodic cleaning of these surfaces is essential to maintain a high level of transmission and disinfection efficacy. Cleaning is done through use of mechanical wipers, ultrasonic transducers or chemical cleaning agents such as mild acid or detergent solutions. Transmission of both Teflon and quartz tubes are found to reduce with lamp age (USEPA

1986; Qasim 1999). A designated portion of the tubes or lamps should therefore be periodically monitored for reductions in transmission such that they may be replaced.

Most commercial UV disinfection systems employ either low or medium pressure mercury vapour lamps (USEPA 1986; Nguyen 1999). Low pressure systems are the most efficacious sources of germicidal radiation – this is because the output is near monochromatic at 254 nm. However, medium pressure lamps offer a greater treatment capacity owing to a greater UV output intensity (Nguyen 1999). Medium pressure lamps also offer the capacity for oxidation of a range of organics due to their broad spectral output (USEPA 1990), and are often employed in advanced oxidation processes (AOP's). Numerous closely-spaced lamps are required in the treatment of wastewater owing to the high liquid absorbance (Qualls and Johnson 1985; Petrasek *et al.* 1980; Qasim 1999). Qualls and Johnson (1985) note that too close a lamp spacing may result in reduced disinfection efficacy, arising from light absorption from adjacent lamps. Pre-filtration can also improve performance by increasing transmission of the wastewater and reducing the likely particle-association of any microbial contaminants. This may also prolong quartz lamp or Telfon tube life.

The criteria for any acceptable UV disinfection unit design are that it must meet both disinfection requirements and head-loss constraints (Loge *et al.* 1996; Qasim 1999).

2.7 · Economics of UV disinfection

UV disinfection is capital intensive, with equipment requirements directly proportional to the peak hydraulic needs. The operational and maintenance needs, however, are reflected more by the average utilisation of the system (USEPA 1986). In particular, the operational and maintenance costs are site specific, and are dependent upon the quality of the water to be treated together with discharge requirements (USEPA 1992). It has been proposed that the cost of UV disinfection can be approximated from the required contact time and length of UV lamp per reactor volume (Qasim 1999; Nguyen 1999).

The installed costs for UV systems have been estimated to be approximately \$US 48,800 kW^{-1} for systems with less than 100 lamps, and \$US 39,000 kW^{-1} for larger systems (USEPA 1986). When considered on the basis of flow for advanced secondary

treatment plants, these costs range from $US 78,000 to $US 97,600 per mgd[4] of average design flow for large (> 1.5 mgd) and smaller (< 1.5 mgd) plants respectively (USEPA 1992). The installed costs of UV systems are generally dominated by the equipment costs. These include (USEPA 1992):

- UV modules with lamps and quartz sleeves
- module support racks
- level control devices
- instrumentation and control panels
- power supply distribution/ballasts
- cables/cableways
- spare parts inventory.

There is an economy-of-scale with UV disinfection, although divided into two distinct sizes: systems with less than 100 lamps, and; those with greater than 100 lamps.

Operation and maintenance labour requirements, exclusive of cleaning, have been estimated at 120 hours per year per 100 lamps for smaller systems, and 55 hours per year per 100 lamps for larger systems (USEPA 1992).

The unit costs of UV disinfection vary significantly depending on: the plant size, wastewater quality, the type of UV reactor used, and; the efficiency of the UV lamps (Savolainen 1991). A sequential application of ozone-UV or UV-ozone is found to be more economical than application of either UV or ozone alone (Venosa *et al.* 1984; Severin and Suidan 1985; Nguyen 1999).

In general, UV disinfection is believed to be cheaper than all forms of wastewater disinfection other than chlorination (Nguyen 1999). Oliver and Cosgrove (1975) calculated total operational costs of UV disinfection systems and found the cost of disinfecting 1,000 US gallons of secondary effluent to be $US 0.012, compared to $US 0.001 for chlorine disinfection – suggesting the operating costs for UV treatment were not excessive. Savolainen (1991) reported the cost of UV disinfection to be comparable with chlorination and ozonation, but added that the cost varied significantly with both the treatment capacity

[4] mgd = mega gallon (US) per day

of the UV disinfection unit and the quality of wastewater to be treated. The costs associated with dechlorination make UV disinfection an increasingly viable alternative (Severin 1980). Taghipour (2004) reported the required energy, and associated cost, for inactivation of *E. coli* by UV treatment to be considerably less than for inactivation utilising ionising radiation. Energies required for a 4-$\log_{10}$ reduction utilising UV and ionising radiation respectively were 8×10^{-2} and 2.5×10^{-1} kWh.m^{-3}, corresponding to associated costs of 0.4 and 1.25 cents m^{-3}.

Alternative analyses have found that costs of UV treatment are comparable to (or slightly higher than) the costs of chlorination, and lower than those of ozonation and chlorine dioxide disinfection (Wolfe 1990). Wolfe (1990) found the capital costs for 0.5 and 1 mgd UV facilities to be greater than those for comparable chlorine, chlorine dioxide, and ozone facilities. However, due to relatively low operation and maintenance requirements for UV disinfection, the total annual cost for UV disinfection was less than that for chlorine dioxide or ozone disinfection. For a 1 mgd facility, the estimated total costs for disinfection by chlorine, UV, ozone and chlorine dioxide were, respectively, $US 0.017, $US 0.053, $US 0.066 and $US 0.086 per 1,000 US gallons (Wolfe 1990). Carnimeo *et al.* (1995) found that when UV irradiation was used in combination with hydrogen peroxide the total cost was $US 19.5 per 1,000 m^3 ($US 0.074 per 1,000 gallons), with optimisation of hydrogen peroxide dosing leading to a possible further reduction in total cost (Carnimeo *et al.* 1995; Nguyen 1999).

Venosa (1983) reported that for UV disinfection of secondary effluent with flows of between 1 and 100 mgd (0.044 and 4.4 m^3 s^{-1}), capital plus operating costs ranged between $US 0.045 and $US 0.03 per 1,000 US gallons respectively (or between $US 12.00 and $US 8.00 per 1,000 m^3). These costs were said to be comparable to combined chlorination/dechlorination.

Based on an estimated operational cost of $US 0.021 per 1,000 US gallons, Severin (1980) determined the respective operating costs for UV treatment of "good-quality" effluent, secondary effluent and sand-filtered secondary effluent to be $US 0.0072, $US 0.0079 and $US 0.015 per 1,000 US gallons, highlighting the benefit of filtration prior to UV disinfection.

Heinonen-Tanski *et al.* (2003) determined the annual maintenance cost of a UV disinfection unit treating an annual flow of 22×10^6 m^3 to be € 137,500. Of this, € 20,000 (~14.5 %) was attributed to general maintenance and other ancillary costs, such as those associated with general testing and lamp disposal.

2.8 Review of the main kinetic models for UV disinfection

Careful analyses of the published literature revealed that early studies into UV disinfection were empirical, and the results often limited to the specific reactor being tested. Even where the same UV reactors are used by separate researchers, it can be difficult to collate data and adequately compare UV disinfection efficacy due to non-standardised reporting (Severin and Suidan 1985). Correlations of specific wastewater parameters to UV disinfection efficacy have been largely unsuccessful (USEPA 1996). The kinetics of UV disinfection are widely assumed (Nguyen *et al.* 1998; Qasim 1999; Loge *et al.* 1996; Savolainen 1991) to follow the form of a first-order chemical reaction with respect to UV dose. Mathematically, this classical log-linear model form is represented by Equation (2.5). However, deviations from first-order kinetics do occur in practice. For example, the tailing often reported (Darby *et al.* 1999; Emerick *et al.* 1999; Emerick *et al.* 2000) is primarily attributed to occlusion or shielding of the micro-organisms by suspended solids (USEPA 1986; Qasim 1999; Oliver and Carey 1976) – and to a lesser extent by the absorbance of the water.

One attempt to account for tailing has been the addition of a term for particulate bacterial density (Qasim 1999; USEPA 1986; Darby *et al.* 1999; Loge *et al.* 1996) such that:

$$N = N_{0.} e^{-k.[dose]} + N_p \qquad (2.13)$$

where N_p = the particulate bacterial density unaffected by UV light. The particulate bacterial density is in turn expressed as a function of either turbidity, or, total suspended solids (TSS):

$$N_p = c(TSS)^m \qquad (2.14)$$

where c and m are experimentally determined constants. It is also widely known that the RTD characteristics of a UV photoreactor have a sizeable influence on the disinfection efficacy. Scheible and Bassell (USEPA 1981) further modified Equation (2.13) to

incorporate the dispersive properties of the reactor, which led to the following generalised model (Qasim 1999):

$$N = N_0 \exp\left[\frac{ux}{2E}\left(1-\left(1+\frac{4Ea\bar{I}^b}{u^2}\right)^{0.5}\right)\right] + c(TSS)^m \qquad (2.15)$$

where u = velocity of water (cm s^{-1}); x = average distance travelled by a water element while exposed to UV (cm); E = dispersion coefficient (cm^2 s^{-1}) estimated from RTD; $\bar{I}$ = average intensity of light in the reactor (μW cm^{-2}); and a and b are constants determined from a linear regression on Equation (2.16):

$$k = a(\bar{I})^b \qquad (2.16)$$

However, the model of Scheible and Bassell does have some problems (USEPA 1981). Estimation of the particulate bacterial density requires generating data under high values of UV dose. The assumption is that the observed bacterial density at high doses can be attributed solely to those bacteria associated with particulate material. These survivors are then correlated to the suspended solids concentration. However, previous studies (Nguyen *et al.* 1998; Nguyen 1999) have found that tailing does in fact occur in the absence of suspended solids, and might to a certain extent result from bacterial clumping.

A further drawback with the model of Equation (2.15) is that; whilst estimation of the particulate bacterial density is performed at high UV doses, the disinfection rate coefficient must generally be determined at lower values of UV dose so that appreciable detail in the kinetics can be observed.

Darby *et al.* (1995) proposed an empirical relationship to describe the tailing region of a UV dose-response curve. The functional form of the relationship is (Darby *et al.* 1999; Tchobanoglous *et al.* 1996):

$$N = A\,(SS)^a\,(UFT)^b\,(N_0)^c\,[dose]^n \qquad (2.17)$$

where N = coliform density after UV exposure (MPN per 100 millilitres); SS = suspended solids (mg L^{-1}); UFT = unfiltered transmittance (% at 253.7 nm); N_0 = influent coliform density (MPN per 100 millilitres), and; A, a, b, c, n = empirical site-specific constants.

The model, Equation 2.17, was initially developed for conventional activated sludge processes with water flow parallel to the UV lamps. The significance of the model coefficients is determined through multiple linear regression (Tchobanoglous *et al.* 1996). However, it may prove difficult to distinguish between the effects of suspended solids and unfiltered transmittance. Figure 2.9 shows typical dose-response curves for varying water quality. A filtered tranmittance (or the colour of a filtered sample) may be a more suitable inclusion in the model as unfiltered transmission is dependent upon suspended solids concentration. This is evident in Figure 2.9, where reduced efficacy is shown to occur for high concentrations of suspended solids, or low levels of unfiltered water transmittance (UFT). No provision is made for water with high UV absorbance arising from the presence of soluble UV absorbing agents. In this case, the suspended solids concentrations could potentially remain low.

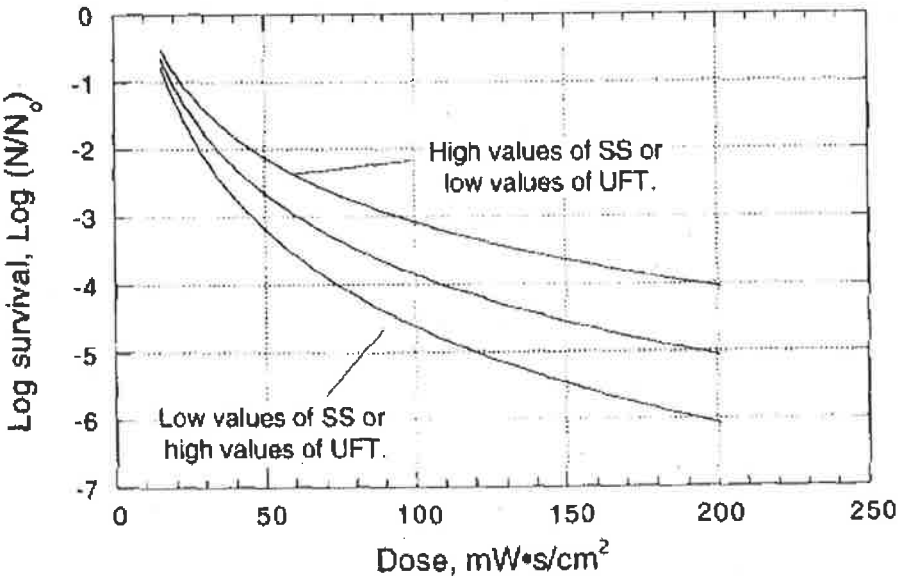

Figure 2.9 Survival curves for varying water quality characteristics (*from* Tchobanoglous *et al.* 1996)

A similar model has been published by Tchobanoglous *et al.* (1999). The model was developed to describe both the first-order and tailing regions of a UV dose-response curve and has the form:

$$N = N_D \exp(-k[dose]) + \frac{\overline{N_P}}{k[dose]}(1 - \exp(-k[dose])) \tag{2.18}$$

where N_D = total number of disperse coliform bacteria prior to UV application per 100 mililitres and $\overline{N_P}$ = total number of particles containing at least one coliform bacterium per 100 mililitres prior to UV application. This model has found widespread use in wastewater treatment (Emerick *et al.* 1999; Emerick *et al.* 2000; Darby *et al.* 1999). Figure 2.10 shows a fit of this model to the UV disinfection data of Darby *et al.* (1999). The disinfection of particle-associated coliform bacteria and disperse coliform bacteria are described by solid lines labelled one and two respectively. The rate of disinfection of disperse coliform bacteria is seen to be high, even for low UV dose (< 25 mWs cm^{-2}). The implicit assumption is that disinfection kinetics in the tailing region are characterised primarily by an association with particulate matter. This coincides with the view of Nelson (2000), that suspended solids concentration is not an appropriate criterion for evaluating suitability of UV treatment to a particular wastewater, and instead the total number of particles that have associated coliforms ($\overline{N_P}$) should be used.

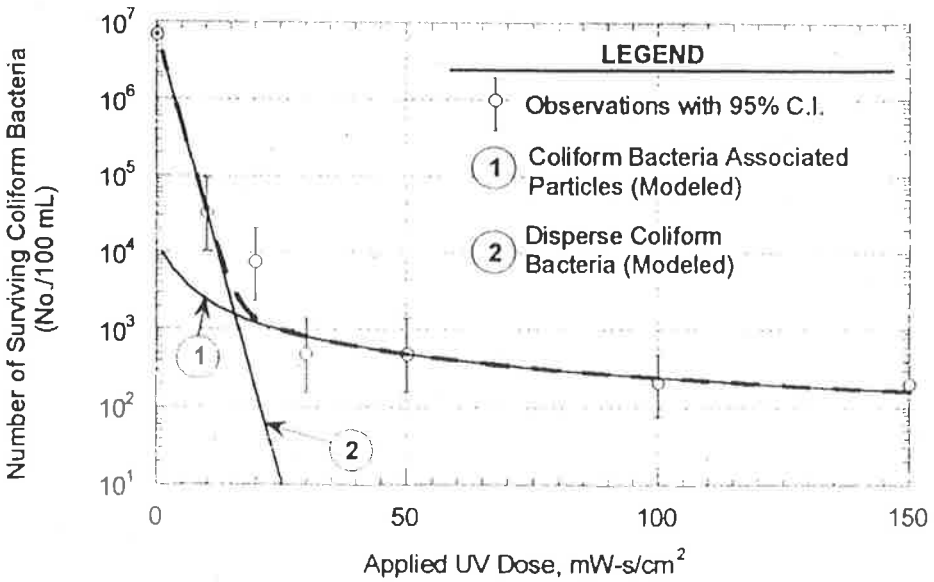

Figure 2.10 Fit of model of Equation (2.18) to dose response data (*from* Darby *et al.* 1999)

The model of Equation (2.18) was developed based on two assumptions. The first, that enumeration of coliform bacteria (by the method of multiple tube fermentation) counts one particle with at least one viable coliform embedded as a single coliform - regardless of the actual number of coliform bacteria embedded (Darby *et al.* 1999; Emerick *et al.* 2000). The second, is that the probability of disinfecting the critical coliform bacterium in each affected particle (coliform bacterium most protected) is independent of the particle containing the micro-organism. This second assumption was found to be true with coliforms for all particles exceeding 10 pm (i.e. 10^{-6} µm). This is in contrast to the assertion of Oliver and Cosgrove (1975) that the size distribution of suspended solids is likely to affect the efficacy of UV disinfection. The first assumption regarding accurate enumeration of contaminant coliforms can be seen to lead the model towards over-prediction of the actual number of coliform bacteria inactivated during disinfection, and could have serious implications of a public health risk as there will be more bacterial survivors than expected.

Severin, Suidan and Engelbrecht (1983) used two standard kinetic models to represent UV disinfection – multi target-kinetics and series-event kinetics. The series-event model for batch reactions is given by:

$$\frac{N}{N_0} = \exp(-k\bar{I}t)\sum_{i=0}^{T-1}\frac{(k\bar{I}t)^i}{i!} \tag{2.19}$$

and the series event model applied to a flow-through completely-mixed reactor is defined as:

$$\frac{N}{N_0} = 1-\left[1+\frac{1}{k\bar{I}t}\right]^T \tag{2.20}$$

In both cases, T = the threshold number of damaged sites required for disinfection (Severin and Suidan 1985; Severin, Suidan and Engelbrecht 1983; Labas *et al.* 2006).

The other model used by Severin, Suidan and Engelbrecht (1983) has been termed as "multi-target series-event kinetics" (Severin and Suidan 1985). This model combines the clumping effects together with viable cell resistance.

This model for batch inactivation is:

$$\frac{N}{N_0} = 1 - \left(1 - \exp(-k\bar{I}t) \sum_{i=0}^{T-1} \frac{(k\bar{I}t)^i}{i!} \right)^L \tag{2.21}$$

where N/N_0 = the survival fraction of clumps in a uniform suspension of clumps with L micro-organisms per clump, and T = the threshold number due to internal resistance (Severin and Suidan 1985). Severin and Suidan (1985) postulate series-event kinetics most adequately fit the expected mechanism of UV inactivation.

2.9 Summary and concluding remarks

1. A critical review of the literature highlights that the combined effect of all three treatment parameters, solids concentration, UV transmission and UV dose, is important to understanding UV efficacy.

2. A number of researchers have attempted to model the combined effect of solids concentration, UV transmission and UV dose on the efficacy of UV disinfection. However, none of these models are universally used. This can be primarily attributed to previous studies being fragmented with inconsistent sampling techniques, variation in methods used for enumeration of viable bacteria and, differences in the nature of the UV reactors studied. These models are also shown to be based on assumptions which in practice may be difficult to justify.

3. Extensive experimental validation of a model for the effect of solids concentration, UV transmission and UV dose has been undertaken by Nguyen (1999). However, this model is not adequate in that it does not include explicitly the effect of concentration of suspended solids together with UV transmission and UV dose.

In the next chapter, the established UV disinfection data of Nguyen (1999) are used to assess four established predictive model forms with the aim of developing a rigorous model that can be used to predict the combined effect of all three treatment parameters, solids concentration, UV transmission and UV dose, on the efficacy of UV disinfection.

CHAPTER 3: EVALUATION OF FOUR ESTABLISHED MODEL FORMS FOR UV DISINFECTION KINETICS

Parts of this chapter have been published as:

Amos S A, Davey K R and Thomas C J 2001 A comparison of predictive models for the combined effect of UV dose and solids concentration on disinfection kinetics of *Escherichia coli* for potable water production. *Transactions of the Institution of Chemical Engineers, Part B, Process Safety and Environmental Protection.* **79** (3): 174-182.

Amos S A, Davey K R and Thomas C J 2001 Predicting the combined effect of UV dose and suspended solids concentration on UV disinfection kinetics of *Escherichia coli.* In: *Proc. 6th World Congress of Chemical Engineering*, Melbourne, Australia, 23-27 September 2001, Health and Safety (Session 3110). p. 107 ff. (ISBN 0 7340 2201 8).

3.1 Introduction

The presence of suspended solids in water is qualitatively known (Qasim 1999; Nguyen *et al.* 1998) to produce tailing (Cerf 1977; Davey, Hall and Thomas 1995; Daughtry *et al.* 1997; Qasim 1999; Taghipour 2004; Cantwell and Hofmann 2008) in UV survivor data. Attempts have been made by a number of researchers to model survivor data (Tchobanoglous *et al.* 1999; Darby *et al.* 1995; Darby *et al.* 1999; Emerick *et al.* 1999; Emerick *et al.* 2000). The development of an adequate model can be justified by an increased confidence in application, and as the necessary first step to process optimisation.

Nguyen (1999) carried out an experimental study of the combined effect of suspended solids concentration, UV transmission and UV dose on survival of *Escherichia coli*, an indicator for presence of enteric pathogens and found in water contaminated by faecal material, to obtain data for model development. However the model failed to adequately account for the effect of suspended solids on the extent of UV disinfection.

In this chapter, the UV disinfection data of Nguyen (1999) are used to assess the adequacy of four established model forms for quantitative prediction of the combined effect of UV dose and suspended solids concentration on disinfection kinetics of *E coli*. In addition to

the classical log-linear model form, these models include the: Davey linear-Arrhenius (DL-A), Square-Root (or Ratkowsky-Belehradek), and; a general n^{th} order polynomial form (*n*OP).

Criteria for fit of an adequate model are established and defined – and a comparative summary is made of the four model forms. The linear-Arrhenius model form of Davey is shown to best fit these data against the established criteria.

3.2 Experimental data of Nguyen (1999)

A pure culture of *E. coli* ATCC 25922 (FDA strain, *Seattle* 1946) was used as the contaminant micro-organism by Nguyen and co-workers in The University of Adelaide's, *Food Research Group*, (FRG) (Nguyen *et al.* 1998; Nguyen 1999). *E. coli* is a motile rod about 1 μm by 2 to 3 μm in length (Brock and Madigan 1991; Stanier, Doudoroff and Adelberg 1971). It satisfied the necessary requirements of: significant sensitivity to UV irradiation, simple growth requirements, and; easy dispersion as individual cells. Feed water transmittance was varied by the addition of either a UV shielding agent (Diatomaceous earth as Celite 503™) or a UV absorbing agent (International Roast™ instant coffee powder). The Celite 503™ consisted of 89% silica (SiO_2) with a median particle size of 23 μm (Nguyen 1999).

The experiments were carried out in a commercial UV disinfection unit (Model LC-5 supplied by Ultraviolet Technology of Australasia Pty. Ltd., Glynde, SA, Australia) that delivered an irradiation intensity of 11,940 μW cm^{-2} at a wavelength corresponding to maximum germicidal effect of 254 nm. The system configuration was that of a single-pass U-tube, in which the flow regime spanned the transition between laminar and turbulent flow, with a Reynolds' Number (*Re*) ranging from 1.98×10^3 to 7.64×10^3.

A block experimental design of four non-zero UV doses (10,800; 14,100; 22,700 and 44,200 μWs cm^{-2}) and five solids concentrations for disinfection of *E. coli* was employed (Nguyen 1999). The non-zero UV doses corresponded to UV exposure times of 0.9, 1.2, 1.9 and 3.7 seconds respectively. Four non-zero, suspended solids concentrations of shielding agent used were: 0.01, 0.05, 0.1 and 0.3 g L^{-1}, whilst for the absorbing agent, concentrations of: 0.001, 0.005, 0.01 and 0.03 g L^{-1} were used. Three replicates were

obtained. This design resulted in n = 75 data sets for each of the shielding and absorbing agents. The temperature of the feed-water ranged between 20 and 24 °C.

3.3 The model of Nguyen (1999)

As highlighted in Chapter 2, the kinetics of UV disinfection are widely assumed (Qasim 1999; Loge *et al.* 1996; Kiely 1998; Nguyen 1999) to follow the form of a first-order chemical reaction with respect to UV dose (Equation 2.5). Equation (2.5) implies that a plot of $-\ln (N/N_0)$ versus UV dose results in a straight line through the origin with slope, k (hence the term log-linear model).

Despite significant tailing apparent in survivor data, Nguyen (1999) proposed a log-linear model to include the effect of UV dose only on the rate coefficient for disinfection.

Careful analyses of these data for *E. coli* disinfection however highlights that the rate coefficient exhibits dependence on both UV dose and suspended solids concentration. The model form of Nguyen (1999) is therefore inadequate. Both because it is not a good descriptor of experimentally observed tailing and because it does not include the effect of suspended solids concentration. There are at least four alternate model forms that could be used to better fit these UV data.

3.4 Four selected model forms

A classical, log-linear model form for the combined effect of both UV dose and suspended solids concentration on kinetics of disinfection of *E.* coli can be given by:

$$\ln k = C_0 + C_1 [dose] + C_2 [C_{agent}] \tag{3.1}$$

The model form of Davey (McMeekin *et al.* 1993; Holdsworth 1997; Davey 1993) for predicting the effect of combined environmental factors on thermal inactivation data was investigated. This model applied to UV disinfection, may be given by (Davey 1993; Holdsworth 1997; Daughtry *et al.* 1997; McMeekin *et al.* 1993):

$$\ln k = C_0 + C_1[dose] + C_2 [dose]^2 + C_3 [C_{agent}] + C_4 [C_{agent}]^2 \tag{3.2}$$

The model form of Equation (3.2) is said to be linear-Arrhenius and *additive* (Davey 1993; Davey 1999; Daughtry *et al.* 1997). That is, the environmental factors, [*dose*] and [C_{agent}], appear to act independently in combination to effect cell inactivation. No statistically significant interaction terms (e.g. [*dose*]×[C_{agent}]^2, [*dose*]^2×[C_{agent}]^2) have been found in this model (as applied to growth and thermal inactivation), despite analysis of some 95 years of published data for bacterial growth and death (McMeekin *et al.* 1993; Davey 1999).

The Square-Root, or Ratkowsky-Belehradek model, has been used widely to predict bacterial growth kinetics (McMeekin *et al.* 1993; Davey 1999). This model form, when applied to disinfection kinetics with combined UV dose and suspended solids concentration, is given by:

$$\sqrt{k} = c\left([dose] - \overline{dose}\right)\left([C_{agent}] - \overline{C_{agent}}\right) \tag{3.3}$$

Using the convention of Belehradek (Belehradek 1926; Davey 1999), the terms $\overline{dose}$ and $\overline{C_{agent}}$ of Equation (3.3) would represent biological "zeros", or limiting conditions at which no disinfection is possible. This is not considered valid however for the *E. coli* disinfection data of Nguyen (1999) owing to the narrow range of both UV dose and suspended solids concentration investigated. Both $\overline{dose}$ and $\overline{C_{agent}}$ are therefore constants in Equation (3.3).

Equation (3.3) should be understood to be *multiplicative* (Davey 1999; McMeekin *et al.* 1993). This is clear in its mathematically expanded form of the model terms, namely:

$$\sqrt{k} = c_0 + c_1[dose] + c_2[C_{agent}] + c_3[dose][C_{agent}] \tag{3.3a}$$

where:

$$c_0 = c.\overline{dose}.\overline{C_{agent}} \tag{3.3b}$$

$$c_1 = -c.\overline{C_{agent}} \tag{3.3c}$$

$$c_2 = -c.\overline{dose} \tag{3.3d}$$

$$c_3 = c \tag{3.3e}$$

In consequence, terms for the Square-Root model are often more difficult to obtain and use than for either the classical log-linear or Davey linear-Arrhenius (DL-A) model forms.

An n^{th} order Polynomial (nOP) form may be assumed to model the disinfection rate. Applying the growth form of Buchanan (McMeekin *et al.* 1993) to UV disinfection kinetics this model form is given by:

$$k = \gamma_0 + \gamma_1 [dose] + \gamma_2 [dose]^2 + \gamma_3 [dose]^3 + \gamma_4 [C_{agent}] + \gamma_5 [C_{agent}]^2 + \gamma_6 [C_{agent}]^3 \qquad (3.4)$$

The nOP model is generally restricted to a cubic order. Higher order forms are notoriously difficult to extrapolate or apply universally (Davey 1993).

3.5 Criteria for fit of an adequate model

The criteria for an adequate model for predicting the effect of combined UV dose and suspended solids concentration on disinfection kinetics must include (Davey 1993; McMeekin *et al.* 1993):

- goodness of fit and accuracy of prediction against observed data
- be as simple as possible (but no simpler) i.e. parsimony
- ease of synthesis and ease of use
- potential for physiological significance and interpretation of model parameters.

A stringent test of goodness of fit is the *percent variance accounted for (%V)*. The *%V* is given by:

$$\%V = \left[1 - \frac{(1-R^2)(n-1)}{(n-N_T-1)}\right] \times 100 \qquad (3.5)$$

The *%V* is a more stringent test of goodness of fit than either the correlation coefficient (r^2) or Mean Square Error (MSE), particularly, when there are few available data and the model form has a large number of terms (Davey 1993; Davey 1999; Daughtry *et al.* 1997). The *%V* permits significant comparison of model forms with different numbers of terms. This is the case with comparison of the foregoing four model forms, Equations (3.1) through (3.4).

The use of r^2 has been widely criticised (Ratkowsky 1990; Davey 1999; Davey 1993) and has little significance if the model form is non-linear. Further, r^2 can be misleading when there are few data and thereby a high value is obtained. MSE has been shown to be an inappropriate measure of goodness of fit in some instances (Davey 1999). It is claimed only to be reliable if the data are normally distributed (McMeekin *et al.* 1993).

A second important criterion for the fit of an adequate model is insight gained from appraisal of plots of residual value (as predicted value *vs.* observed value). Adequate model parameterisation and a guide to complexity of the model form can be estimated from residual plots (Ratkowsky 1990; Montgomery 2001). Diagnosis of residuals can shed light on model fits and the influence of inherent assumptions made in model development (Snedecor and Cochran 1969; Montgomery 2001).

Parsimony and ease of use are important. Parsimony entails that: "*Entities are not to be multiplied beyond necessity*" (McMeekin *et al.* 1993). That is, the model should contain the minimum number of justifiable terms. From a process engineering point-of-view, the model should, in addition, be of a form that can be readily integrated with other equations describing the nature of the liquid and hydrodynamics of flow to simulate a complete UV disinfection process operation (Davey, Hall and Thomas 1995). The kinetic model of Schoolfield, Sharpe and Magnuson (1981), for example, would be rejected on this basis as it involves a complex non-linear regression, making it difficult to obtain coefficients for all but the most sophisticated (Davey 1993).

3.6 Fitting of model forms

Regression analyses (Snedecor and Cochran 1969; McMeekin *et al.* 1993; Montgomery 2001) on linearised versions of each of the model forms fitted to the raw disinfection data for *E. coli* of Nguyen (1999) were carried out using Microsoft *Excel*® 2000 Edition, on an IBM® compatible desktop PC with an Intel Pentium® III microprocessor.

3.7 Results

Table 3.1 summarizes the values of the model coefficients obtained for the log-linear form for both the shielding and absorbing agents. Tables 3.2 through 3.4, respectively, summarize the model coefficients obtained for the disinfection rate for the Davey linear-Arrhenius (DL-A), Square-Root and third order *n*OP model forms.

The value of the disinfection rate coefficient (k) at each combination of UV dose and suspended solids concentration was obtained using Equation (2.5). The value of the disinfection rate coefficient was calculated using the terminal conditions of the dose interval investigated, with the justifiable assumption that there was no reduction in the number of viable bacteria at zero UV dose. This condition of zero UV dose was used as a datum in all rate coefficient calculations (and is analogous to calculation of apparent shear rate in rheological studies). This technique is recommended in fitting of an appropriate model to these disinfection data (*pers. comm.* B J Daughtry & K R Davey).

Table 3.1 Fit of the log-linear model for the disinfection rate coefficient:
$\ln k = C_0 + C_1 [dose] + C_2 [C_{agent}]$

Data	C_0	C_1 $\times 10^5$	C_2	n	%V	MSE $\times 10^2$
E. coli and shielding agent[1]	-6.78	-3.63	-0.685	20	95.3	1.19
E. coli and absorbing agent[2]	-6.64	-4.10	-11.04	20	90.7	3.20
				MEAN	93.0	2.19

[1] Diatomaceous earth as Celite 503™
[2] International Roast™ instant coffee powder

Substitution for the values of the model coefficients from Table 3.1 in the log-linear model for UV disinfection of *E. coli* in the presence of shielding agent (Celite 503™) yields:

$$\ln k = -6.78 - 3.63\times10^{-5} [dose] - 0.685 [C_{agent}] \qquad (3.6)$$

And, that for the effect of absorbing agent (International Roast ™ instant coffee powder) yields:

$$\ln k = -6.64 - 4.10\times10^{-5} [dose] - 11.04 [C_{agent}] \qquad (3.7)$$

Substitution for [*dose*] in μWs cm^{-2} and [C_{agent}] in g L^{-1} in Equations (3.6) and (3.7), gives k in μWs^{-1} cm^2. This model explained an overall 93.0%V in the two data sets for shielding and absorbing agents.

Table 3.2 Fit of the Davey linear-Arrhenius model for the disinfection rate coefficient:
$$\ln k = C_0 + C_1 [dose] + C_2 [dose]^2 + C_3 [C_{agent}] + C_4 [C_{agent}]^2$$

Data	C_0	C_1 ×10^4	C_2 ×10^9	C_3	C_4	n	%V	MSE ×10^2
E. coli and shielding agent[1]	-6.344	-0.771	0.723	-0.685	†	20	97.7	0.57
E. coli and absorbing agent[2]	-5.866	-1.14	1.30	-11.04	†	20	96.6	1.17
						MEAN	97.2	0.87

† not significant (P>0.05)
[1] Diatomaceous earth as Celite 503™
[2] International Roast™ instant coffee powder

Similarly, appropriate substitution for the value of the coefficients from Table 3.2 gives the Davey linear-Arrhenius (DL-A) model for shielding agent as:

$$\ln k = -6.334 - 7.71\times10^{-5} [dose] + 7.23\times10^{-10} [dose]^2 - 0.685 [C_{agent}] \quad (3.8)$$

And that for absorbing agent as:

$$\ln k = -5.866 - 1.14\times10^{-4} [dose] + 1.30\times10^{-9} [dose]^2 - 11.04 [C_{agent}] \quad (3.9)$$

This model explained an overall 97.2%V in these data.

Table 3.3 Fit of the Square-Root model for the disinfection rate coefficient:
$$k^{1/2} = c_0 + c_1 [dose] + c_2 [C_{agent}] + c_3 [C_{agent}][dose]$$

Data	c_0 ×10^2	c_1 ×10^7	c_2 ×10^3	c_3	n	%V	MSE ×10^6
E. coli and shielding agent[1]	3.14	-3.70	-7.46	†	20	90.8	2.52
E. coli and absorbing agent[2]	3.19	-4.19	†	†	20	82.6	6.49
					MEAN	86.7	4.51

† not significant (P>0.05)
[1] Diatomaceous earth as Celite 503™
[2] International Roast™ instant coffee powder

Table 3.4 Fit of the *n*OP model for the disinfection rate coefficient:
$k = \gamma_0 + \gamma_1 [dose] + \gamma_2 [dose]^2 + \gamma_3 [dose]^3 + \gamma_4 [C_{agent}] + \gamma_5 [C_{agent}]^2 + \gamma_6 [C_{agent}]^3$

Data	γ_0 $\times 10^3$	γ_1 $\times 10^8$	γ_2 $\times 10^{13}$	γ_3	γ_4 $\times 10^3$	γ_5	γ_6	n	%V	MSE $\times 10^9$
E. coli and shielding agent[1]	1.31	-5.32	6.66	†	-0.345	†	†	20	94.7	2.77
E. coli and absorbing agent[2]	1.57	-7.24	9.68	†	-4.91	†	†	20	96.6	2.47
								MEAN	95.6	2.62

† not significant (P>0.05)
[1] Diatomaceous earth as Celite 503™
[2] International Roast™ – instant coffee powder

The two *n*OP model forms for shielding agent and absorbing agent respectively (see Table 3.4), are given by:

$$k = 1.31\times10^{-3} - 5.32\times10^{-8} [dose] + 6.66\times10^{-13} [dose]^2 - 3.45\times10^{-4} [C_{agent}] \quad (3.10)$$

and:

$$k = 1.57\times10^{-3} - 7.24\times10^{-8} [dose] + 9.68\times10^{-13} [dose]^2 - 4.91\times10^{-3} [C_{agent}] \quad (3.11)$$

Over these two data sets a mean of 95.6%*V* is explained by the *n*OP model form.

Figures 3.1 through 3.4, respectively, are plots of residuals, as predicted value *vs.* observed value, of the disinfection coefficient for each of the four model forms with the addition of absorbing agent (instant coffee).

It is seen from the figures that the residual value appears uniformly spread over the observed range of the data for all but the Square-Root model. The non-uniform spread of the residuals in the figure for the Square-Root model (Figure 3.4) implies that the model is poorly parameterised (Ratkowsky 1990).

Overall the Davey linear-Arrhenius (DL-A) model is seen to give the best fit as defined by the criteria of %*V* and residual plots.

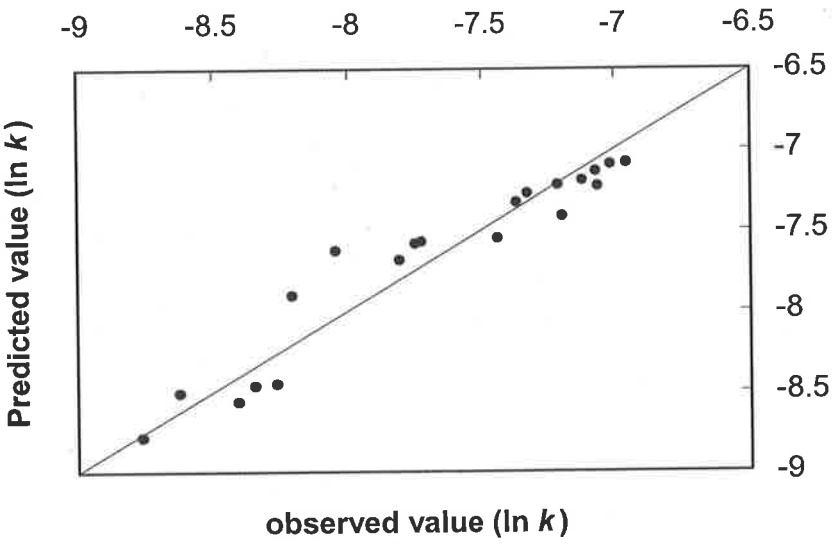

Figure 3.1 Predicted value *vs.* observed value of the disinfection rate coefficient (expressed as ln k) for the log-linear model with the presence of absorbing agent (coffee powder) in the range 0 to 0.03 g L^{-1}

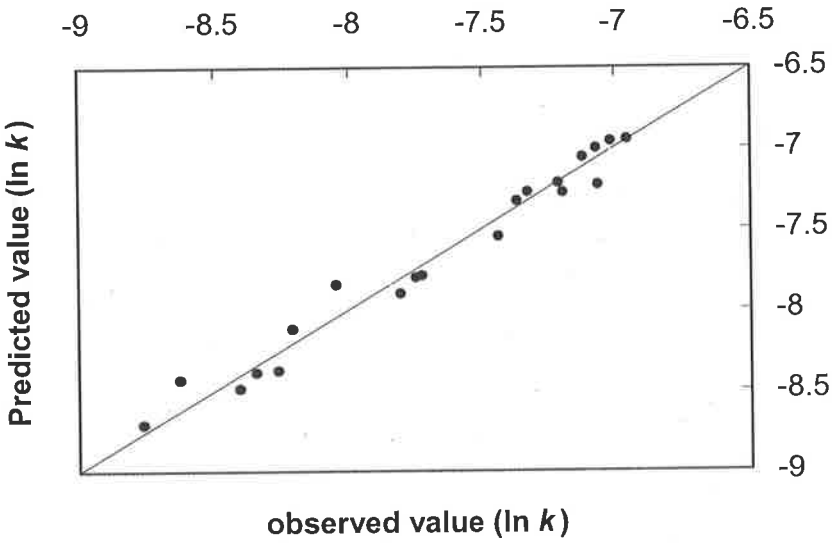

Figure 3.2 Predicted value *vs.* observed value of the disinfection rate coefficient (expressed as ln k) for the Davey linear-Arrhenius (DL-A) model with the presence of absorbing agent (coffee powder) in the range 0 to 0.03 g L^{-1}

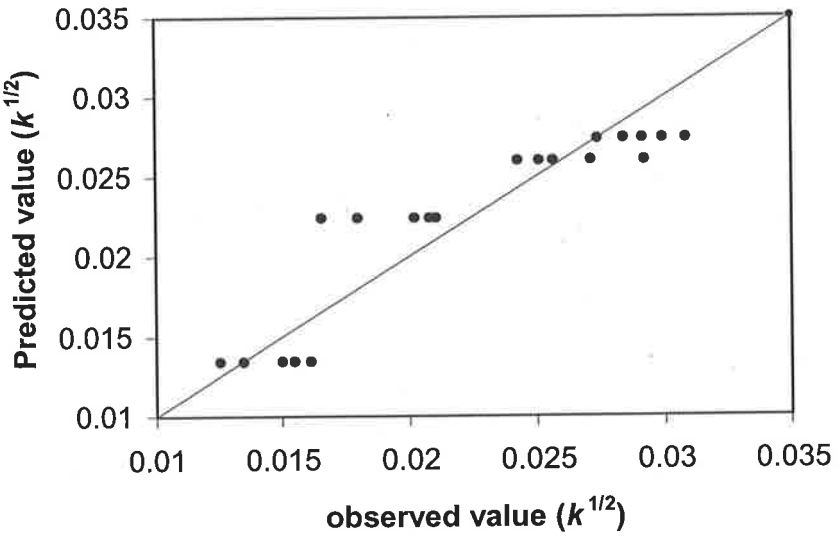

Figure 3.3 Predicted value *vs.* observed value of the disinfection rate coefficient (expressed as $k^{1/2}$) for the square-root model with the presence of absorbing agent (coffee powder) in the range 0 to 0.03 g L^{-1}

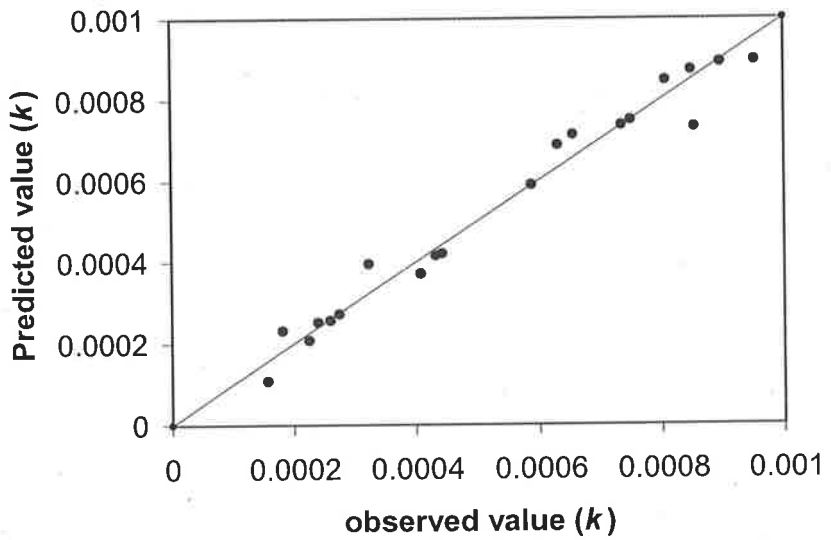

Figure 3.4 Predicted value *vs.* observed value of the disinfection rate coefficient (expressed as k) for the *n*OP model with the presence of absorbing agent (coffee powder) in the range 0 to 0.03 g L^{-1}

Figure 3.5 illustrates the smooth nature of the predicted surface of this (N_T equals) three-term model for the disinfection rate coefficient. The figure shows the effect of combined UV dose and shielding agent (Celite 503^{TM}) concentration (over the range of data). The additional lines shown in the [*dose*]-[C_{agent}] plane are contour lines. (i.e. lines of constant value of k).

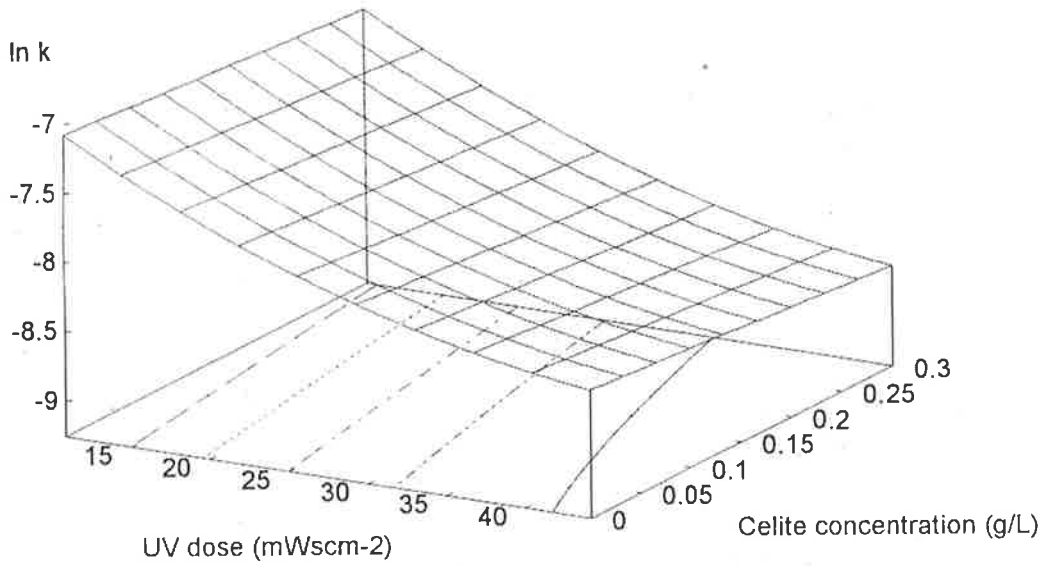

Figure 3.5 Predicted surface of the disinfection rate coefficient (expressed as ln k) for a range of shielding agent (Celite 503^{TM}) concentrations

The polynomial model form (nOP) proposed to simulate the disinfection data was restricted to a cubic in both UV dose [*dose*] and suspended solids concentration [C_{agent}]. A higher order polynomial would present certain difficulty, in addition to limited potential for extrapolation, for any attempted physiological interpretation of coefficients (Davey 1993). Importantly, there were no significant ($P<0.05$) interaction terms, for example, $[C_{agent}]^2\times[dose]^2$; $[C_{agent}]^2\times[dose]$, in the model for these *E. coli* disinfection data. A major disadvantage of the nOP model form however in consisting of six terms, namely; [*dose*], $[dose]^2$, $[dose]^3$, [C_{agent}], $[C_{agent}]^2$ and $[C_{agent}]^3$ is that it potentially fails the test of parsimony, an important criterion for an adequate predictive model. For both shielding agent (Celite 503^{TM}) and absorbing agent (instant coffee), the regression analyses for fit of the nOP model showed the disinfection rate to be quadratic with respect to [*dose*] and linear with respect to [C_{agent}] (Table 3.4).

The Square-Root model in its expanded form contains three terms: $[dose]$, $[C_{agent}]$ and $[dose]\times[C_{agent}]$. The interaction term, $[dose]\times[C_{agent}]$, was not statistically significant ($P>0.05$) for either the shielding agent or absorbing agent. The Square-Root model therefore becomes (substituting the coefficients from Table 3.3), for the shielding agent:

$$\sqrt{k} = 3.14\times10^{-2} - 3.70\times10^{-7}\,[dose] - 7.46\times10^{-3}\,[C_{agent}] \qquad (3.12)$$

And that for the absorbing agent:

$$\sqrt{k} = 3.19\times10^{-2} - 4.19\times10^{-7}\,[dose] \qquad (3.13)$$

The Square-Root model in its reduced form of Equations (3.12) and (3.13), does not reveal the inherent, multiplicative nature of the model form. A mean value of 86.7 $\%V$ is explained by the Square-Root model, over the fit of equations (3.12) and (3.13). This compares with that of 95.6$\%V$ for the nOP, and; respectively, 93.0$\%V$ and 97.2$\%V$ for the log-linear and Davey linear-Arrhenius (DL-A) models.

The better fit of the three models: nOP, log-linear and Davey linear-Arrhenius over the Square-Root model underscores that $[dose]$ and $[C_{agent}]$ appear to act independently to effect disinfection of the bacterial cells. For the log-linear model, an advantage is that it only has two terms: $[dose]$ and $[C_{agent}]$, both of which are significant ($P<0.05$) for addition of shielding and absorbing agent. This better fits the criterion of parsimony than the nOP model with its potentially six terms, but only three significant terms for these *E. coli* data ($[dose]$, $[dose]^2$ and $[C_{agent}]$), and; that of the three significant terms of the Davey linear-Arrhenius model ($[dose]$, $[dose]^2$ and $[C_{agent}]$). However the Davey linear-Arrhenius model gave a better fit in terms of *percent variance accounted for* ($\%V$) than either the log-linear or nOP models.

The reader might note from Tables 3.1, 3.2 and 3.4 that the magnitude of the coefficient for $[C_{agent}]$ is consistently about one order of magnitude lower for the shielding agent (Celite 503™) than for the absorbing agent (coffee). This reflects the difference in the range of concentrations used for each agent. The maximum concentration of the shielding agent is one order of magnitude greater than for the absorbing agent (i.e. 0.3 g L^{-1} *cf.* 0.03 g L^{-1}).

This is consistent with the fact that at lower concentrations of the shielding agent there will be reduced physical shielding of viable *E. coli* cells to UV irradiation.

The similarities in form between the two best-fit models, *n*OP and Davey linear-Arrhenius forms, suggest that UV disinfection kinetics are quadratically dependent on UV dose and linearly dependent on solids concentration, irrespective of the mechanism by which protection is afforded to the viable *E. coli* cells (i.e. same terms are significant for both the shielding and absorbing agents in each model). The improved fit of the Davey linear-Arrhenius model over that of the *n*OP does suggest some degree of exponential behaviour in disinfection kinetics (i.e. modelled as ln *k cf. k*).

A convenient summary and comparison of the general properties of the four predictive models is presented in Table 3.5. Using summation of checks over important model characteristics as the basis for comparison, it appears that the log-linear and Davey linear-Arrhenius (DL-A) model forms are best suited to these disinfection data for *E. coli*. On the basis of accuracy of fit (i.e. *%V*) alone however, the Davey linear-Arrhenius and *n*OP are better model forms. Both the log-linear and Davey linear-Arrhenius models are parsimonious and empirical.

Table 3.5 Comparison of general properties of the four predictive models

	MODEL			
	log-linear	DL-A	Square-Root	*n*OP*
Accuracy of Model	×	✓	×	✓
Ease of obtaining and use	✓	✓	×	×
Physiological interpretation	×	×	×	×
Theoretical basis	×	×	×	×
Parsimony	✓	✓	×	✓
Predicted limits	×	×	✓	×
Reliability of extrapolation	✓ ×	✓ ×	×	×
Simple structure	✓	✓	×	×
Linear model	✓	✓	×	✓
Integration with process models	✓	✓	×	✓
SUM OF CHECKS	**6 -**	**7 -**	**1**	**4**

* $n = 3$ for a third order polynomial

Analyses of other disinfection data for different micro-organisms might show the DL-A model to be of a generalized and universal model form. A physiological interpretation of the model coefficients would thereby be strengthened. A disadvantage of the DL-A model however, is that it does not predict a limiting value whereas the Square-Root form does (Davey 1999). This suggests that an asymptotic model may be preferable to more accurately describe UV disinfection kinetics exhibiting tailing. The DL-A model nevertheless gives the greatest degree of accuracy of prediction of the four forms, which is arguably the most influential criterion for choice of a suitable model, for these disinfection data.

Tables 3.6 and 3.7 summarise values of the residuals from the DL-A model (Equations 3.8 and 3.9), over the range of experimentally observed [*dose*] and [C_{agent}] values for shielding agent and absorbing agent respectively. The random and evenly distributed residuals of these tables suggest the model is neither over- nor under-parameterised (Ratkowsky 1990). The distribution of residuals shows that the model (generally) over-predicts (shown by negative value of the residual) the value of the disinfection rate coefficient at shielding agent concentrations of both 0 g L^{-1} and 0.1 g L^{-1} (Table 3.6). For addition of absorbing agent (Table 3.7), the model generally over-predicts the value of the disinfection rate coefficient for suspended solids concentrations of 0.01 g L^{-1} and 0.03 g L^{-1}.

Figures 3.6 and 3.7, respectively, show the predictions of the Square-Root and Davey linear-Arrhenius (DL-A) models over the range of [*dose*] and shielding agent concentrations [C_{agent}] studied experimentally. It is evident that the predictions of the Square-Root model of Figure 3.6 do not adequately simulate the form of tailing in the original disinfection data of Nguyen (1999). A high degree of tailing (Davey, Hall and Thomas 1995; Cerf 1977) is evident in Figure 3.7, suggesting the Davey linear-Arrhenius model is better suited to predicting the effect of suspended solids on the extent of UV disinfection. As the UV dose is extended beyond the observed range however, a rapid increase in the predicted level of disinfection occurs as a result of the quadratic nature of the Davey linear-Arrhenius model. These data suggest an asymptotic model may be better suited to represent the tailing phenomenon observed during UV disinfection.

Table 3.6 Comparison between predicted value and observed value of the disinfection rate coefficient (ln *k*) from the Davey linear-Arrhenius model with shielding agent (Celite 503^{TM}) present to 0.3 g L^{-1}

UV dose (=*It*) ($\mu Ws\ cm^{-2}$)	Shielding Agent ($g\ L^{-1}$)	Disinfection Rate ($\mu Ws^{-1}cm^{2}$)		Residual
		Observed	Predicted	
10,800	0	-6.956	-7.092	0.136
	0.01	-7.215	-7.287	0.072
	0.05	-7.723	-7.721	-0.002
	0.1	-8.261	-8.338	0.077
	0.3	-7.124	-7.099	-0.025
14,100	0	-7.367	-7.294	-0.073
	0.01	-7.778	-7.728	-0.050
	0.05	-8.344	-8.345	0.001
	0.1	-7.149	-7.126	-0.023
	0.3	-7.358	-7.321	-0.037
22,700	0	-7.812	-7.755	-0.057
	0.01	-8.405	-8.372	-0.033
	0.05	-7.213	-7.161	-0.052
	0.1	-7.444	-7.355	-0.089
	0.3	-7.614	-7.789	0.175
44,200	0	-8.463	-8.406	-0.057
	0.01	-7.255	-7.297	0.042
	0.05	-7.485	-7.492	0.007
	0.1	-7.946	-7.926	-0.020
	0.3	-8.536	-8.543	0.007

Table 3.7 Comparison between predicted value and observed value of the disinfection rate coefficient (ln k) from the Davey linear-Arrhenius model with absorbing agent (coffee powder) present to 0.03 g L^{-1}

UV dose ($=It$) ($\mu Ws\ cm^{-2}$)	Absorbing Agent ($g\ L^{-1}$)	Disinfection Rate ($\mu Ws^{-1}cm^{2}$)		Residual
		Observed	Predicted	
10,800	0	-6.956	-6.948	-0.008
	0.001	-7.215	-7.218	0.003
	0.005	-7.723	-7.789	0.066
	0.01	-8.261	-8.378	0.117
	0.03	-7.017	-6.959	-0.058
14,100	0	-7.065	-7.229	0.164
	0.001	-7.748	-7.800	0.052
	0.005	-8.341	-8.389	0.048
	0.01	-7.072	-7.003	-0.069
	0.03	-7.328	-7.273	-0.055
22,700	0	-8.041	-7.844	-0.197
	0.001	-8.623	-8.434	-0.189
	0.005	-7.123	-7.058	-0.065
	0.01	-7.369	-7.328	-0.041
	0.03	-7.805	-7.899	0.094
44,200	0	-8.404	-8.489	0.085
	0.001	-7.196	-7.279	0.083
	0.005	-7.438	-7.549	0.111
	0.01	-8.206	-8.120	-0.086
	0.03	-8.764	-8.710	-0.054

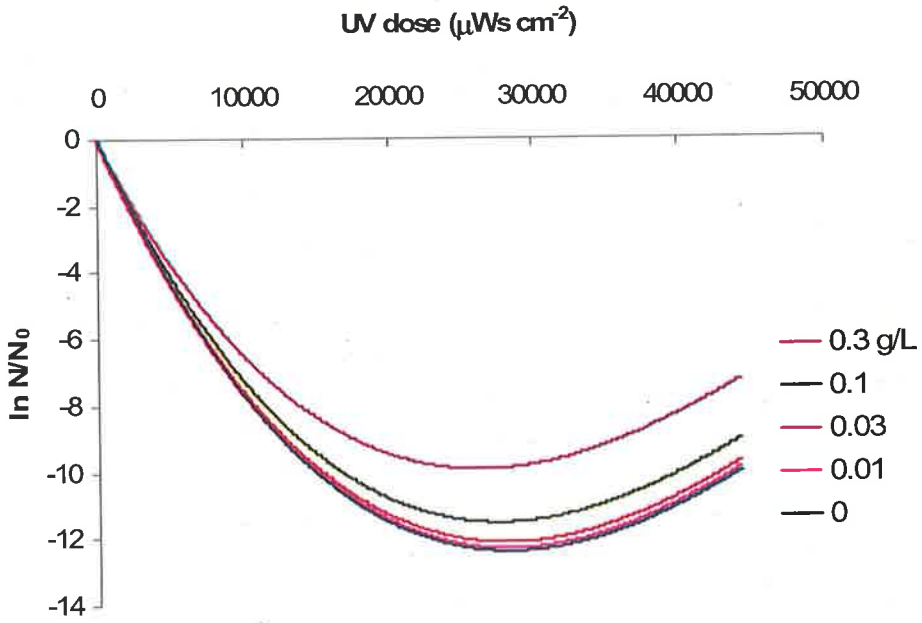

Figure 3.6 Predicted survivor curve from the Square-Root model with the effect of shielding agent concentration (Celite 503^{TM}) to 0.3 g L^{-1}

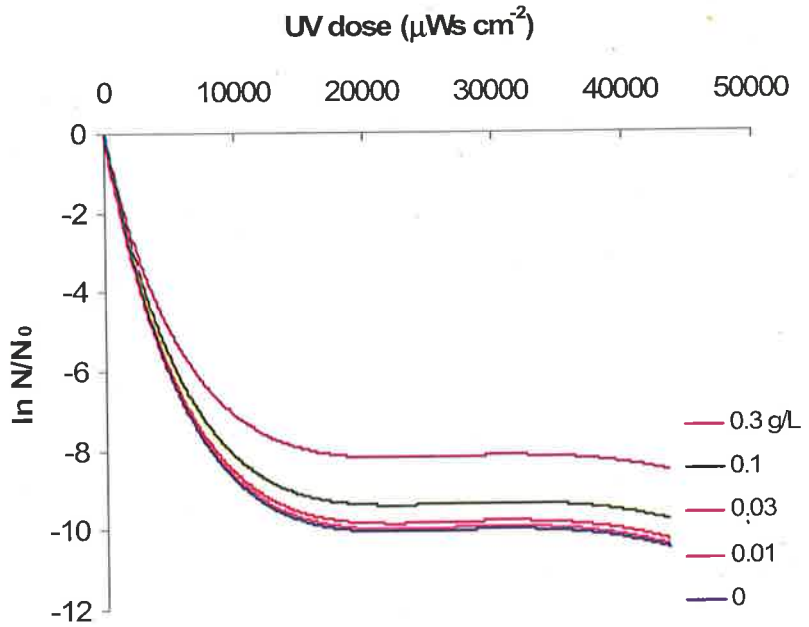

Figure 3.7 Predicted survivor curve from the Davey linear-Arrhenius model with the effect of shielding agent concentration (Celite 503^{TM}) to 0.3 g L^{-1}

It is axiomatic that extrapolation of empirical models should not be carried out beyond the experimental limits from which they are obtained without caution (Davey 1999; Daughtry *et al.* 1997; Ratkowsky 1990). Although the four model forms studied are smooth functions, extrapolation beyond the experimental range cannot be readily justified for these *E. coli* disinfection data.

The potential for physiological interpretation of coefficients of a predictive model is arguably important (Davey 1993). However generation of more data, particularly within the lower range of UV dose (0 to 10,000 μWs cm^{-2}), is required. Physiological insights may proceed from an established and widely demonstrated empirical model, to a form including a mechanistic basis for UV disinfection.

3.8 Concluding remarks

1 The combined effect of UV dose and suspended solids concentration on the rate coefficient for UV disinfection of *E. coli* in purified water is significant. This effect is more pronounced at low values of UV dose and higher solids concentrations. The combined effect of the absorbing agent and UV dose is significant also.

2. On the basis of *percent variance accounted for (%V)*, analyses of residual plots, sum of checks, and criteria including: parsimony and ease of use, and ready integration with additional equations to describe a UV disinfection unit operation, the Davey linear-Arrhenius model (DL-A) is ranked as the most suitable (of the four assessed forms) for UV disinfection of viable *E. coli* cells in purified water.

3. Although, the DL-A model was found to best fit the UV disinfection data, a shortcoming is that it is not amenable to extrapolation – and further it does not model the reduction in viable bacteria directly (i.e. as $\log_{10} N/N_0$), but rather models the disinfection rate coefficient (as ln k). Its use therefore predicates the need for the model to be coupled with the general first-order rate equation (Equation 2.5).

4. Drawbacks with the DL-A model have underscored the need for a new and non-linear model form to adequately describe tailing observed in UV disinfection data. An asymptotic form may be better suited to prediction of UV disinfection kinetics exhibiting tailing, and may be used to determine a limiting rate of disinfection.

5. It should be noted that, despite the emergence of UV treatment as a viable alternative to traditional means of wastewater disinfection such as chlorination, there are actually few published robust disinfection data suitable for model development.

In the following chapter, two new non-linear models for UV disinfection are proposed and assessed to overcome the shortcomings of the Davey linear-Arrhenius model. These two new models are, initially, validated against the independent published data of Nelson (2000) for UV disinfection of faecal coliforms in waste stabilisation pond effluent.

CHAPTER 4: SYNTHESIS OF TWO NEW MODELS FOR UV DISINFECTION KINETICS

Parts of this chapter have been published as:

Amos, S. A., Davey, K. R. and Thomas, C. J. (2003). A new EDP model for predicting UV disinfection kinetics of coliforms as effected by dose and suspended solids. In: *Proc. 31st Australasian Chemical Engineering Conference (Products and Processes for the 21st Century)*, CHEMECA 2003, Stamford Plaza, Adelaide, South Australia, Australia, September 28 – October 1, paper 185. (ISBN 0 8639 6829 5).

Amos, S. A., Davey, K. R. and Thomas, C. J. (2004). A new Weibull model for prediction of tailing in UV disinfection survivor data. In *Proc. 32nd Australasian Chemical Engineering Conference (Sustainable Processes)*, CHEMECA 2004, Australian Technology Park, Sydney, NSW, Australia, September 26 – 29, paper 106. (ISBN 1 8770 4012 6).

4.1 Introduction

In the previous chapter it was shown that of four widely used established model forms, the Davey linear-Arrhenius (DL-A) model best satisfied the criteria established for fit of an adequate model. This model however, was found to have shortcomings in prediction of numbers of survivors at high values of UV dose (> 40,000 $\mu Ws\ cm^{-2}$).

In this chapter, two new non-linear models for UV disinfection are synthesised in an attempt to overcome these shortcomings of the Davey linear-Arrhenius model. These two new models are assessed against the independent published data of Nelson (2000) for UV disinfection of faecal coliforms in a range of waste stabilisation pond effluents. These data of Nelson (2000) exhibit tailing for the disinfection of a range of waste stabilisation pond effluents, and are some of the few available data suitable for use in model assessment – despite the recent advances in UV technology and its emergence as an alternative disinfectant for potable water production, and wastewater treatment.

The two new model forms are: a modified exponentially damped polynomial (EDP_m), and; a form based on the Weibull probability distribution. Both models are found to accurately simulate the tailing phenomena in the disinfection data of Nelson (2000) over a range of

treatment conditions. Each model has the advantage of reduction to a log-linear kinetic form in the tailing region – suggesting extrapolation over small increments beyond the reported UV dose range may be justifiable in some instances. The EDP_m model is treated first (Section 4.4), followed by the modified Weibull form (Section 4.5).

4.2 UV data of Nelson (2000)

The UV disinfection data of Nelson (2000) are appropriate for model development in that they exhibit tailing in the presence of a range of solids concentrations – and are for a variety of treated effluents. The survival of total coliform bacteria as a function of UV dose was reported by Nelson (2000) for eight different treatment effluents, namely: conventional activated sludge (AS), AS utilising high purity oxygen, AS with chemical phosphorus removal, AS with biological nitrogen and phosphorus removal, AS with biological nitrogen removal, trickling filter, *facultative* pond, and; aerated pond effluents (Nelson 2000; Emerick *et al.* 1999).

These data, reported graphically, *see* Figure 4.1, were photographically enlarged and digitised. All resulting survivor curves (each with n = 5 to 8) showed an initial linear region of UV inactivation followed by tailing. Tailing manifested at a UV dose of between 50 and 150 mWs cm^{-2}.

4.3 Fitting of new model forms

Non-linear regression analyses (Snedecor and Cochran 1989; Ratkowsky 1990) of the new models to the data of Nelson (2000) were carried out using Microsoft Excel® 2000 Edition and the statistics package, R© Version 1.3.0, on an IBM® compatible desktop PC with an Intel Pentium® III microprocessor. In addition to the established criteria developed for fit of an adequate model (*see* Chapter 3.5) the residual sum-of-squares (RSS) is used. The residual sum-of-squares (in this instance) is defined by:

$$\sum (Predicted \log_{10} N/N_0 - Observed \log_{10} N/N_0)^2 \qquad (4.1)$$

Large values of the residual sum-of-squares indicate a poor fit of the model to data. This criterion is used as the primary measure of fit for both the modified exponentially damped polynomial (EDP_m) and Weibull model forms.

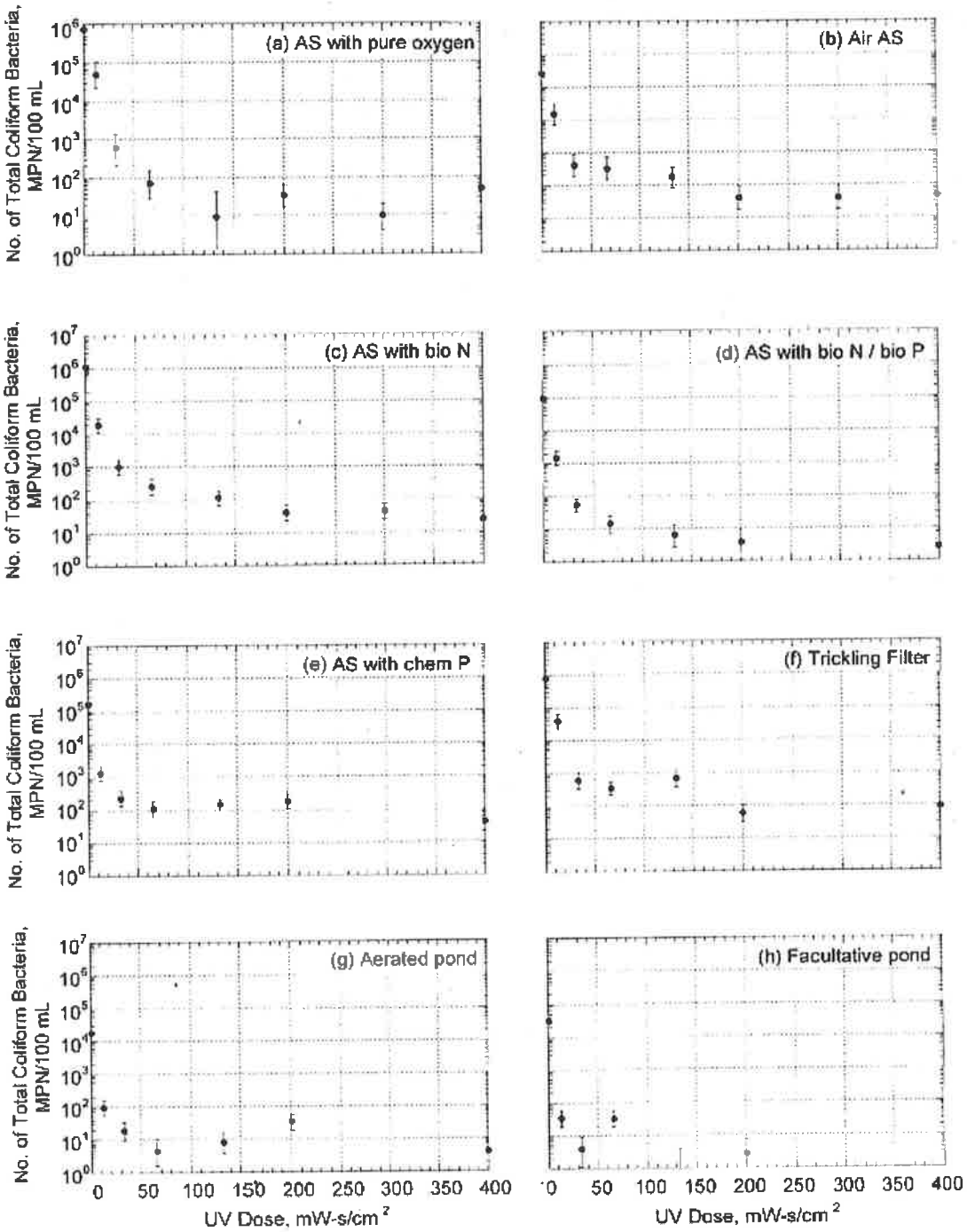

Figure 4.1 UV disinfection data of Nelson (2000) reported graphically as survival of total coliform bacteria as a function of UV dose for eight effluent treatments

(a) AS* utilizing pure oxygen	(e) AS with chemical P removal
(b) AS utilizing air	(f) Trickling filter
(c) AS with biological N removal	(g) Aerated pond
(d) AS with biological N and P removal	(h) Facultative pond

* AS denotes activated sludge.

4.4 Exponentially Damped Polynomial

An exponentially damped polynomial (EDP) form was successfully used by Daughtry *et al.* (1997) to model non log-linear thermal inactivation kinetics of bacterial cells based on the generalised form of Crowder and Tredger (1981) and Crowder (1983). The EDP model has also been used to analyse the melting kinetics of DNA (Kühne and Walter 1975a, b), suggesting it may be of a form suitable to modelling the denaturation of DNA which forms the basis for UV disinfection (Cano and Colome 1986; USEPA 1986).

When applied to UV disinfection, the EDP model takes the form:

$$\log_{10}\frac{N}{N_0} = -k[dose]\exp(-\lambda[dose]) \tag{4.2}$$

where the model parameters k (mWs^{-1} cm^2) and λ (mWs^{-1} cm^2) = the initial disinfection rate coefficient, and damping coefficient, respectively. N_0 and N =, respectively, the viable coliform counts (MPN per 100 millilitres) before and after UV treatment.

A drawback with the EDP model of Equation (4.2), however, is that $N \rightarrow N_0$ as the UV dose [*dose*] increases (i.e. the predicted log-reduction of coliforms will approach zero).

4.4.1 Modified Exponentially Damped Polynomial

To obviate this problem, a new modified form (EDP_m) was synthesised (*pers. comm.* B J Daughtry) such that:

$$\log_{10}\frac{N}{N_0} = -\delta_1 k[dose]\exp(-\lambda[dose]) - \delta_2(k'[dose]+c) \tag{4.3}$$

where: if $[dose] \leq [dose]_B$ then $\delta_1 = 1$; $\delta_2 = 0$

if $[dose] > [dose]_B$ then $\delta_1 = 0$; $\delta_2 = 1$

This modified model (EDP_m) of Equation 4.3 has three coefficients, namely: the rate coefficient for UV disinfection (k) and the damping coefficient (λ) as defined for Equation (4.2), and the *breakpoint dose*, $[dose]_B$ ($mWs\ cm^{-2}$).

Practically, the term k' (mWs^{-1} cm^2) is the disinfection rate coefficient in the tailing region of the survival curve (once the breakpoint dose has been exceeded), and the term $-c$ is the predicted log-reduction at the breakpoint dose. These terms may be respectively defined by Equations (4.4) and (4.5) as follows:

$$k' = k.\exp(-\lambda[dose]_B)(1-\lambda[dose]_B) \quad (4.4)$$

$$c = k.\exp(-\lambda[dose]_B).[dose]_B \quad (4.5)$$

The breakpoint dose is the UV dose at which the survivor curve response changes from an exponentially damped polynomial (high rate of disinfection) to log-linear (low rate of disinfection), and indicates the onset of tailing.

This modified exponentially damped polynomial form (EDP_m) is a piecewise-continuous function with respect to UV dose [*dose*], and is advantageous over the unmodified form in that it will simulate tailing in UV survivor data beyond the initial period of disinfection. Consequently, the EDP_m model is of a form which might be more reliably extrapolated beyond the experimental UV dose range – in contrast to the unmodified form. This feature of the EDP_m form may prove beneficial in scale-up of UV disinfection reactors.

4.4.2 Results and analyses

Table 4.1 summarises and compares the fits of both EDP and EDP_m models to the data of Nelson (2000) for each of the eight different treatments. For each data set (treatments a through h), it can be seen from Table 4.1 that values of the disinfection rate coefficient (k) and of the damping coefficient (λ) range about one order of magnitude greater for the EDP_m form when compared with the EDP. The values of the residual sum-of-squares are significantly lower for the EDP_m form – indicating a statistically better fit of the EDP_m to these disinfection data.

A comparison of predictions for survival from both the EDP and EDP_m model forms for activated sludge treatment with biological nitrogen removal is given in Figure 4.2. The EDP form is seen to predict a discrete optimum in disinfection efficacy with respect to UV dose. However, as the dose exceeds that at which maximum disinfection is observed (~ 200 mWs cm^{-2}); the predicted reduction in viable coliforms is seen to decrease for

increasing values of dose. Intuitively, this response would not be expected because effects on cellular material are said to be cumulative. This is provided however the irradiation dose to induce irreparable damage is exceeded (Harm 1980).

A limiting case would expect no further increase in the level of disinfection once the optimum is reached (i.e. a limiting value of zero for the disinfection rate coefficient in the tailing region, k'). The observed response of the EDP model would present difficulty in affording any physiological interpretation (*see* Section 3.5) to these UV disinfection data, and may preclude progression from an empirical model towards a mechanistic basis for UV disinfection.

The modified exponentially damped polynomial form (EDP_m) however exhibits a good fit to the disinfection data, and better represents tailing than the unmodified form. It could be argued that the EDP_m model might be reliably extrapolated beyond the observed maximum UV dose of 400 mWs cm^{-2} with some caution, owing to the log-linear approximation of disinfection kinetics in the tailing region.

Table 4.1 EDP and EDP_m model parameters for eight data sets and treatments of Nelson (2000)

Treatment	n	Model						
		EDP			EDP_m			
		k	λ	RSS**	k	λ	$[dose]_B$	RSS**
		($mWs^{-1}cm^2$)	($mWs^{-1}cm^2$)		($mWs^{-1}cm^2$)	($mWs^{-1}cm^2$)	(mWs cm^{-2})	
(a) AS* with pure O_2	8	0.0777	5.379×10^{-3}	2.38	0.1117	8.511×10^{-3}	121.02	0.43
(b) Air AS	8	0.0554	4.836×10^{-3}	2.79	0.1383	1.690×10^{-2}	56.62	0.28
(c) AS with bio N	8	0.0653	4.789×10^{-3}	3.96	0.1602	1.662×10^{-2}	57.27	0.12
(d) AS with bio N/bio P	7	0.0709	4.970×10^{-3}	4.41	0.1736	1.668×10^{-2}	58.00	0.07
(e) AS with chem P	7	0.0587	5.508×10^{-3}	6.58	0.2687	3.474×10^{-2}	28.35	0.15
(f) Trickling filter	7	0.0581	4.836×10^{-3}	4.11	0.1489	1.706×10^{-2}	56.66	0.58
(g) Aerated pond	7	0.0681	6.078×10^{-3}	7.90	0.2775	3.284×10^{-2}	30.17	0.62
(h) Facultative pond	5	0.1268	9.790×10^{-3}	5.16	0.4116	4.505×10^{-2}	21.81	0.48

* AS denotes activated sludge.
** RSS denotes residual sum-of-squares.

Figure 4.3 shows the predicted *vs.* observed value of reduction in viable coliforms (as $\log_{10} N/N_0$) for the EDP_m model applied for all eight treatment conditions of Nelson (2000).

It can be seen from Figure 4.3 that, importantly, the data are evenly and randomly distributed over the entire range of data – this implies that the EDP_m model is well parameterised (Ratkowsky 1990). It is clear from Figures 4.2 and 4.3 that the UV disinfection data of Nelson (2000) do not obey first-order chemical reaction kinetics. Therefore non-linear modelling of these UV disinfection data is justified and necessary.

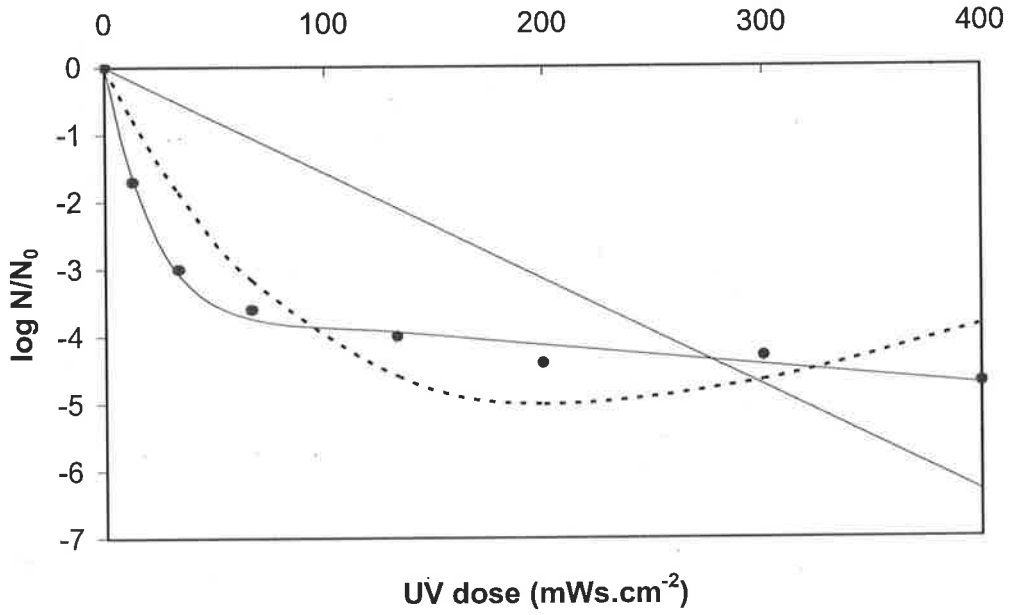

Figure 4.2 Comparison of EDP (----) and EDP_m (—) fits to independent, published data of Nelson (2000), together with predictions of the classical log-linear model (for treatment of activated sludge with biological nitrogen removal)

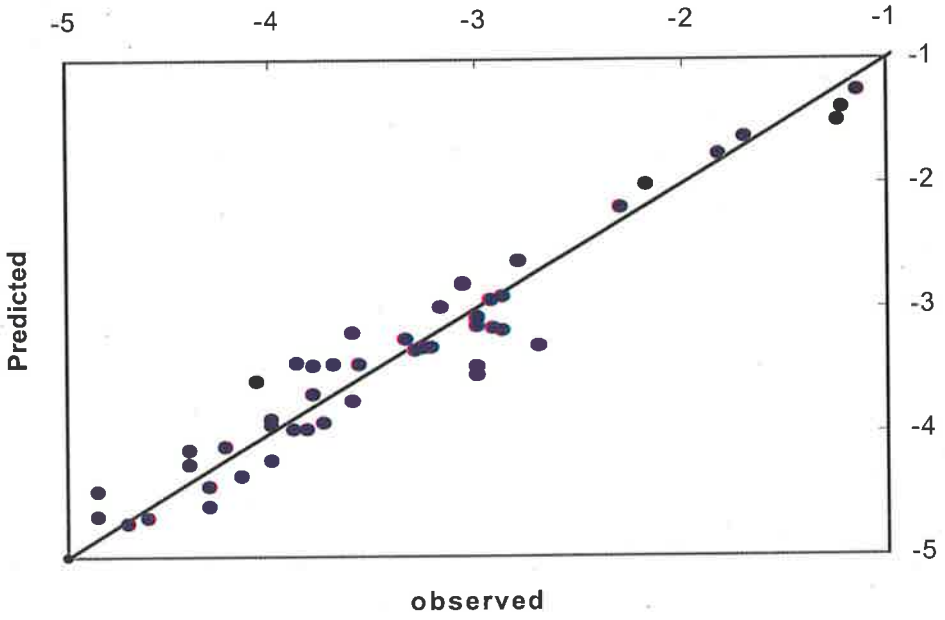

Figure 4.3 Predicted *vs.* observed value of the log-reduction in viable coliforms (as $\log_{10} N/N_0$) from the EDP_m model fitted to the independent, published data of Nelson (2000) for treatment of a range of effluents (a to h)

Similarly, Figure 4.4 shows the predicted *vs.* observed value of reduction in viable coliforms (as $\log_{10} N/N_0$) for the EDP model (unmodified) applied to the data of Nelson (2000).

The data appear randomly distributed. However, the EDP model is seen to generally under-predict the extent of disinfection when the observed level of disinfection is less than two $\log_{10}$ reductions. It should also be noted that the predicted and observed values of disinfection are more poorly correlated for the EDP model (Figure 4.4) than those for the modified (EDP_m) form (Figure 4.3), with greater spread in data about the line of equivalence. This is in agreement with comparison of the residual sum-of-squares for the two EDP models (Table 4.1), and underscores the better fit of the EDP_m model to the disinfection data.

A projected axis intercept, α, can be defined using the disinfection rate coefficient for the tailing region, k', and the breakpoint dose, $[dose]_B$:

$$\alpha = k' [dose]_B - c \qquad (4.6)$$

The projected axis intercept can be used as a measure of deviation from log-linear disinfection kinetics – provided the disinfection rate coefficient in the tailing region is non-negative (Block 1983).

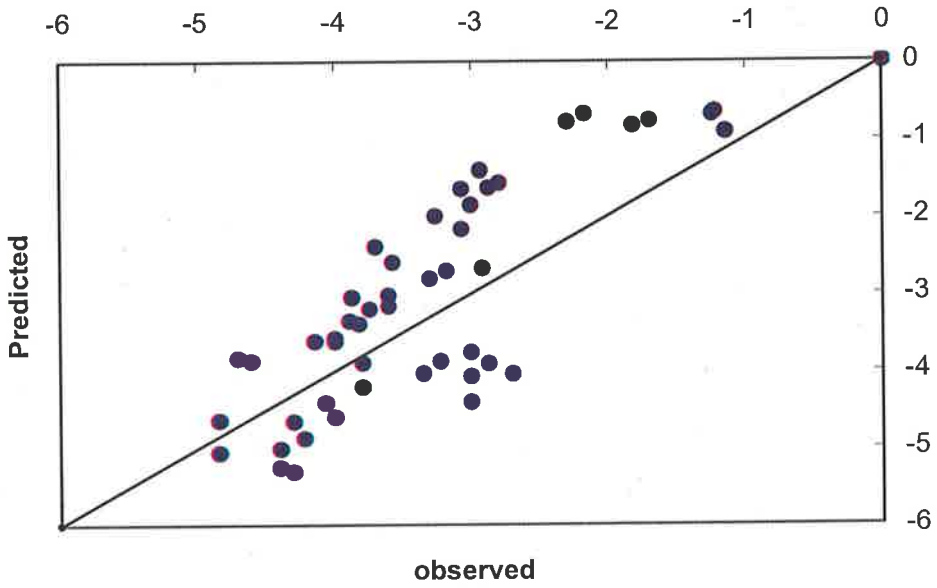

Figure 4.4 Predicted *vs.* observed value of the log-reduction in viable coliforms (as $\log_{10} N/N_0$) from the EDP model fitted to the independent, published data of Nelson (2000) for treatment of a range of effluents (a to h)

For a given breakpoint dose (and predicted log-reduction at this dose), a decrease in value of the projected axis intercept (α) represents a further deviation from log-linear disinfection kinetics, or, an increased degree of tailing. Where the projected axis intercept is zero, classical log-linear kinetics (i.e. first-order) are observed.

Table 4.2 summarises predicted parameter values (α, k' and $-c$) associated with tailing (Equation 4.6) of the UV disinfection data. For activated sludge utilising pure oxygen (AS with pure O_2), the disinfection rate coefficient for the tailing region (k') is seen to be negative – that is, the number of survivors is predicted to increase with increasing UV dose after the breakpoint dose is exceeded.

Examination of the graphical UV disinfection data of Nelson (2000) for this case however, suggests the response of the EDP_m model is not unexpected, with the observed number of

surviving coliforms increasing from approximately 10 to 50 MPN per 100 millilitres for a, respective, increase in UV dose from 300 to 400 mWs cm^{-2} (Figure 4.1).

Table 4.2 EDP_m tailing properties for the eight treatments of Nelson (2000)

Treatment	k' (mWs^{-1} cm^2)	$-c$ (as $\log_{10}$ N/N_0)	α (as $\log_{10}$ N/N_0)	k/k' (dimensionless)
(a) AS* with pure O_2	-1.20×10^{-3}	-4.83	-4.97	-93.3
(b) Air AS	2.28×10^{-3}	-3.01	-2.88	60.6
(c) AS with bio N	2.97×10^{-3}	-3.54	-3.37	53.9
(d) AS with bio N/bio P	2.15×10^{-3}	-3.83	-3.70	80.9
(e) AS with chem P	1.53×10^{-3}	-2.85	-2.80	176.2
(f) Trickling filter	1.90×10^{-3}	-3.21	-3.10	78.5
(g) Aerated pond	9.63×10^{-4}	-3.11	-3.08	288.3
(h) Facultative pond	2.66×10^{-3}	-3.36	-3.30	154.9

* AS denotes activated sludge.

Comparison of the value of the initial disinfection rate coefficient (k) (Table 4.2) with that in the region of tailing (k') for each of the treatment conditions of Nelson (2000) shows that the initial rate of disinfection is between one and two orders of magnitude greater than that in the tailing region – with one exception of the case of activated sludge utilising pure oxygen. Figure 4.5 highlights the difference in the initial rate of disinfection predicted by the EDP_m model, to that predicted in the tail for disinfection of activated sludge effluent treated with biological nitrogen and phosphorous removal. The dashed lines represent the rates of disinfection observed initially and in the tail of the survivor data.

The initial rate of disinfection is seen to be high, with a 3-$\log_{10}$ reduction in viable numbers observed for a UV dose less than 50 mWs cm^{-2}. The predicted disinfection rate coefficient (k) representative of this initial region of rapid inactivation is 1.74×10^{-1} mWs^{-1} cm^2 (*see* Table 4.1 – treatment d), compared to a rate (k') of 2.15×10^{-3} mWs^{-1} cm^2 predicted in the tail – approximately eighty times smaller (*see* Table 4.2 – treatment d). Whilst Figure 4.5 shows some additional disinfection is predicted in the tail, the rate of disinfection is small by comparison.

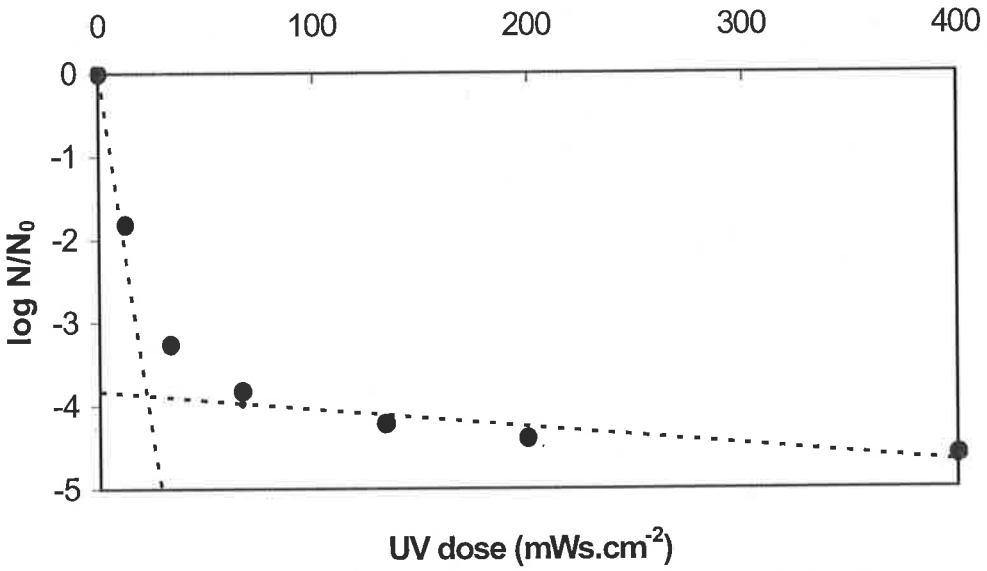

Figure 4.5 Comparison of the initial disinfection rate coefficient to that predicted for the tail by the EDP_m model fitted to the data of Nelson (2000) for treatment of activated sludge with biological nitrogen and phosphorous removal

A practical limiting case would likely be that in which the predicted disinfection rate coefficient in the tailing region is zero. This suggests use of a non-negative constraint might be required when modelling the rate of UV disinfection for data exhibiting tailing.

Analyses found the parameters of the EDP_m model not to display any meaningful correlations with measured wastewater characteristics for each of the eight treatments (*see* Table 4.1) of Nelson (2000). These characteristics include the: suspended solids (SS) concentration (mg L^{-1}), water transmission (%T at 254 nm), and; residual coliform concentration remaining after UV treatment (MPN per 100 millilitres). The breakpoint dose $[dose]_B$ however does appear to decrease with increasing suspended solids concentration as shown by Figure 4.6. This suggests that the onset of tailing will occur at lower values of UV dose when the suspended solids concentration is high, consistent with the findings of others (Taghipour 2004; Cantwell and Hofmann 2008).

Figure 4.6 also illustrates a spread in the breakpoint dose data for suspended solids concentrations less than 40 mg L^{-1}. It follows therefore that suspended solids concentration alone is not a good predictor of the onset of tailing, supporting the notion of others that particle size and association are more important (Cantwell and Hofmann 2008).

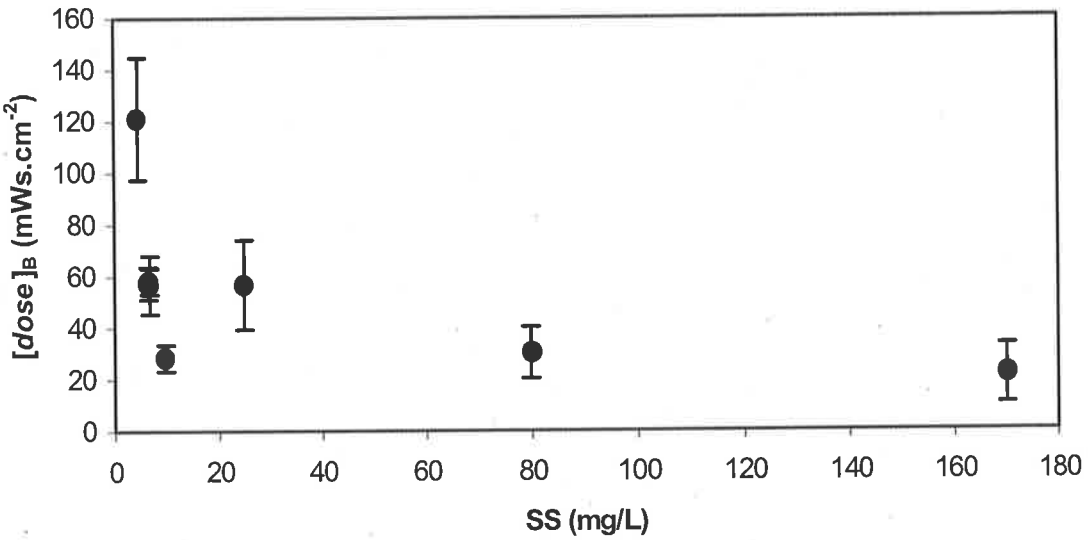

Figure 4.6 Breakpoint dose $[dose]_B$ as a function of suspended solids concentration for the EDP_m model fitted to the data of Nelson (2000). Error bars represent standard errors for each estimate of breakpoint dose

Figure 4.7 shows the derived parameters (k, λ and $[dose]_B$) for the EDP_m model for each of the eight treatments of Nelson (2000). The data sets are labelled (a) through (h) as per Tables 4.1 and 4.2. Lower values of the disinfection rate coefficient (k) and damping coefficient (λ) were obtained for effluents treated, in part, utilising activated sludge (treatments a – d). One exception being the case of activated sludge treatment utilising chemical phosphorous removal (treatment e), where the disinfection rate coefficient and damping coefficient were both higher than values obtained for remaining activated sludge treatments. The predicted values of breakpoint dose ($[dose]_B$) for disinfection of the aerated and facultative pond effluents (treatments g and h) in particular are low by comparison to predictions for the remaining treatments employed by Nelson (2000).

The EDP_m model parameters were found to be highly correlated for the fits of the model to the UV disinfection data of Nelson. Figure 4.8 presents, respectively: (a) disinfection rate coefficient (k) *vs.* damping coefficient (λ), (b) disinfection rate coefficient (k) *vs.* breakpoint dose $[dose]_B$, and; (c) damping coefficient (λ) *vs.* breakpoint dose $[dose]_B$. The disinfection rate coefficient (k) and the damping coefficient (λ) were found to be linearly dependent (Figure 4.8a), with an increase in the damping coefficient leading to a corresponding increase in the disinfection rate coefficient.

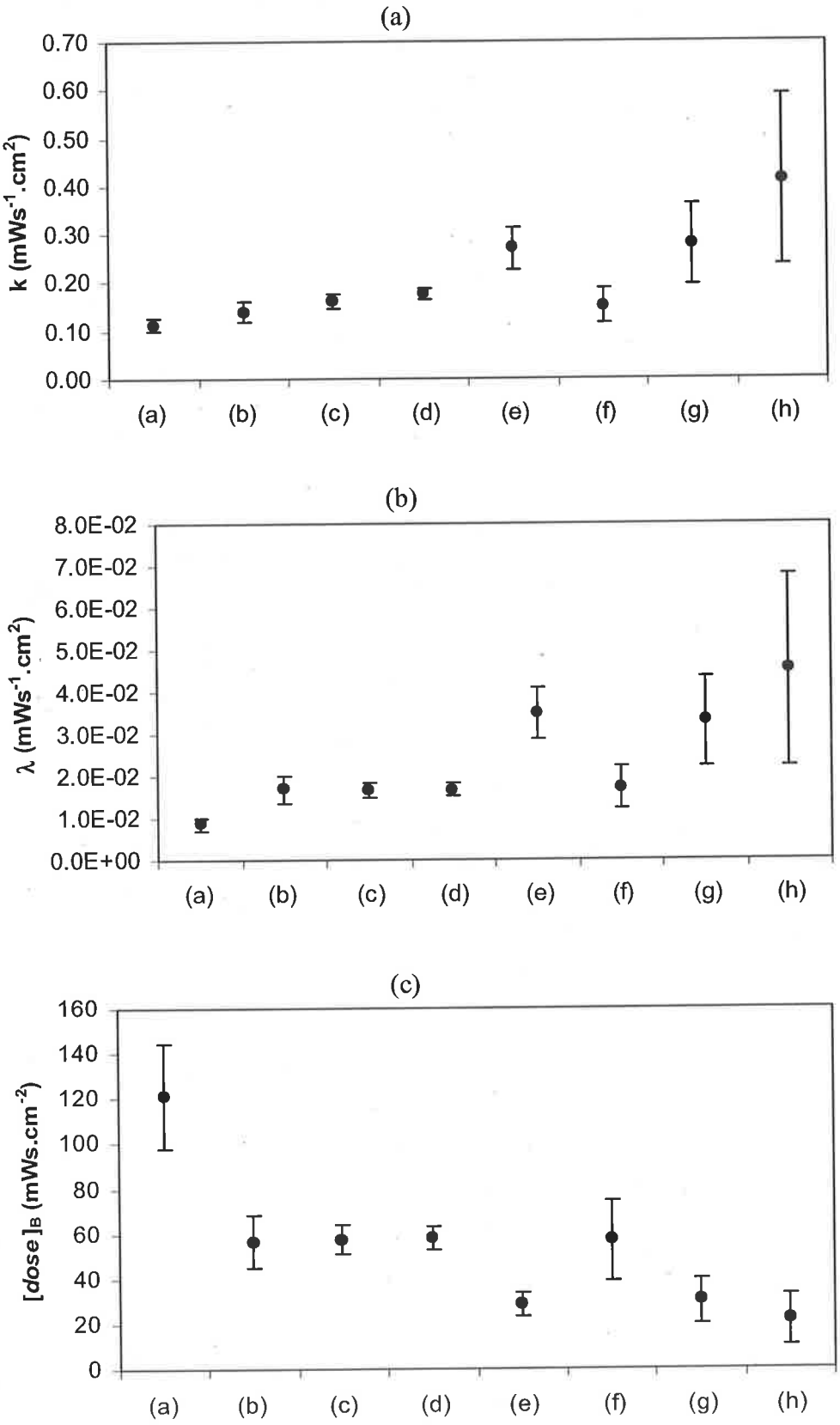

Figure 4.7 EDP_m model parameters for each of the eight wastewater effluents treated by Nelson (2000): (a) disinfection rate coefficient (k), (b) damping coefficient (λ), and; (c) breakpoint dose $[dose]_B$. Error bars show standard error for each parameter estimate

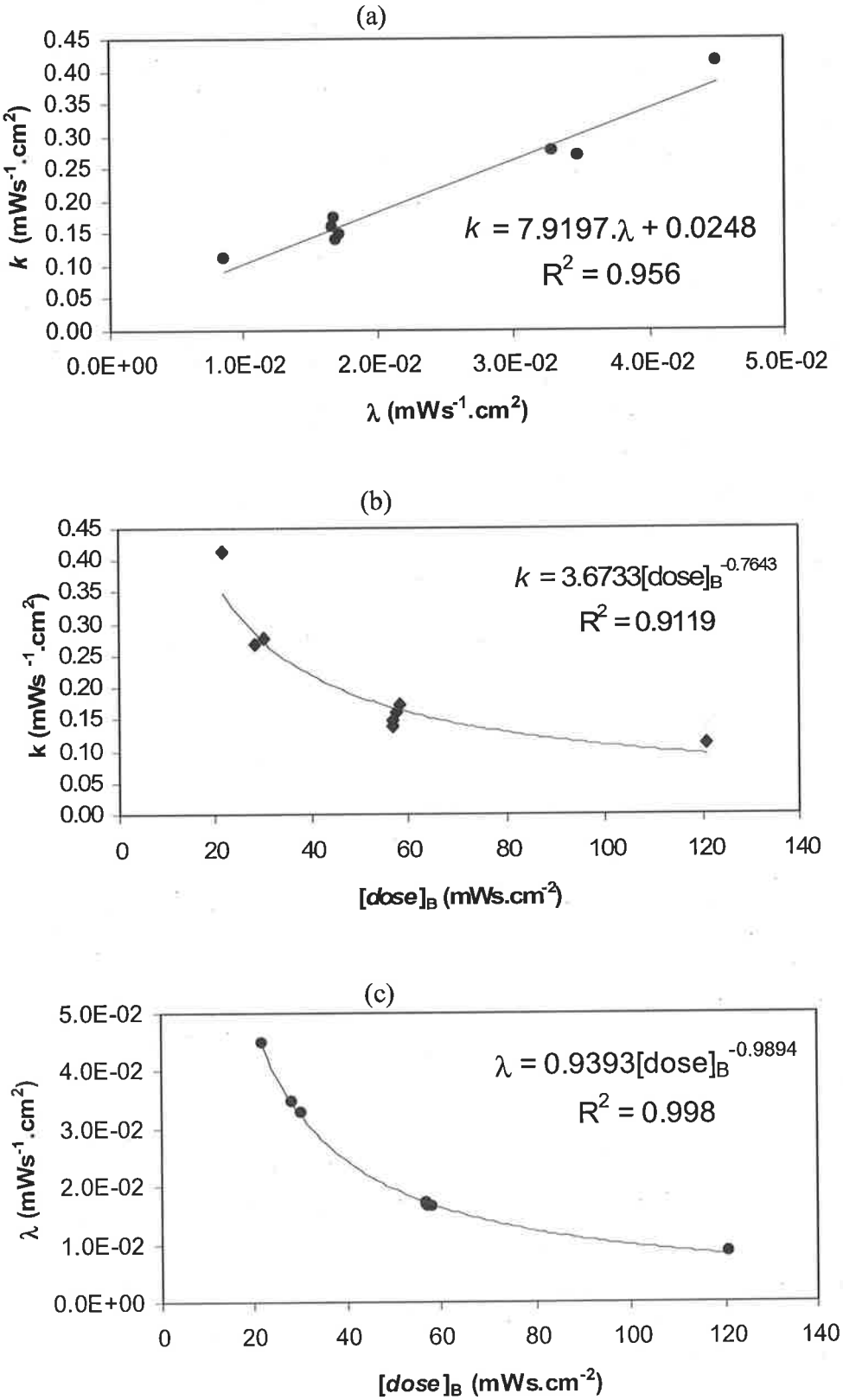

Figure 4.8 Observed correlations between EDP_m model parameters fitted to the UV disinfection data of Nelson (2000): (a) k *vs.* λ, (b) k *vs.* $[dose]_B$, and; (c) λ vs $[dose]_B$

It follows that both the disinfection rate coefficient and the damping coefficient will exhibit similar responses with respect to breakpoint dose because they are linearly dependent. As highlighted in Figures 4.8b and 4.8c respectively, both the disinfection rate coefficient (k) and the damping coefficient (λ) were found to decrease with respect to breakpoint dose $[dose]_B$ – and were well represented by a power law relationship. This was not unexpected as both k and λ are measures of the rapid disinfection observed at low UV dose. Higher values of both the disinfection rate coefficient and the damping coefficient correspond to a greater rate of disinfection initially observed – meaning the onset of tailing occurs at a lower breakpoint dose.

In summary, Figure 4.8 shows that for an increase in the breakpoint dose, the initial rate of disinfection and the level of damping will decrease. Practically this leads to a reduction in the extent of tailing predicted by the EDP_m model. Similarly, if one of the EDP_m parameters is known, then the remaining model parameters are implicitly defined. This will likely have beneficial implications when using the EDP_m model to predict tailing observed in UV disinfection data, and may provide a basis for comparison between independently measured disinfection data. (These issues are further addressed in Chapter 6).

4.4.3 Summary

Findings show that the EDP_m model appears to be an appropriate model form to adequately simulate UV disinfection data exhibiting significant tailing for a range of treatment conditions. By imposing a constraint (non-negative) on the rate of disinfection in the tailing region (k'), the EDP_m model is of a form that can be optimised for process treatment.

Further analysis of independent UV disinfection data may show this EDP_m model form can be generalised. Physiological interpretation of model coefficients, together with mechanistic insights, could follow.

4.5 Weibull model

Weibull model forms are based on the Weibull probability distribution (Ratkowsky 1990; D'Agostino and Stephens 1986; Mafart *et al.* 2002). These have been used to model the non log-linear thermal inactivation kinetics of both vegetative bacteria and spores (van Boekel 2002; Mafart, Couvert and Leguérinel 2001; Mafart *et al.* 2002; Peleg and Cole 1998; Fernández *et al.* 2002). The form has been found to better predict thermal inactivation kinetics of data exhibiting tailing than the traditional first-order chemical reaction equation (van Boekel 2002).

Also, this form has been used to model deviations from first-order kinetics in inactivation by pulsed electric fields (Lebovka and Vorobiev 2004; Álvarez *et al.* 2003), and in modelling dose-response behaviour in aquatic toxicity testing (Christensen 1984). Other applications include use in reliability engineering to measure "time-to-failure" of electrical and mechanical systems (van Boekel 2002).

When applied to UV disinfection kinetics, a possible form for the Weibull model is:

$$\log_{10}\frac{N}{N_0} = -\beta_0\left[1-\exp\left(-\beta_1[dose]\right)\right] \tag{4.7}$$

where N_0 and N = respectively, the viable coliform counts (MPN per 100 millilitres) before and after UV treatment.

Equation (4.7) shows the model consists of two parameters: namely the dimensionless scale parameter (β_0) and the shape parameter (β_1). Practically, the scale parameter (as defined, $\beta_0 > 0$) is a measure of the maximum achievable level of disinfection, and quantifies the log-reduction observed in the tailing region. The shape parameter (β_1) takes positive values, with a larger value (for fixed β_0) giving a higher initial rate of disinfection, with the onset of tailing occurring at a reduced UV dose.

The rate of disinfection predicted by the Weibull model can be determined through differentiation of Equation (4.7) with respect to UV dose. Evaluation of the derivative for an initial UV dose of zero defines the initial rate of disinfection predicted by the model as

$\beta_0.\beta_1$. Equally, the predicted rate of disinfection may also be determined as $\beta_0.\beta_1 \exp(-\beta_1 [dose])$ for non-zero values of UV dose.

A potential drawback with the Weibull model however is that the scale and shape parameters are generally not independent (Mafart *et al.* 2002; van Boekel 2002), causing potential instability of parameter estimates (Mafart *et al.* 2002).

Although Equation (4.7) is empirical, it is nevertheless a statistical model derived from a distribution of inactivation times (or UV doses in this case), and a link can be made with physiological effects (van Boekel 2002). This view contrasts however with that of Mafart *et al.* (2002) who state that parameters of empirical models generally have no easily interpretable physical or biological significance.

4.5.1 Results and analyses

Table 4.3 summarises the fit of the Weibull model to the UV disinfection data of Nelson (2000) for each of the eight different treatments. The scale parameter, β_0, can be seen to vary from 3.14 for activated sludge treatment with chemical phosphorous removal (treatment e), to a maximum of 4.56 for disinfection following activated sludge treatment utilising pure oxygen (treatment a). This corresponds to between 3 and 4.5-$\log_{10}$ reductions predicted as the limiting extent of disinfection in the tailing region across all data sets (or between 99.9 to 99.997% inactivation). The shape parameter, β_1, ranges from 3.08×10^{-2} to 1.37×10^{-1} mWs^{-1} cm^2 for activated sludge utilising pure oxygen (treatment a) and for facultative pond treatments (treatment h) respectively.

Relatively large values for the shape parameters are noted for both the aerated and facultative pond treatments (9.12×10^{-2} and 1.37×10^{-1} mWs^{-1} cm^2 respectively), when compared with the remaining treatments employed by Nelson (2000). This might be attributable to the high concentrations of suspended solids present in each case, with suspended solids concentrations of 79.8 and 170 mg L^{-1} reported by Nelson (2000) for the aerated and facultative pond treatments respectively. However, the scale parameters of 3.31 and 3.63 for each of these respective treatments are comparable to those observed for the remaining treatments employed by Nelson (2000).

Table 4.3 shows the residual sum-of-squares to vary from 0.14 for activated sludge treatment utilising both biological nitrogen and phosphorous removal (treatment d), to a maximum of 0.82 observed for disinfection following treatment via trickling filter (treatment f). The residual sums-of-squares for each set of the data are of the same order of magnitude, suggesting the Weibull model gives a comparable fit to the disinfection data regardless of the treatment employed.

Table 4.3 Weibull model parameters for each of the eight treatments of Nelson (2000)

Treatment	n	β_0 (dimensionless)	β_1 ($mWs^{-1}\ cm^{-2}$)	RSS**
(a) AS* with pure O_2	8	4.56	3.08×10^{-2}	0.56
(b) Air AS	8	3.62	3.50×10^{-2}	0.43
(c) AS with bio N	8	4.33	3.40×10^{-2}	0.35
(d) AS with bio N/bio P	7	4.37	4.00×10^{-2}	0.14
(e) AS with chem P	7	3.14	9.10×10^{-2}	0.30
(f) Trickling filter	7	3.66	4.16×10^{-2}	0.82
(g) Aerated pond	7	3.31	9.12×10^{-2}	0.64
(h) Facultative pond	5	3.63	1.37×10^{-1}	0.62

* AS denotes activated sludge.
** RSS denotes residual sum-of-squares.

The standard errors of the scale and shape parameters have not been reported in Table 4.3. However, the standard errors for estimates of the scale parameter (β_0) range from 2.75×10^{-1} to 9.40×10^{-2}. For estimates of the shape parameter, standard errors range from 6.36×10^{-2} to 3.68×10^{-3} $mWs^{-1}\ cm^2$.

Figure 4.9 illustrates the efficacy of disinfection predicted by the Weibull model fitted to the data of Nelson (2000) for disinfection following activated sludge treatment utilising pure oxygen (AS with pure O_2). The observed disinfection kinetics are clearly non-linear. The Weibull model adequately predicts the tailing of the UV disinfection data, with no further disinfection predicted at UV doses in excess of approximately 150 mWs cm^{-2}. This is equivalent to a negligible rate of disinfection in the tailing region. However, on closer inspection, the observed data exhibit some evidence of an apparent negative rate of disinfection in the tailing region, with the number of survivors observed for a dose of 400 mWs cm^{-2} being greater than that observed for respective doses of 130, 200, and 300 mWs cm^{-2} (if only slightly). It should also be noted that the value of the scale parameter obtained for this data set (β_0 = 4.56, or 4.56-$\log_{10}$ reductions) is representative of the

predicted limit of disinfection observed in the tailing region shown by Figure 4.9. Data representing the tail exhibit some variation about this predicted mean level of disinfection, and span a range covering approximately 0.5-$\log_{10}$ reductions.

Figure 4.10 presents the predition of the Weibull model fitted to the data of Nelson (2000) for UV disinfection following activated sludge treatment with biological nitrogen removal (treatment c). The Weibull model is seen to predict the observed tailing; however it is restricted by the fact that it is of a form whereby the limiting rate of disinfection predicted in the tailing region is zero. Clearly, these UV disinfection data shown in Figure 4.10 exhibit an increasing level of disinfection as the UV dose is increased from 70 to 400 mWs cm^{-2} – data that represents the tail. In comparison, the scale parameter obtained for this data set (β_0 = 4.33, or 4.33-$\log_{10}$ reductions), or the limiting predicted extent of disinfection, under-predicts the level of disinfection delivered at a UV dose of 400 mWs cm^{-2}.

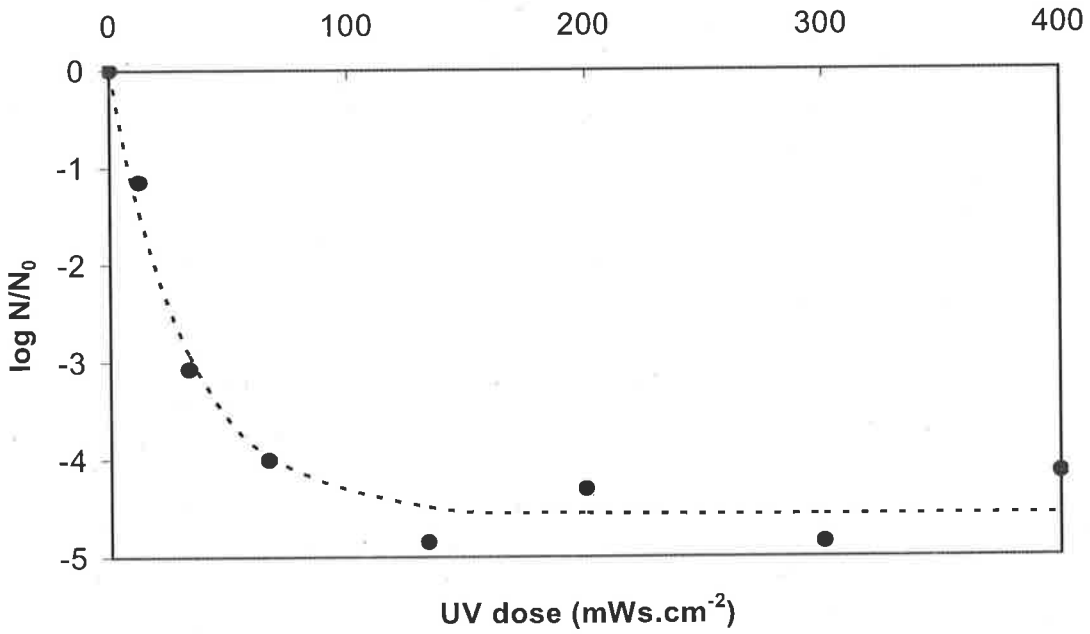

Figure 4.9 Fit of the Weibull model to the data of Nelson (2000) for the treatment of activated sludge utilising pure oxygen (AS with pure O_2)

In this instance (Figure 4.10), where there appears to be some continuing level of disinfection in the tailing region, the scale parameter is representative of the "average" level of disinfection observed in the tail of these data, and does not represent a limiting case. Here, the scale parameter is likely to over-predict the level of disinfection at the onset

of tailing, and under-predict the level of disinfection as the UV dose is increased. This could result in excessive doses being delivered in some instances, representing an increase in operating costs.

In fact, for disinfection following activated sludge treatment with biological nitrogen removal (treatment c), the observed level of disinfection is 3.60-$\log_{10}$ reductions at the onset of tailing (UV dose of 70 mWs cm^{-2}), and 4.70-$\log_{10}$ reductions at a UV dose of 400 mWs cm^{-2}.

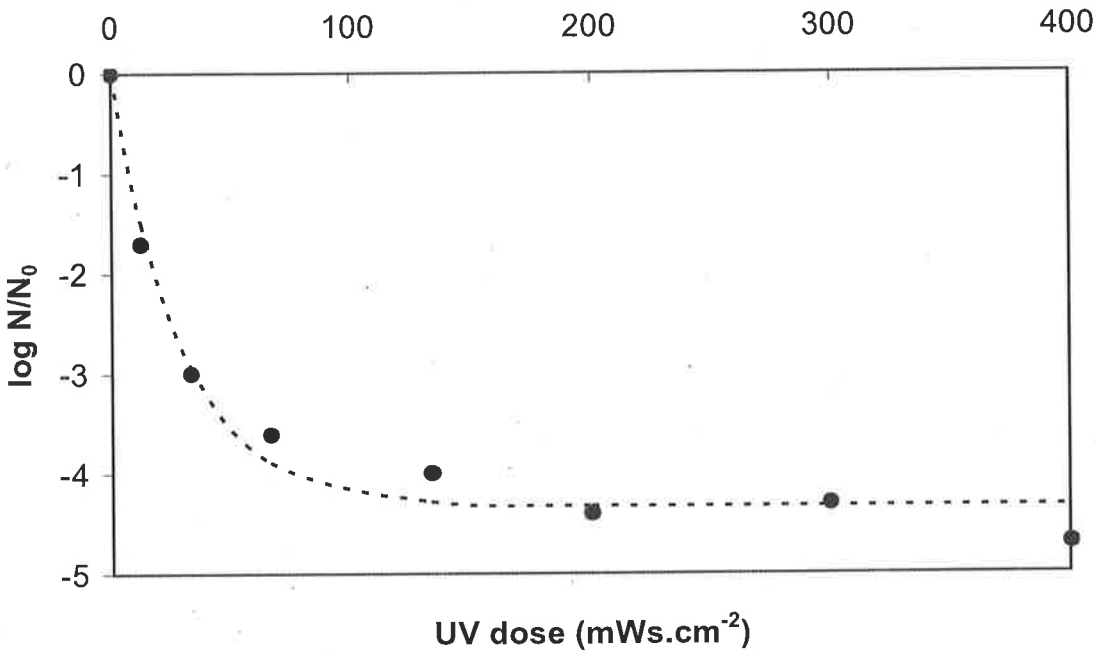

Figure 4.10 Fit of the Weibull model to the data of Nelson (2000) for the treatment of activated sludge with biological nitrogen removal (AS with pure O_2)

Figure 4.11 shows the predicted *vs.* observed values of reduction in viable coliforms ($\log_{10}$ N/N_0) for the Weibull model applied to the eight treatment conditions of Nelson (2000). Deviations in the predictions of the Weibull model from these UV disinfection data become more apparent as the level of disinfection exceeds 3-$\log_{10}$ reductions. Nevertheless, and importantly, it can be seen that the data are evenly and randomly distributed over the entire range of observed reductions, indicating that the model is well parameterised (Ratkowsky 1990). This is further evidence to suggest that non-linear models, and in particular the Weibull model form, are suitable to account for tailing phenomena often observed in practical UV disinfection kinetics.

Table 4.4 shows the rates of disinfection predicted by the Weibull model when fitted to the UV disinfection data of Nelson (2000), for UV doses of 0 and 200 mWs cm^{-2} respectively. Evaluation of the rate of disinfection at UV dose = zero gives a measure of the initial rate of disinfection, which is relatively high compared with those rates predicted for data describing the tail. Evaluation of the rate of disinfection at a UV dose of 200 mWs cm^{-2} is intended to give a measure of the rate of disinfection observed in the tail of the UV disinfection data.

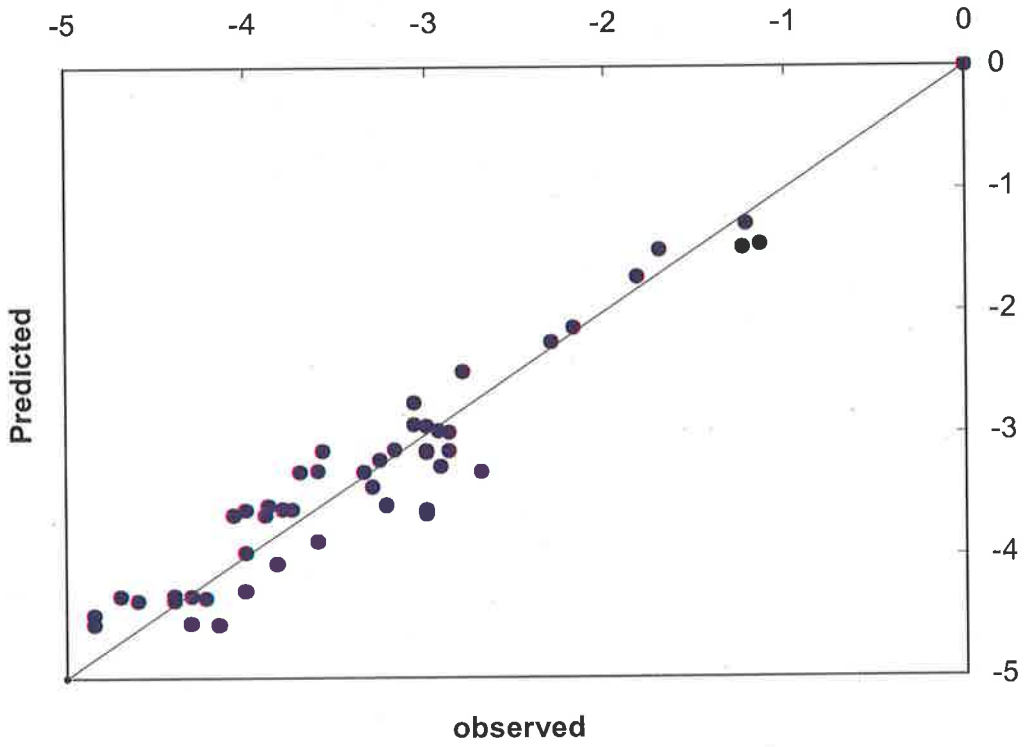

Figure 4.11 Predicted *vs.* observed value of the log-reduction in viable coliforms (as $\log_{10} N/N_0$) for the Weibull model fitted to the data of Nelson (2000)

Close inspection of Figure 4.1 shows clearly that a UV dose of 200 mWs cm^{-2} is representative of a mid-range UV dose describing the region of tailing for all of the eight treatment options employed by Nelson (2000).

The initial rates of disinfection (at UV dose = zero) predicted by the Weibull model when fitted to the UV disinfection data of Nelson are seen to vary between 1.27×10^{-1} mWs^{-1} cm^2 for activated sludge treatment fed by air (treatment b), and 4.97×10^{-1} mWs^{-1} cm^2 for facultative pond treatment (treatment h), as shown by Table 4.4. The initial rates of disinfection are seen to be of the same order of magnitude for all eight treatments.

Table 4.4 also shows the predicted rates of disinfection at a UV dose of 200 mWs cm^{-2} to vary between 2.98×10^{-4} and 6.22×10^{-13} mWs^{-1} cm^2 for activated sludge supplemented with oxygen (treatment a), and; disinfection of facultative pond effluents (treatment h) respectively.

Table 4.4 Rates of disinfection predicted by the Weibull model fitted to the data of Nelson (2000) for each of eight treatments

Treatment	rate of disinfection (mWs^{-1} cm^2)		Initial/Tail
	Initial (dose = 0 mWs cm^{-2})	Tail (dose = 200 mWs cm^{-2})	
(a) AS* with pure O_2	1.40×10^{-1}	2.98×10^{-4}	4.72×10^{2}
(b) Air AS	1.27×10^{-1}	1.15×10^{-4}	1.10×10^{3}
(c) AS with bio N	1.47×10^{-1}	1.63×10^{-4}	9.03×10^{2}
(d) AS with bio N/bio P	1.75×10^{-1}	5.82×10^{-5}	3.00×10^{3}
(e) AS with chem P	2.86×10^{-1}	3.54×10^{-9}	8.07×10^{7}
(f) Trickling filter	1.52×10^{-1}	3.75×10^{-5}	4.06×10^{3}
(g) Aerated pond	3.02×10^{-1}	3.62×10^{-9}	8.35×10^{7}
(h) Facultative pond	4.97×10^{-1}	6.22×10^{-13}	7.98×10^{11}

* AS denotes activated sludge.

The variation in the rate of disinfection in the tailing region spans nine orders of magnitude across the eight treatment options, and suggests the fit of the Weibull model to disinfection data is more sensitive to data comprising the tail than to that governing the initial period of disinfection. With the predicted rates of disinfection in the tail negligible (compared with initial rates), this further highlights the nature of the Weibull model in that it approaches a limiting level of disinfection in the tail (given as scaling parameter β_0), where the rate of disinfection is effectively zero. The ratio of the initial rate of disinfection to that observed in the tail is seen from Table 4.4 to vary between 400 and 7.98×10^{11}, highlighting further the negligible rate of disinfection predicted in the tail, and the inability of the model to account for continued disinfection over this region.

Figure 4.12 displays each of the derived Weibull model parameters (β_0 and β_1) and their respective standard errors, as shown by error bars, for fits of the model to disinfection data for each of the treatments of Nelson (2000). The data sets are labelled (a) through (h) as per Tables 4.3 and 4.4. Figure 4.12b shows values of the shape parameter (β_1) for activated sludge treatments (treatments a. through e. inclusive) to be relatively low, in the most part,

when compared with remaining treatments. The notable exception the case of activated sludge treatment utilising chemical phosphorus removal (treatment e). Figure 4.12a shows the distribution of predicted values for the scale parameter (β_0) for each of the treatments. The values do not appear to display bias towards a particular type of treatment, contrary to prediction of lower values for the shape parameter in the case of activated sludge treatments (treatments a – d).

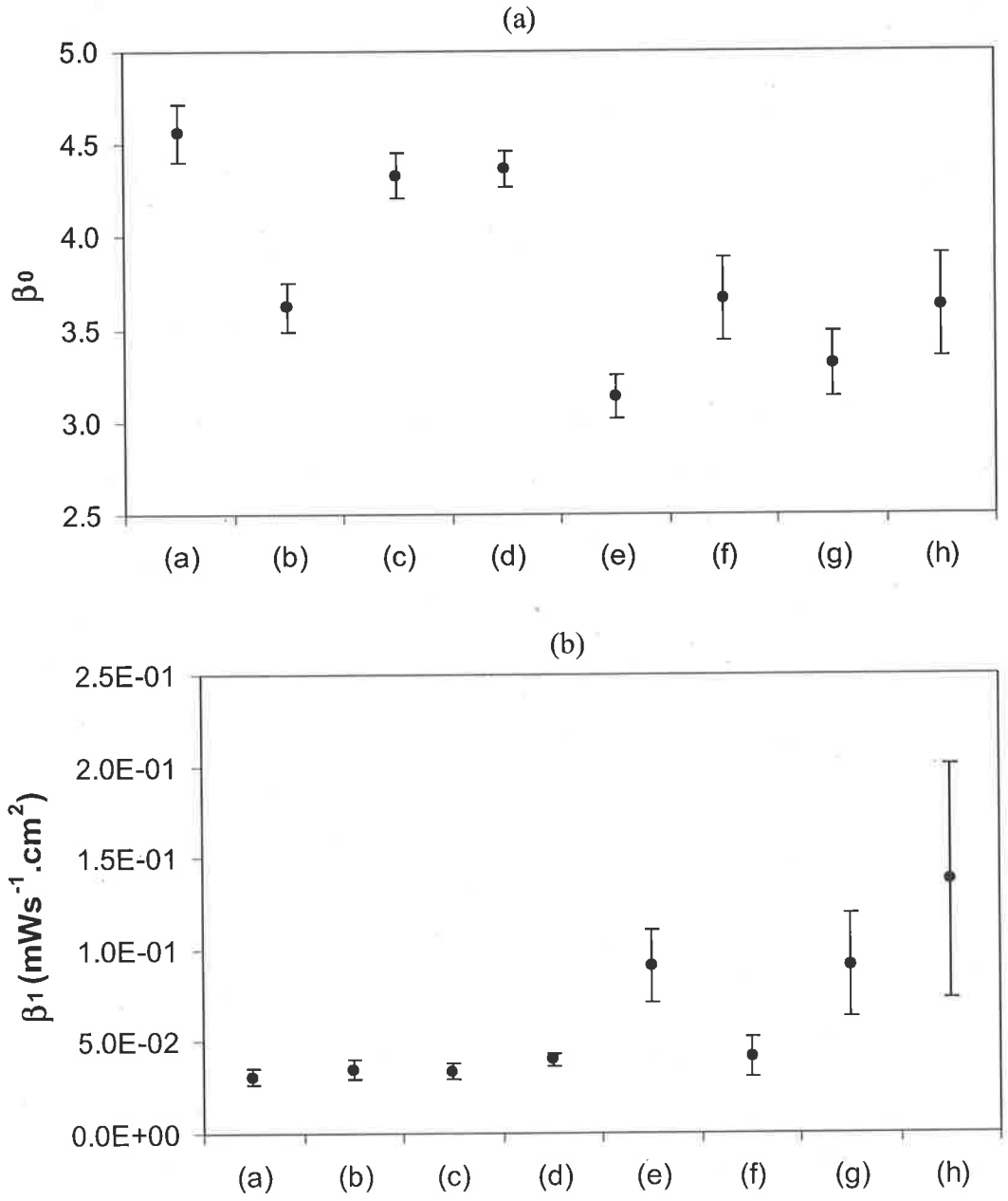

Figure 4.12 The Weibull model parameters for each of the wastewater effluents treated by Nelson (2000), respectively: (a) scale parameter (β_0), and; (b) shape parameter (β_1). Error bars denote standard error for each parameter estimate

The standard errors associated with the shape parameter (β_1) are seen in Figure 4.12 to be small for the majority of activated sludge treatments (excluding the case coupled with chemical phosphorous removal – e), suggesting some stability of model predictions for these disinfection data. The same cannot be said for aerated and facultative pond treatments (treatments g and h respectively). The predictions of scale parameter (β_0) are generally relatively high for the activated sludge treatments (treatments a, c and d particularly), compared with the remaining treatments of Nelson (2000).

Figure 4.13 presents the Weibull scale parameter (β_0) plotted against measured wastewater characteristics: (a) suspended solids concentration, (b) percent transmission, and; (c) residual coliform concentration, for each of the treatment options of Nelson (2000). Error bars show the standard error obtained for each estimate of β_0. Figures 4.13a and 4.13b respectively show pronounced variation in the scale parameter (β_0) to be observed at low suspended solids concentrations (< 30 mg L^{-1}), and consequently at higher values of percent transmission (>70 %).

This suggests that neither suspended solids or percent transmission alone are good predictors of the scale parameter (β_0), and therefore for predicting the limiting level of disinfection in UV data exhibiting tailing. The scale parameter is also seen to range between 3 to 4.5 for residual coliform levels less than 40 MPN per 100 millilitres as shown by Figure 4.13c. However, the lowest value of the scale parameter ($\beta_0 \sim 3.2$) is observed at the highest residual coliform concentration of 120 MPN per 100 millilitres. This underscores that low predicted levels of disinfection (characterised by small β_0) are asscociated with high residual coliform concentrations (often particle associated) in the effluent, and not necessarily with low suspended solids concentration as shown by Figure 4.13a. This is consistent with the findings of others (Nelson 2000; Taghipour 2004; Templeton, Andrews and Hofmann 2005; Hu *et al.* 2007; Cantwell and Hofmann 2008) who argue particle size distribution and particle association to be more important than concentration alone.

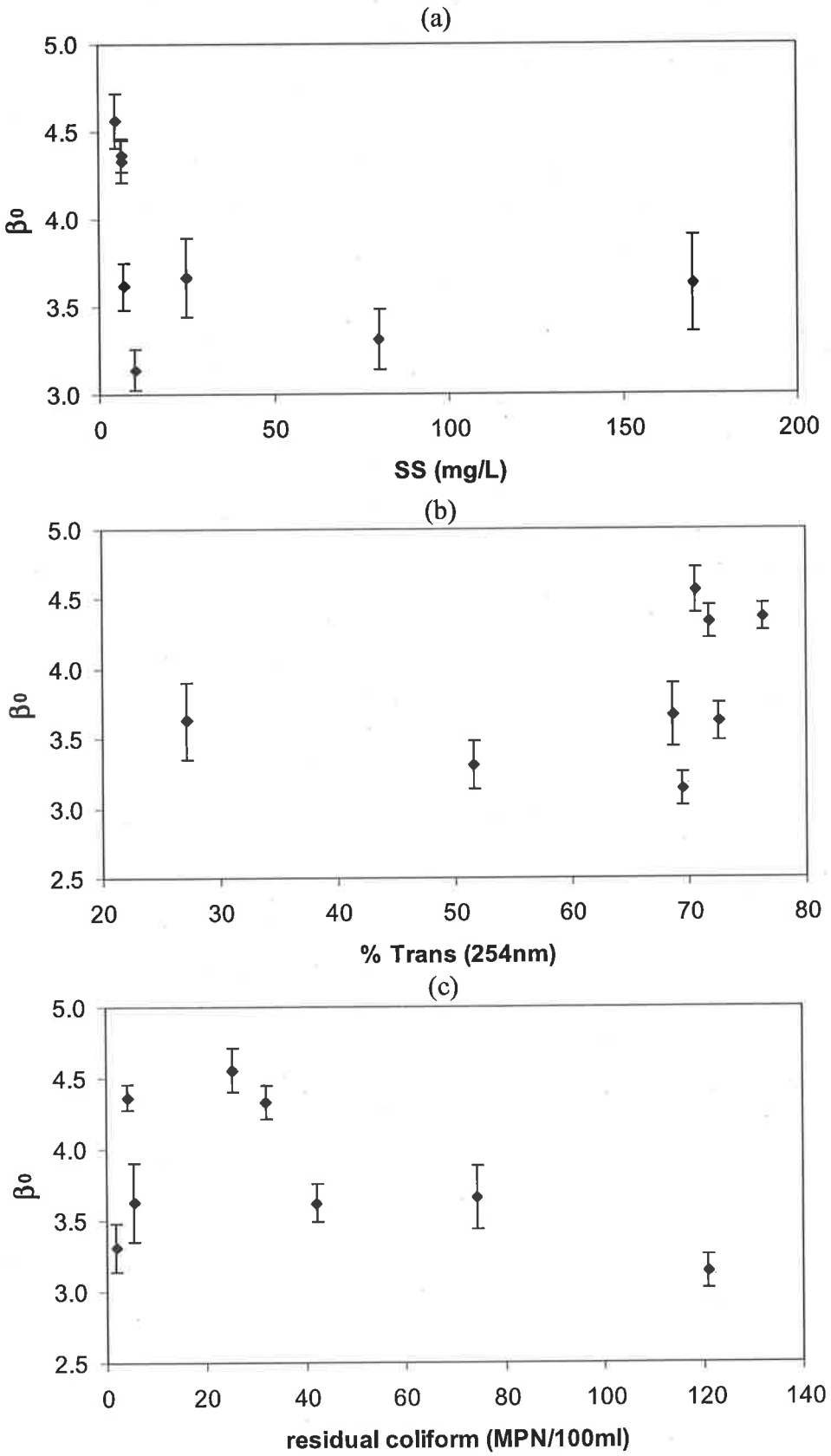

Figure 4.13 The scale parameter (β_0) of the Weibull model plotted against selected wastewater characteristics for the UV disinfection data of Nelson (2000): (a) suspended solids, (b) percent transmission, and; (c) residual coliform concentration. Error bars denote standard error for each parameter estimate

Figure 4.14 presents the Weibull shape parameter (β_1) plotted against measured wastewater characteristics: (a) suspended solids concentration, (b) percent transmission, and; (c) residual coliform concentration, for each of the treatment options of Nelson. Error bars show the standard error obtained for each estimate of β_1.The shape parameter (β_1) is seen to increase with suspended solids concentration (Figure 4.14a), and accordingly to decrease for a corresponding increase in transmission of the effluent (Figure 4.14b). This implies that suspended solids concentration may be a useful wastewater characteristic to assess the extent, or onset, of tailing – with an increase in the shape parameter signifying a more rapid onset of tailing. It should be emphasised however, that while suspended solids concentration may be a useful indicator to predict the onset of tailing, it has been shown in Figure 4.13a not to be a reliable index on which the limiting extent of disinfection (as β_0) can be predicted. No obvious trend was observed in values of the shape parameter with respect to the residual coliform concentration as shown by Figure 4.14c. Significant variation in the shape parameter is however observed for residual coliform concentrations less than 20 MPN per 100 millilitres.

Figure 4.15 presents the scale parameter (β_0) plotted against the shape parameter (β_1) of the Weibull model fitted to UV disinfection data for each of the eight treatments of Nelson. From the figure, there appears no significant correlation between the Weibull model parameters. This finding contrasts with that for the EDP_m model (*see* Section 4.4.2), and the widely held view that the scale and shape parameters of the Weibull model are not independent (Mafart *et al.* 2002; van Boekel 2002).

However, greater values of the shape parameter (β_1) tend to correspond to lower values of the scale parameter (β_0), and similarly; greater values of the scale parameter (β_0) correspond to lower values of the shape parameter (β_1). Despite these general trends, no clear relationship between the scale and shape parameters was apparent from extensive analyses.

The effects of environmental variables should therefore be more easily attributed to either the scale or shape parameters when using the Weibull model to simulate UV disinfection kinetics. This is advantageous in moving from an empirical model to a possible mechanistic basis for UV disinfection.

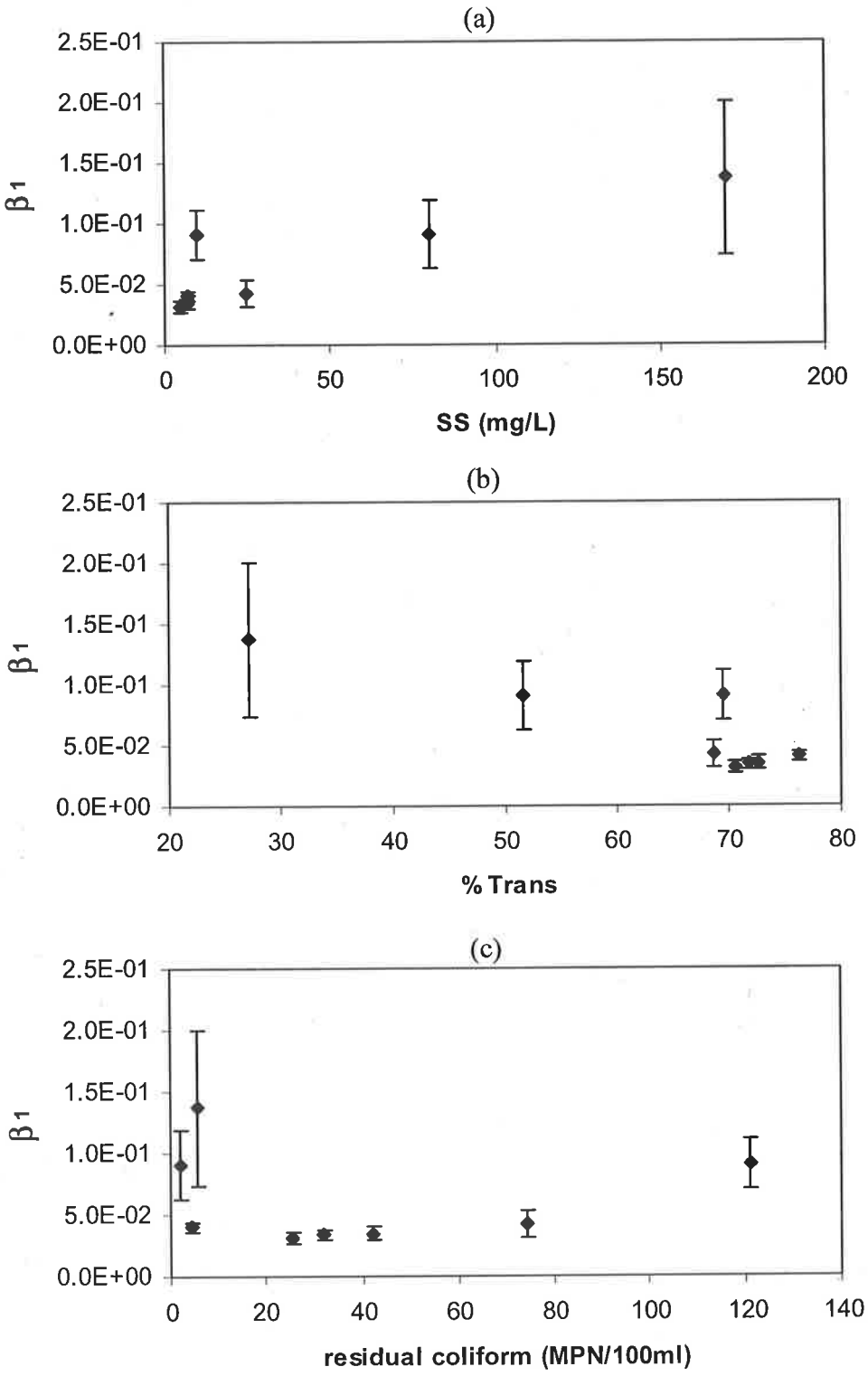

Figure 4.14 The shape parameter (β_1) of the Weibull model plotted against selected wastewater characteristics for the UV disinfection data of Nelson (2000): (a) suspended solids, (b) percent transmission, and; (c) residual coliform concentration. Error bars denote standard error for each parameter estimate

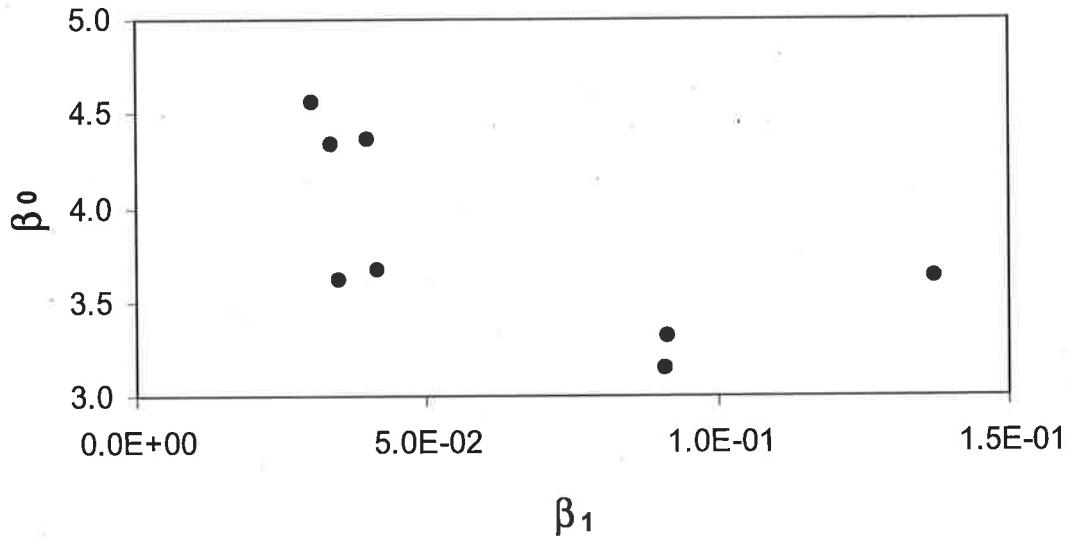

Figure 4.15 The scale parameter (β_0) correlated with the shape parameter (β_1) for the Weibull model fitted to the eight UV disinfection treatments Nelson (2000)

4.5.2 Summary

Findings highlight that the Weibull model is of an appropriate form to simulate tailing often observed in practical UV disinfection data for a range of treatment conditions. The model is based on the Weibull probability distribution, and contains two parameters: the dimensionless scale parameter (β_0) and the shape factor (β_1). An advantageous property of the model is that it is monotonic, and; approaches a limiting slope (or rate of disinfection) of zero in the tail – an intuitive limiting case.

4.6 Discussion

A comparative summary of the residual sums-of-squares (RSS) of both the EDP and EDP_m models with those for the Weibull form for the UV data of Nelson (2000), is given in Table 4.5. On the basis of RSS, the modified exponentially damped polynomial form (EDP_m) is seen to best fit these disinfection data. The unmodified exponentially damped form (EDP), expectedly (*see* Section 4.4.2), gives the poorer fit. The value of RSS for both the Weibull and EDP_m models are all but identical – these are both about an order of magnitude less than the values for the unmodifed EDP model.

The Weibull model form has only two model parameters (β_0 and β_1) compared with the three of the EDP_m model (k, λ and $[dose]_B$). A practical implication when fitting the model forms to UV disinfection data, particularly when few data are observed, is therefore that the confidence intervals for the respective Weibull parameters can be expected to be smaller than those for the parameters of the EDP_m model (Snedecor and Cochran 1969; Bates and Watts 1988; D'Agostino and Stephens 1986).

Table 4.6 presents a comparison between the Weibull scale parameter (β_0) and the predicted log-reduction at the breakpoint dose ($-c$) for the EDP_m model. Importantly, both of these terms are measures of the predicted level of disinfection at the onset of tailing. Generally, the magnitude of the scale parameter (presented as $-\beta_0$) is seen to be greater than of the predicted log-reduction at the breakpoint dose ($-c$) of the EDP_m model. This arises from the capability of the EDP_m model to account for a level of continuing disinfection in the tail, whereas the Weibull model cannot. As a result, the scale parameter of the Weibull model is more representative of an "average" level of disinfection in the tail, whilst the level of disinfection predicted by the EDP_m model at the breakpoint dose is indicative of the extent of disinfection at the onset of tailing.

One exception to these overall findings is for activated sludge with pure oxygen (treatment a: Table 4.6). The scale parameter, β_0, of the Weibull model represents a lower level of disinfection than at the breakpoint dose of the EDP_m model, $-c$ (i.e. 4.56 *cf.* 4.83-$\log_{10}$ reductions). This can be attributed to the presence of more survivors following UV treatment at a dose of 400 mWs cm^{-2} than are observed after treatment at 130, 200 and 300 mWs cm^{-2} (treatment a: Figure 4.1). That is, an apparent negative rate of disinfection is

observed in data representative of the tail. This is further supported by the prediction of a negative rate of disinfection (-1.20×10^{-3} mWs^{-1} cm^2) in the tail by the EDP_m model for this treatment (Table 4.2).

Table 4.5 Comparison of the residual sum-of-squares (RSS) obtained for the fits of the EDP, EDP_m and Weibull models fitted to the data of Nelson (2000)

Treatment	RSS		
	EDP	**EDP_m**	**Weibull**
(a) AS* with pure O_2	2.38	0.43	0.56
(b) Air AS	2.79	0.28	0.43
(c) AS with bio N	3.96	0.12	0.35
(d) AS with bio N/bio P	4.41	0.07	0.14
(e) AS with chem P	6.58	0.15	0.30
(f) Trickling filter	4.11	0.58	0.82
(g) Aerated pond	7.90	0.62	0.64
(h) Facultative pond	5.16	0.48	0.62

* AS denotes activated sludge.

The capability of the EDP_m model to predict a negative rate of disinfection in data describing the tail highlights both: the flexibility of the model in that it is capable of accounting for continuing disinfection as the UV dose is increased throughout the tail; as well as the need for imposition of a constraint in some circumstances. This is to ensure that the rate of disinfection predicted in the tail is restricted to taking non-negative values, and is limited to a maximum of zero – an intuitive limiting case.

Table 4.6 Comparison between the Weibull model, β_0, and the EDP_m model, $-c$, parameters as measures of the onset of tailing

Treatment	$-\beta_0$ (dimensionless)	$-c$ (dimensionless)
(a) AS* with pure O_2	-4.56	-4.83
(b) Air AS	-3.62	-3.01
(c) AS with bio N	-4.33	-3.54
(d) AS with bio N/bio P	-4.37	-3.83
(e) AS with chem P	-3.14	-2.85
(f) Trickling filter	-3.66	-3.21
(g) Aerated pond	-3.31	-3.11
(h) Facultative pond	-3.63	-3.36

* AS denotes activated sludge.

A comparison between predicted rates of disinfection from the EDP_m and Weibull models is given in Table 4.7 (the disinfection rate coefficient, k, and; the disinfection rate coefficient for the tailing region, k', of the EDP_m model are defined in Equations 4.3 and 4.4 respectively). Disinfection rates predicted at UV doses of 0 and 200 mWs cm^{-2} by the Weibull model give respective measures of the initial rate of disinfection, and that observed in the tail of the disinfection data.

Table 4.7 Comparison of predicted disinfection rates for the EDP_m and Weibull models for the UV disinfection treatments of Nelson (2000)

Treatment	rate of disinfection (mWs^{-1} cm^2)			
	EDP_m		Weibull	
	k	k'	initial (dose = 0 mWs cm^{-2})	tail (dose = 200 mWs cm^{-2})
(a) AS* with pure O_2	1.12×10^{-1}	-1.20×10^{-3}	1.40×10^{-1}	2.98×10^{-4}
(b) Air AS	1.38×10^{-1}	2.28×10^{-3}	1.27×10^{-1}	1.15×10^{-4}
(c) AS with bio N	1.60×10^{-1}	2.97×10^{-3}	1.47×10^{-1}	1.63×10^{-4}
(d) AS with bio N/bio P	1.74×10^{-1}	2.15×10^{-3}	1.75×10^{-1}	5.82×10^{-5}
(e) AS with chem P	2.69×10^{-1}	1.53×10^{-3}	2.86×10^{-1}	3.54×10^{-9}
(f) Trickling filter	1.49×10^{-1}	1.90×10^{-3}	1.52×10^{-1}	3.75×10^{-5}
(g) Aerated pond	2.78×10^{-1}	9.63×10^{-4}	3.02×10^{-1}	3.62×10^{-9}
(h) Facultative pond	4.12×10^{-1}	2.66×10^{-3}	4.97×10^{-1}	6.22×10^{-13}

* AS denotes activated sludge.

The disinfection rate coefficient (k) of the EDP_m model and the initial rate of disinfection predicted by the Weibull model are seen from Table 4.7 to be comparable for each of the treatments of Nelson (2000). This suggests that both the EDP_m and Weibull model forms are equally capable of predicting the rate of disinfection during the early stages of UV treatment (i.e. at low UV dose).

However, the rate of disinfection predicted in the tailing region is much higher for the EDP_m model than for predictions of the Weibull model form. The predicted rate of disinfection in the tailing region (k') for the EDP_m model varies over one order of magnitude for all eight treatments (a – h) of Nelson (2000), and is generally 50 to 300 times smaller than the initial rate, as the disinfection rate coefficient (k). The rates of disinfection predicted in the tail (i.e. at 200 mWs cm^{-2}) by the Weibull model vary by nine orders of magnitude over all eight treatments.

Despite the overall suitability of the new model forms, there are shortcomings. For the Weibull model this is that it is not amenable to extrapolation where a level of disinfection continues to occur throughout the tail. However, the Weibull form is advantageous when there is large variance in data in the tail.

A shortcoming of the EDP_m model is that it is defined by three parameters (k, λ and $[dose]_B$), compared with two parameters (β_0 and β_1) for the Weibull model. This has important implications for the standard errors associated with the EDP_m model parameters (as highlighted in the preceding discussion); particularly when few data are available (Snedecor and Cochran 1969; Montgomery 2001; Bates and Watts 1988). The illustrated inter-dependence of these three parameters might present difficulties when attempting to attribute influence of environmental variables on UV efficacy. This inter-dependence could be exploited to provide a convenient basis for comparison of UV disinfection data generated under different treatments. This contrasts with the Weibull model parameters which appear independent in this case. The scale parameter (β_0) of the Weibull model however does provide a useful measure of the predicted maximum level of disinfection.

Practical problems might arise however when few data are available to fit the EDP_m model. These problems might stem from the piecewise nature of the model – that can present difficulties for convergence during regression analyses, particularly when fitted to smaller data sets. However, the breakpoint dose, $[dose]_B$, defining this piecewise nature of the EDP_m model is arguably an important design criterion in that it de-lineates between the kinetics representing the tailing region and the initial period of rapid disinfection. Further studies are required to determine whether this threshold dose is characteristic: of water quality parameters (including any contaminants present), or; of the properties of the disinfection unit (such as residence time distributions and intensity profiles within the reactor). It could prove a useful criterion to scale-up UV disinfection kinetics for use in reactor design.

Overall, the rates of disinfection predicted by the Weibull model for data of the tail are effectively zero, and are at least three orders of magnitude less than the equivalent rates predicted by the EDP_m model for identical treatments.

These findings highlight further the inability of the Weibull model to account for continuing levels of disinfection in the tailing region, and might also explain why the EDP_m model consistently produced lower residual sums-of-squares than the Weibull model for the same UV disinfection data. The flexibility of the EDP_m model to simulate the continuing disinfection observed in the tail of practical UV disinfection data is the main advantage over the Weibull form.

4.7 Concluding remarks

1. Both the newly synthesised EDP_m and Weibull models forms are of a form suitable to adequately simulate tailing often seen in practical UV disinfection kinetics.

2. For the independent disinfection data of Nelson (2000), the EDP_m model gives a better fit than the Weibull model for a range of treatments.

3. There appears to be no significant correlation between the parameters of either model form with respect to typical wastewater characteristics: suspended solids concentration, percent transmission, and; residual coliform concentration.

4. Parameters of the EDP_m model (k, λ, $[dose]_B$) all are highly inter-dependent for the published disinfection data of Nelson (2000).

5. The scale (β_0) and shape (β_1) parameters of the Weibull model appear to be independent of each other for the published disinfection data of Nelson (2000).

6. The question of general suitability of these two newly synthesised models for adequate simulation of UV disinfection must be rigorously validated against a further, suitable set of carefully determined, robust experimental data.

In the following chapter, experimental materials, apparatus and procedures used for careful generation of suitable UV disinfection data for validation of the new, non-linear model forms are outlined. Particular emphasis is given to determining data at low UV dose ($< 10{,}000$ $\mu W s\ cm^{-2}$). In Chapter 6, these data are initially used to rigorously validate the suitability of both the EDP_m and Weibull models that were synthesised and assessed against independent published data in this chapter.

CHAPTER 5: EXPERIMENTAL STUDIES

5.1 Introduction

This chapter describes a pilot apparatus and experimental methods used to carefully obtain UV survival data for disinfection of a pure strain of *Escherichia coli* in the presence of either a shielding agent (particulate diatomaceous earth present as Celite 503™) or a UV absorbing agent (soluble UV absorbing agents present as International Roast™ instant coffee powder) over a range of defined concentrations in purified water.

Adequate, robust UV disinfection data are generated, with emphasis on low values of UV dose (<10,000 μWs cm^{-2}), to rigorously validate the two new model forms developed and initially assessed in Chapter 4

Dye trace studies are carried out using Methylene Blue to investigate the hydrodynamics of flow of water in the UV pilot disinfection unit and digital video results presented. Examination of flow profiles generated for each of the flow rates used revealed turbulent profiles in all cases other than for a flow rate of 0.4 L min^{-1}. A minimum flow rate of 1 L min^{-1} is used in the experimental trials however. The experimental disinfection data, together with extensive analyses, are presented in Chapter 6.

5.2 Commercial LC5™ disinfection pilot apparatus

A commercially available LC5™ UV disinfection unit, manufactured by Ultraviolet Technology of Australasia (UVTA) Pty. Ltd., was used as the pilot apparatus. The LC5™ unit was designed to disinfect up to 5 L min^{-1} of clean, clear-quality, drinking water (turbidity < 5 NTU and Colour < 5 HU), and up to 2 L min^{-1} of industrial wastewater (Nguyen 1999). The unit can be operated continuously at a pressure of 552 kPa for a liquid temperature of 24°C, with the pressure rating decreasing by 2% for every 1°C rise in temperature (UVTA – Product Specification LC Series).

The unit comprises a single-pass advanced fluoropolymer U-tube that carries water alongside a XUV low-pressure mercury vapour lamp. It provides a nominal UV intensity of 11,940 μWs cm^{-2} (Nguyen 1999). The fluoropolymer used for water flow has low fouling characteristics – and is also FDA approved for use with food and beverages (UVTA – Product Specification LC Series). The lamp and fluoropolymer U-tube are

enclosed in a robust, powder-coated aluminium case, with the vapour-lamp mounted in an easy-turn lamp-holder to permit ready lamp replacements.

5.3 Experimental loop

The LC5^{TM} UV disinfection unit was connected in a flow-loop fed from a 20 L glass feed-tank. Water used was purified by *Reverse Osmosis* (RO). A centrifugal pump (PV 52 – James Beresford & Sons Ltd, Birmingham, England) was used to circulate water through the flow-loop. The rate of water flow was adjusted with a control-valve (Swagelok^{TM} – Adelaide Valve & Fitting, South Australia), and measured using a variable area flow-meter (Platon VA – ABB Kent Taylor, England) graduated linearly from 0.4 to 4.4 L min^{-1}. The disinfected solution was discharged into a 20 L glass effluent tank for additional treatment prior to disposal.

The experimental flow-loop is shown schematically in Figure 5.1. A photograph of the LC5^{TM} disinfection unit with cover removed is presented as Figure 5.2. A photograph of the experimental arrangement, showing the pilot disinfection unit and flow-loop, is presented as Figure 5.3. An enlarged photograph of the hydrodynamic flow profile within the UV disinfection unit for a water flow of 0.4 L min^{-1} is presented as Figure 5.4. The flow profile is seen to be well developed and parabolic, characteristic of laminar pipe-flow.

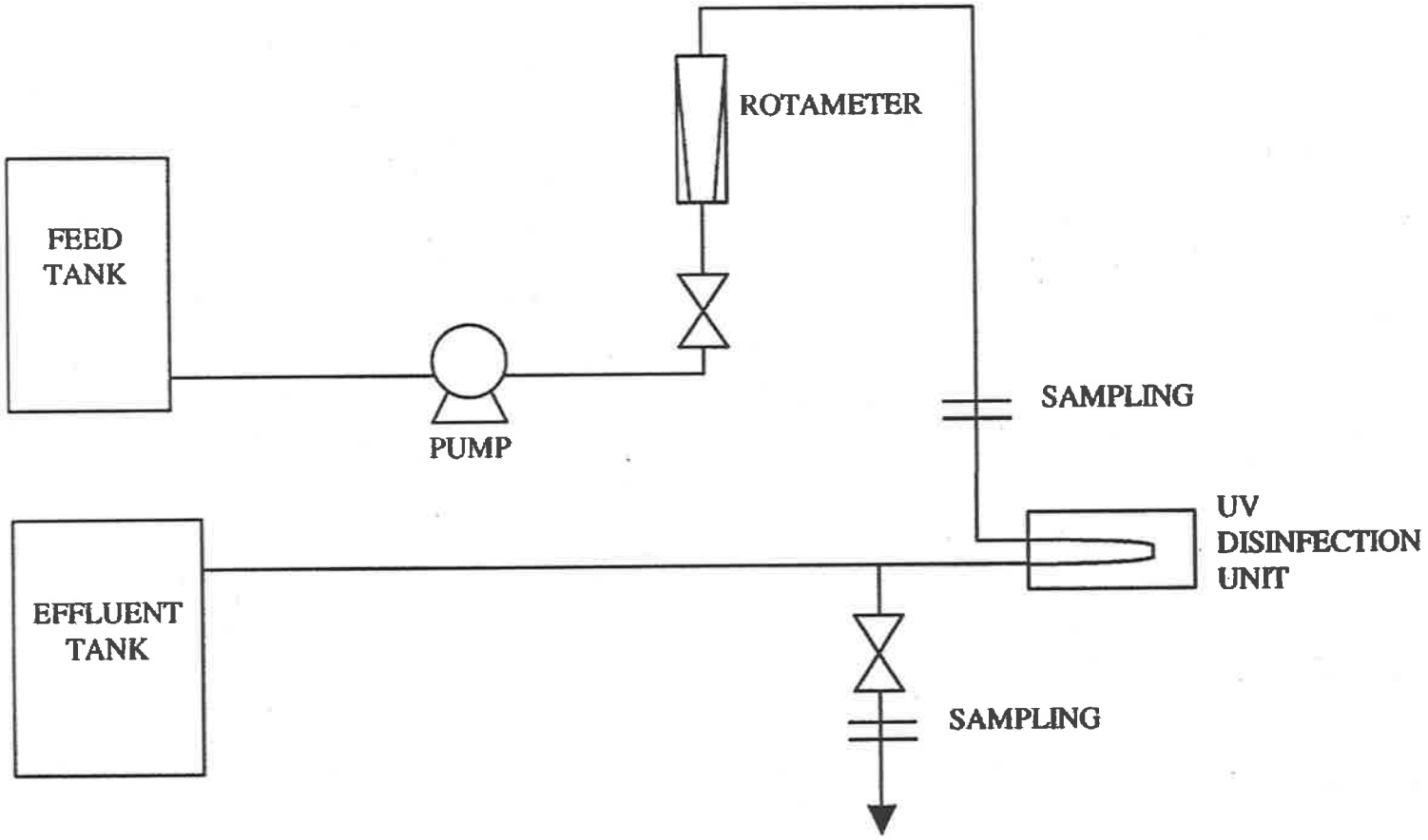

Figure 5.1 Schematic of the pilot UV disinfection apparatus and flow-loop

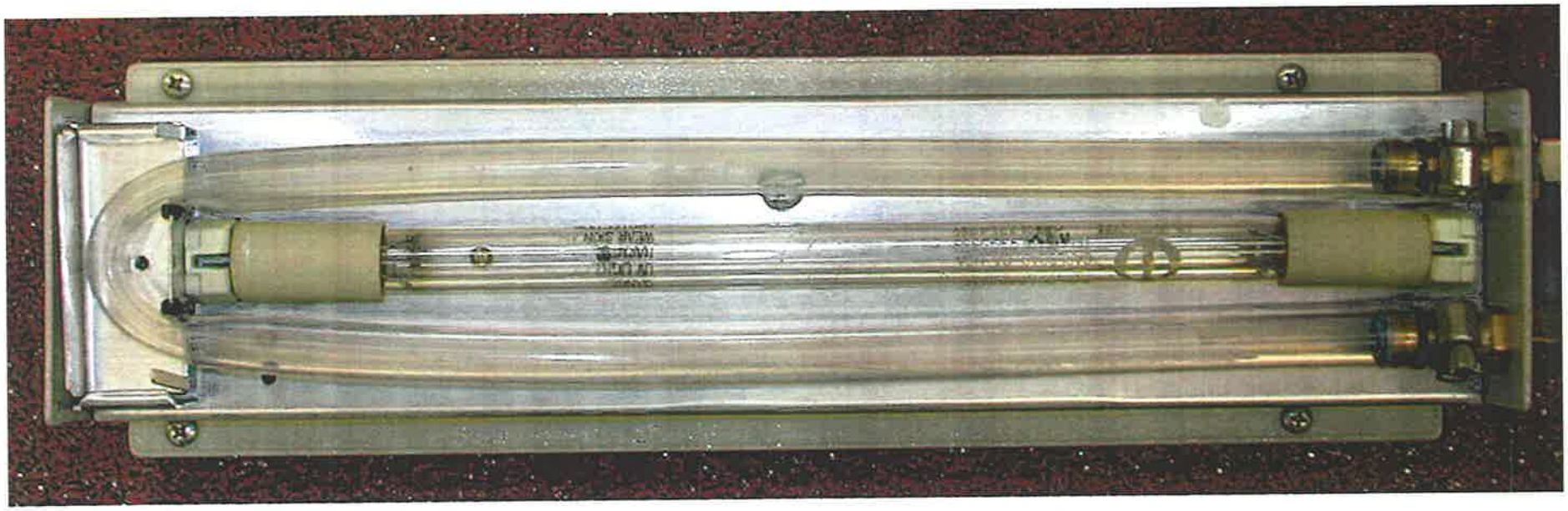

Figure 5.2 Photograph of the LC5^{TM} disinfection unit with lamp cover removed

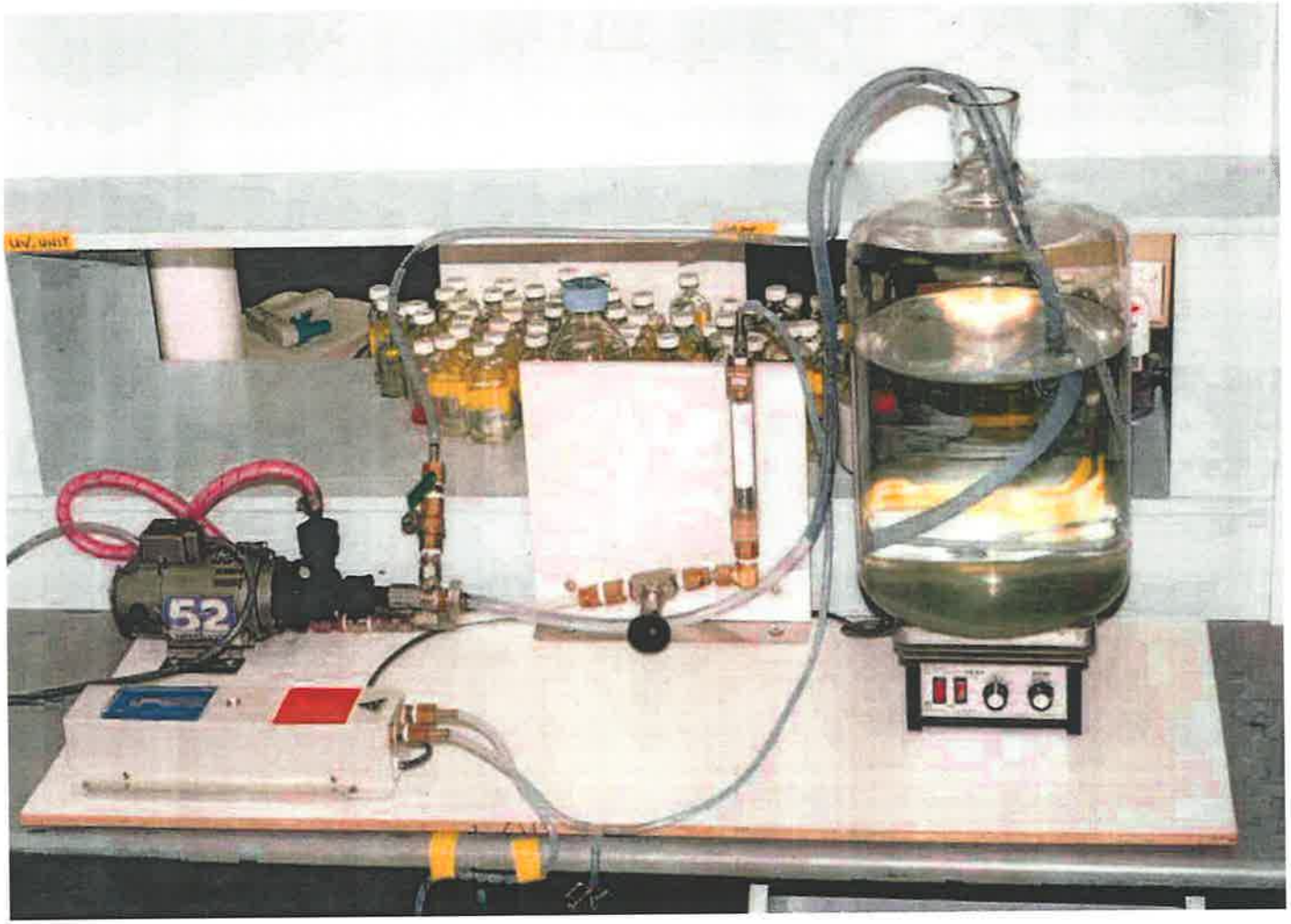

Figure 5.3 Photograph of the pilot UV disinfection apparatus and flow loop

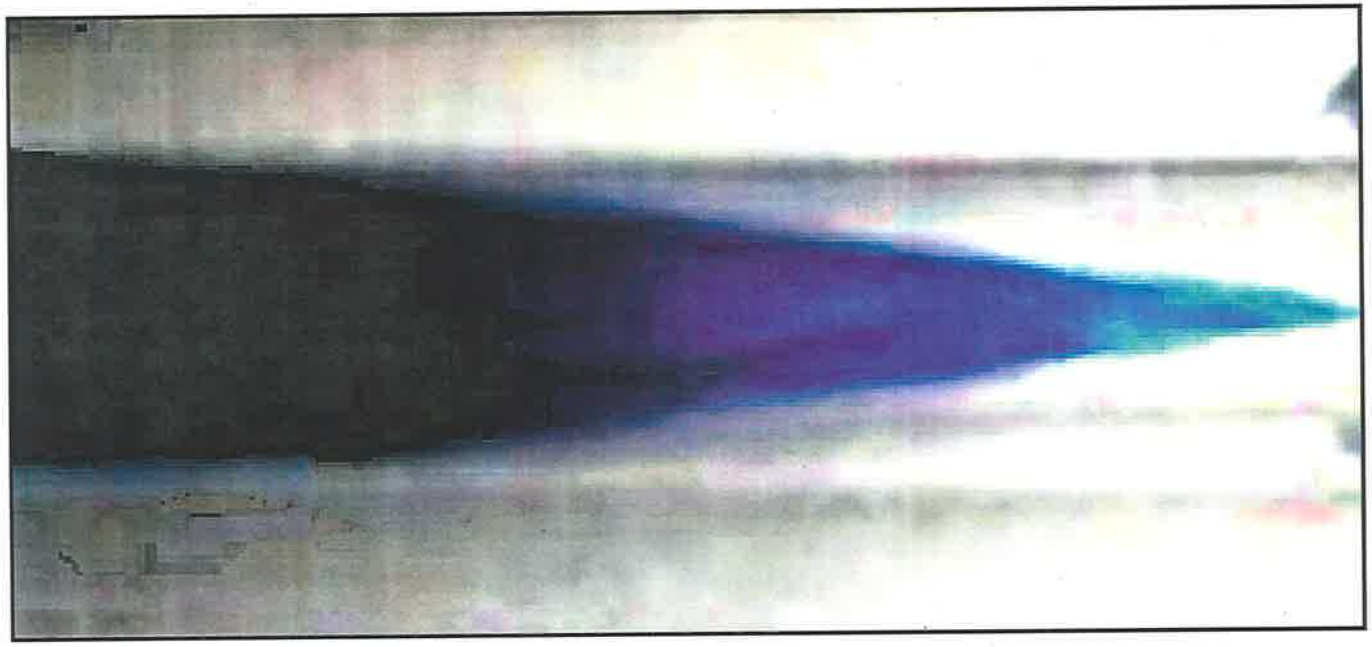

Figure 5.4 Enlarged photograph of the hydrodynamic profile at a flow of 0.4 L min^{-1}

5.4 Test micro-organism

The test micro-organism selected for the experimental trials was *Escherichia coli*.

This bacterium is a motile rod about 1 μm, by 2 to 3 μm in length (Brock and Madigan 1991; Stanier, Doudoroff and Adelberg 1971) and is widely used as an indicator for the presence of *enteric* pathogens in both water (USEPA 1986; Kiely 1998; Qasim 1999) and food (Davey 1993; Davey, Hall and Thomas 1995; Chiruta 2000; Daughtry *et al.* 1997). It should not be present in potable water (*see* Section 3.2). The particular strain was the FDA "Seattle strain" American Type Culture Collection (ATCC) 25922. A culture of this pure strain was supplied by, and is maintained within, the *Food Research Group* (FRG), University of Adelaide.

This bacterium satisfies the necessary requirements of: availability from accessible stocks, significant sensitivity to UV irradiation, simple growth requirements, and; easy dispersion as individual cells.

5.5 UV shielding and UV absorbing agents

Transmittance (%T 254 nm) of the water in the feed-tank was varied by addition of either a suspended solid (diatomaceous earth as Celite 503™ – Ace Chemical Company, South Australia), or, a soluble UV absorbing agent (International Roast™ instant coffee powder).

The Celite 503™ consisted of 89 % silica (SiO_2) with median particle size of 23 μm (Nguyen 1999). Particle size analysis showed the limiting particle diameter for a 90% cumulative under-size to be 46 μm, with a maximum observed particle size of 120 μm (*see* Appendix C).

The suspended solid, diatomaceous earth as Celite 503™, is formed from fossilised remains of microscopic single-celled alga (i.e. diatoms), as is almost pure silica. Some of the components identified in the instant coffee (aborbing agent) include: caffeine, chlorogenic and other acids, carbonyl compounds, alcohols, esters, and; aromatic and heterocyclic compounds (Trugo, Macrae and Dick 1983). Ultraviolet irradiation may

be absorbed by those compounds containing conjugated double-bonds (Cano and Colome 1986; Harm 1980; Kohler 1965).

These two agents have been used extensively in ongoing studies on UV disinfection within the *Food Research Group* (FRG) (e.g. Nguyen 1999; Nguyen *et al.* 1998; Davey *et al.* 1995; Manning 1994).

5.6 Experimental methodology

These experimental trials involved: cultivation and harvesting of the test micro-organism, UV exposure of the test micro-organism, enumeration of viable cells remaining post-UV treatment, and; dye studies to investigate the hydrodynamics of flow in the pilot disinfection unit.

5.6.1 Cultivation and harvesting of the test micro-organism

Nutrient Broth (NB) was routinely prepared by dissolution of: 10 g Oxoid peptone, 10 g Oxoid Lab Lemco powder, and; 5 g NaCl (salt) in one litre of RO water. The neck of the conical flask was sealed with a cotton-bung, and then autoclaved at 121 °C for 30 minutes. Nutrient Agar (NA) was prepared by solidification of Nutrient Broth with 15 g L^{-1} of Oxoid agar.

The test micro-organism was regularly cultivated from glycerol stock cultures maintained at a temperature of minus 70 °C. Aseptic technique (Meynell and Meynell 1970) was used to streak a loop of frozen culture on the surface of nutrient agar, and the plate incubated at 37 °C for eight hours. A single colony was then used to inoculate 100 mL of nutrient broth, which was then incubated at 37°C for eight hours. Four conical flasks, each containing 500 mL of nutrient broth, were then inoculated with 10 mL of inoculum per flask. The flasks were sealed with a sterile cotton-bung, and incubated with mild agitation at 37 °C for eight hours. This ensured all harvested cells were in the exponential phase of growth (*pers. comm.* C J Thomas).

Bacterial cells were then harvested by centrifugation (Beckman JA 10 rotor at 5000 rpm and 4 °C for 30 minutes). The resulting cell pellets were re-suspended in phosphate-buffered saline (0.8% w/v NaCl and 0.1% w/v peptone) such that the total

volume of concentrate was between 80 to 100 mL. The viable concentration of cells ranged from 10^{10} to 10^{11} mL^{-1}. Cell concentration was determined indirectly by standard measurements of optical density at a fixed wavelength (of 600 nm).

5.6.2 UV exposure of the test micro-organism

Prior to each experimental trial, the pump and all flow-lines were primed with RO water. This was achieved by filling the feed-line to the pump with water, and allowing the pump to fill under gravity. The pump was then set to a maximum flow (~ 4.4 L min^{-1}) for 2 – 3 minutes to ensure both the flow-lines and pump contained no air. The pump was then switched off, and the discharge line elevated to ensure the flow-loop remained primed.

The feed-tank was filled with 18 L of RO water. A fixed volume (ranging from 3 – 10 mL) of the bacterial concentrate was added to the feed-tank water to give a target viable cell concentration of between 1×10^{7} and 3×10^{7} mL^{-1}. To ensure homogeneity of the feed-tank content, it was circulated through the flow-loop (with the disinfection unit switched off) for a minimum of 10 minutes. Four water samples from the flow-loop were used to determine the transmittance of the feed-water due to the presence of the bacterial cells.

A pre-set amount of, either, the suspended solid or UV absorbing agent was added to the feed-tank to give a required concentration. The feed-tank contents were circulated through the flow loop to again ensure homogeneity. A magnetic bar-stirrer was used in the feed-tank to ensure added suspended solids remained suspended, and did not settle in the tank. Four samples were used to determine the transmittance of the feed-water due to the combined effect of: the bacterial cells, and; of the respective agent added. These samples were immediately stored in an ice-slurry (4 °C) for subsequent enumeration of viable cells.

The UV dose was controlled by one of two means. The flow rate could be adjusted, using the control-valve, to values of 1, 3 and 4 L min^{-1}. These flow rates corresponded to respective UV doses of: 44,200, 14,100 and 10,800 μWs cm^{-2}. A proportion of the exposed length of flow-tube within the LC5™ disinfection unit could be covered with

aluminium foil. At a flow rate of 4 L min^{-1}, covering half and three-quarters of the exposed length, respectively, generated the delivered doses of 5,400 and 2,700 μWs cm^{-2}. The UV dose was calculated as the product of the UV intensity, *I*, and the exposure time, *t* (*see* Appendix F).

Following UV exposure, four (4) samples of the disinfected water were taken immediately downstream of the disinfection unit for each of the five UV doses investigated. These samples were stored in an ice-slurry (4 °C) for later enumeration of viable cells.

5.6.3 Enumeration of viable cells

The numbers of viable bacterial cells were counted by the standard Plate Count Method (Meynell and Meynell 1970). Serial 10-fold dilutions of all samples taken were made by 1 mL transfers (of sample) into 9 mL saline. Samples were homogenised by a bench-top, vortex-mixer between successive dilutions. This constant 1 in 10 dilution factor was used exclusively throughout experimentation to reduce the likelihood of error when conducting large numbers of counts. For each sample, a minimum of three dilutions were each plated in duplicate. Plating consisted of spreading 0.1 mL of an appropriate culture over the surface of nutrient agar. The plates were incubated at 37 °C for between 20 and 24 hours. Those plates with between 30 and 300 colonies were counted. This method assumes each viable cell will yield a single colony following incubation (Meynell and Meynell 1970). There were no airborne contaminants visible on the agar plates during the experimental trials. These could easily have been differentiated on the basis of colonial size and morphology, and would therefore not affect counts of the contaminant micro-organism.

For those samples where expected survival was low (less than 30 colonies per plate by standard plate count), the Pour Plate Technique was employed (Meynell and Meynell 1970). This involved the addition of liquid agar to 1 mL sample volumes. These were incubated at 37 °C for between 20 and 24 hours.

The number of surviving bacteria (mL^{-1}) was evaluated as the mean number of colonies (of the duplicates) for a given dilution, multiplied by the dilution factor (Meynell and Meynell 1970; Nguyen 1999). The resulting concentrations of viable bacteria were then averaged across all samples.

5.6.4 UV transmittance measurement

The UV transmittance of each sample was measured in a 10 mm path-length quartz cuvette using a BioRad SmartSpec^{TM} 3000 Spectrophotometer (BioRad Laboratories). All measurements were made at a wavelength of 254 nm with the transmittance reported as absorbance units per centimetre (cm^{-1}). The transmittance of each sample was measured in triplicate, with the average reported. The spectrophotometer was calibrated with RO water set to have no absorbance at the specified wavelength of 254 nm.

5.6.5 pH and temperature measurement

The pH of the feed-tank contents was measured using a TPS digital pH-mV-T meter (TPS Pty. Ltd., 901-PH), coupled with standardised pH electrodes. Regular instrument calibration was carried out against standard buffer solutions at pH 4, 7 and 10. The pH value reported for the feed-tank contents is the average of four samples. The temperature of the feed-tank contents was measured using a standard alcohol thermometer (range 0 to 100°C, with 1°C graduations).

5.6.6 Dye studies (Methylene Blue)

Methylene Blue (Ace Chemical Company, South Australia) was prepared to a concentration of 1% (w/w) in RO water and used as a tracer to investigate the hydrodynamics within the LC5^{TM} disinfection unit. At each of the flow rates studied, a 0.5 mL pulse of the Methylene Blue solution was injected axially into the flow upstream of the UV disinfection unit. The resultant flow profiles through the pilot disinfection unit were recorded using digital video photography.

Corresponding Reynolds' numbers (*Re*) for flow rates of between 1 and 4 L min^{-1} are from 1.9×10^3 to 7.6×10^3 respectively (*see* Appendix E). Consequently, flow is not highly turbulent, but rather spans the transitional region between laminar and turbulent flow (Gerhart, Gross and Hochstein 1992). Gerhart, Gross and Hochstein

(1992) suggest the minimum Reynolds' number for stable turbulent flow in a pipe to be 4,000 – with any increase above this value indicating that flow is usually turbulent.

Some axial dispersion was evident from the digital video recorded during these dye studies. Figure 5.4 presents an enlarged photograph of a velocity profile obtained at a very low flow rate of 0.4 L min^{-1} (*Re* = 760). It can be seen that the flow profile is both well-developed and parabolic, the latter characteristic of laminar flow. Efforts to quantify the extent of dispersion were hampered by difficulties associated with estimation of colour intensity during image processing.

These dye studies showed clearly however (*see* Chapter 6), that at flow rates used during disinfection trials (1 – 4 L min^{-1}), there were no stationary, or eddying, liquid elements within the disinfection reactor (i.e. no dead-space within the reactor volume). Consequently, nominal exposure time (and therefore UV dose) may be simply, and reliably, determined.

5.7 A typical experiment

A typical experimental trial involved:

- Thorough rinsing of the flow loop with RO water prior to priming
- Addition of 18 L of RO water to the feed-tank
- Addition of a defined volume of bacterial concentrate to the feed-tank to give an initial viable cell concentration of ~ 10^7 mL^{-1}
- Addition of either the suspended solid (Celite 503™) or the soluble UV absorbing agent (International Roast™ instant coffee powder) to yield a specified concentration in the feed tank
- Circulation of feed-tank contents to ensure homogeneity prior to sampling
- Sampling of feed-tank contents prior to treatment for determination of: water transmission, pH, temperature, and; initial viable cell concentration
- Control of the UV dose by systematically varying the flow rate of water, and exposed length within the disinfection reactor
- Sampling of four replicates of the treated water for each controlled UV dose
- Assay and enumeration of samples pre- and post-treatment to determine disinfection efficacy.

5.8 Concluding remarks

A pilot apparatus was successfully developed to permit experimental investigation of the effects of suspended solids and soluble UV absorbing agents, together with UV dose, on the efficacy of UV disinfection of *E. coli* in a model water. Generation of disinfection data at low UV doses (< 10,000 $\mu Ws\ cm^{-2}$) is possible by modification of the exposed length of flow-loop within the LC5^{TM} disinfection unit. Hydrodynamics of flow within the pilot disinfection unit span the transitional regime between laminar and turbulent flow. There are no stationary, or eddying, elements of water within the disinfection reactor for the range of flow rates of interest (i.e. 1 – 4 $L\ min^{-1}$).

In the next chapter the experimental results obtained with this pilot apparatus are presented, together with associated detailed analyses. The generated UV data are used to rigorously validate the EDP_m and Weibull model forms synthesised in Chapter 4.

CHAPTER 6: RESULTS AND DISCUSSION

6.1 Introduction

This chapter presents the experimental UV disinfection data obtained using the pilot apparatus presented in Chapter 5 together with extensive analyses.

The pilot experimental data are used to validate the EDP_m and Weibull models that were synthesised in Chapter 4. The suitability of these model forms to represent tailing in UV disinfection kinetics is critically assessed. The influence of both a shielding agent (diatomaceous earth as Celite 503™) and a soluble UV absorbing agent (International Roast™ instant coffee powder) on the parameters of both models is established.

The results of the Methylene Blue dye studies described in Chapter 5 are presented and assessed. The digital images are used to investigate the hydrodynamic significance of flow on the residence time distribution of fluid elements in the LC5™ UV disinfection unit.

A brief comparative study of experimentally determined data is made with those of Nguyen (1999).

6.2 Experimental data

A total of 138 UV disinfection trials were conducted. Effects of four concentrations of shielding agent and six concentrations of absorbing agent on UV disinfection kinetics of *Escherichia coli* were studied. The experimental design gave 23 sets of experimental data. For each, measurement of the initial concentration of bacterial contaminants prior to UV exposure plus those surviving post-treatment was made. The summary design for each of the 23 sets is presented as Table 6.1.

A summary of a typical experimental UV disinfection trial is presented as Table 6.2 for data set 4, namely, experimental disinfection trials 19 through 24. A complete summary of all 23 data sets for each of the 138 disinfection trials is presented as Appendix O – Experimental disinfection data.

A convenient summary of the settings of the LC5™ UV disinfection unit, highlighting flow rate and exposure time, is presented as Table 6.3.

Table 6.1. Summary of experimental trials

Data Set	N_0 mL^{-1}	Agent $g\ L^{-1}$
1	2.99×10^8	zero
2	1.27×10^7	zero
3	6.64×10^6	zero
4	3.49×10^6	0.001 absorbing agent (as coffee)
5	9.70×10^6	0.005 absorbing agent
6	4.96×10^6	0.01 absorbing agent
7	2.06×10^6	0.005 absorbing agent
8	2.74×10^7	0.03 absorbing agent
9	2.78×10^6	0.1 shielding agent (as Celite 503™)
10	2.07×10^7	0.5 shielding agent
11	9.45×10^7	0.5 shielding agent
12	1.19×10^8	0.7 shielding agent
13	1.05×10^8	0.3 shielding agent
14	2.60×10^7	0.3 shielding agent
15	5.80×10^7	0.5 shielding agent
16	5.58×10^7	0.005 absorbing agent
17	1.60×10^8	0.03 absorbing agent
18	1.03×10^9	0.05 absorbing agent
19	1.41×10^8	0.07 absorbing agent
20	8.89×10^7	0.7 shielding agent
21	7.02×10^7	0.3 shielding agent
22	7.58×10^7	zero
23	8.51×10^7	0.3 shielding agent

Table 6.2. Illustrative summary of experimental data for disinfection trials 19 – 24 (data set 4)

Disinfection trial	19	20	21	22	23	24
UV dose ($\mu Ws\ cm^{-2}$)	0	2700	5400	10800	14100	44200
agent	coffee	coffee	coffee	coffee	coffee	coffee
agent conc ($g\ L^{-1}$)	0.001	0.001	0.001	0.001	0.001	0.001
UV trans - wo* bacteria (%)	98	98	98	98	98	98
UV trans - w** bacteria (%)	91	91	91	91	91	91
Temperature (°C)	24	24	24	24	24	24
pH	6.84	6.84	6.84	6.84	6.84	6.84
Initial number, N_0 (mL^{-1})	3.49×10^6	3.49×10^6	3.49×10^6	3.49×10^6	3.49×10^6	3.49×10^6
Survival number, N (mL^{-1})	3.49×10^6	5.50×10^1	6.88×10^0	1.58×10^1	6.13×10^0	1.31×10^1
$\log_{10}(N/N_0)$	0.00	-4.80	-5.71	-5.34	-5.76	-5.43

* wo = without
** w = with

Table 6.3. Nominal UV dose applied by the LC5™ disinfection unit as a function of flow rate, exposed length and exposure time

Flow rate ($L\ min^{-1}$)	Exposed length (mm)	Exposure time (s)	Nominal UV dose ($\mu Ws\ cm^{-2}$)*
1	636.6	3.70	44,200
3	636.6	1.20	14,100
4	636.6	0.90	10,800
4	318.3	0.45	5,400
4	159.2	0.23	2,700

* The LC5™ disinfection unit delivers a nominal intensity of 11,940 $\mu W.cm^{-2}$ (Nguyen 1999).

Figure 6.1 displays the experimentally determined data plotted as the $\log_{10}$ reduction in viable numbers of bacteria *vs.* UV dose for both absorbing agent (International Roast™ – instant coffee powder: 0.001 to 0.07 g L^{-1}) and shielding agent (Celite 503™ – diatomaceous earth: 0.1 to 0.7 g L^{-1}). The data are labelled (in parentheses) in the order in which they appear in Table 6.1.

To help distinguish between the effects of different concentrations of each agent on disinfection, the data were pooled according to additive concentration. Figure 6.2 presents the pooled data for both absorbing and shielding agent. To further differentiate between different concentrations of each agent, the pooled data were averaged at each UV dose. Figure 6.3 displays the resulting averaged data for both shielding and absorbing agents. The data are presented as the average $\log_{10}$ reduction *vs.* UV dose for each concentration of agent. The variance in the measured $\log_{10}$ reduction for each concentration is presented as standard deviation of the $\log_{10}$ N/N_0 values.

The disinfection data of Figure 6.1 show typical tailing. It is of interest to note that for a zero concentration of agent, the data also show a tail, namely about a 5-$\log_{10}$ reduction in viable cells at a dose from about 5,400 $\mu Ws\ cm^{-2}$. There is only a further 1-$\log_{10}$ reduction as the dose is increased nearly 10-fold to 44,200 $\mu Ws\ cm^{-2}$.

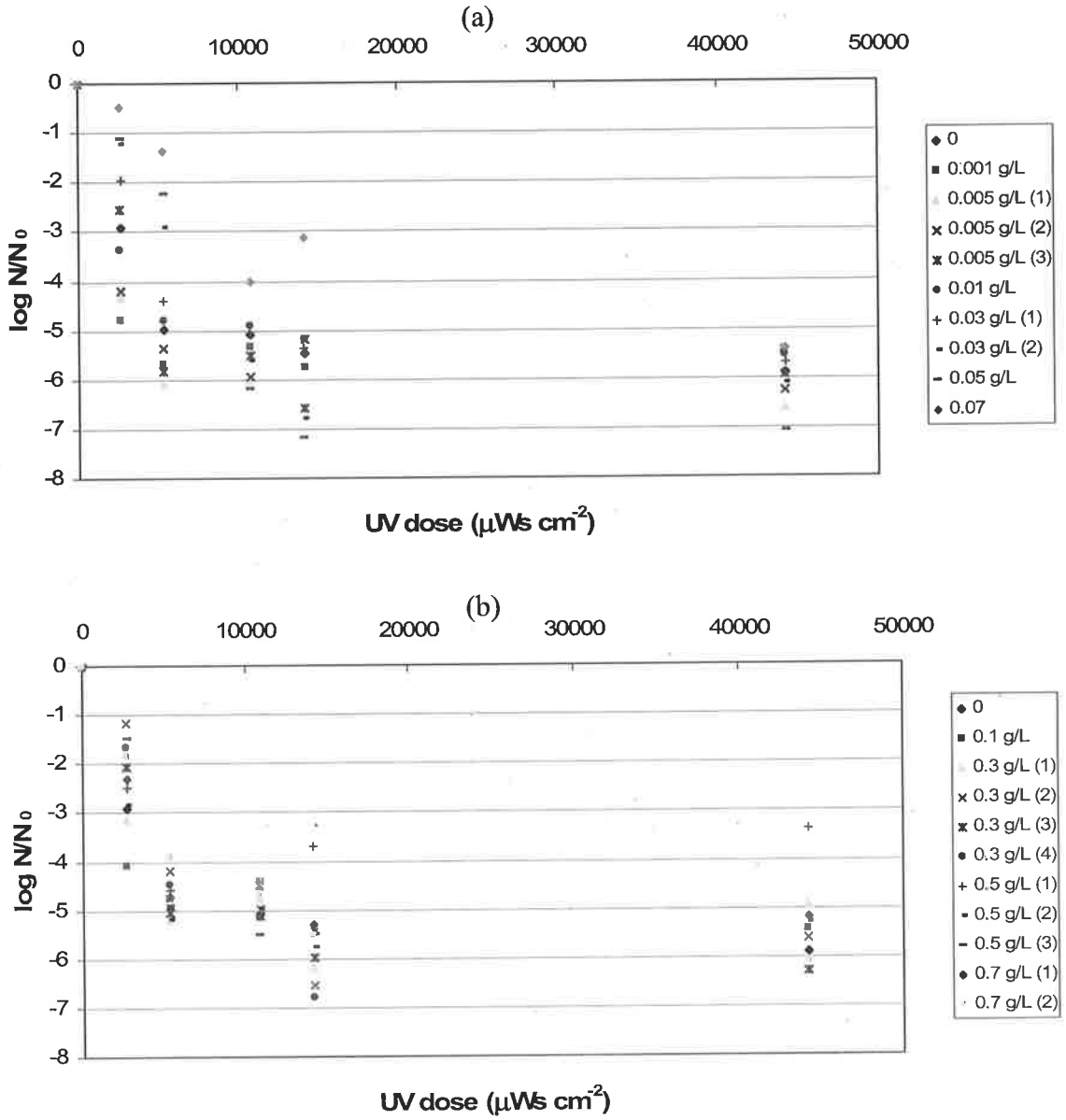

Figure 6.1. Experimental UV disinfection data for *Escherichia coli* in RO water (presented as $\log_{10} N/N_0$) in the presence of: (a) absorbing agent, and (b) shielding agent

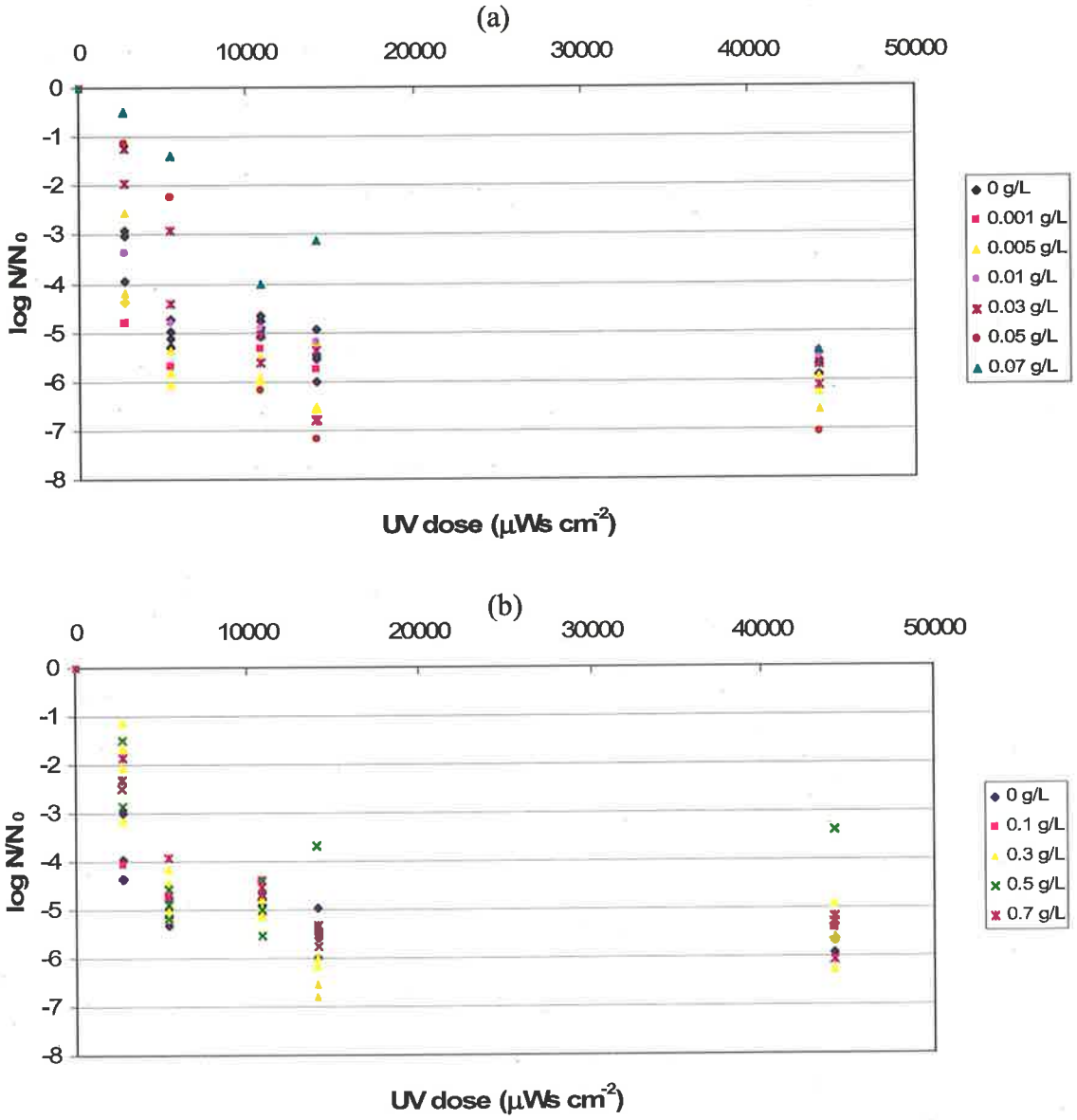

Figure 6.2. Experimental UV disinfection data for *Escherichia coli* in RO water (presented as $\log_{10} N/N_0$) in the presence of: (a) absorbing agent, and (b) shielding agent, with data pooled according to agent concentration

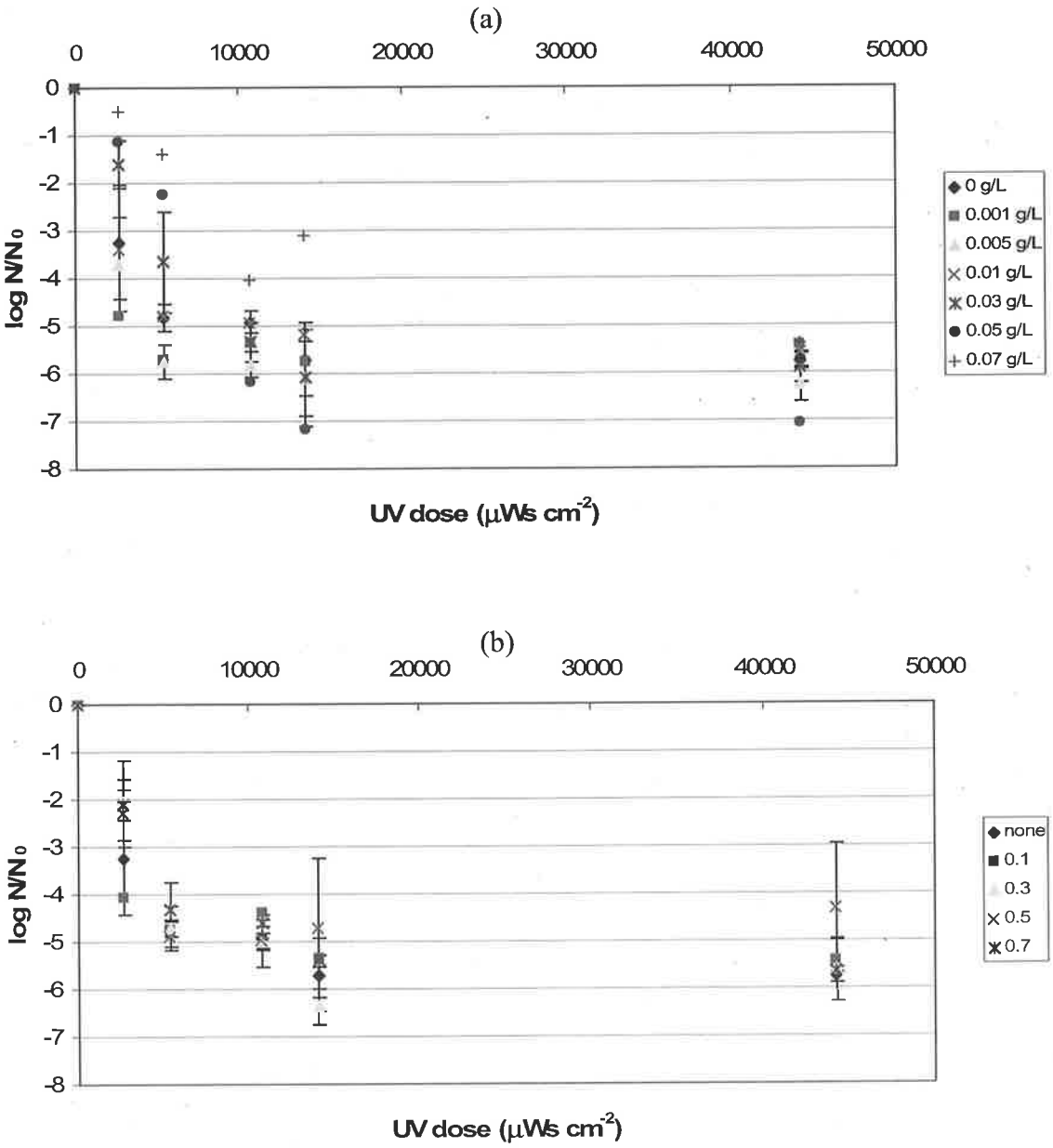

Figure 6.3. Experimental UV disinfection data for *Escherichia coli* in RO water (presented as $\log_{10} N/N_0$) in the presence of: (a) absorbing agent, and (b) shielding agent, with data averaged based on agent concentration

Figure 6.2a shows the disinfection data pooled on the basis of absorbing agent concentration. A trend is observed for concentrations of 0.01, 0.03, 0.05 and 0.07 g L^{-1} at the UV dose of 2,700 μWs cm^{-2}. This is that as absorbing agent concentration is increased over the range of 0.01 to 0.07 g L^{-1}, a lower level of disinfection is observed. This suggests that the initial rate of disinfection might depend on the concentration of absorbing agent present. Any decrease in absorbing agent below 0.01 g L^{-1} might be insufficient to appreciably affect the initial rate of UV disinfection.

Figures 6.3a and 6.3b respectively present the averaged disinfection response for fixed concentrations of absorbing and shielding agent. From Figure 6.3a, a variation in the level of disinfection efficacy can be seen of 4-$\log_{10}$ reductions at the initial UV dose of 2,700 μWs cm^{-2}. In the tailing region the level of disinfection efficacy ranges from 5 to 7-$\log_{10}$ reductions. The variation in the level of disinfection for the shielding agent (Figure 6.3b) is greater, with between 3 to 7-$\log_{10}$ reductions in the tail (UV dose > 14,100 μWs cm^{-2}). For the averaged disinfection data, where there exists only a single set for a given concentration of either additive, no representation of the variance is made.

Overall the experimental disinfection data reveal a level of disinfection efficacy of between 5 to 7-$\log_{10}$ reductions with a minimum UV dose of ~14,100 μWs cm^{-2} when absorbing agent is present. And, that there is no apparent difference in the maximum level of disinfection efficacy using the LC5™ disinfection unit over the range of concentrations of both shielding and UV absorbing agent. This means there is no systematic effect on the level of disinfection with suspended solids or absorbing agent concentrations.

An attempt was made to more clearly distinguish between the effects of different additive concentrations on the observed level of disinfection by pooling the disinfection data for each concentration of additive. Figure 6.2 shows the disinfection data for both absorbing and shielding agent, where the data sets obtained for a given concentration of either additive have been pooled.

Figure 6.2b shows the disinfection data pooled on the basis of shielding agent concentration. No observations can be made other that the data set for the shielding agent concentration of 0.3 g L^{-1} largely spans the remaining data. However, at the initial UV dose of 2,700 μWs cm^{-2}, the disinfection data for a concentration of 0.3 g L^{-1} spans those data for concentrations of 0.5 and 0.7 g L^{-1} respectively – describing between 1 and 3-log_{10} reductions. For lower concentrations of shielding agent (0.1 g L^{-1} and none), a 4-log_{10} reduction is observed at the initial UV dose of 2,700 μWs cm^{-2}. This variance in the UV disinfection data (particularly for a shielding agent concentration of 0.3 g L^{-1}) may make it difficult to deduce the effect of the shielding agent concentration on the initial rate of disinfection. An elevated level of disinfection is also observed for a shielding agent concentration of 0.3 g L^{-1} and UV dose of 14,100 μWs cm^{-2}, where a 6 to 7-log_{10} reduction is observed. This compares to between 4 to 6-log_{10} reductions for the remaining disinfection data.

A further attempt was made to more clearly distinguish between the data sets corresponding to different concentrations of additive, by averaging the observed levels of disinfection (measured as log_{10} reductions) at a given UV dose, and representing the variance in the data as standard deviations.

6.2.1 Effect of initial concentration of viable bacteria (N_0)

The initial concentration of viable bacteria in the feed-tank ranged from 2×10^6 to 10^9 bacteria mL^{-1}. Four series of disinfection trials were conducted in the absence of any additive, with initial bacterial concentrations ranging from about 6×10^6 to 3×10^8 bacteria mL^{-1} (These trials are presented as data sets 1, 2, 3 and 22 in Appendix O – Experimental disinfection data).

Figure 6.4 presents UV disinfection data for *E. coli* when neither agent is present for initial viable cell concentrations ranging from 6.60×10^6 to 3×10^8 mL^{-1}. The kinetics shown exhibit the typical tailed response associated with practical UV disinfection. A disinfection level of between 5 to 6-log_{10} reductions is observed in the tail across all data. There is a large variance in the data at low values of UV dose. It appears that when no agent is present, the initial rate of disinfection increases for decreasing initial levels of contaminant bacteria as observed at a UV dose of 2,700 μWs cm^{-2}.

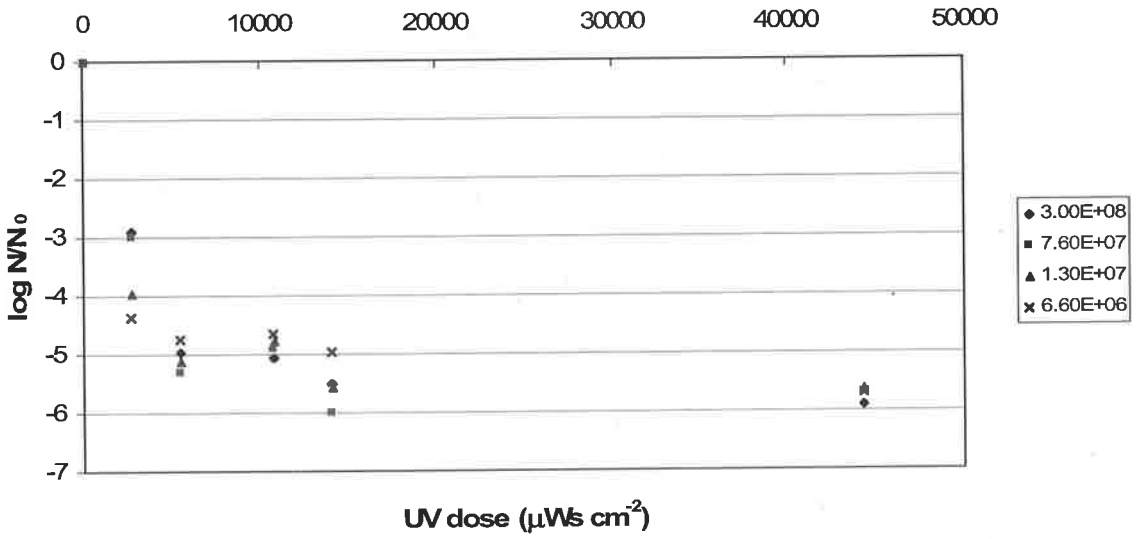

Figure 6.4. Experimental UV disinfection efficacy for *Escherichia coli* in RO water (presented as $\log_{10} N/N_0$) in the absence of absorbing or shielding agent for a range of initial cell concentrations: 6.60×10^6 to 3×10^8 mL^{-1}

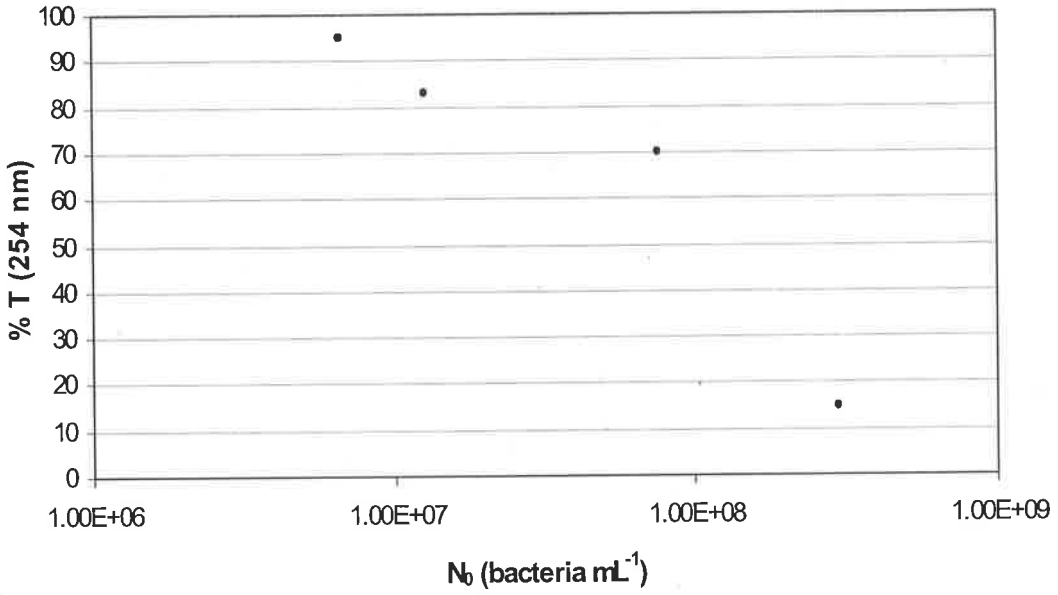

Figure 6.5. Percent transmission (at 254 nm) of feed-water as affected by initial concentration of viable bacteria (N_0)

Figure 6.5 shows the effect of initial concentration of bacteria (bacteria mL^{-1}) on transmission of the feed-water without absorbing or shielding agent present. The transmission is seen from the figure to decrease from 95 to 15 % for a respective increase in initial viable bacteria concentration from 6.64×10^6 to 2.99×10^8 mL^{-1} – and is seen to decrease log-linearly with respect to initial bacteria concentration.

The effect of the initial concentration of viable bacteria on transmission of a given feed-water (containing no agent) can be coupled with the observed initial rates of disinfection. Namely, at low UV doses (< 5,000 $\mu Ws\ cm^{-2}$), a reduced transmission (afforded by a high concentration of bacteria) appears sufficient to reduce the level of disinfection (i.e. the initial rate of disinfection). However, as the UV dose is increased (> 10,000 $\mu Ws\ cm^{-2}$) from the initial region of disinfection, the dose received by the cells is likely to be that to give a maximum level of disinfection – regardless of the transmission of the feed-water. This feature will be characteristic of the contact time and UV intensity distributions within the UV disinfection unit.

6.2.2 Effect of agent concentration on transmission

The effect of concentration of both absorbing and shielding agent on the transmission of unseeded feed-water (i.e. with no bacteria present) was quantified in a set of calibration studies. Figure 6.6 presents a set of calibration curves for the effect of absorbing agent (Figure 6.6a: instant coffee) and shielding agent (Figure 6.6b: Celite 503™) on UV transmission. Both curves show reduced levels of transmission with increases in agent concentration. The calibration data are the mean of three replicates at each agent concentration.

The figure highlights that, when in comparable concentrations (i.e. < 0.1 g L^{-1} for Celite 503™), the absorbing agent has a greater effect on reducing UV transmission than the shielding agent. For example, to achieve a transmission of ~50 % in the unseeded feed-water, 0.04 g L^{-1} of absorbing agent would be required in comparison to 0.7 g L^{-1} of shielding agent. Similarly, the transmission for absorbing agent at a concentration of 0.07 g L^{-1} is less than 30 %, whereas for an absorbing agent concentration 10 times greater, the transmission is reduced to only 50 %.

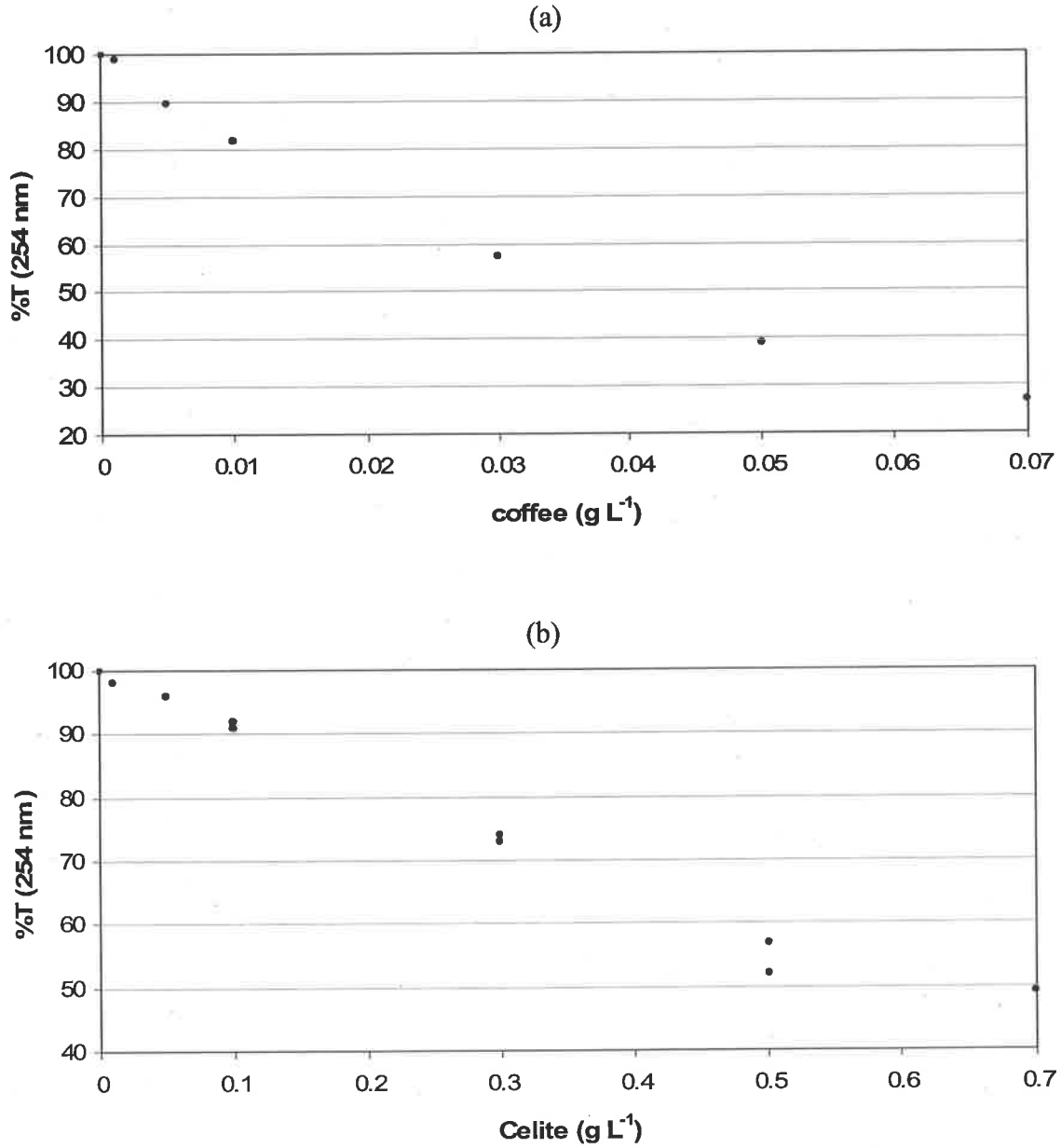

Figure 6.6. Calibration curves for the effect of: (a) absorbing agent, and (b) shielding agent on the percent transmission of unseeded RO water

6.2.3 Influence of pH and temperature

During the disinfection trials, the pH of the feed-water varied from 4.61 to 7.07 in the presence of absorbing agent (coffee), and from 6.02 to 7.82 in the presence of the shielding agent (Celite 503^{TM}). These ranges are not considered to have any impact on the viability of the contaminant cells of *E. coli*, or on the disinfection kinetics. Further, the temperature of the feed-water ranged from 23 to 26 °C over the trials. It is known that temperature has little effect on UV disinfection (Meulemans 1987; Nguyen 1999). There was no need therefore to control the feed-water temperature during the experimental evaluation of the pilot scale UV disinfection apparatus.

Figure 6.7 illustrates the effect of concentration of both absorbing agent and shielding agent on feed-water pH. Large variation in measured values of pH can be seen from the figure for both agents.

No obvious trend in pH value with absorbing agent concentration can be gleaned from the figure. However, it can be seen that pH is lowest (<5) for the two highest absorbing agent concentrations (0.05 and 0.07 g L^{-1}). The feed-water solution overall is seen to be slightly acidic when absorbing agent is present. The data presented in Figure 6.7 underscores that it is not possible to adequately correlate observed pH with the concentration of either additive over the ranges studied.

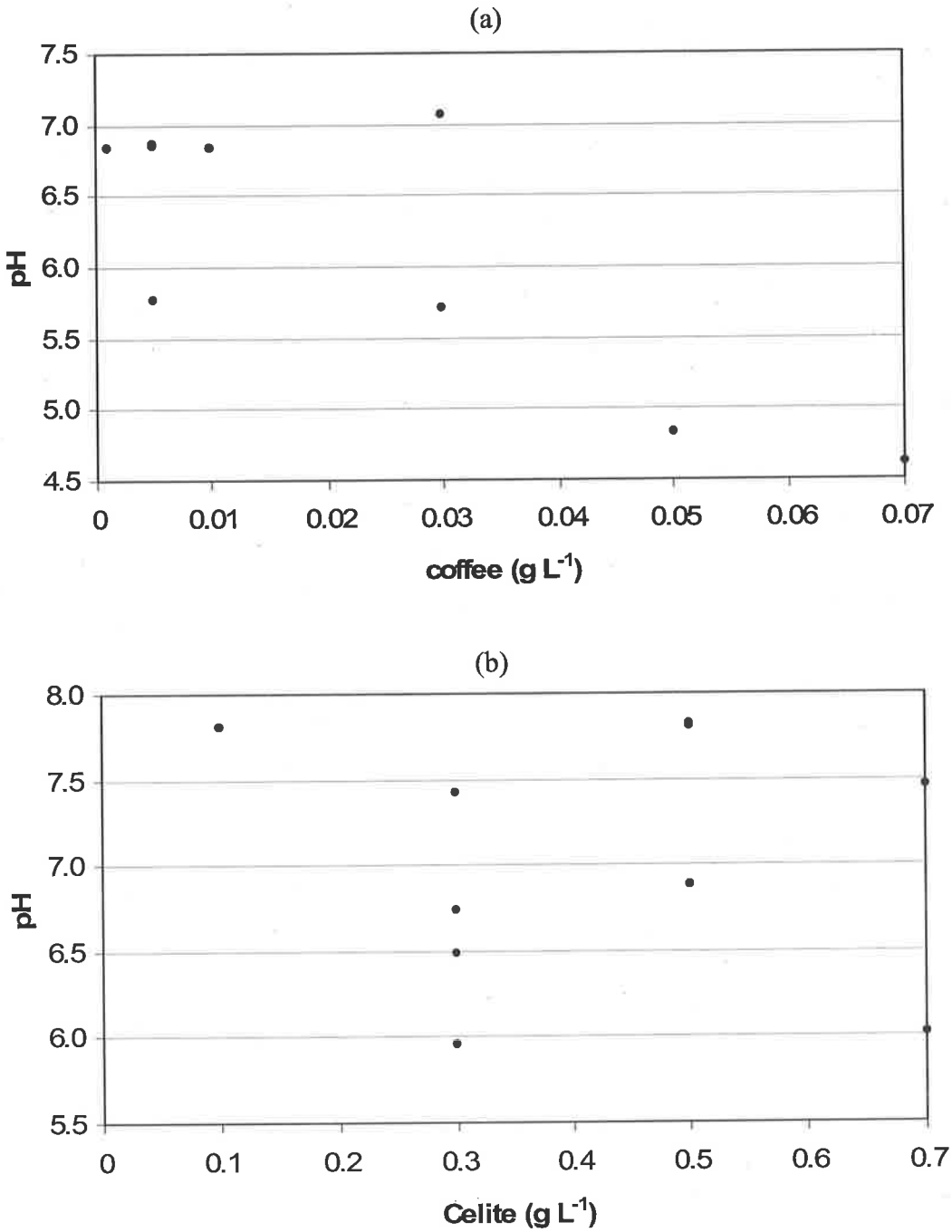

Figure 6.7. Effects of additive concentration on measured pH: (a) absorbing agent and (b) shielding agent

6.2.4 Dye studies

The range of flow rates utilised in this UV disinfection study ranged from 1 to 4 L min^{-1}. This corresponds to a Reynolds' number range of 1,900 to 7,600 (*see* Appendix E). From the Reynolds' number it is clear that the hydrodynamic regime spans the transitional region between laminar and turbulent (Gerhart, Gross and Hochstein 1993). This may lead to a non-uniform distribution of residence times through the UV disinfection unit, particularly at low flow rates, and hence give rise to a range of dose distributions within the disinfection control-volume. This clearly has implications for the modelling of observed UV disinfection kinetics. At the higher flow rates, the deviation from the plug flow assumption may be negligible as a Reynolds' number in excess of 4000 usually indicates stable turbulent flow in a pipe (Gerhart, Gross and Hochstein 1993).

Figure 6.8 is a composite of six typical time-lapse digital images of the Methylene Blue dye studies. The flow rate is the maximum used in this study of 4 L min^{-1} (Re = 7,600), and the water temperature is ~ 22 °C. From part (a) of the figure, in the lower left of the image, dye can be seen to enter the LC5^{TM} disinfection unit. Each successive image (parts (b) through (f)) illustrates the time-lapse of the dye as it proceeds through the disinfection unit. Some axial dispersion, indicated by the light tip of the velocity profile, can be seen upon entry to the LC5^{TM} disinfection unit in part (a). This is seen to increase along the length of the tube in part (b). The water flow through the bend begins breaks down the established hydrodynamic flow pattern. There is increasing dispersion evident in the water as it leaves the bend shown by parts (c) and (d). The flow pattern begins to re-develop however prior to exiting the LC5^{TM} disinfection unit seen in parts (e) and (f). Overall, however, the effects of dispersion on mean residence time appear negligible other than for flow exiting the bend., The flow hydrodynamics can therefore be considered uniform through the LC5^{TM} disinfection unit at the maximum flow rate of 4 L min^{-1}.

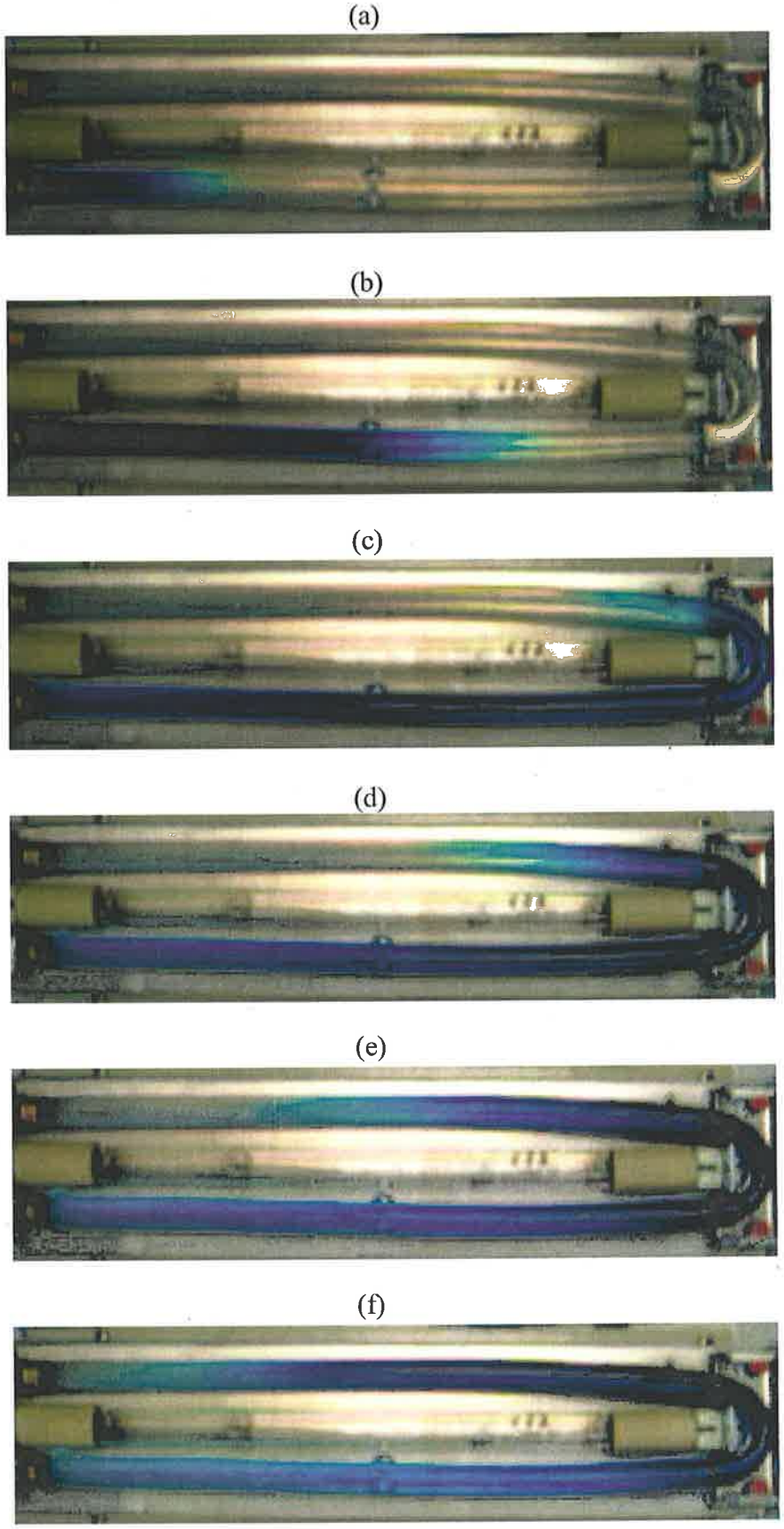

Figure 6.8. Time-lapse digital record of flow hydrodynamics in the LC5^{TM} disinfection unit for a water flow rate of 4 L min^{-1}.

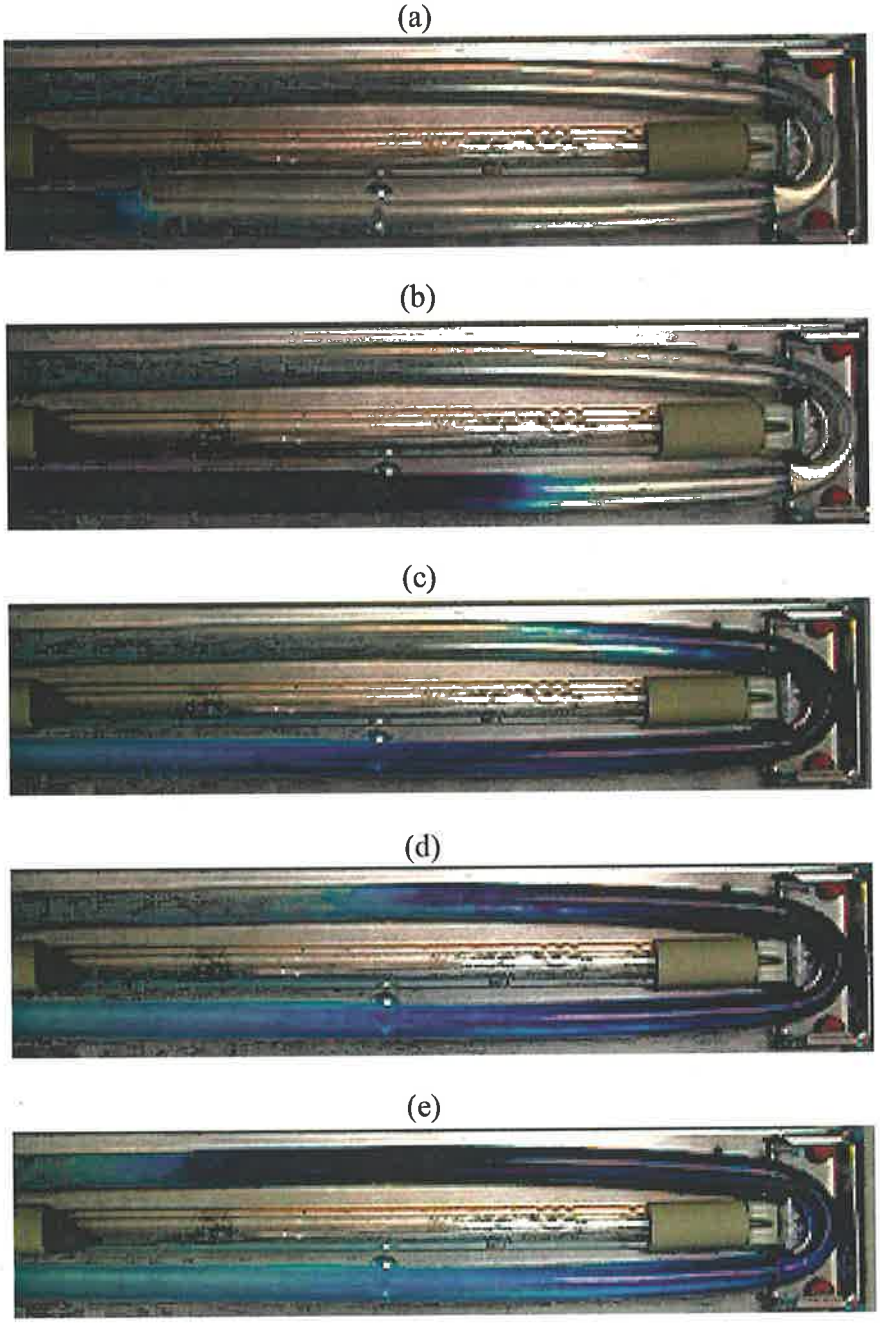

Figure 6.9. Time-lapse digital record of flow hydrodynamics in the LC5^{TM} disinfection unit for a water flow rate of 1 L min^{-1}

It was also of interest to investigate the flow hydrodynamics at the minimum experimental flow rate of 1 L min^{-1} (Re = 1,900). Figure 6.9 is a composite of five typical time-lapse images at a flow rate of 1 L min^{-1}. From this figure, some axial dispersion prior to entering the bend can be seen in part(b), but it is observed that the bend exerts substantial drag on the fluid and causes disruption of the hydrodynamic flow pattern leaving the bend (part (c)). In particular, the flow velocity on the interior of the bend can be inferred from the

figure to be slowed. This will result in a high UV dose delivered to those bacteria occupying these fluid elements. The hydrodynamic flow remains disturbed for a short duration (part (c)) then appears to re-develop (parts (d) and (e)) prior to leaving the LC5^{TM} disinfection unit. For these low flow rates, it appears that a significant proportion of the water flow leaving the bend might be flowing slower than the bulk velocity.

From observation of both Figures 6.8 and 6.9, it can be concluded that there is importantly no gross hold-up or short-circuiting of water in the UV disinfection unit control volume. Excessive non-uniform water hydrodynamics, and the resultant distribution of residence times through the UV disinfection unit, will give rise to a complex dose distribution within elements of water in the disinfection unit. The experimental evidence carefully obtained from these dye studies utilising digital photography highlights that at the higher flow rates used in the UV disinfection trials (1 to 4 L min^{-1}), any deviation from the assumption of plug flow can be assumed negligible. This finding is underscored by that of Gerhart, Gross and Hochstein (1993) who state that at Reynolds' numbers in excess of 4,000, flow in a smooth pipe is typically stable and turbulent.

6.2.5 Assessment of pre-exposure to UV on resulting disinfection efficacy

An assessment of whether prior UV irradiation of bacterial cells of *E. coli* may have an effect on the subsequent disinfection kinetics of daughter cells was made.

A single viable colony was exposed to a UV dose of 44,200 μWs cm^{-2} (the maximum experimental dose), and was subsequently used to inoculate sterile Nutrient Broth. A bacterial concentrate prepared from this Nutrient Broth was used to seed the feed-water for a subsequent UV disinfection trial.

Figure 6.10 presents the efficacy of UV disinfection (as $\log_{10} N/N_0$) for the bacteria cultured from the sub-lethally damaged single-cell, and also for pooled survival data generated in the absence of either agent (Table 6.1: data sets 1, 2 and 3). No difference in the response of the two data sets is evident through inspection of Figure 6.10. These findings strongly suggest that prior UV exposure has no effect on disinfection kinetics for subsequently cultured bacterial cells of *E. coli*.

It was hypothesized that there is no accumulated UV resistance or susceptibility within a sub-lethally damaged bacterial cell, and hence; subsequently cultured daughter cells will exhibit an unchanged kinetic response. Statistical tests have shown there to be no difference in the UV response of the bacteria grown from the sub-lethally damaged survivors. These tests are outlined in Appendix D.

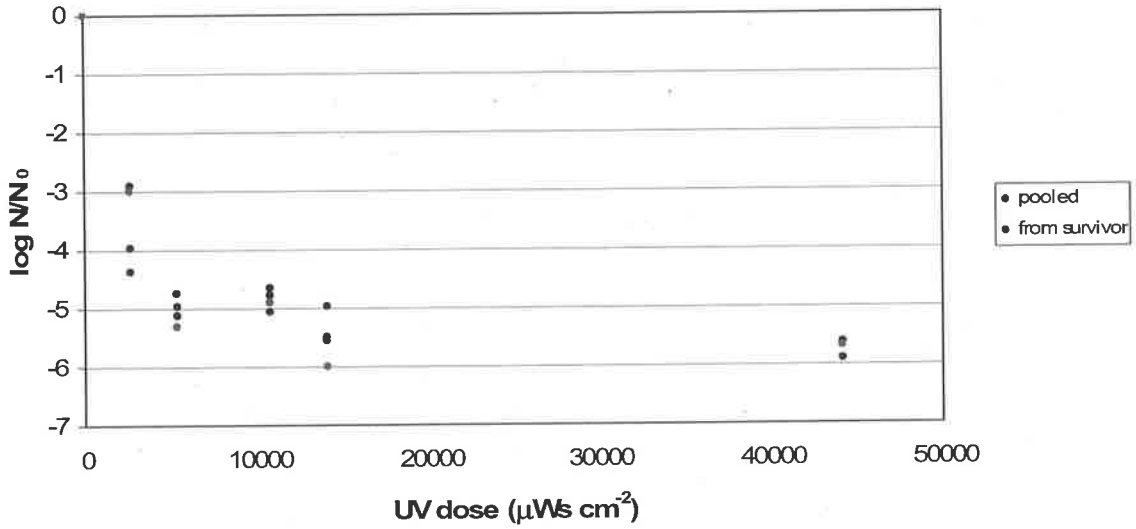

Figure 6.10. Reduction in viable numbers of bacteria following UV exposure. The pooled data are displayed as ●, with the data from the cultured survivor shown as ●

Importantly, these results show that exposure to a sub-lethal UV dose does not make a bacterial contaminant, specifically *E coli* ATCC 25922, more susceptible to UV damage or, more importantly, increasingly resistant to subsequent UV exposure. No UV induced resistance appears to be passed on to successive generations of daughter cells.

Blatchley *et al.* (2001) also found no discernable difference in the kinetic response of parent and daughter cells of *E. coli* over the UV dose range of 0 to 100,000 µWs cm^{-2}.

6.3 Validation of two new models for UV disinfection

The following presents a validation of the two new models for UV disinfection, namely the modified exponentially damped polynomial (EDP_m) and Weibull forms, fitted to the extensive experimental disinfection data. These disinfection data are of a form suitable to assess the ability of a model to predict tailing observed in UV disinfection data. This validation is coupled with an in-depth analysis of the experimental UV disinfection kinetics.

The influence of six (6) non-zero absorbing agent concentrations, ranging from 0.001 to 0.07 g L^{-1}, and four (4) non-zero concentrations of shielding agent, ranging from 0.1 to 0.7 g L^{-1}, on the UV disinfection kinetics of *E. coli* (ATCC 25922) are investigated throughout this study. The five (5) UV doses considered are: 2,700; 5,400; 10,800; 14,100; and, 44,200 μWs cm^{-2}.

Both models were found to be of a suitable form to account for the tailing observed in the experimental UV disinfection data.

6.3.1 Modified Exponentially Damped Polynomial

The EDP_m model parameters are summarised in Table 6.4, for the model fitted to each of the experimental data sets (as outlined in Table 6.1). The model was typically fitted to a set containing six (6) data points, with data-set 15 consisting only of four (4) data points, to describe the observed disinfection kinetics. The *P-values* associated with each of the model parameters generally have a value of less than 0.05, indicating the model parameters are highly (statistically) significant. The noticeable exceptions are P-values of: 0.197 and 0.334 for the damping coefficient (λ) and breakpoint dose ($[dose]_B$) respectively for data set 14; 0.152, 0.606 and 0.751 for the disinfection rate coefficient (k), damping coefficient and breakpoint dose respectively for data set 19, and; 0.060, 0.138 and 0.211 for the disinfection rate coefficient, damping coefficient and breakpoint dose respectively for data set 23. The reduced significance of model parameters fitted against data set 23 is due in part to five (5) data only used to fit the model as opposed to six (6) data in most other cases – affording one less degree of freedom for a fit of the model in this instance. This extra degree of freedom is particularly significant when fitting models to small sets of data (Snedecor and Cochran 1969; Montgomery 2001). The residual sum of squares for each of the model fits ranged from a value of 0.03 (data set 6) to 2.13 (data set 18).

Table 6.4. EDP_m model parameters for each experimentally observed data set

Data Set	n	Model Parameters									
		k			λ			$[dose]_B$			
		estimate	t-value	P-value	estimate	t-value	P-value	estimate	t-value	P-value	RSS *
1	6	1.60×10^{-3}	8.8	3.10×10^{-3}	1.14×10^{-4}	6.8	6.53×10^{-3}	8.51×10^{3}	6.4	7.63×10^{-3}	0.25
2	6	2.34×10^{-3}	6.6	7.17×10^{-3}	1.70×10^{-4}	5.7	1.09×10^{-2}	5.78×10^{3}	5.6	1.15×10^{-2}	0.23
3	6	3.46×10^{-3}	8.4	3.55×10^{-3}	2.81×10^{-4}	7.7	4.54×10^{-3}	3.49×10^{3}	7.8	4.44×10^{-3}	0.04
4	6	3.03×10^{-3}	11.5	1.41×10^{-3}	1.97×10^{-4}	10.1	2.05×10^{-3}	5.09×10^{3}	9.8	2.23×10^{-3}	0.10
5	6	2.38×10^{-3}	12.6	1.08×10^{-3}	1.42×10^{-4}	10.2	2.03×10^{-3}	6.94×10^{3}	9.8	2.29×10^{-3}	0.14
6	6	1.85×10^{-3}	20.4	2.56×10^{-4}	1.39×10^{-4}	16.4	4.94×10^{-4}	7.04×10^{3}	15.8	5.48×10^{-4}	0.03
7	6	2.46×10^{-3}	6.5	7.26×10^{-3}	1.68×10^{-4}	5.6	1.12×10^{-2}	5.82×10^{3}	5.5	1.17×10^{-2}	0.33
8	6	1.13×10^{-3}	7.1	5.74×10^{-3}	7.95×10^{-5}	5.4	1.26×10^{-2}	1.23×10^{4}	4.9	1.59×10^{-2}	0.44
9	6	2.71×10^{-3}	4.4	2.18×10^{-2}	2.15×10^{-4}	3.9	3.01×10^{-2}	4.56×10^{3}	3.9	3.05×10^{-2}	0.39
10	6	1.44×10^{-3}	5.1	1.43×10^{-2}	1.16×10^{-4}	3.9	2.91×10^{-2}	9.12×10^{3}	3.5	3.91×10^{-2}	0.55
11	6	1.57×10^{-3}	6.5	7.42×10^{-3}	1.05×10^{-4}	5.0	1.57×10^{-2}	9.64×10^{3}	4.5	2.02×10^{-2}	0.56
12	6	1.35×10^{-3}	5.2	1.39×10^{-2}	1.00×10^{-4}	4.0	2.86×10^{-2}	9.89×10^{3}	3.6	3.56×10^{-2}	0.74
13	6	1.65×10^{-3}	4.7	1.82×10^{-2}	1.07×10^{-4}	3.6	3.69×10^{-2}	9.59×10^{3}	3.2	4.76×10^{-2}	1.12
14	6	7.63×10^{-4}	3.7	3.39×10^{-2}	3.77×10^{-5}	1.7	1.97×10^{-1}	3.09×10^{4}	1.1	3.34×10^{-1}	1.51
15	4	1.20×10^{-3}	-	-	8.51×10^{-5}	-	-	1.08×10^{4}	-	-	1.82
16	6	1.58×10^{-3}	-	-	9.36×10^{-5}	-	-	1.08×10^{4}	-	-	1.66
17	6	7.17×10^{-4}	-	-	3.15×10^{-5}	-	-	3.85×10^{4}	-	-	0.53
18	6	7.34×10^{-4}	-	-	3.04×10^{-5}	-	-	3.85×10^{4}	-	-	2.13
19	6	3.70×10^{-4}	1.9	1.52×10^{-1}	2.50×10^{-5}	0.6	6.06×10^{-1}	4.03×10^{4}	0.3	7.51×10^{-1}	1.57
20	6	9.73×10^{-4}	8.7	3.21×10^{-3}	7.11×10^{-5}	6.3	8.26×10^{-3}	1.32×10^{4}	5.8	1.04×10^{-2}	0.27
21	6	1.29×10^{-3}	4.8	1.71×10^{-2}	8.61×10^{-5}	3.8	3.20×10^{-2}	1.11×10^{4}	3.6	3.70×10^{-2}	1.11
22	6	1.67×10^{-3}	5.1	1.45×10^{-2}	1.12×10^{-4}	3.9	2.94×10^{-2}	8.85×10^{3}	3.7	3.54×10^{-2}	0.85
23	5	1.05×10^{-3}	3.9	6.04×10^{-2}	7.07×10^{-5}	2.4	1.38×10^{-1}	1.11×10^{4}	1.8	2.11×10^{-1}	0.82

* RSS denotes residual sum of squares

Bates and Watts (1988) state that it is insufficient to reject model parameters on the basis of *P-value* alone, with the primary aim of model development to describe behaviour of the data. Clearly, all three EDP_m parameters are significant in describing the fundamental action of UV disinfection kinetics. The observed *t-values*, or test statistic, (measure of the parameter estimate in relation to its associated standard error) for parameter estimates of each data set further support the notion that each of the model parameters is significant when fitted to these experimental UV disinfection data.

The model parameters of Table 6.4 show, across the range of experimental data, the disinfection rate coefficient (k) can be seen to vary from 3.70×10^{-4} to 3.46×10^{-3} μWs^{-1} cm^2, whilst the damping coefficient (λ) was seen to vary from 2.50×10^{-5} to 2.81×10^{-4} μWs^{-1} cm^2 – approximately an order of magnitude change in each case. The breakpoint dose ($[dose]_B$) was seen to range between values of 3.49×10^3 and 4.03×10^4 μWs cm^{-2}. The data-set for which the maximum values of the disinfection rate coefficient and the damping coefficient were observed (data set 3), is that for which the minimum breakpoint dose was also observed. This further supports the earlier finding that the EDP_m parameters are correlated.

Convergence of the parameter estimates was not possible for data sets 15 to 18 inclusive, as shown in Table 6.4, using the non-linear regression techniques employed. As such, *P-values* (or the test statistic) for model parameter estimates could not be determined in these instances. The parameter estimates included for these data sets (Table 6.4) were made through trial and error. It was observed that the residual sum of squares had not converged for these data sets for the values of each of the model parameters reported. This is despite the values obtained for the residual sums of squares in these instances (0.53 to 2.13) being comparable to those of the other data sets.

The predicted *vs.* observed values of the reduction in viable bacteria are displayed by Figure 6.11 (as $\log_{10} N/N_0$) for the EDP_m model applied to all of the (23) experimental disinfection data sets. It is noticed that at low observed levels of disinfection (less than 3-$\log_{10}$ reductions), the EDP_m model generally over-predicts the observed level of disinfection. The data presented in Figure 6.11 show that, importantly however, the model predictions are evenly and randomly distributed over the entire range of data, implying that

the EDP_m model is well parameterised (Ratkowsky 1990), and of a form well suited to describe the tailing behaviour in these UV disinfection data.

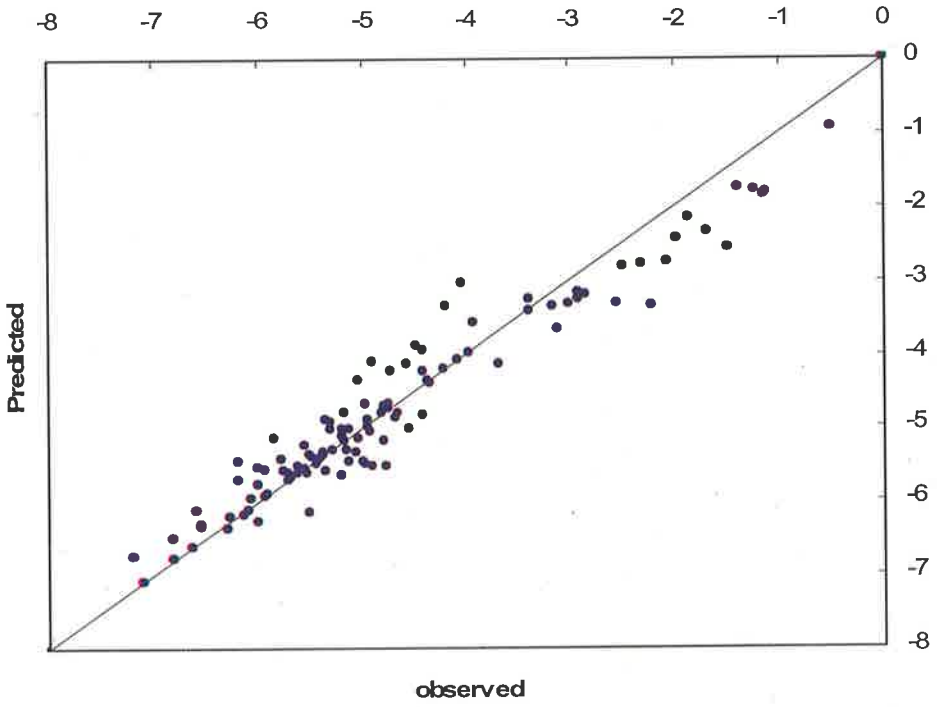

Figure 6.11. Predicted *vs.* observed value of the log-reduction in viable bacteria (as $\log_{10} N/N_0$) from the EDP_m model for the experimental UV disinfection data

The derived model parameters (k, λ and $[dose]_B$ respectively) for fits of the EDP_m model to each of the experimental data-sets are presented by Figures 6.12 to 6.14, together with associated standard errors. Collectively across all data-sets, Figures 6.12 and 6.13 illustrate that a high value for the disinfection rate coefficient (k) is associated with a corresponding high value for the damping coefficient (λ). Namely, where a high initial rate of disinfection is observed, the resulting UV disinfection kinetics will exhibit a high degree of tailing. This is not unexpected since the disinfection rate coefficient (k) and the damping coefficient (λ) were previously found to be linearly dependent, as shown by Figure 4.8a.

Figure 6.14 presents the breakpoint dose, $[dose]_B$, predictions for each data set. The breakpoint dose remains relatively constant across most data sets, except for sets 14, 17, 18 and 19, where an elevated breakpoint dose is observed. Experimental data sets 14 and 19 also display particularly high standard errors in the predicted value of breakpoint dose,

with the standard error associated with data-set 19 distorting the relative values of the remaining data sets.

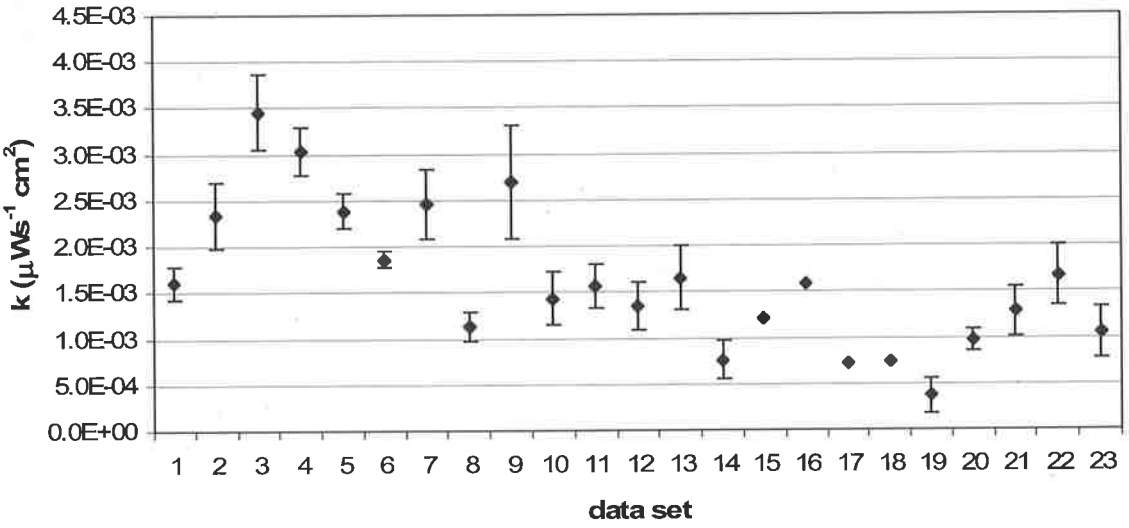

Figure 6.12. The EDP_m disinfection rate coefficient for each of the experimental data sets

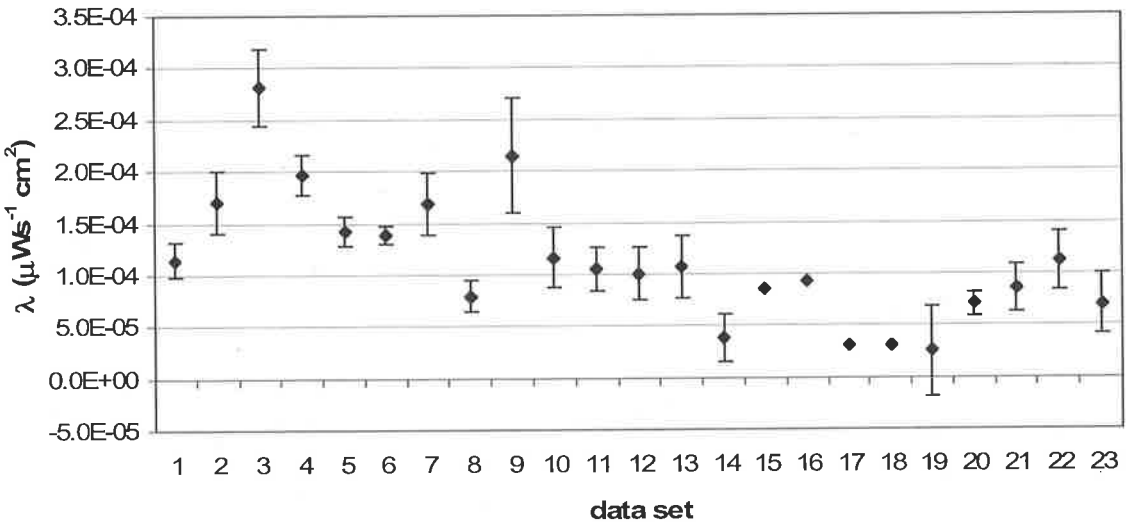

Figure 6.13. The EDP_m damping coefficient for each of the experimental data sets

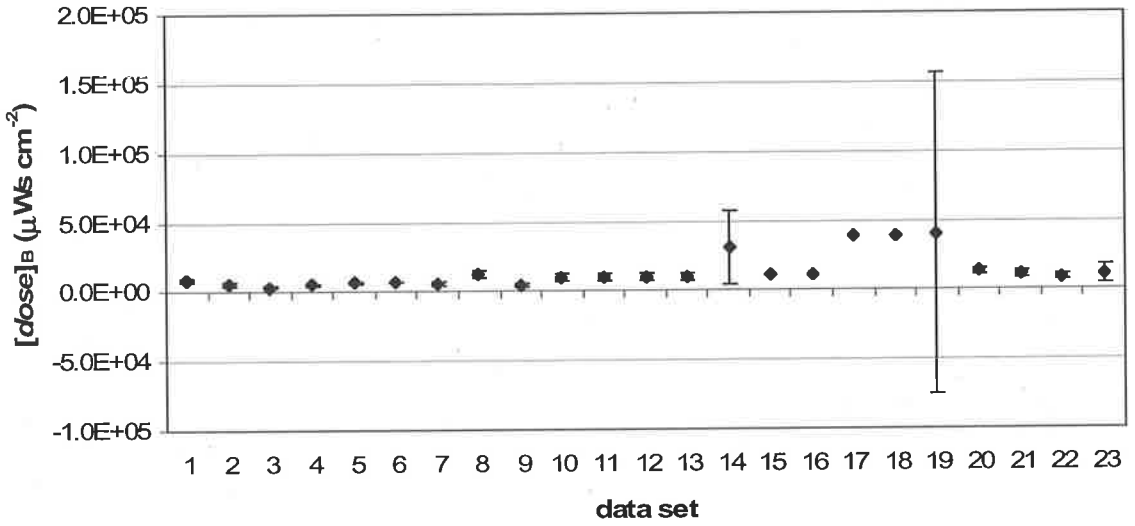

Figure 6.14. The EDP_m breakpoint dose for each of the experimental data sets

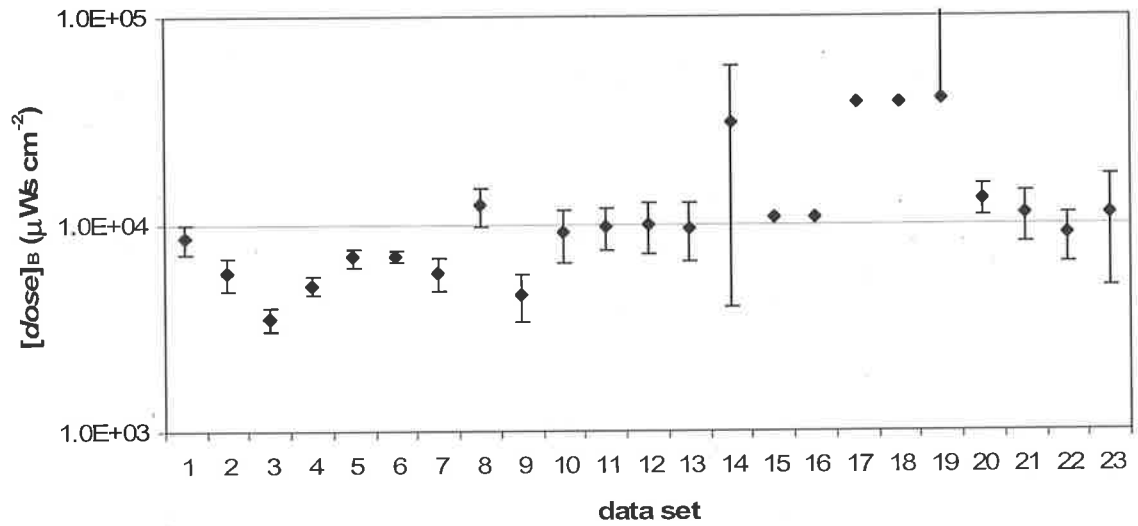

Figure 6.15. The EDP_m breakpoint dose for each of the experimental data sets presented on a logarithmic scale

Figure 6.15 displays the breakpoint dose against the data-set from which it was derived on logarithmic coordinates so as to give a clearer representation of the variation in values across data-sets. It is now evident that the determined values for breakpoint dose vary largely between 5,000 and 10,000 $\mu Ws\ cm^{-2}$. The regression output was found to be highly dependent on the initial estimate of breakpoint dose, and is particularly sensitive to slight variations in some instances.

The EDP_m model parameters were plotted against the concentration of both shielding agent and absorbing agent in order to determine whether either additive had a systematic influence of the EDP_m model parameters over the range of concentrations investigated.

The effect of absorbing agent (as International Roast^{TM} – instant coffee powder) on each of the EDP_m model parameters is presented in Figure 6.16. For an increase in absorbing agent concentration, both the disinfection rate coefficient (k) and the damping coefficient (λ) are seen to decrease. The reduction in rate may be attributed to the lower UV transmittance resulting from an increased concentration of absorbing agent. This, in turn, leads to a reduction in the damping coefficient (since k and λ are proportionally dependent), and less pronounced tailing in the UV survivor response.

Substantial variation in the values of the rate coefficient and the damping coefficient at low concentrations of absorbing agent (< 0.01 g L^{-1}) are evident in Figures 6.16a and 6.16b respectively. This is attributable to the variation in initial concentrations of bacteria present prior to UV exposure, which varies appreciably between sets of data and has a significant effect on UV transmission.

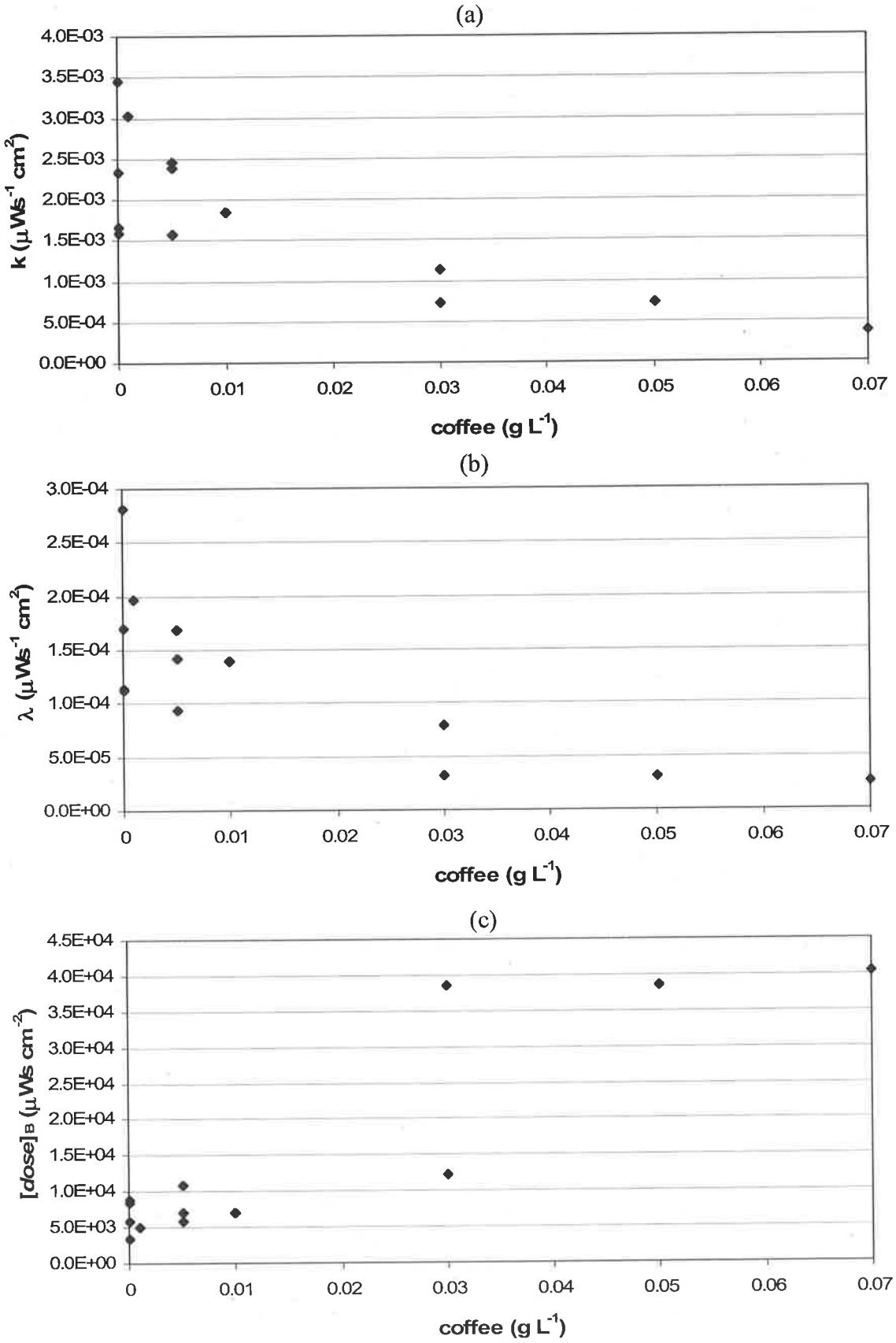

Figure 6.16. The EDP_m model parameters *versus* absorbing agent concentration (a) disinfection rate coefficient k (b) damping coefficient λ (c) breakpoint dose $[dose]_B$

The breakpoint dose $[dose]_B$ is seen to increase with absorbing agent concentration in Figure 6.16c. Higher values for breakpoint dose represents more gradual tailing, and are characteristic of a reduced initial rate of disinfection as measured by k. Notably, for a fixed absorbing agent concentration of 0.03 g L^{-1}, the breakpoint dose varies between 1.23×10^4 and 3.85×10^4 μWs cm^{-2} – almost spanning the entire range of UV doses studied. At this absorbing agent concentration, the reduced initial rate of disinfection (7.17×10^{-4} *cf.* 1.13×10^{-3} μWs^{-1} cm^2) characterised by the higher breakpoint dose of 3.85×10^4 μWs cm^{-2}, is due to a higher concentration of viable bacteria initially present in the water to be treated (1.6×10^8 *cf.* 2.7×10^7 mL^{-1}). For the lower breakpoint dose of 1.2×10^4 $\mu Ws.cm^{-2}$, the initial population of viable bacteria was approximately an order of magnitude lower (2.7×10^7 mL^{-1}), resulting in a higher transmittance of the water, and hence a higher initial rate of disinfection. It should be noted, that of the three breakpoint doses exceeding 35,000 μWs cm^{-2}, two of the parameter estimates are from non-convergent regression analyses (data-sets 17 and 18).

The effect of shielding agent concentration (as Celite 503™) on each of the EDP_m model parameters (when fitted to the experimental disinfection data) is presented in Figure 6.17. As was the case for the absorbing agent, an increase in the concentration of shielding agent led to a reduction in both the disinfection rate coefficient (k) and the damping coefficient (λ). The breakpoint dose ($[dose]_B$) increased accordingly. In particular, the breakpoint dose was seen to vary over a narrower range in the presence of shielding agent, than was generally observed with the absorbing agent. A noticeable outlier at a breakpoint dose of 30,000 μWs cm^{-2} for a shielding agent concentration of 0.3 g L^{-1} was observed. The concentration of viable bacteria present prior to treatment for this data-set is 2.6×10^7 mL^{-1}. This is the lowest initial concentration of viable bacteria for all sets of data generated in the presence of shielding agent at a concentration of 0.3 g L^{-1}.

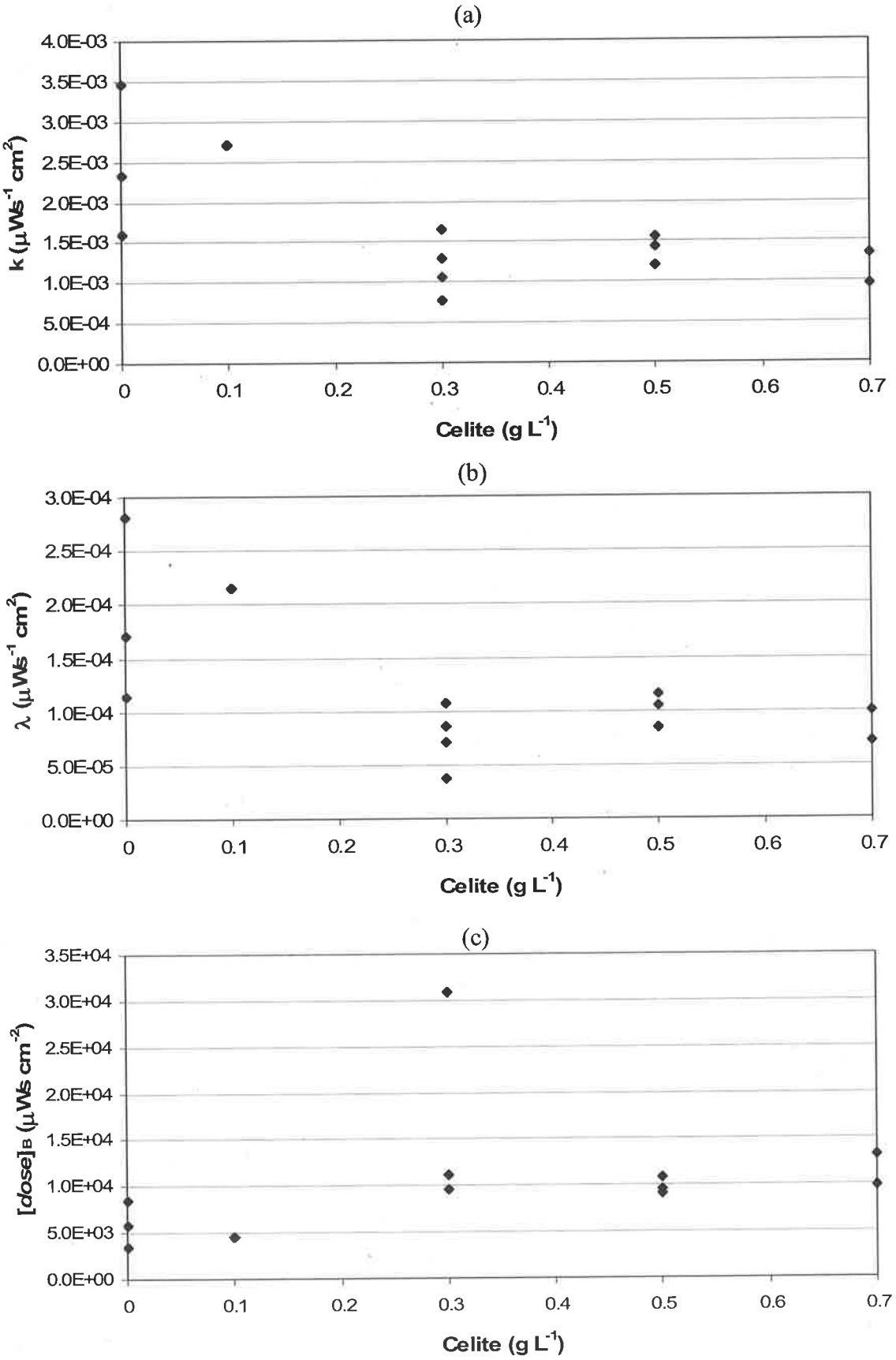

Figure 6.17. The EDP_m model parameters *vs.* shielding concentration (a) disinfection rate coefficient k (b) damping coefficient λ (c) breakpoint dose $[dose]_B$

The remaining disinfection data-sets generated for 0.3 g L^{-1} of shielding agent, namely data sets 13 and 21, both had higher concentrations of viable bacteria present prior to treatment (1.05×10^8 and 7.02×10^7 mL^{-1} respectively), whilst also maintaining higher transmittance (47 % and 57 % respectively compared with 42 %) than for the sample with fewer bacteria initially present before disinfection. Intuitively, this finding makes no sense. The data-set (data-set 14) corresponding to this highest breakpoint dose may therefore have been affected by an unforeseen contaminant, reducing the bulk transmittance of the sample.

The effect of the initial concentration of bacteria prior to treatment (N_0) on the EDP_m parameters for fixed concentrations of both additives was also assessed. The effect of the concentration of viable bacteria prior to treatment on the EDP_m parameters for fixed concentrations of absorbing agent and shielding agent is presented by Figures 6.18 and 6.19 respectively. The response for no additive present is included in each as a point of reference.

In the absence of absorbing agent, Figure 6.18 highlights that both the disinfection rate coefficient and the damping coefficient decrease for increasing concentrations of viable bacteria present prior to UV exposure. Both parameters (k and λ) are sensitive to changes in initial bacterial population below values of 7×10^7 cells mL^{-1}, and are relatively insensitive beyond this initial concentration of viable bacteria.

The breakpoint dose is seen to increase with respect to increasing initial concentrations of viable bacteria when no additive is present. Similarly, the breakpoint dose becomes relatively insensitive to the initial concentrations of viable bacteria once 7×10^7 cells mL^{-1} is exceeded. This indicates a delayed onset of tailing for high concentrations of bacteria to be disinfected (when no additive is present).

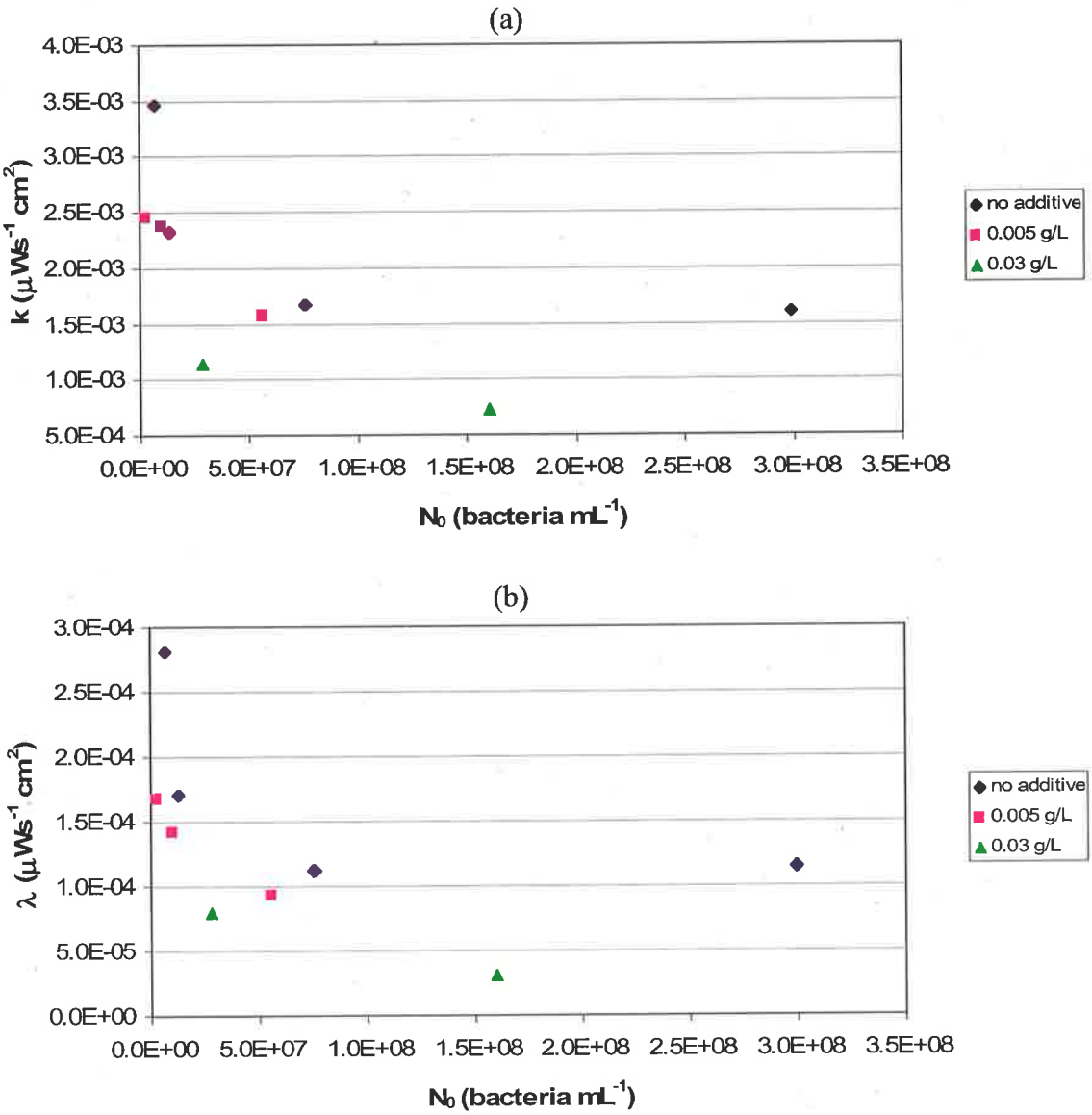

Figure 6.18. The EDP_m model parameters *vs.* initial concentration of viable bacteria for fixed concentrations of absorbing agent: (a) disinfection rate coefficient k (b) damping coefficient λ

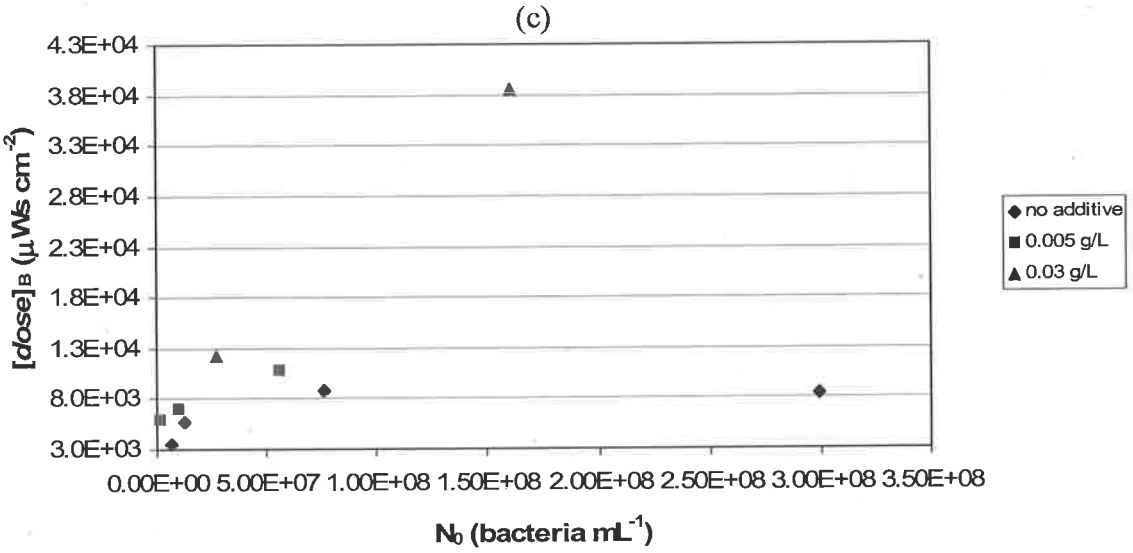

Figure 6.18 (continued). The EDP_m model parameters *vs.* initial concentration of viable bacteria for fixed concentrations of absorbing agent: (c) breakpoint dose $[dose]_B$

It is also clear that when absorbing agent is present (at a given concentration), both the disinfection rate coefficient and the damping coefficient decrease for increases in the concentration of viable bacteria initially present before treatment. Again the breakpoint dose increases with increasing viable populations of bacteria prior to disinfection. It is also noted that both the disinfection rate coefficient and the damping coefficient become increasingly insensitive to changes in the concentration of viable bacteria initially present as the concentration of absorbing agent is increased from 0.005 to 0.03 g L^{-1}. Conversely, the breakpoint dose becomes increasingly sensitive to changes in the initial bacterial population as the concentration of absorbing agent increases. This is consistent with small changes in the initial concentration of viable bacteria present having little, or no, effect on the breakpoint dose when the concentration of absorbing agent is low (or zero). This again highlights the reciprocal nature of breakpoint dose with respect to the remaining EDP_m parameters. Collectively, this illustrates that increasing concentrations of both, bacteria initially present prior to treatment, and soluble UV absorbing agents, act to make the disinfection rate coefficient and the damping coefficient less sensitive to changes in the initial concentration of viable bacteria.

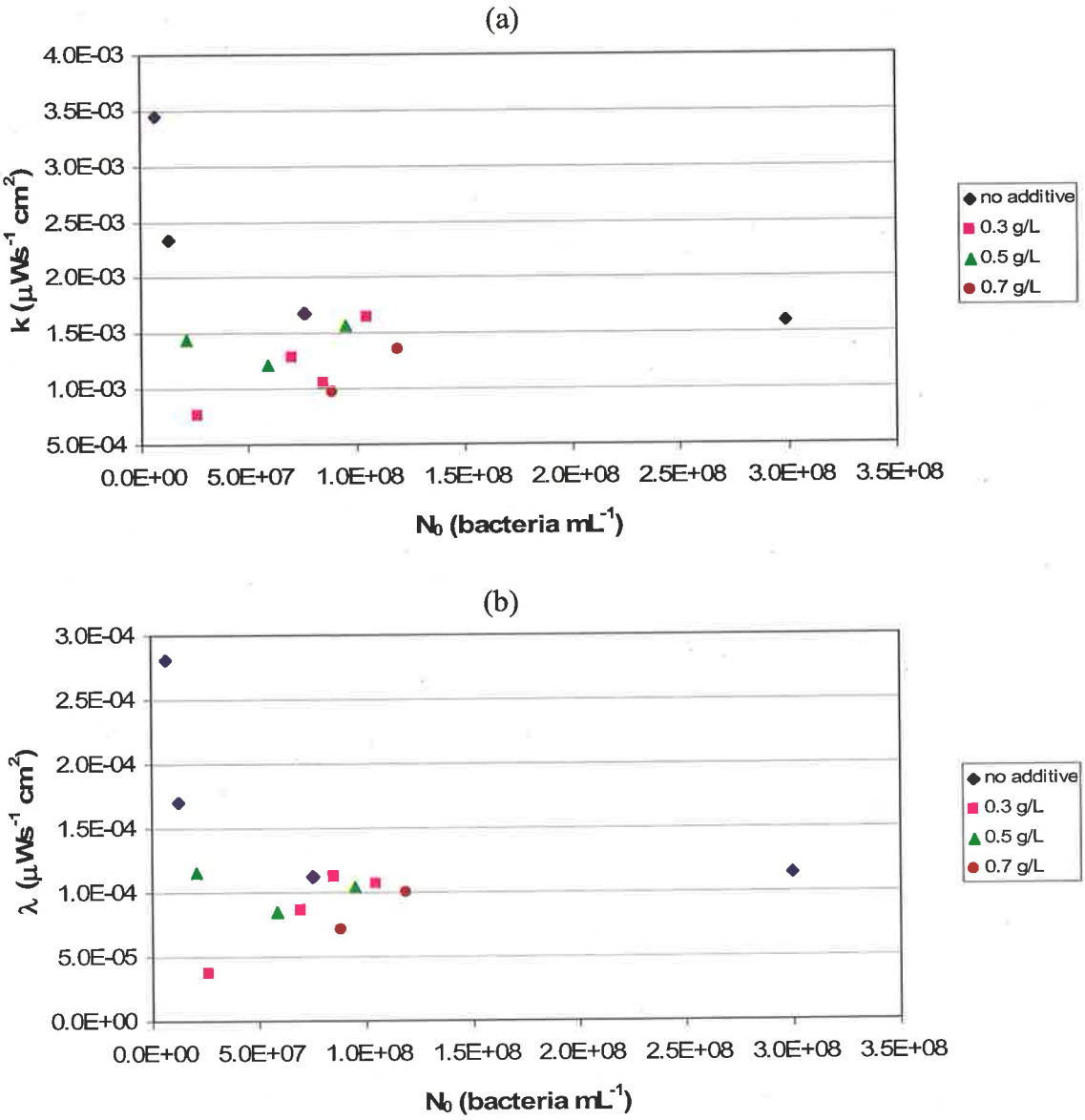

Figure 6.19. The EDP_m model parameters *vs.* initial concentration of viable bacteria for fixed concentrations of shielding agent (a) disinfection rate coefficient k (b) damping coefficient

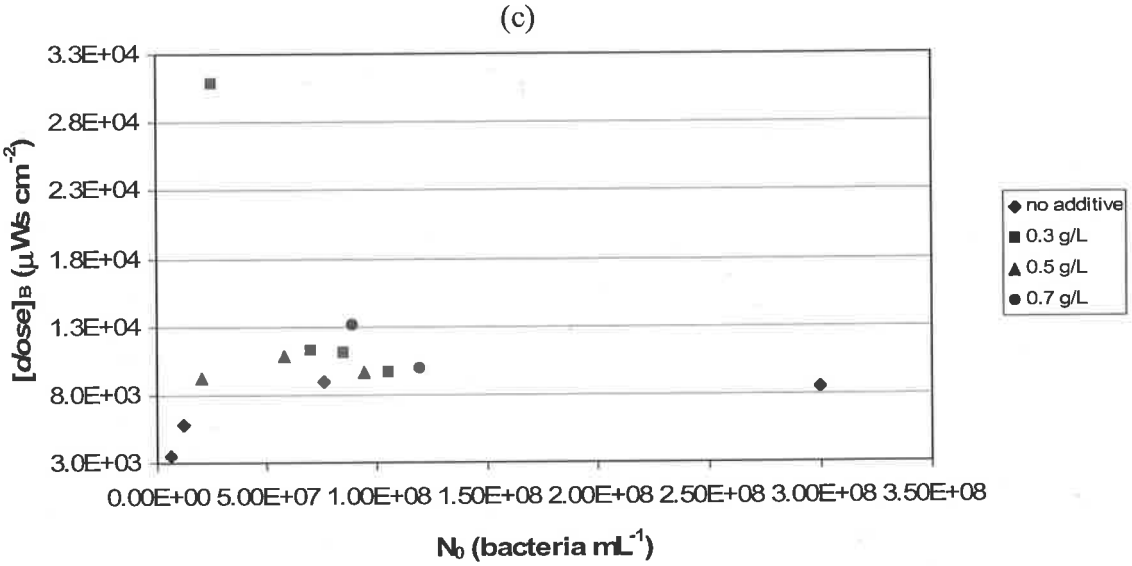

Figure 6.19 (continued). The EDP_m model parameters *vs.* initial concentration of viable bacteria for fixed concentrations of shielding agent (c) breakpoint dose $[dose]_B$

Figure 6.19 highlights that when shielding agent is present at a given concentration, both the disinfection rate coefficient (k) and the damping coefficient (λ) increase with respect to an increase in the concentration of viable bacteria initially present prior to UV treatment. This corresponds to a respective decrease in the observed breakpoint dose under the same conditions. This is despite the data presented (Figure 6.19) for a shielding agent concentration of 0.5 g L^{-1} exhibiting no obvious trends. These findings are in contradiction to those found at fixed absorbing agent levels (Figure 6.18). This highlights that the shielding and absorbing agents differ in the way they effect the EDP_m parameters, and supports the notion that they shielding and absorbing agents differ in the mode by which they act to inhibit UV disinfection.

It is believed that significant amounts of bacteria are being adsorbed to the shielding agent, with clumps of bacteria enumerated as single colonies only, giving an increased estimate of the extent of disinfection. The data presented in Figure 6.19 support the notion that as the concentration of bacteria increases, the shielding agent is occluding a larger number of bacteria. This is in contradiction with the finding of Nguyen (1999) that there was no significant adsorption of *E. coli* to the shielding agent (Celite 503^{TM}) for concentrations as high as 3 g L^{-1}.

The dependent nature of the EDP_m model parameters is again evident when observing the effects of either a fixed agent or bacterial concentration across respective sets of data. Correlations observed between the EDP_m model parameters obtained for fits of the model each of the experimental data sets are presented in Figure 6.20. Standard errors of the respective model parameters have been omitted for clarity.

The correlation between each of the model parameters was of the same nature as those observed when the EDP_m model was fitted to the UV disinfection data of Nelson (2000), namely: the disinfection rate coefficient (k) and the damping coefficient (λ) were again found to be linearly dependent as shown in Figure 6.20a. The correlation of both the disinfection rate coefficient (k) and the damping coefficient (λ) with respect to breakpoint dose $[dose]_B$ was again well represented by a power law relationship. This further highlights that for UV disinfection kinetics exhibiting tailing, a high initial rate of disinfection is coupled with a low breakpoint dose – indicating a rapid onset of tailing.

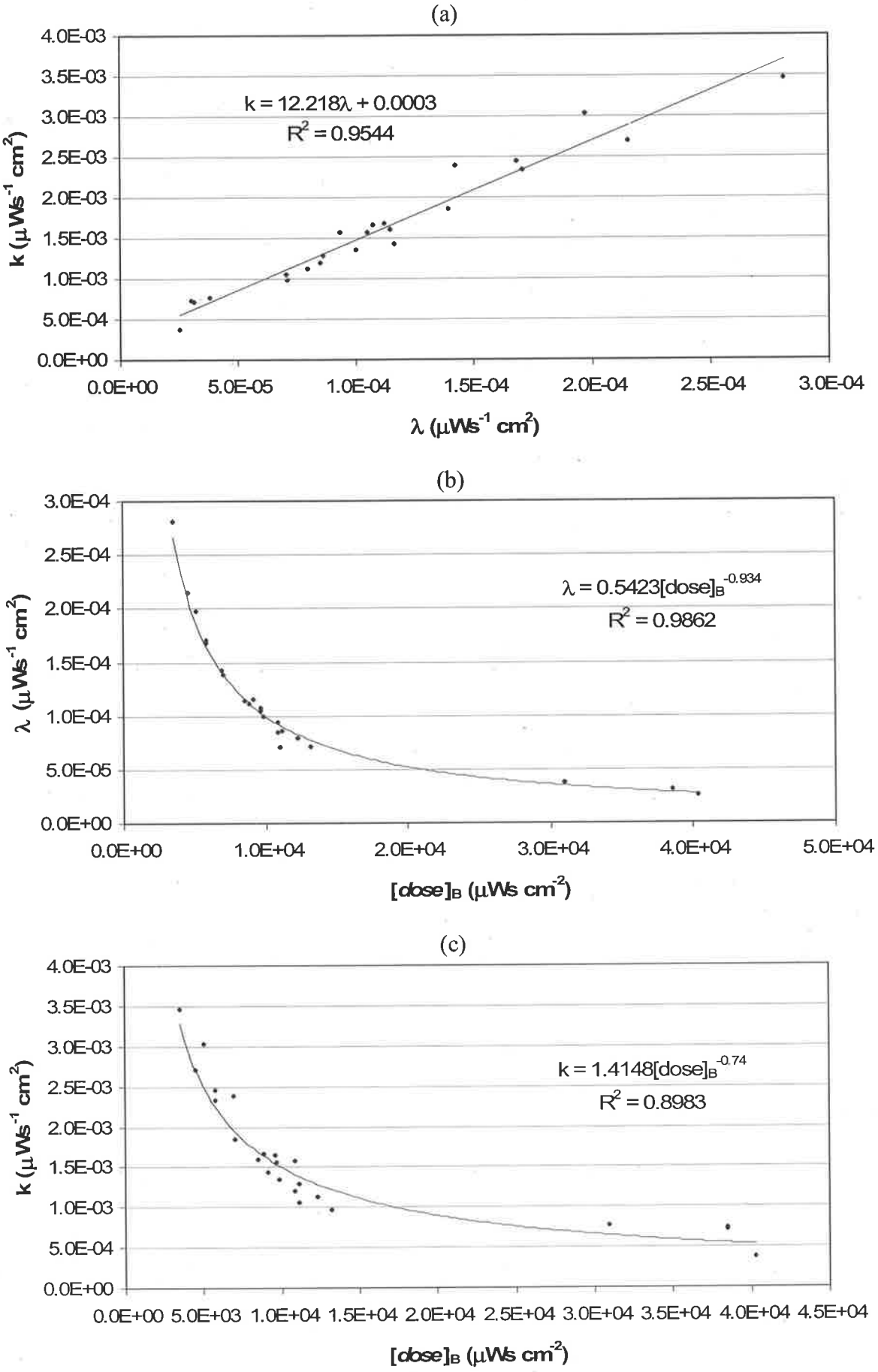

Figure 6.20. Observed correlations between EDP_m model parameters when fitted against the experimental UV disinfection data: (a) *k vs.* λ; (b) λ *vs.* $[dose]_B$; (c) *k vs.* $[dose]_B$

The correlations observed between the EDP_m parameters for fits of the model to both the experimental disinfection data generated during this study, and the UV disinfection data of Nelson (2000) are summarised in Table 6.5.

Table 6.5. Correlation between the EDP_m parameters for fits of the model to the experimental disinfection data, and to the disinfection data of Nelson (2000)

Source		R^2	Equation
Experimental	$k = 12.2.\lambda + 0.003$	0.9544	(6.1)
	$\lambda = 0.5423[dose]_B^{-0.93}$	0.9862	(6.2)
	$k = 1.41[dose]_B^{-0.74}$	0.8983	(6.3)
Nelson (2000)	$k = 7.92.\lambda + 0.025$	0.9560	(6.4)
	$\lambda = 0.9393[dose]_B^{-0.99}$	0.9980	(6.5)
	$k = 3.67[dose]_B^{-0.76}$	0.9120	(6.6)

The constants defining correlations between each respective pair of EDP_m parameters are seen to be of comparable orders of magnitude for both the experimental data, and the disinfection data of Nelson (2000). The correlations are strong in both instances. This is despite only 8 data defining the correlation between derived parameters when fit to the data of Nelson (2000), compared to 23 data defining each correlation when fit to data generated from the current study. These values for the coefficient of determination, R^2, give a measure of the strength of correlation between the EDP_m parameters.

These constants obtained defining the correlation between EDP_m parameters may provide a useful basis for comparison of independent sets of UV disinfection data, as in this case, and may be suitable criteria for definition of the scale of a UV disinfection facility (i.e. scale-up). Interpretation of any associated physical meaning may prove more difficult. Clearly, the correlation of EDP_m parameters makes it difficult to restrict the influence of a given environmental variable to a single model parameter. This may be a source of concern for further modelling studies.

The EDP_m model may be used to define some interesting kinetic properties associated with the tailing region typically displayed in practical UV disinfection data.

The predicted disinfection rate coefficient in the tailing region (k'), and level of disinfection (as $\log_{10}$ reductions) at the breakpoint dose ($-c$) for fits of the EDP_m model to the experimental data is presented in Table 6.6. The rate of disinfection in the tailing region is seen to vary between $1.04\times10^{-4}$and 4.58×10^{-6} μWs^{-1} cm^2, that is, from 10 to 300 times less than the disinfection rate coefficient, k (i.e. measure of the initial rate of disinfection). This does not include those data-sets for which the EDP_m model was constrained to ensure a non-negative rate of disinfection in the tailed data. In these cases, the rate of disinfection in the tail is by default set as zero. The predicted reduction of viable bacteria at the breakpoint dose ($-c$) ranges between 4 and 7.5-$\log_{10}$ reductions, and is a measure of the level of disinfection prior to the onset of tailing.

Table 6.6. EDP_m tailing properties for each experimentally observed data set

Data Set	k' (μWs^{-1} cm^2)	c (as $\log_{10}$ N/N_0)	α (as $\log_{10}$ N/N_0)	k/k'
1	1.68×10^{-5}	-5.15	-5.01	95.4
2	1.31×10^{-5}	-5.05	-4.97	178.7
3	2.60×10^{-5}	-4.52	-4.43	133.1
4	-4.81×10^{-6}	-5.65 (-5.56)	-5.68	infinite
5	1.05×10^{-5}	-6.16	-6.09	226.3
6	1.49×10^{-5}	-4.89	-4.79	124.1
7	1.93×10^{-5}	-5.37	-5.26	127.3
8	1.10×10^{-5}	-5.21	-5.08	102.1
9	1.94×10^{-5}	-4.63	-4.54	139.3
10	-2.90×10^{-5}	-4.55 (-3.97)	-4.81	infinite
11	-5.03×10^{-6}	-5.51 (-5.40)	-5.56	infinite
12	4.58×10^{-6}	-4.96	-4.92	295.3
13	-1.57×10^{-5}	-5.68 (-5.34)	-5.83	infinite
14	-3.93×10^{-5}	-7.35 (-6.01)	-8.57	infinite
15	3.91×10^{-5}	-5.19	-4.77	30.8
16	-6.19×10^{-6}	-6.20 (-6.08)	-6.27	infinite
17	-4.56×10^{-5}	-8.20 (-6.60)	-9.96	infinite
18	-3.85×10^{-5}	-8.78 (-7.51)	-10.26	infinite
19	-1.19×10^{-6}	-5.44 (-5.39)	-5.49	infinite
20	2.49×10^{-5}	-5.03	-4.70	39.1
21	1.99×10^{-5}	-5.48	-5.26	64.6
22	4.62×10^{-6}	-5.48	-5.44	361.4
23	1.04×10^{-4}	-5.33	-4.18	10.1

Inspection of Table 6.6 shows that a negative rate of disinfection in the tailing region is predicted for fits of the EDP_m model to some sets of experimental data. In this instance, the ratio of the disinfection rate coefficient (k) to the rate of disinfection in the tailing region (k') has been reported as infinite. This is also reflected in values of the projected axis intercept (α). In the case of a negative rate of disinfection in the tailing region, the level of disinfection projected at a zero dose by the tail (or α) becomes greater than that predicted at the onset of tailing (as $-c$). In this case, $\alpha < c$. Clearly, this presents a problem when attempting to model UV disinfection kinetics in the tailing region of these UV disinfection data. The projected axis intercept (α) may only take values between the predicted log-reduction at the breakpoint dose ($-c$) and zero to ensure a non-negative rate of disinfection is predicted for the tailed data. When the projected axis intercept and the predicted level of disinfection at the breakpoint dose are equal, the disinfection rate coefficient for the tailing region is by definition zero.

As the projected axis intercept tends towards zero (for a given predicted level of disinfection at the breakpoint dose), the UV disinfection kinetics approach log-linear, or the extent of tailing decreases. The predicted rates of disinfection in the tailing region (k') and predicted level of disinfection at the breakpoint dose ($-c$) for fits of the EDP_m model to the experimental data pooled according to concentration of both absorbing and shielding agents are shown in Table 6.7.

The projected axis intercept (α) has physical significance in the case of multi-component kinetics (Block 1983), where the bacterial population is characterised by a range of sub-populations, each with a different sensitivity to UV irradiation. It the case of two-component kinetics (or simply put, a population consisting of a UV susceptible and a UV resistant fraction) the projected intercept represents the proportion of the initial population which displays the elevated resistance. The biological significance of the projected axis intercept is confounded in this study by the presence of either the shielding or absorbing agent.

Table 6.7. EDP_m tailing properties for experimental data pooled according to concentration of either absorbing or shielding agent

Pooled data set	k' (μWs^{-1} cm^2)	$-c$ (as $\log_{10}$ N/N_0)	α (as $\log_{10}$ N/N_0)
none	1.58×10^{-5}	-5.03	-4.92
0.001 g/L coffee	-4.81×10^{-6}	-5.65 (-5.56)	-5.68
0.005 g/L coffee	6.48×10^{-6}	-5.94	-5.89
0.01 g/L coffee	1.49×10^{-5}	-4.89	-4.79
0.03 g/L coffee	-1.86×10^{-5}	-6.73 (-6.09)	-7.19
0.05 g/L coffee	-3.85×10^{-5}	-8.78 (-7.51)	-10.26
0.07 g/L coffee	-1.19×10^{-6}	-5.44 (-5.39)	-5.49
0.1 g/L Celite 503™	1.94×10^{-5}	-4.63	-4.54
0.3 g/L Celite 503™	-9.47×10^{-6}	-6.03 (-5.86)	-6.18
0.5 g/L Celite 503™	-1.70×10^{-5}	-5.02 (-4.71)	-5.18
0.7 g/L Celite 503™	1.83×10^{-5}	-4.90	-4.70

A constraint was imposed on the EDP_m model ($[dose]_B \leq \lambda^{-1}$) to ensure that the rate of disinfection predicted in the tailing region (k') would not become negative, and was restricted to a limiting value of zero. Derivation of this constraint is outlined in Appendix J, together with development of the modified exponentially damped polynomial (EDP_m) model form.

Fitting the constrained EDP_m form to those experimental data sets for which a negative rate of disinfection (in the tail) was initially observed (i.e. sets 4, 10, 11, 13, 14 and 16 – 19), showed the predicted level of disinfection at the breakpoint dose ($-c$) was now reduced. These reduced values are shown in parentheses in Table 6.6. In all cases, the level of disinfection predicted at the breakpoint dose by the constrained EDP_m model (i.e. $-c$ in parentheses) is less than the level of disinfection represented by the projected axis intercept (α) for the unconstrained model form. This is expected as the rate of disinfection in the tail (k') predicted by the constrained EDP_m model is convergent towards zero.

Imposition of this necessary constraint ($[dose]_B \leq \lambda^{-1}$) causes the EDP_m model parameters (k, λ and $[dose]_B$) to vary as they each contribute to defining the kinetics in the tailing region, as shown previously by Equations 4.4 and 4.5.

Figure 6.21 presents a comparison of the EDP_m model parameters before and after inclusion of the constraint for the experimental data-sets where a negative rate of disinfection was initially observed in the tailing region (k'). After imposition of the constraint, the values obtained for the disinfection rate coefficient (k) and the damping coefficient (λ) were seen to increase slightly, whereas values of the breakpoint dose ($[dose]_B$) were seen to decrease. This is in agreement with the observed inverse dependence of the disinfection rate and damping coefficients on the breakpoint dose. In particular, the decreases in breakpoint dose for data-sets 14, 17 and 18 were relatively large, with a decrease in excess of 10,000 $\mu Ws\ cm^{-2}$ in each case. In the case of data-set 14, the breakpoint dose was reduced from above 30,000 to below 20,000 $\mu Ws\ cm^{-2}$. For data set 17, the decrease in breakpoint dose is closer to 20,000 $\mu Ws\ cm^{-2}$.

A comparison between the fit of both the EDP_m model and the constrained EDP_m model to the experimentally obtained UV disinfection data is presented in Figure 6.22 for an initial viable bacteria concentration of $1.08\times10^8\ mL^{-1}$, at a shielding agent concentration of 0.3 $g\ L^{-1}$ (i.e. data-set 13). The constrained model clearly predicts a limiting extent of disinfection (~ 5.3 $\log_{10}$ reductions. *see.* Table 6.6), characterised by a zero- rate of disinfection in the tail. This is a practical limiting case. The unconstrained EDP_m model continues to predict a reduced extent of disinfection as the breakpoint dose (~ $9.6\times10^3\ \mu Ws\ cm^{-2}$, *see.* Table 6.4) is exceeded.

A comparison between the residual sums of squares (RSS) obtained when fitting the EDP_m and the constrained EDP_m forms is presented in Table 6.8, for all sets of disinfection data for which a negative rate of disinfection was initially predicted in the tail (*see.* Table 6.6). As expected, the residual sum of squares increased where the constrained EDP_m model was fitted to a given data set, with the largest observed increase from 0.53 to 1.61 for data-set 17. No difference in the RSS is observed however when the EDP_m and constrained EDP_m forms are fitted to the disinfection data of set 19.

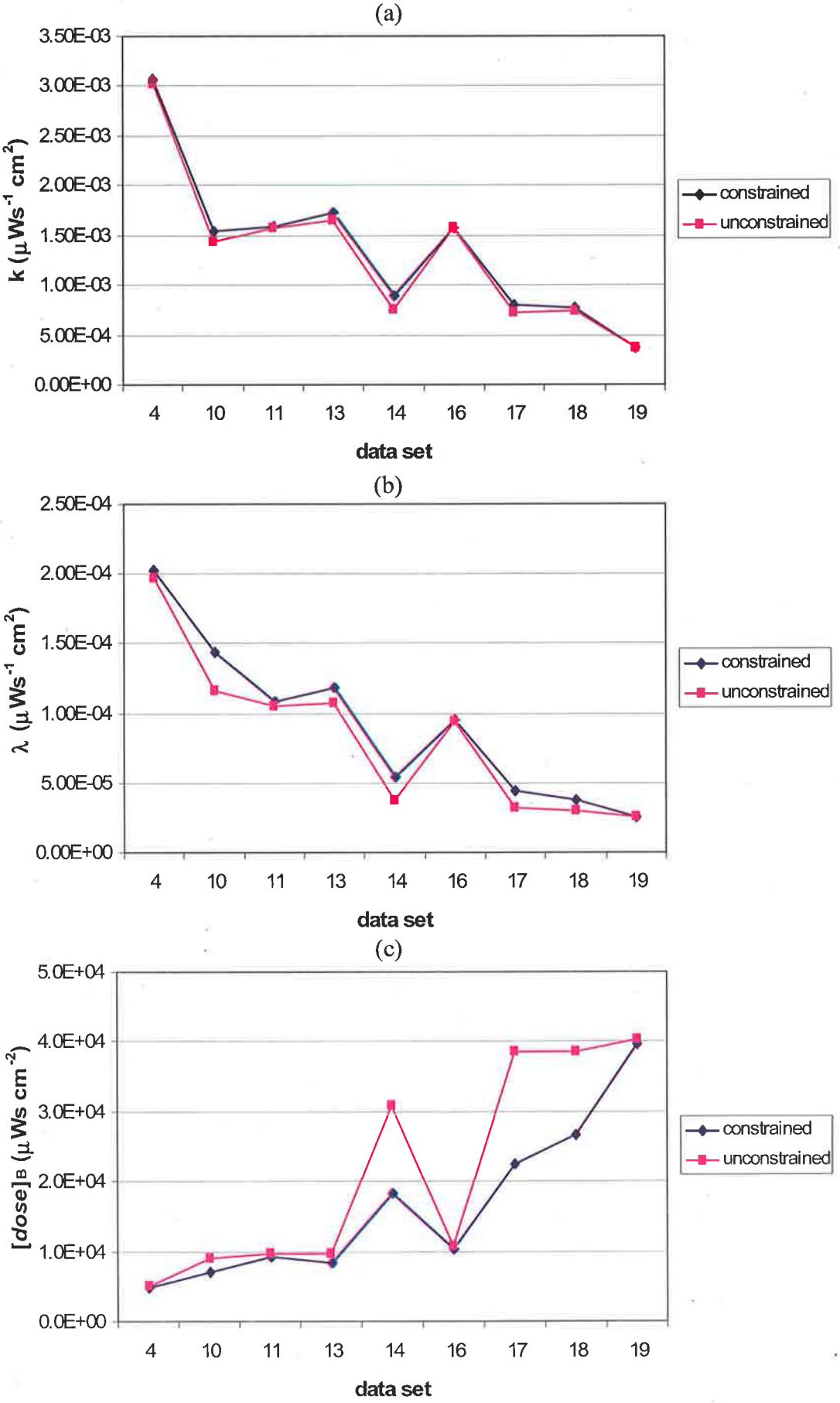

Figure 6.21. Comparison of the EDP_m model parameters before and after inclusion of the constraint: $[dose]_B \leq \lambda^{-1}$. (a) k, (b) λ, and (c) $[dose]_B$

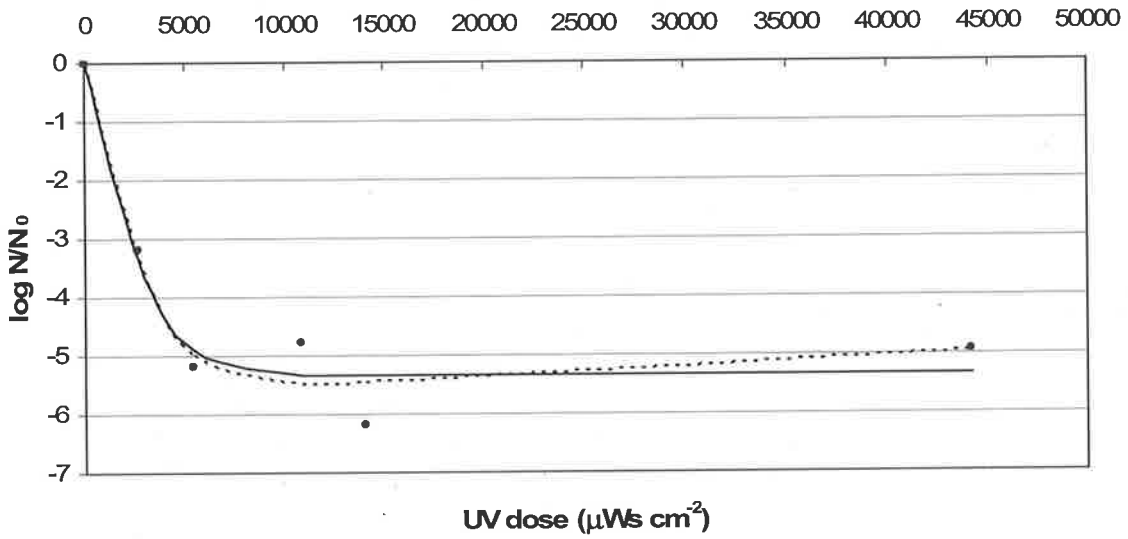

Figure 6.22. Fit of the EDP_m (---) and the constrained EDP_m model (continuous straight line) to experimentally observed UV disinfection data for 0.3 g L^{-1} of shielding agent and $N_0 = 1.05\times10^8$ mL^{-1} (data set 13)

Table 6.8. A comparison between residual sums of squares for fits of the EDP_m and constrained EDP_m forms to experimental disinfection data where an negative rate of disinfection in the tail was predicted

data set	RSS*	
	EDP_m	constrained EDP_m
4	0.10	0.12
10	0.55	1.27
11	0.56	0.58
13	1.12	1.30
14	1.51	2.03
16	1.66	1.70
17	0.53	1.61
18	2.13	3.10
19	1.57	1.57

* RSS denotes residual sum of squares

The variation in the value of the EDP_m tailing parameters predicted (k', $-c$ and α) with absorbing and shielding agent concentration respectively is presented in Figures 6.23 and 6.24. The data-sets when no additive is present (sets 1, 2, 3 and 22) have been included for comparison in each case. None of the tailing parameters (k', $-c$ or α) display a clear dependence with respect to concentration in the case of either absorbing or shielding agent.

The disinfection rate coefficient for the tailing region (k') is seen to exhibit large variation, as shown in Figure 6.23a, particularly for absorbing agent concentrations less than 0.01 g L^{-1}. This variation is larger if constrained values of the disinfection rate coefficient in the tail (k') are neglected in the analysis (i.e. negative values are included). The log-reduction predicted at the breakpoint dose ($-c$), and the projected axis intercept (α), also appear to display substantial variability for absorbing agent concentrations less than 0.01 g L^{-1}.

Through inspection of Figure 6.24, the tailing parameter data for the shielding agent appears to be inconclusive. No discernable trends in any of the EDP_m tailing parameters (k', $-c$ or α) are evident with respect to shielding agent concentration. The predicted disinfection efficacy at the breakpoint dose ($-c$) and the projected axis intercept (α) are seen to vary over the range of 4 to 6-$\log_{10}$ reductions. The disinfection rate coefficient for the tailing region (k') appears to be independent of shielding agent concentration as highlighted by Figure 6.24a.

The experimental UV disinfection data were also pooled according to concentration of either absorbing or shielding agent as part of these analyses. This was in an attempt to more easily identify the effect of agent concentration on, and to reduce the variance in, parameter estimates obtained for each of the models tested. Experimental disinfection data obtained at fixed concentrations of absorbing or shielding agent are, however, confounded by variation in the initial concentrations of viable bacteria between experimental data-sets. Consequently, by pooling the data on the basis of concentration of either agent, any influence of the initial concentration of viable bacteria on the UV disinfection kinetics of may not be clear.

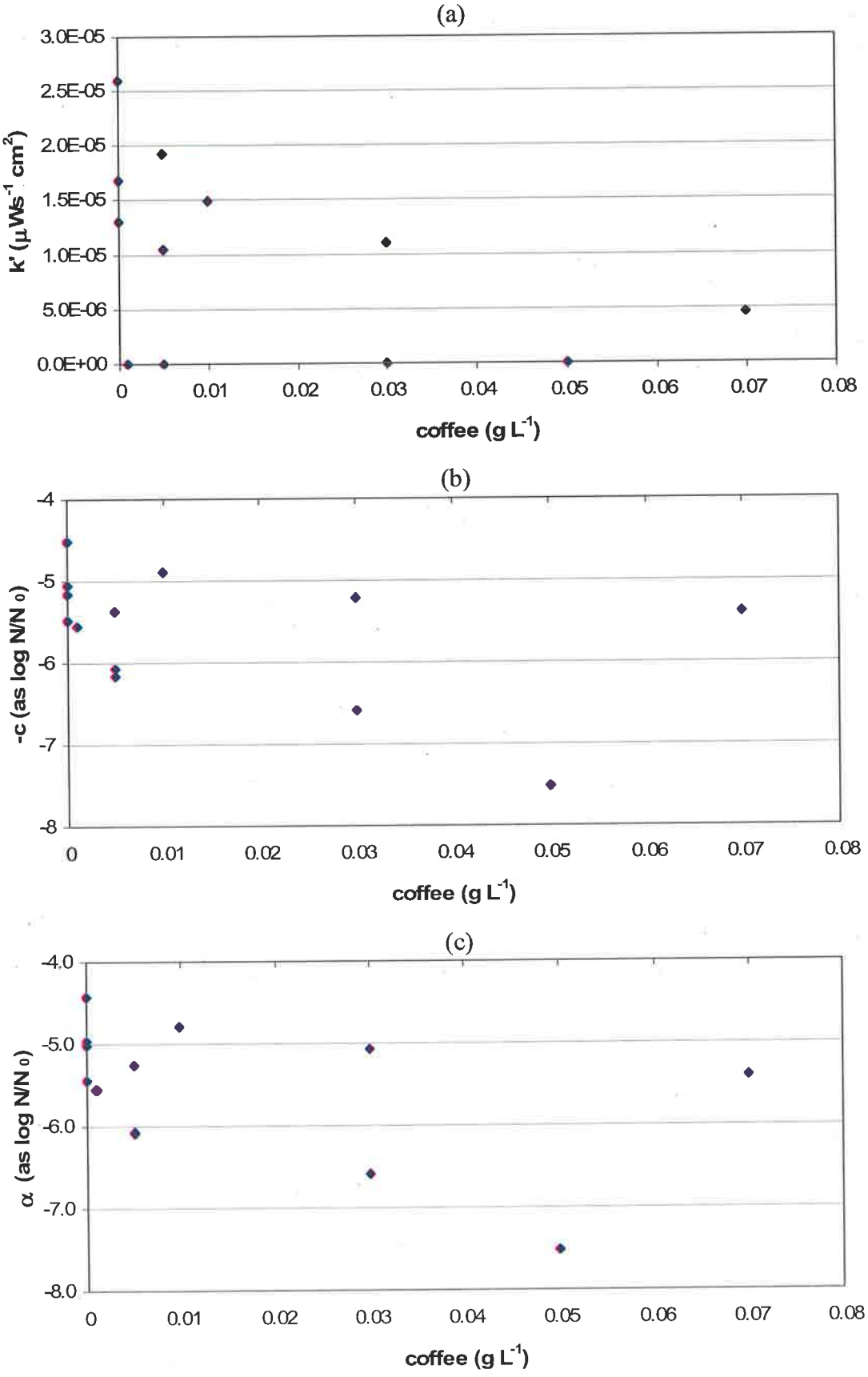

Figure 6.23. EDP_m tailing parameters presented against absorbing agent concentration for the experimental disinfection data: (a) k' (b) $-c$, and (c) α

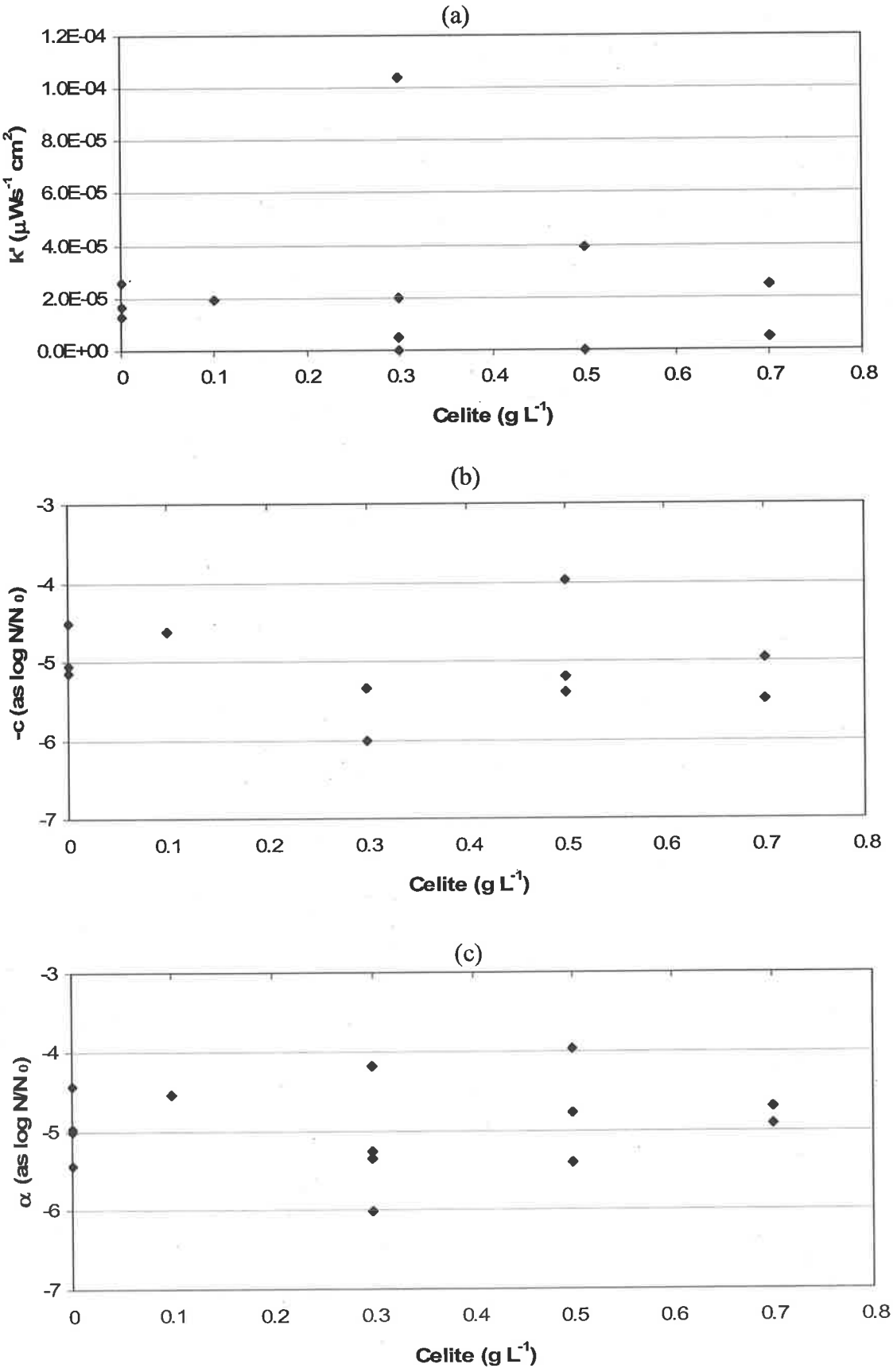

Figure 6.24. EDP_m tailing parameters presented against shielding agent concentration for the experimental disinfection data: (a) k' (b) $-c$, and (c) α

The EDP_m model parameters obtained when the experimental UV disinfection data are pooled on the basis of the type and concentration of agent present are presented in Table 6.9. Data-set 15 has been omitted from the analysis due to difficulties with convergence of the EDP_m model to the data-set. For those instances where there exists only a single data-set for a given concentration of either agent, the model parameters (and respective P-values) remain unchanged in comparison to the previous fit of the EDP_m model (*see.* Table 6.4), and are included for comparative purposes only.

The statistical significance of each of the pooled EDP_m parameters are seen to be much higher than the respective values corresponding to single sets of data (*see.* Table 6.4). This is made evident by comparison of the associated *P-values* for the pooled data in Table 6.9, which are typically of the order of 10^{-3} to 10^{-10} for the pooled estimates, to those derived from single disinfection data-sets only in Table 6.4, typically ranging from 10^{-1} to 10^{-3}. Consequently, the standard error associated with each of the pooled EDP_m parameter estimates is markedly reduced. This is due to the larger number of data in each of the pooled sets providing more available degrees of freedom for regression analyses. The standard error on each of the EDP_m parameter estimates has not been explicitly reported for the pooled disinfection data in Table 6.9. However, the test-statistic (or t-value) is reported, which is the ratio of a given parameter estimate to its respective standard error. Values of the test-statistic reported in Table 6.9 highlight that for fits of the EDP_m model to the pooled disinfection data, each of the model parameters are highly significant. Corresponding values for the test-statistic are also much higher when the disinfection data are pooled.

The model parameters presented in Table 6.9 further highlight when a minimum of 2 original sets of disinfection data are pooled, all EDP_m parameters become significant (i.e. P-value < 0.05). This is in contrast to singular sets of the experimental disinfection data. Table 6.4 shows for fits of the EDP_m model to data sets 19 and 23, the P-values corresponding to each of the parameter estimates all exceed 0.05, indicating limited statistical significance.

Table 6.9. EDP_m model parameters for experimental data pooled according to agent concentration

Agent	Source data sets	n	Model Parameters									
			k			λ			$[dose]_B$			
			estimate	t-value	P-value	estimate	t-value	P-value	estimate	t-value	P-value	RSS *
none	1, 2, 3, 22	24	1.99×10^{-3}	11.0	3.79×10^{-10}	1.46×10^{-4}	8.9	1.38×10^{-8}	6.71×10^{3}	8.7	2.28×10^{-8}	3.24
0.001 g L^{-1} coffee	4	6	3.03×10^{-3}	11.5	1.41×10^{-3}	1.97×10^{-4}	10.1	2.05×10^{-3}	5.09×10^{3}	9.8	2.23×10^{-3}	0.10
0.005 g L^{-1} coffee	5, 7, 16	18	2.00×10^{-3}	9.2	1.50×10^{-7}	1.24×10^{-4}	7.2	3.22×10^{-6}	8.01×10^{3}	6.8	6.38×10^{-6}	4.16
0.01 g L^{-1}coffee	6	6	1.85×10^{-3}	20.4	2.56×10^{-4}	1.39×10^{-4}	16.4	4.94×10^{-4}	7.04×10^{3}	15.8	5.48×10^{-4}	0.03
0.03 g L^{-1}coffee	8, 17	12	7.97×10^{-4}	6.5	1.07×10^{-4}	4.35×10^{-5}	3.3	8.97×10^{-3}	2.46×10^{4}	2.5	3.26×10^{-2}	2.99
0.05 g L^{-1}coffee	18	6	7.34×10^{-4}	-	-	3.04×10^{-5}	-	-	3.85×10^{4}	-	-	2.13
0.07 g L^{-1}coffee	19	6	3.70×10^{-4}	1.9	1.52×10^{-1}	2.50×10^{-5}	0.6	6.06×10^{-1}	4.03×10^{4}	0.3	7.51×10^{-1}	1.57
0.1 g L^{-1} Celite 503™	9	6	2.71×10^{-3}	4.4	2.18×10^{-2}	2.15×10^{-4}	3.9	3.01×10^{-2}	4.56×10^{3}	3.9	3.05×10^{-2}	0.39
0.3 g L^{-1} Celite 503™	13, 14, 21, 23	23	1.06×10^{-3}	9.3	1.09×10^{-8}	6.49×10^{-5}	6.8	1.37×10^{-6}	1.58×10^{4}	5.9	8.26×10^{-6}	9.16
0.5 g L^{-1} Celite 503™	10, 11 #	12	1.50×10^{-3}	4.8	1.04×10^{-3}	1.10×10^{-4}	3.6	5.42×10^{-3}	9.38×10^{3}	3.3	9.47×10^{-3}	5.00
0.7 g L^{-1} Celite 503™	12, 20	12	1.17×10^{-3}	8.3	1.63×10^{-5}	8.76×10^{-5}	6.6	9.61×10^{-5}	1.10×10^{4}	6.3	1.43×10^{-4}	1.80

* RSS denotes residual sum of squares

Data set 15 has been omitted

The residual sums of squares for each of the pooled sets (Table 6.9) are now larger than those values observed for single data sets, with values ranging between 1.80 and 9.16 for the pooled data sets. This compares to values ranging from 0.03 to a maximum of 2.13 for the unpooled disinfection data (*see*. Table 6.4). These residual sums of squares may be standardised on the basis of available degrees of freedom, in which case larger pools of data are preferable. However, this was not deemed necessary in this case.

The predicted *vs*. observed values of reduction in viable bacteria (as $\log_{10} N/N_0$) for the predictions of the EDP_m model applied to each of the pooled data sets are summarised by Figure 6.25. Those predictions where a given concentration of either absorbing or shielding agent is represented by a single data-set only are also included. The predictions based on the pooled disinfection data are again evenly and randomly distributed, suggesting the EDP_m model is of a form suitable to representing the tailing observed in the pooled disinfection data. However, the effects of variations in the initial concentration of viable bacteria on the model predictions have in effect been weighted by pooling the data, when it may not be justifiable to do so over the range of initial concentrations of viable bacteria observed. The predicted vs. observed values of reduction in viable bacteria for predictions of the EDPm model fitted to individual, or unpooled, data sets has been included as a basis for comparison. The distributions of both the pooled and unpooled data remain comparable. The distribution of pooled data appears no more widely spread, for observed levels of disinfection in excess of 4-$\log_{10}$ reductions. However, as the observed level of disinfection is reduced (< 4-$\log_{10}$ reductions), predictions of the EDP_m model fitted to the pooled disinfection data become more widely spread about the line of equivalence.

This may be a result of differences in the numbers of viable bacteria initially present, when the experimental disinfection data were pooled. Inspection of Figures 6.18a and 6.18b show that the disinfection rate coefficient (k) and the damping coefficient (λ) are particularly sensitive to variation in the initial concentration of viable bacteria (N_0) when neither absorbing nor shielding agents are present. This holds equally for low concentrations of absorbing agent. In these instances, variation in the initial concentration of viable bacteria is particularly influential in determining the initial rates of disinfection, when typically less than 4-$\log_{10}$ reductions are observed at relatively low UV doses.

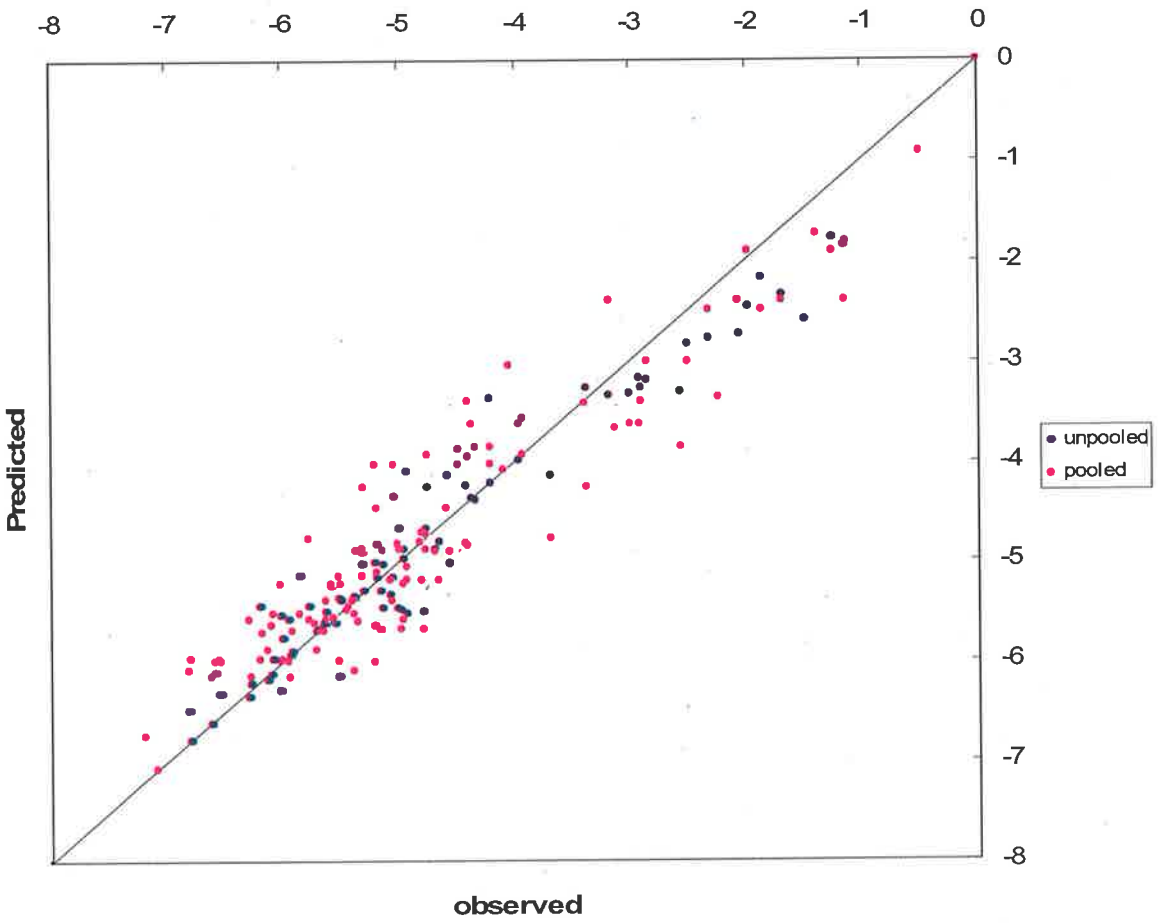

Figure 6.25. Predicted *versus* observed value of the log reduction in viable bacteria (as log N/N_0) from the EDP_m model for both the pooled and unpooled experimental UV disinfection data

Figures 6.26 and 6.27 display the EDP_m (k, λ and $[dose]_B$) parameters against the absorbing agent and shielding agent concentrations respectively for fits of the model to the pooled sets of disinfection data. The effect of absorbing agent concentration on the respective EDP_m parameters is clearer than for the shielding agent. Both the disinfection rate coefficient (k) and damping coefficient (λ) appear to decrease exponentially with increases in absorbing agent concentration, whilst the predicted breakpoint dose ($[dose]_B$) clearly increases to a maximum of approximately 40,000 μWs cm^{-2} as the absorbing agent concentration is increased to 0.05 g L^{-1} and beyond.

Clearly, pooling the survivor data in this instance has made it easier to assess the general effect of absorbing agent concentration (or UV absorbance) on the EDP_m model parameters. Pooling the survivor data in this manner effectively negates any influence of differences in initial concentrations of viable bacteria on the regressed EDP_m parameters. The variability in the EDP_m parameter estimates (at a fixed absorbing agent concentration) displayed in Figure 6.23 may be due, in part, to differences in the initial concentration of viable bacteria present between data sets. This variability was sufficient to prevent suitable assessment of the effect of absorbing agent concentration on the EDP_m parameters. However, the effect of the initial concentration of viable bacteria on the EDP_m parameters remains unclear, as it is confounded with absorbing agent concentration in this instance.

The effect of shielding agent concentration on the pooled EDP_m parameter estimates is shown to be less clear through inspection of Figure 6.27. An increase in shielding agent concentration leads to a general decrease in both the disinfection rate coefficient (k) and the damping coefficient (λ), and a corresponding increase in the breakpoint dose ($[dose]_B$). It is apparent that an outlier may occur for a shielding agent concentration of 0.3 g L^{-1}. If the apparent outlier was omitted, the dependence of each EDP_m parameter on shielding agent concentration may be cautiously approximated as linear. Examination of Figure 6.27, however shows the dependence of the pooled EDP_m parameter estimates on shielding agent concentration to be described by five (5) data only, whereas the dependence of the pooled estimates on absorbing agent concentration is described by seven (7) data (*see*. Figure 6.26).

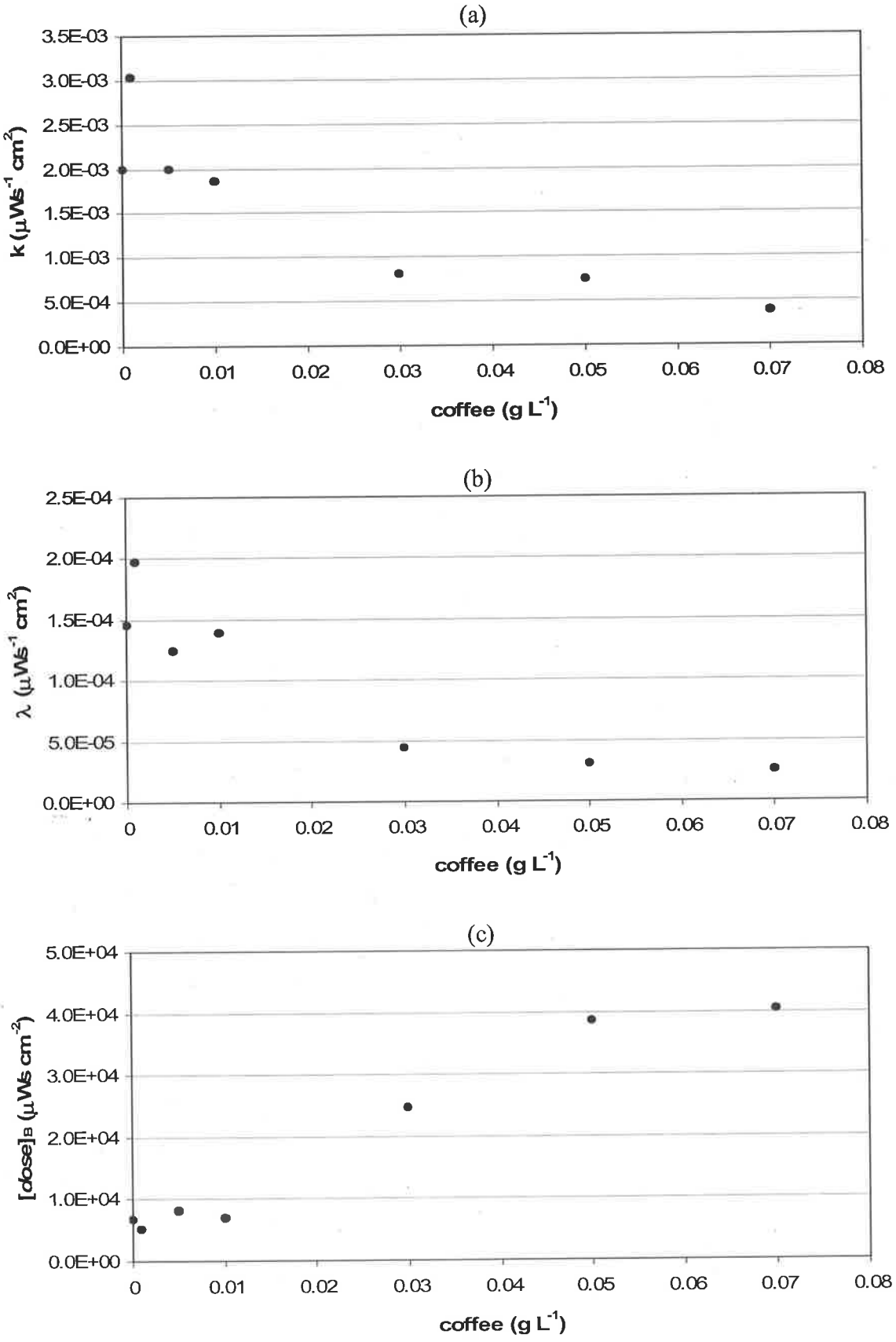

Figure 6.26. The EDP_m parameters derived from the pooled disinfection data against concentration of absorbing agent (a) k (b) λ, and (c) $[dose]_B$

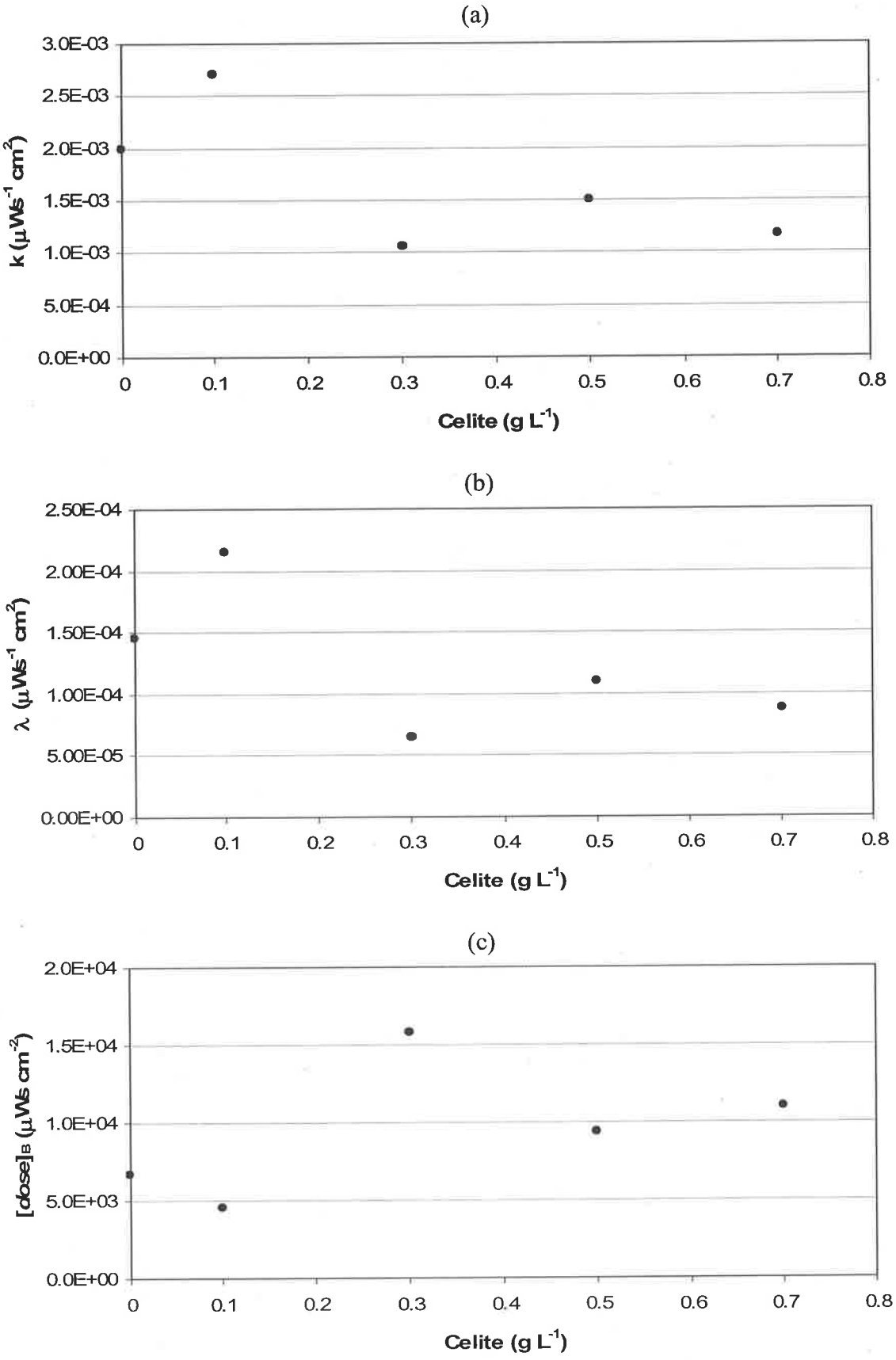

Figure 6.27. The EDP_m parameters derived from the pooled disinfection data against concentration of shielding agent (a) k (b) λ, and (c) $[dose]_B$

The predicted rates of disinfection in the tailing region (k'), and level of disinfection at the breakpoint dose ($-c$) for fits of the EDP_m model to the pooled experimental disinfection data are given in Table 6.10. The disinfection rate coefficient for the tailing region is observed to be negative in a number of instances, requiring the EDP_m model to again be constrained with respect to the breakpoint dose ($[dose]_B \leq \lambda^{-1}$). The level of disinfection predicted at the breakpoint dose ($-c$) after the constraint is introduced is again reduced, and included in parentheses in Table 6.10. Also, the value of the disinfection rate coefficient predicted in the tail for the constrained EDP_m model is by default zero. For the pooled disinfection data, the disinfection rate coefficient in the tailing region varied from 6.48×10^{-6} to 1.94×10^{-5} μWs^{-1} cm^2, with imposition of the constraint yielding between 4.6 and 7.5-$\log_{10}$ reductions predicted at the breakpoint dose (i.e. $-c$).

Table 6.10. EDP_m tailing properties for experimental data pooled according to concentration of either absorbing or shielding agent

Agent	k' (μWs^{-1} cm^2)	$-c$ (as $\log_{10}$ N/N_0)	α (as $\log_{10}$ N/N_0)
none	1.58×10^{-5}	-5.03	-4.92
0.001 g L^{-1} coffee	-4.81×10^{-6}	-5.65 (-5.56)	-5.68
0.005 g L^{-1} coffee	6.48×10^{-6}	-5.94	-5.89
0.01 g L^{-1}coffee	1.49×10^{-5}	-4.89	-4.79
0.03 g L^{-1}coffee	-1.86×10^{-5}	-6.73 (-6.09)	-7.19
0.05 g L^{-1}coffee	-3.85×10^{-5}	-8.78 (-7.51)	-10.26
0.07 g L^{-1}coffee	-1.19×10^{-6}	-5.44 (-5.39)	-5.49
0.1 g L^{-1} Celite 503™	1.94×10^{-5}	-4.63	-4.54
0.3 g L^{-1} Celite 503™	-9.47×10^{-6}	-6.03 (-5.86)	-6.18
0.5 g L^{-1} Celite 503™	-1.70×10^{-5}	-5.02 (-4.71)	-5.18
0.7 g L^{-1} Celite 503™	1.83×10^{-5}	-4.90	-4.70

By definition, imposition of the constraint ($[dose]_B \leq \lambda^{-1}$) causes the rate of disinfection in the tailing region to converge to zero for these pooled disinfection data. Consequently, there are too few data to assess the effect of variation in the concentration of either the absorbing or shielding agent on the disinfection rate coefficient for the tailing region.

Where a negative rate of disinfection in the tail was initially observed for fits of the EDP_m model to the pooled data (*see*. Table 6.10), a comparison of the EDP_m parameters (k, λ and $[dose]_B$) before and after imposition of the constraint ($[dose]_B \leq \lambda^{-1}$) is presented in Figure 6.28. The change in disinfection rate coefficient, damping coefficient and breakpoint dose respectively, for fits of the EDP_m model to the pooled disinfection data (as compared to the unpooled data) are presented in Figures 6.28a, 6.28b and 6.28c.

As was previously observed for fits of the EDP_m model to the unpooled disinfection data, the disinfection rate coefficient and the damping coefficient remain relatively unchanged upon inclusion of the constraint in the EDP_m model. Imposition of the constraint causes a minor increase in the disinfection rate coefficient and the damping coefficient as shown in Figures 6.28a and 6.28b respectively. The most noticeable differences occur with respect to the effect on breakpoint dose, with decreases of approximately 5,000 and 10,000 $\mu Ws\ cm^{-2}$ observed for the pooled disinfection data sets representing concentrations of 0.03 $g\ L^{-1}$ and 0.05 $g\ L^{-1}$ of absorbing agent respectively.

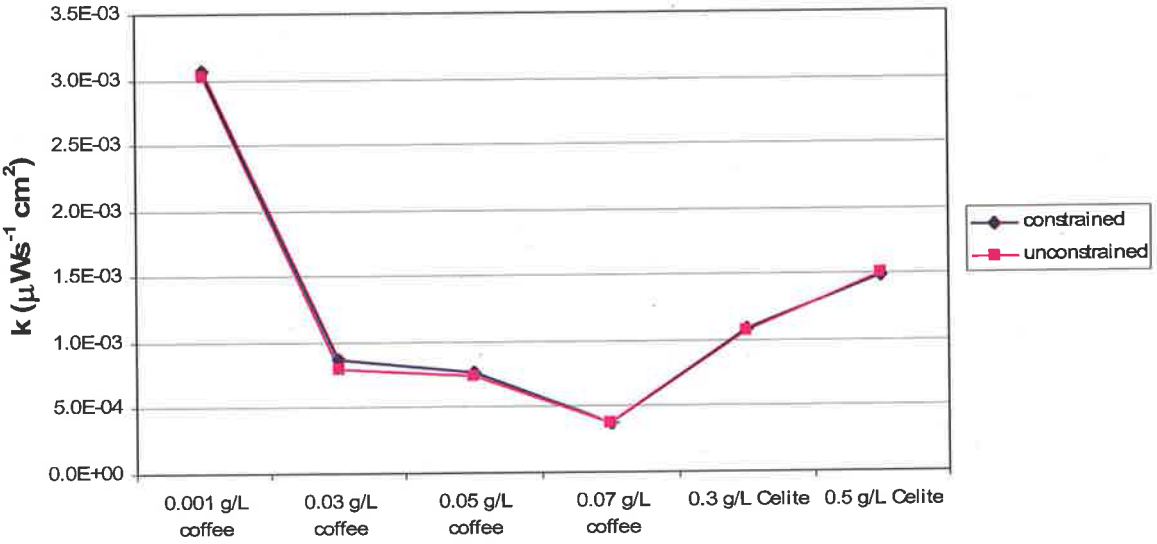

Figure 6.28a. Comparison of the EDP_m disinfection rate coefficient (k) for pooled data sets before and after inclusion of the constraint: $[dose]_B \leq \lambda^{-1}$

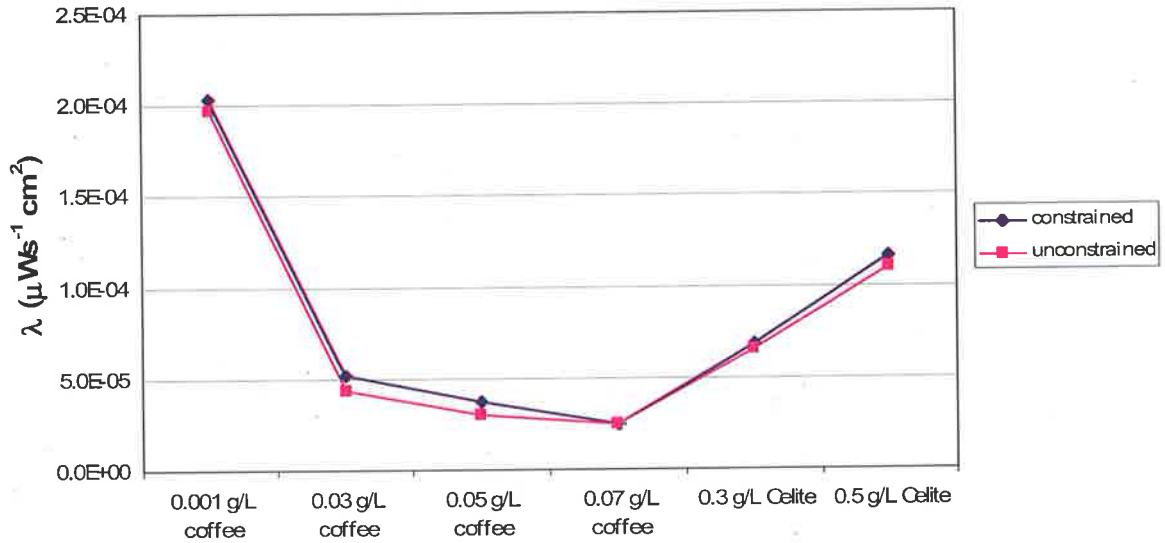

Figure 6.28b. Comparison of the EDP_m damping coefficient (λ) for pooled data sets before and after inclusion of the constraint: $[dose]_B \leq \lambda^{-1}$

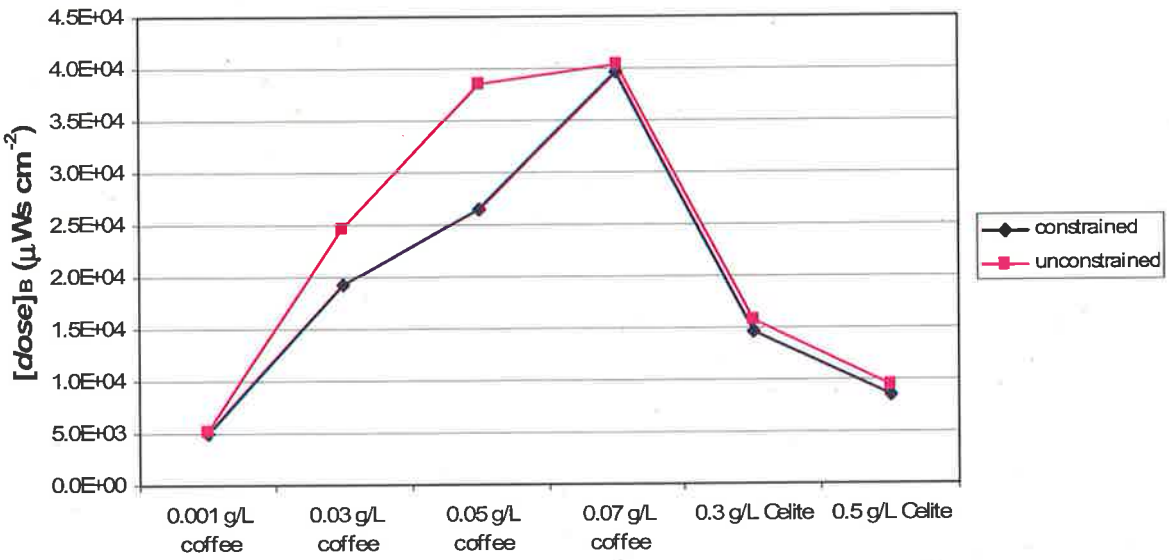

Figure 6.28c. Comparison of the EDP_m breakpoint dose ($[dose]_B$) for pooled data sets before and after inclusion of the constraint: $[dose]_B \leq \lambda^{-1}$

For the pooled disinfection data, the predicted $\log_{10}$ reduction in viable bacteria at the breakpoint dose ($-c$), for addition of both absorbing and shielding agent respectively is presented by Figure 6.29. There is no apparent dependence of the predicted level of disinfection at the breakpoint dose on the concentration of either additive when the data is pooled. The predicted levels of disinfection at the onset of tailing range from 5 to 7.5-$\log_{10}$ reductions and from 4.5 to 6-$\log_{10}$ reductions for the effect of absorbing agent and shielding agent concentrations respectively.

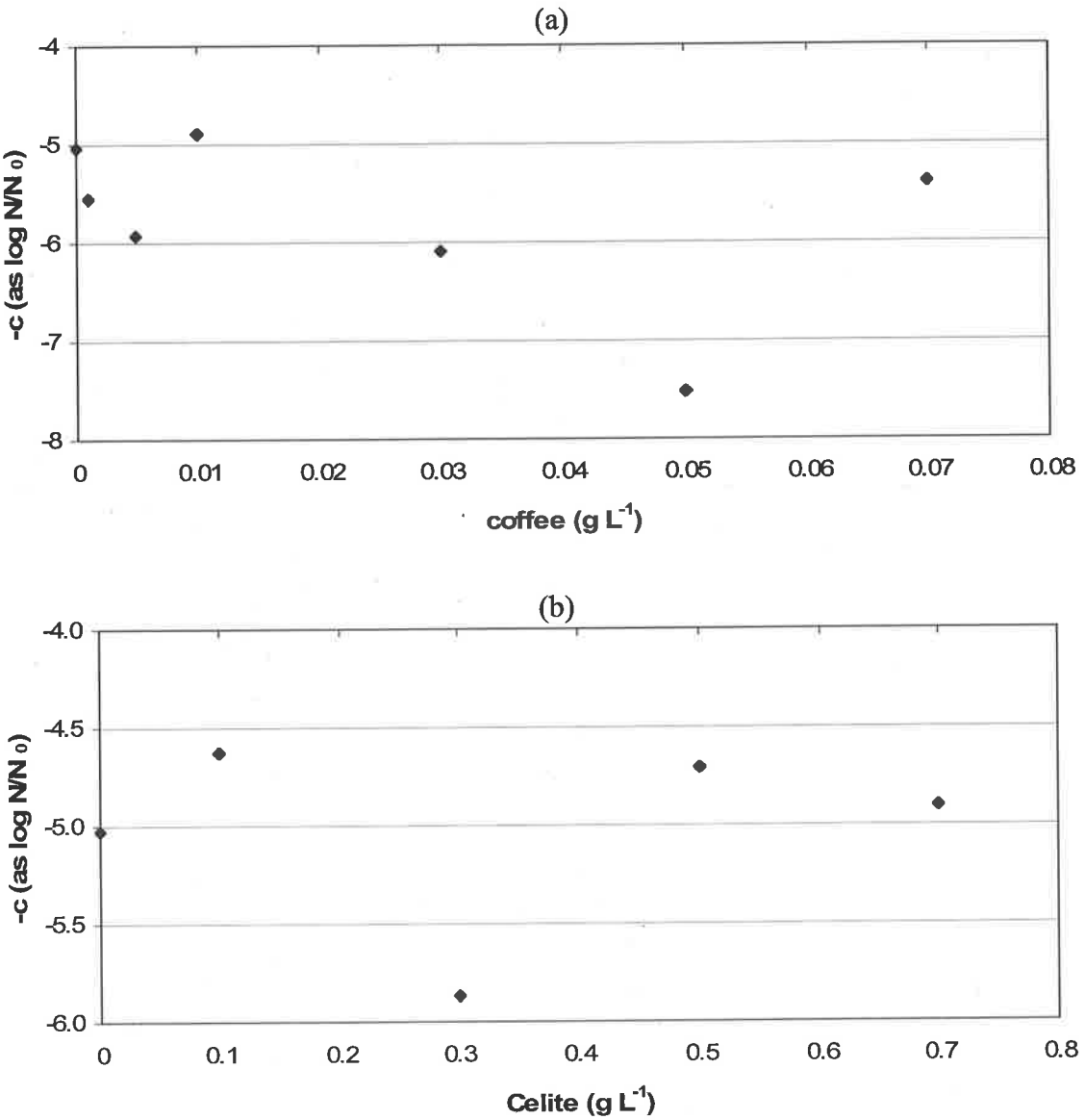

Figure 6.29. The predicted log-reduction in viable bacteria (as $\log_{10} N/N_0$) at the breakpoint dose ($-c$) presented against: (a) absorbing agent, and (b) shielding agent concentration for the pooled disinfection data

In summary, no clear systematic trends in the EDP_m parameters (k, λ and $[dose]_B$) are evident with respect to concentration of either agent when the UV disinfection data remain unpooled. This may, in part, be attributable to variation between the experimental data sets in the initial concentrations of viable bacteria prior to UV treatment; with order-of-magnitude differences often observed for equal concentrations of shielding or absorbing agent. This was despite efforts to standardise the initial concentration of bacteria between data sets.

Pooling of the disinfection data on the basis of agent concentration was beneficial however, in that the influence of concentration on the EDP_m parameters was made more clear. When considering the absorbing agent, pooling of disinfection data showed both the disinfection rate coefficient (k) and the damping coefficient (λ) to decrease exponentially with increasing agent concentration, whilst simultaneously the breakpoint dose ($[dose]_B$) increased. The effect of shielding agent on pooled estimates of the EDP_m parameters was unclear.

Pooled estimates of the EDP_m parameters however, remain confounded by variation in the initial numbers of viable bacteria, with the general effect of bacterial concentration on the model parameters remaining unknown.

6.3.2 Weibull model

Table 6.11 presents the Weibull model parameters, the dimensionless scale parameter β_0 and the shape parameter β_1, for the model fitted to each of the experimental disinfection data sets (as outlined in Table 6.1). The Weibull model parameters fitted against the experimental UV disinfection data, where the data have been pooled on the basis of concentration of absorbing or shielding agent, are presented in Table 6.12. Fits of the Weibull model to these pooled disinfection data will be discussed later in this chapter.

Table 6.11. Weibull model parameters for each experimentally observed data set

Data Set	n	Model Parameters						RSS *
		β_0			β_1 ($\mu Ws^{-1} cm^2$)			
		estimate	t-value	P-value	estimate	t-value	P-value	
1	6	5.67	25.0	1.51×10^{-5}	3.00×10^{-4}	6.4	3.04×10^{-3}	0.46
2	6	5.36	28.4	9.10×10^{-6}	5.05×10^{-4}	5.3	6.04×10^{-3}	0.44
3	6	5.05	24.1	1.77×10^{-5}	7.09×10^{-4}	3.3	3.08×10^{-2}	0.61
4	6	5.57	52.3	8.00×10^{-7}	7.64×10^{-4}	6.5	2.87×10^{-3}	0.16
5	6	6.45	43.1	1.73×10^{-6}	4.32×10^{-4}	9.0	8.48×10^{-4}	0.26
6	6	5.29	39.9	2.36×10^{-6}	3.89×10^{-4}	8.9	8.92×10^{-4}	0.19
7	6	5.81	26.1	1.28×10^{-5}	4.76×10^{-4}	5.1	7.00×10^{-3}	0.59
8	6	5.71	19.7	3.93×10^{-5}	2.11×10^{-4}	6.0	3.83×10^{-3}	0.54
9	6	5.05	22.4	2.34×10^{-5}	5.91×10^{-4}	3.7	2.14×10^{-2}	0.66
10	6	3.98	11.0	3.86×10^{-4}	5.04×10^{-4}	2.1	1.08×10^{-1}	1.60
11	6	5.50	19.4	4.15×10^{-5}	3.35×10^{-4}	4.7	9.34×10^{-3}	0.78
12	6	5.22	16.5	7.90×10^{-5}	2.84×10^{-4}	4.4	1.21×10^{-2}	0.85
13	6	5.42	14.6	1.28×10^{-4}	3.79×10^{-4}	3.3	3.00×10^{-2}	1.45
14	6	6.18	8.6	9.97×10^{-4}	1.69×10^{-4}	2.9	4.22×10^{-2}	2.70
15	4	7.16	2.3	1.50×10^{-1}	1.52×10^{-4}	1.2	3.48×10^{-1}	1.70
16	6	6.25	12.9	2.11×10^{-4}	2.84×10^{-4}	3.4	2.76×10^{-2}	2.00
17	6	6.77	8.7	9.80×10^{-4}	1.36×10^{-4}	3.3	3.06×10^{-2}	2.69
18	6	7.73	7.2	2.00×10^{-3}	1.11×10^{-4}	2.9	4.27×10^{-2}	4.37
19	6	5.67	6.6	2.69×10^{-3}	7.09×10^{-5}	3.1	3.70×10^{-2}	1.62
20	6	6.05	22.9	2.14×10^{-5}	1.61×10^{-4}	8.0	1.30×10^{-3}	0.35
21	6	6.23	13.9	1.55×10^{-4}	2.09×10^{-4}	4.3	1.29×10^{-2}	1.28
22	6	5.70	17.9	5.73×10^{-5}	3.29×10^{-4}	4.4	1.20×10^{-2}	0.97
23	5	8.02	4.0	2.78×10^{-2}	1.18×10^{-4}	2.1	1.29×10^{-1}	1.22

* RSS denotes residual sum of squares

Table 6.12. Weibull model parameters for experimental data pooled according to additive level

Additive	Source data sets	n	Model Parameters						RSS *
			β_0			β_1 ($\mu Ws^{-1} cm^2$)			
			estimate	t-value	P-value	estimate	t-value	P-value	
No additive	1, 2, 3, 22	24	5.44	42.2	$< 2\times10^{-16}$	4.08×10^{-4}	9.1	6.17×10^{-9}	4.03
0.001 g L^{-1} coffee	4	6	5.57	52.3	8.00×10^{-7}	7.64×10^{-4}	6.5	2.87×10^{-3}	0.16
0.005 g L^{-1} coffee	5, 7, 16	18	6.17	32.1	6.66×10^{-16}	3.76×10^{-4}	7.3	1.81×10^{-6}	4.66
0.01 g L^{-1} coffee	6	6	5.29	39.9	2.36×10^{-6}	3.89×10^{-4}	8.9	8.92×10^{-4}	0.19
0.03 g L^{-1} coffee	8, 17	12	6.27	15.5	2.59×10^{-8}	1.60×10^{-4}	5.4	2.90×10^{-4}	4.13
0.05 g L^{-1} coffee	18	6	7.73	7.2	2.00×10^{-3}	1.11×10^{-4}	2.9	4.27×10^{-2}	4.37
0.07 g L^{-1} coffee	19	6	5.67	6.6	2.69×10^{-3}	7.09×10^{-5}	3.1	3.70×10^{-2}	1.62
0.1 g L^{-1} Celite 503™	9	6	5.05	22.4	2.34×10^{-5}	5.91×10^{-4}	3.7	2.14×10^{-2}	0.66
0.3 g L^{-1} Celite 503™	13, 14, 21, 23	23	6.05	20.5	2.44×10^{-15}	2.14×10^{-4}	6.5	2.09×10^{-6}	10.08
0.5 g L^{-1} Celite 503™	10, 11, 15	16	4.89	13.9	1.37×10^{-9}	3.41×10^{-4}	3.6	2.66×10^{-3}	9.66
0.7 g L^{-1} Celite 503™	12, 20	12	5.58	22.4	7.00×10^{-10}	2.13×10^{-4}	6.8	4.58×10^{-5}	2.00

* RSS denotes residual sum of squares

The scale parameter, β_0, is seen to vary from 3.98 to 8.02 across the experimental data sets as shown by Table 6.11, and is a measure of the limiting observed level of disinfection (as $\log_{10} N/N_0$). The shape parameter, β_1, ranges from 7.09×10^{-5} to a maximum of 7.64×10^{-4} μWs^{-1} cm^2 over the sets of experimental disinfection data – an order of magnitude difference. The *P-values* associated with the estimates of both the scale and shape parameters generally have values of less than 0.05, indicating the model parameters are highly (statistically) significant.

The *P-values* associated with the scale parameter of the Weibull model typically take orders of magnitude between 10^{-2} and 10^{-7}, whereas those associated with the shape parameter vary over a narrower range of between 10^{-1} and 10^{-4} orders of magnitude. This highlights the relative statistical importance of the scale and shape parameters in definition of the Weibull model form, with the *P-value* of the scale parameter typically between 2 to 4 orders of magnitude less than that observed for the shape parameter. This is further supported by the observed values for the test statistic, ranging from 2.3 to 52.3 for the scale parameter (β_0) and from 1.2 to 9.0 for the shape parameter (β_1). Arguably however, both parameters are important for adequate definition of observed UV disinfection kinetics. For example, each of the Weibull parameters are seen to not be statistically significant ($P > 0.05$) for a fit of the model to the disinfection data in set 15, owing to the fewer than usual data defining the set (4 *cf.* 6 data). In this instance, the respective *P-values* of the scale and shape parameters are 1.50×10^{-1} and 3.48×10^{-1}, both greater than 0.05. The only remaining instances of parameters not being statistically significant for the Weibull model are for the values obtained for the shape parameter for fits of the model to data sets 10 and 23 respectively, where the associated *P-values* are 1.08×10^{-1} and 1.29×10^{-1}. The residual sum of squares ranged from 0.16 (data set 4) to 4.37 (data set 18) for fits of the Weibull model to the experimental disinfection data.

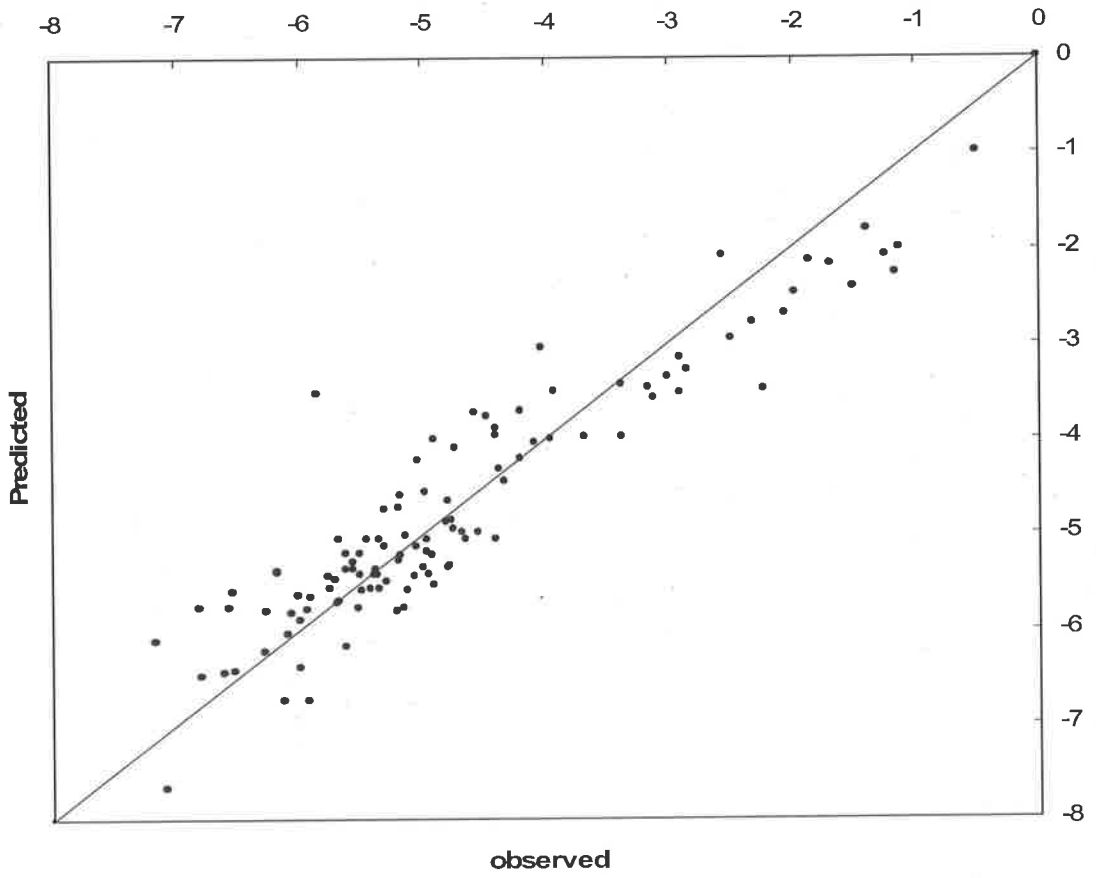

Figure 6.30. Predicted *vs.* observed value of the log-reduction in viable bacteria (as $\log_{10} N/N_0$) for the Weibull model fitted to the experimental UV disinfection data

The predicted *versus* observed levels of disinfection for the Weibull model (as $\log_{10} N/N_0$) fitted to the experimental disinfection data are presented in Figure 6.30. Importantly, the predictions of Weibull model are evenly and randomly distributed over the entire range of data, indicating that the Weibull model form is well parameterised and of a form suited to modelling tailing observed in these experimental UV disinfection data. The Weibull model generally over-predicts the extent of disinfection when the observed level of inactivation is less than 99.99% (4-$\log_{10}$ reductions). That is, the Weibull model generally over-estimates the initial rate of disinfection prior to the onset of tailing.

Estimates of the Weibull scale (β_0) and shape (β_1) parameters respectively, for fits of the model to each of the experimental disinfection data sets are presented in Figures 6.31 and 6.32, together with the associated standard error. It is clear that the standard errors associated with the scale parameter for fits of the Weibull model to experimental data

derived from data-sets 15 and 23 are comparatively large – owing to the reduced number of data in each of these sets (4 and 5 data *cf.* 6 data for the remaining sets respectively). The standard error of estimates of the shape parameter (β_1) are shown to range from approximately 2.5×10^{-4} μWs^{-1} cm^2 to less than 5×10^{-5} μWs^{-1} cm^2 as seen in Figure 6.32.

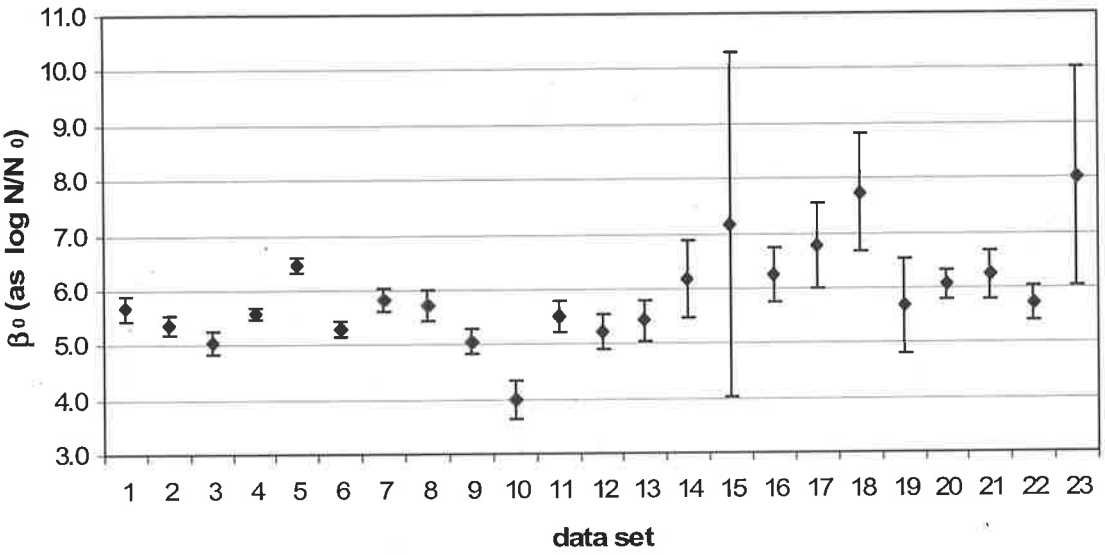

Figure 6.31. The Weibull scale parameter (β_0) for each of the experimental data sets

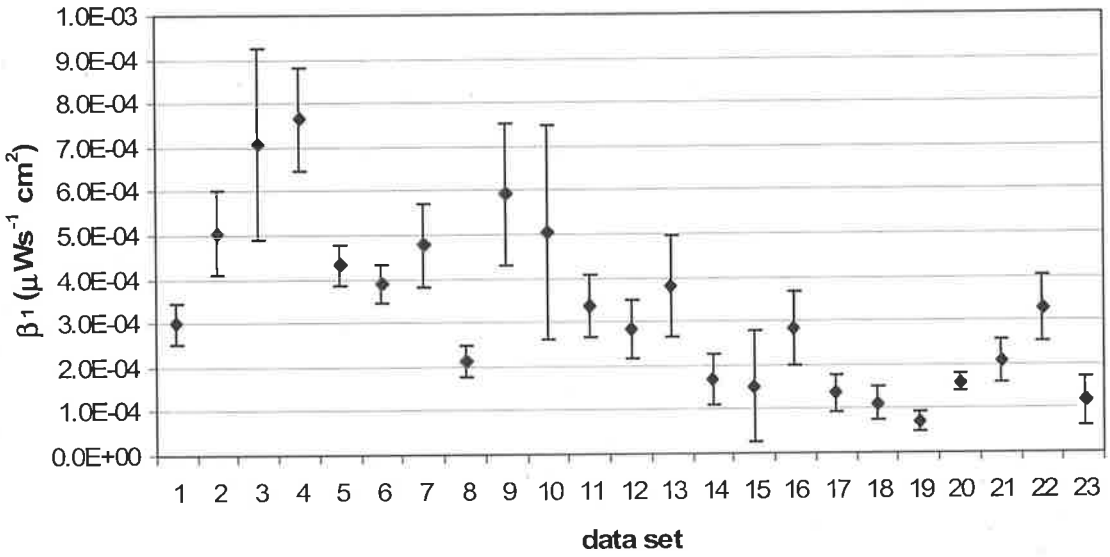

Figure 6.32. The Weibull shape parameter (β_1) for each of the experimental data sets

The respective effects of absorbing agent and shielding agent concentration on the Weibull scale and shape parameters, β_0 and β_1 are displayed in Figures 6.33 and 6.34. Error bars representing standard error have been omitted for clarity. There appears to be no clear effect of the concentration of either additive on the scale parameter, β_1, as shown by

Figures 6.33a and 6.34a. Values for the scale parameter range from limiting values of 5 to 8-$\log_{10}$ reductions as affected by absorbing agent (Figure 6.33a), and from 4 to 8-$\log_{10}$ reductions in the presence of shielding agent (Figure 6.34a). In this instance, Figures 6.33a and 6.34a show the minimum limiting extent of disinfection predicted by the Weibull model to be one order of magnitude lower (on basis of $\log_{10}$ reduction) in the presence of a suspended shielding agent as opposed to a soluble UV absorbing agent.

A significant variation in the scale parameter (β_0) predicted by the Weibull model in the presence of UV absorbing agent is also evident in 6.33a. The predicted limiting extent of disinfection ranges from 5 to 6.5 $\log_{10}$ reductions, for absorbing agent concentrations as low as 0.005 g L^{-1} and below. Correspondingly, predicted values of the shape parameter span a broad range, from 3×10^{-4} to 8×10^{-4} μWs^{-1} cm^2, at these low concentrations of absorbing agent also ($\leq$0.005 g L^{-1}).

An apparent exponential decrease in the predicted value of the shape parameter (β_1) is seen in Figure 6.33b, for increases in concentration of absorbing agent up to 0.7 g L^{-1}. The shape parameter decreases from near 7.5×10^{-4} to 1×10^{-4} μWs^{-1} cm^2 for a respective increase in absorbing agent concentration of from 0.001 to 0.05 g L^{-1}. Since the shape parameter largely governs the rate of disinfection predicted by the Weibull model, this finding (i.e. exponential decay) further highlights the inhibitory effect of absorbing agent concentration, in particular, on the rate of UV disinfection.

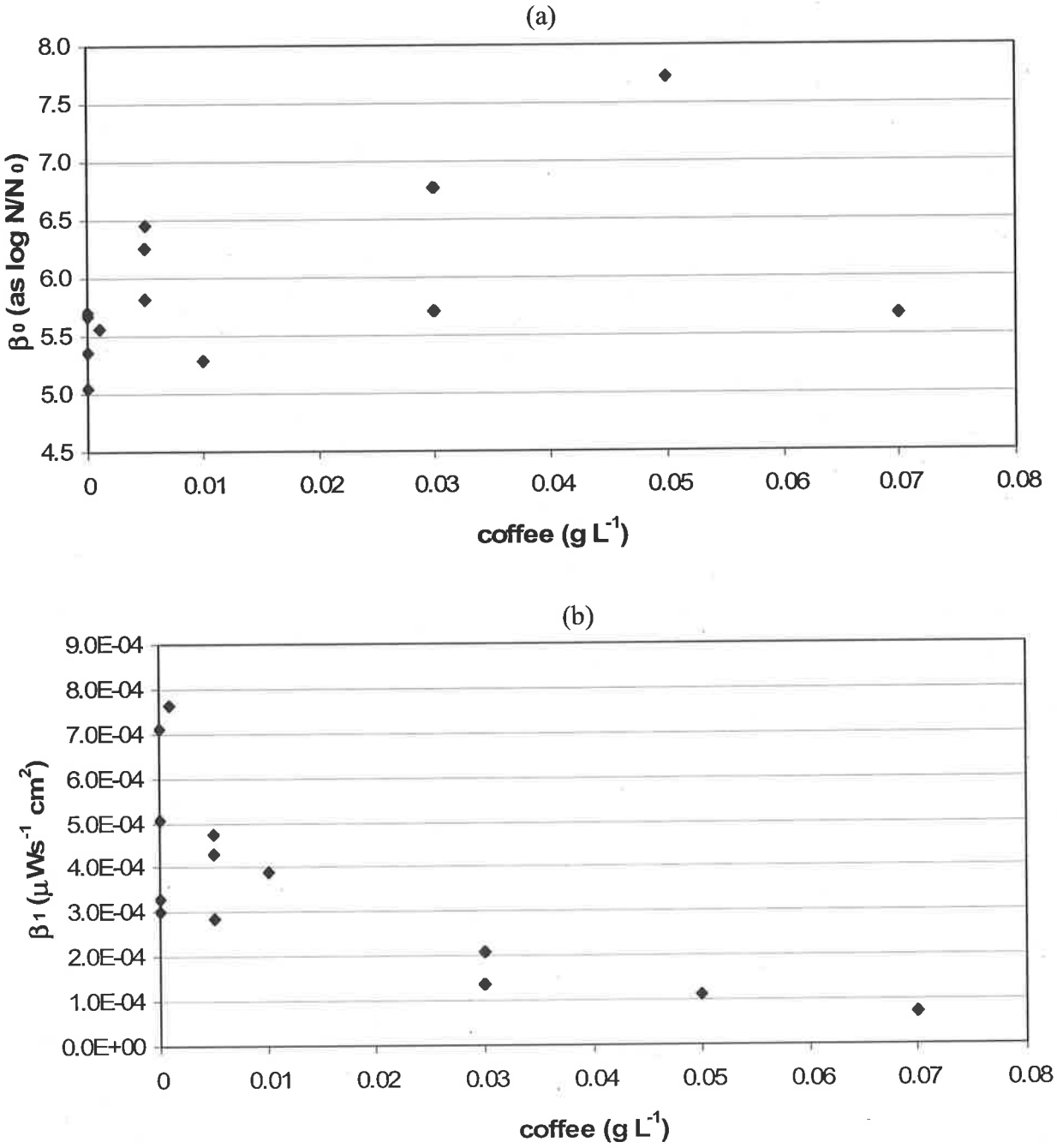

Figure 6.33. The Weibull model parameters *versus* absorbing agent concentration (a) scale parameter β_0 (b) shape parameter β_1

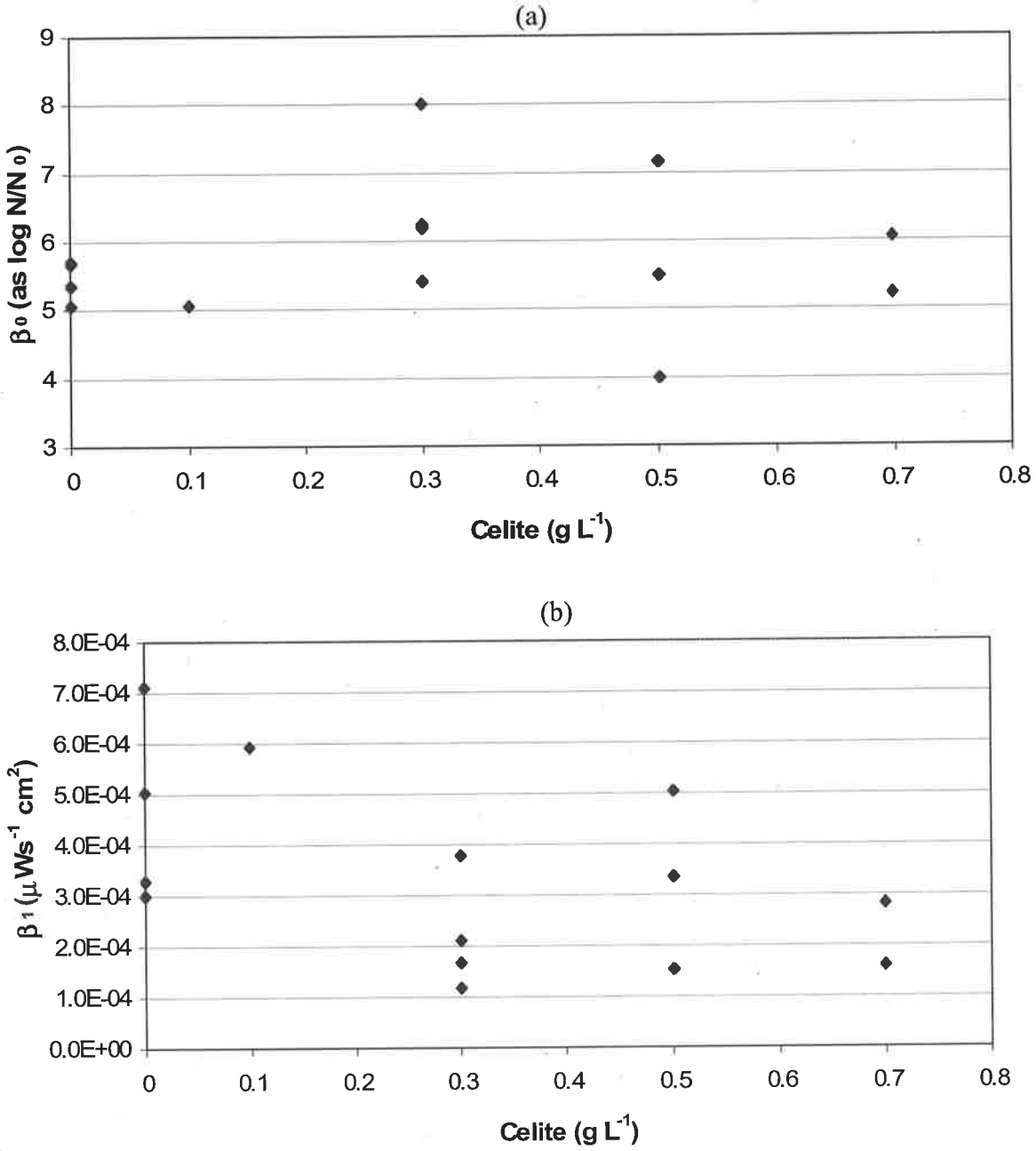

Figure 6.34. The Weibull model parameters *versus* shielding agent concentration (a) scale parameter β_0 (b) shape parameter β_1

The effect of shielding agent concentration on the scale and shape parameters is unclear, as evident through inspection of Figure 6.34.

The observed variation in the Weibull model parameters at fixed concentration (particularly low concentrations) of both absorbing and shielding agent (*see* Figures 6.33 and 6.34 respectively) suggest variations in the initial viable concentrations of bacteria prior to UV disinfection might be having a confounding effect on parameter estimates.

The effects of variation in the initial concentration of viable bacteria (prior to disinfection) on the Weibull parameters estimates are shown by Figures 6.35 and 6.36 respectively, for fixed concentrations of absorbing and shielding agent. The case when no additive is present has been included as a basis for comparison in each case.

When absorbing agent is present, Figure 6.35a highlights that the Weibull scale parameter (β_0) appears to increase with the concentration of viable bacteria initially present prior to treatment. For a fixed absorbing agent concentration of 0.005 g L^{-1} however, the data remains inconclusive. For the case when no additive is present, the scale parameter increases with increasing concentration of bacteria initially present, becoming less sensitive to changes in the initial number of bacteria as the viable population initially present increases. In this case, the scale parameter stabilises at a value of approximately 5.7-$\log_{10}$ reductions once an initial concentration of 7.6×10^{7} mL^{-1} is reached. Further increases in the concentration of viable bacteria initially present appear to have no additional effect on the scale parameter.

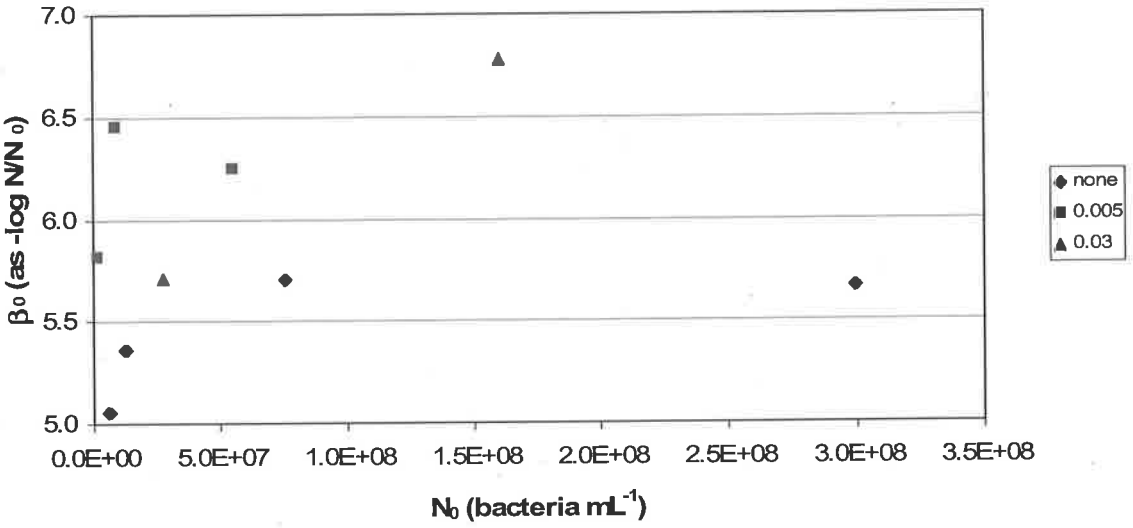

(b)

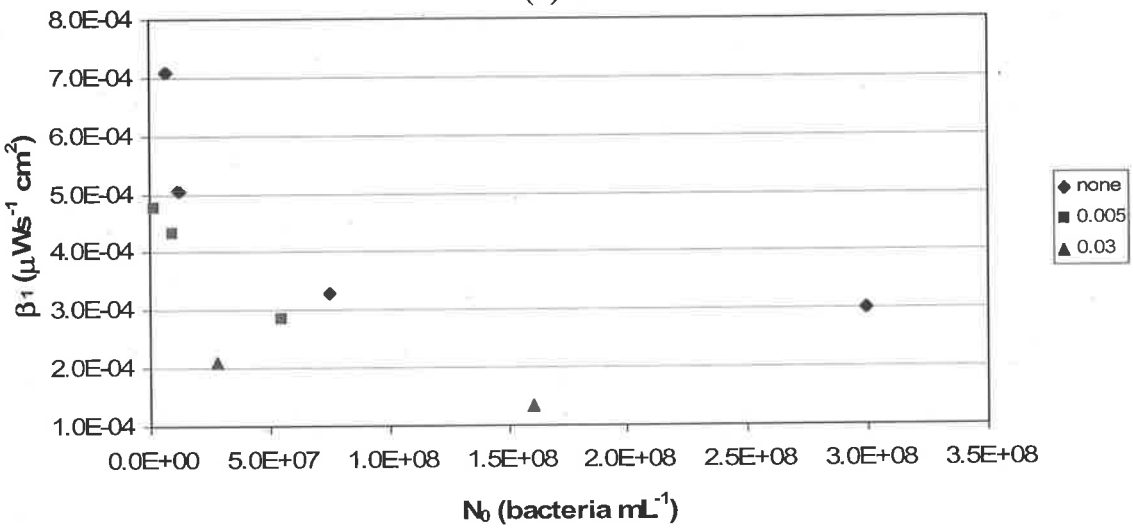

Figure 6.35. The Weibull model parameters versus initial concentration of viable bacteria for fixed concentrations (g L^{-1}) of absorbing agent (a) scale parameter β_0 (b) shape parameter β_1

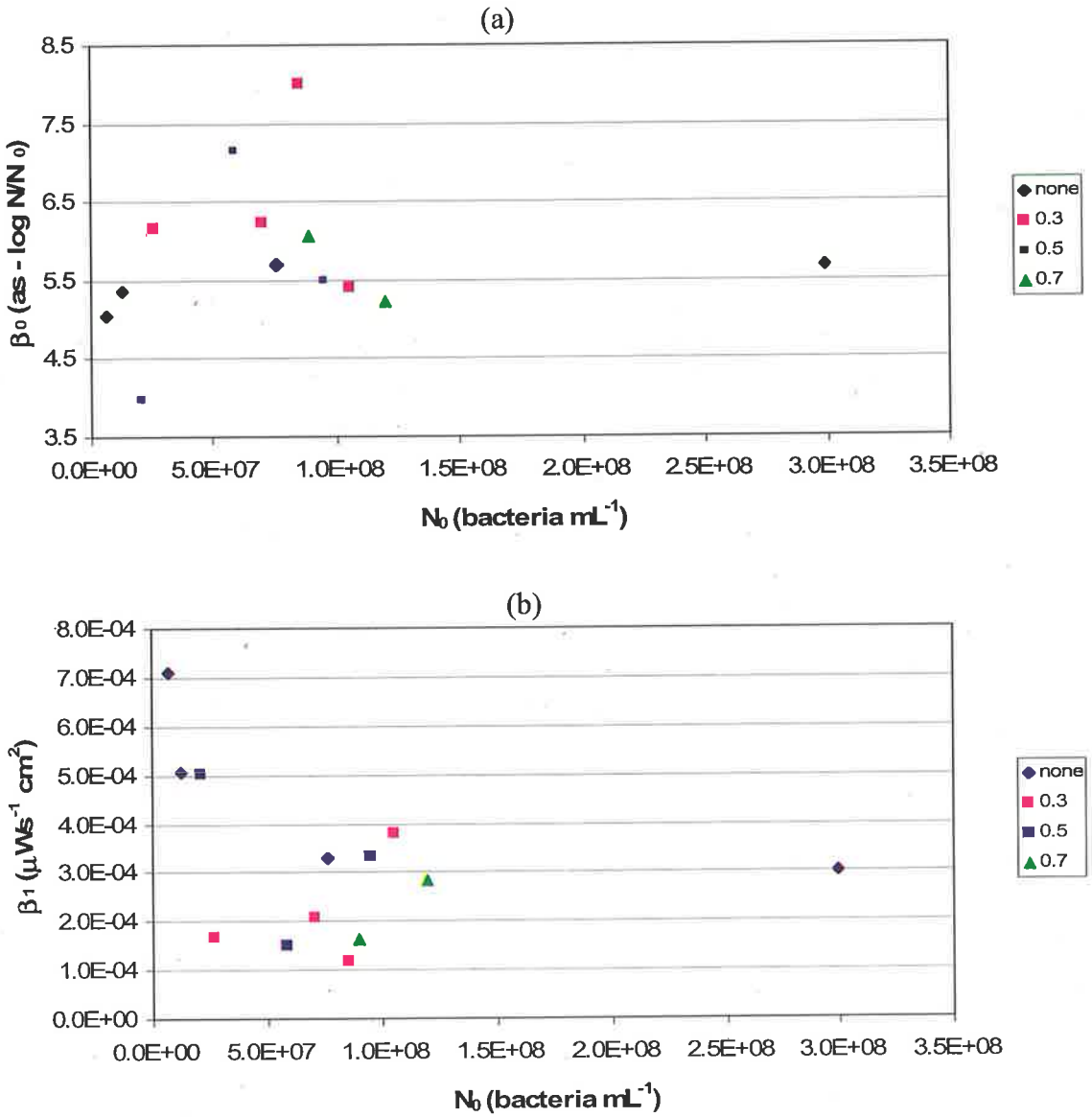

Figure 6.36. The Weibull model parameters versus initial concentration of viable bacteria for fixed concentrations (g L^{-1}) of shielding agent (a) scale parameter β_0 (b) shape parameter β_1

For a fixed concentration of absorbing agent, Figure 6.35b shows the shape parameter (β_1) is reduced for increases in the concentration of viable bacteria initially present prior to UV treatment. As the concentration of absorbing agent is increased (to maximum of 0.03 g L^{-1}), the shape parameter becomes less sensitive to changes in the concentration of viable bacteria initially present. This equates to a reduction in UV transmission to a limiting value.

When neither agent (absorbing or shielding) is present, a decrease in the concentration of viable bacteria initially present (N_0), leads to a decrease in the shape parameter (β_1), towards a limiting a value. The shape parameter stabilises at a value of approximately 3.0×10^{-4} μWs^{-1} cm^2 once an initial concentration of 7.6×10^7 mL^{-1} is reached, and is well represented by the relationship:

$$\beta_1 = 2.01\times10^{-2} N_0^{-0.22} \qquad (6.7)$$

The correlation between the shape parameter and initial viable concentration of bacteria described by Equation (6.7) is strong, with a coefficient of determination (R^2) of 0.92. However, the correlation is defined by four (4) data only. Too few experimental data are available to extend such a relationship to include the effect of concentration of either soluble UV absorbing, or UV shielding agents.

For a given concentration of shielding agent, Figure 6.36 shows the effect of increasing concentration of viable bacteria initially present on both the scale and shape parameters to be largely inconclusive.

The correlation between the Weibull scale and shape parameters, β_0 and β_1, derived for fits of the model to all sets of experimental disinfection data is presented in Figure 6.37. Standard errors of the respective model parameters have been omitted for clarity. No obvious correlation between the Weibull model parameters is apparent, despite the observation that large values of the scale parameter, β_0 (> 6.5-$\log_{10}$ reductions) are only observed for corresponding low values of the shape parameter, β_1 (< 2×10^{-4} μWs^{-1} cm^2). The majority of data are seen to lie between 1×10^{-4} and 7×10^{-4} μWs^{-1} cm^2 for the shape parameter, and between 5 and 6.5-$\log_{10}$ predicted reductions for the scale parameter.

This lack of correlation between model parameters may prove useful when attempting to isolate the effects of an environmental variable (such as absorbance or suspended solids concentration) upon a single parameter when modelling UV disinfection data exhibiting tailing.

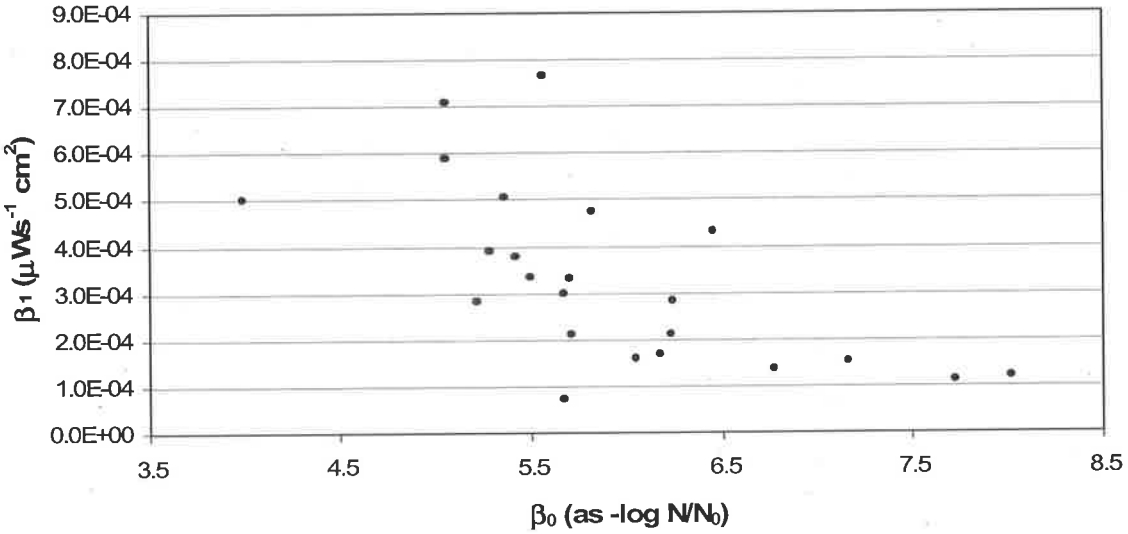

Figure 6.37. Observed correlation of Weibull model parameters when fitted against the experimental UV disinfection data

The Weibull model may be differentiated with respect to UV dose in order to evaluate a measure of the rate of disinfection. The model presented does not explicitly include a single parameter defining the rate of disinfection. At zero- UV dose, the product of the Weibull scale and shape parameters is a measure of the initial rate of disinfection (i.e.β_0, β_1). Herein the derivative of the Weibull model is evaluated at respective UV doses of zero and the maximum experimentally observed UV dose (44,200 μWs cm^{-2}) to give measures of the initial rate of disinfection (k_0), and of a rate of disinfection characteristic of the tailing region (k_T).

Table 6.13. Kinetic rate constant data for the Weibull model

Data set	k_0 ($\mu Ws^{-1}.cm^2$)	k_T ($\mu Ws^{-1}.cm^2$) (at 44200 $\mu Ws.cm^{-2}$)
1	1.70×10^{-3}	2.94×10^{-9}
2	2.71×10^{-3}	5.50×10^{-13}
3	3.58×10^{-3}	8.68×10^{-17}
4	4.25×10^{-3}	9.39×10^{-18}
5	2.78×10^{-3}	1.45×10^{-11}
6	2.06×10^{-3}	7.04×10^{-11}
7	2.77×10^{-3}	2.03×10^{-12}
8	1.20×10^{-3}	1.08×10^{-7}
9	2.99×10^{-3}	1.34×10^{-14}
10	2.00×10^{-3}	4.31×10^{-13}
11	1.84×10^{-3}	6.77×10^{-10}
12	1.48×10^{-3}	5.35×10^{-9}
13	2.05×10^{-3}	1.08×10^{-10}
14	1.04×10^{-3}	5.95×10^{-7}
15	1.09×10^{-3}	1.32×10^{-6}
16	1.78×10^{-3}	6.19×10^{-9}
17	9.18×10^{-4}	2.30×10^{-6}
18	8.58×10^{-4}	6.32×10^{-6}
19	4.02×10^{-4}	1.75×10^{-5}
20	9.72×10^{-4}	8.03×10^{-7}
21	1.30×10^{-3}	1.25×10^{-7}
22	1.87×10^{-3}	9.14×10^{-10}
23	9.43×10^{-4}	5.21×10^{-6}

The rates of disinfection predicted by the Weibull model at UV doses of 0 and 44,200 $\mu Ws\ cm^{-2}$ (k_0 and k_T respectively) when fit against the experimental UV disinfection data are presented in Table 6.13. The initial rate of disinfection predicted by the Weibull model at zero- UV dose (k_0) ranges between 4.02×10^{-4} and 4.25×10^{-3} $\mu Ws^{-1}\ cm^2$, compared to between 9.39×10^{-18} and 1.75×10^{-5} $\mu Ws^{-1}\ cm^2$ predicted as the rate of disinfection at a UV dose of 44,200 $\mu Ws\ cm^{-2}$. Simply, the rate of disinfection predicted at zero UV dose varies by an order of magnitude across all sets of experimental data, whereas the rate predicted at the maximum experimentally observed UV dose (of 44,200 $\mu Ws\ cm^{-2}$) spans 13 orders of magnitude. This is symptomatic of the inherent property of the Weibull model in the prediction of a limiting extent of disinfection (as β_0), whereby the corresponding rate of disinfection becomes negligible.

The rates of disinfection predicted by the Weibull model at zero UV dose (k_0) are presented against absorbing and shielding agent concentration on semi-logarithmic coordinates in Figure 6.38. The dependence of the predicted rate of disinfection (at zero dose) appears log-linear with respect to the absorbing agent concentration, with increasing concentration of absorbing agent leading to a reduction in the predicted initial rate of disinfection (k_0). The dependence of the initial rate of disinfection upon shielding agent concentration is unclear however. For shielding agent concentrations of 0.3 g L^{-1} or greater, no systematic effect of concentration on the predicted initial rate of disinfection is clear, with the predicted rates ranging from 1×10^{-3} to 2×10^{-3} μWs^{-1} cm^2.

It is noted, that in order to achieve comparable predicted initial rates of disinfection (i.e. k_0), the concentration of shielding agent required is approximately an order of magnitude greater than the absorbing agent. This equates to reduction of the UV transmission to a comparable value when each of the agents are in these relative proportions. Or simply, when in comparable concentrations, the soluble absorbing agent affords a greater reduction in UV transmission than the suspended shielding agent.

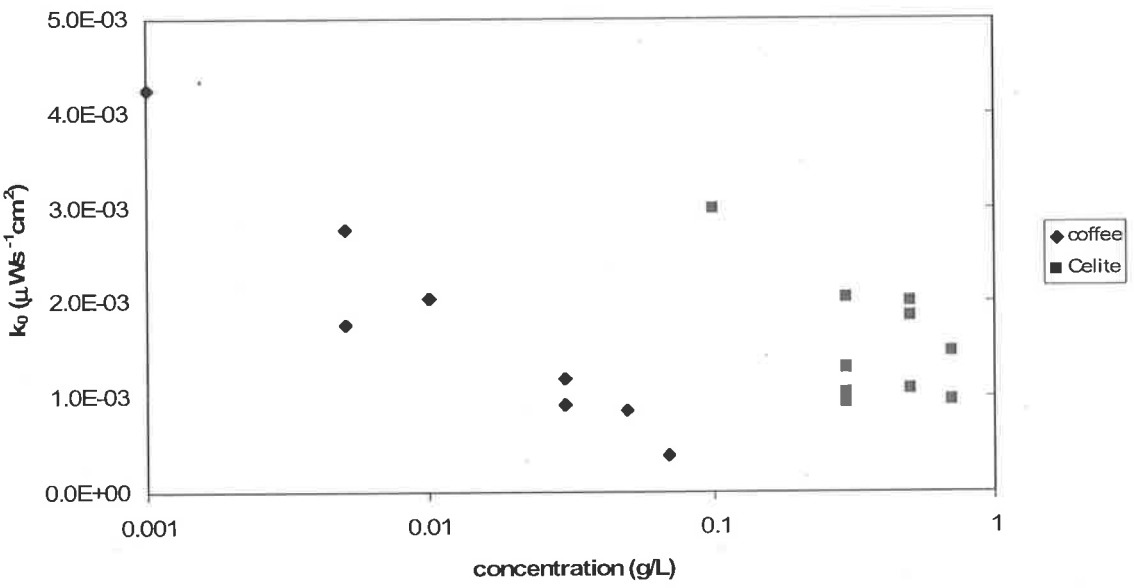

Figure 6.38. Rate of disinfection predicted by the Weibull model at zero UV dose (k_0) against absorbing and shielding agent concentration

Pooling of the experimental disinfection data on the basis of absorbing and shielding agent concentration was also performed to clarify whether either the Weibull scale or shape parameters exhibited any systematic dependence on concentration of either agent.

The predicted values for the Weibull model parameters (β_0 and β_1) obtained when the experimental UV disinfection data are pooled according to the type and concentration of agent present are displayed in Table 6.12. When only one original disinfection data-set is present for a given concentration of absorbing or shielding agent, the model parameters remain unchanged from those derived from the unpooled disinfection data. The statistical significance of the fitted Weibull parameters is increased when the data is pooled, with *P-values* associated with the pooled estimates of the scale parameter (β_0) ranging from 2.59×10^{-8} to less than 2×10^{-16}, compared to between 1.5×10^{-1} and 8×10^{-7} for fits of the model to the unpooled data (*see* Table 6.11). The *P-values* for the shape parameter derived from the pooled disinfection data range between 2.66×10^{-3} and 6.17×10^{-9} – which is typically between two (2) and five (5) orders of magnitude lower than for those values associated with estimates from the unpooled data (*see.* Table 6.11). However, despite the increased statistical significance of the pooled parameter estimates, values of the test statistic (t-value) obtained for the pooled disinfection data are comparable to those when the data remains unpooled. For estimates of the scale parameter (β_0), values of the test statistic range from 15.5 to 42.2 and 2.3 to 52.3 for the pooled and unpooled disinfection data respectively. In the case of the shape parameter (β_1), the test statistic ranged from 3.6 to 9.1 and 1.2 to 9.0 respectively for the pooled and unpooled disinfection data. In either case, the maximum values of the test statistic remain comparable for fits of the Weibull model to the pooled and unpooled data, whilst the minimum value of the test statistic is higher when the data is pooled.

The residual sums of squares derived from the pooled data (*see.* Table 6.12) are again increased in comparison to the observed values obtained for fits of the Weibull model to the unpooled disinfection data (*see.* Table 6.11). When the disinfection data is pooled, values of the residual sum of squares range between 2.00 and 10.08, compared to between 0.16 and 4.37 for fits of the Weibull model to the unpooled disinfection data. This is due to pooled disinfection data comprising of between 12 and 24 data per set, compared to a maximum of six (6) data only describing each of the unpooled sets.

The predicted *versus* observed values of the reduction in viable bacteria following UV treatment (as $\log_{10} N/N_0$) for fits of the Weibull model applied to each of the pooled disinfection data-sets (•) are presented in Figure 6.39, together with those predictions where the disinfection data remain unpooled (•) (i.e. one concentration only for a given agent). Importantly, the predictions based on the pooled data are evenly and randomly distributed. When an observed level of disinfection of less than 4-$\log_{10}$ reductions is observed, the distribution of predictions base on pooled data is broader than when the data remains unpooled. Predictions based on the pooled disinfection data also consistently over-predict the delivered level of disinfection when fewer than 4 $\log_{10}$ reductions are observed experimentally.

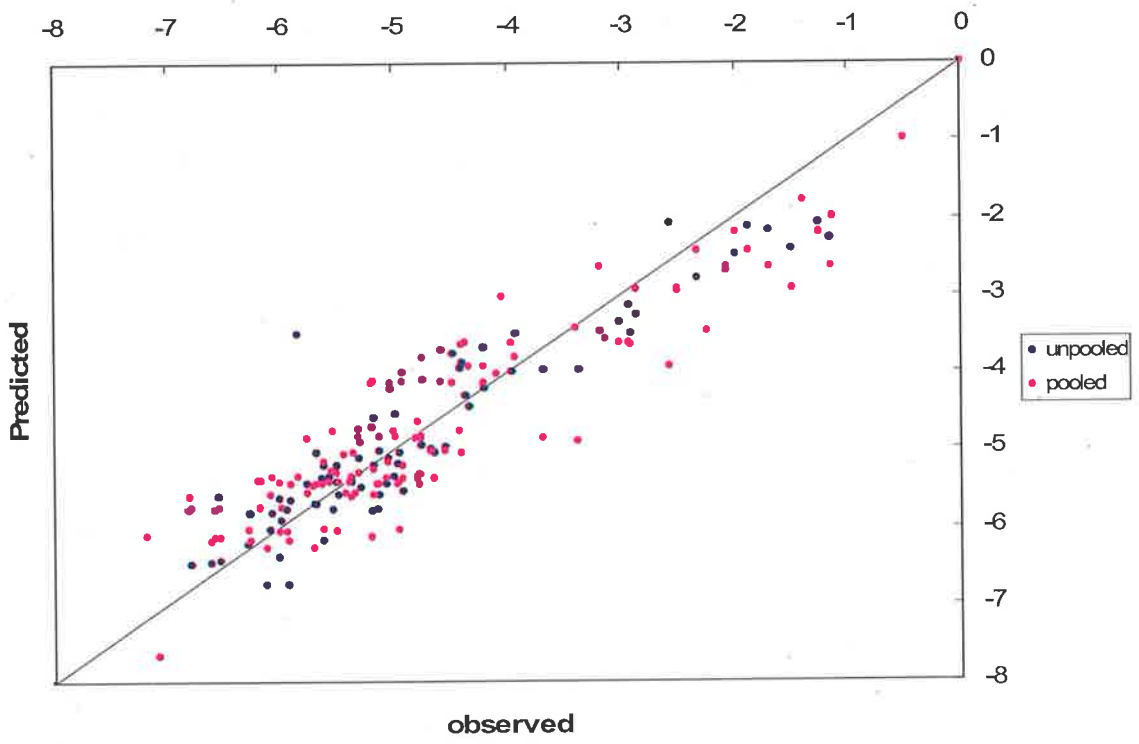

Figure 6.39. Predicted *versus* observed value of the log-reduction in viable bacteria (as $\log_{10} N/N_0$) from the Weibull model for the pooled UV disinfection data

The respective effects of absorbing and shielding agent concentration on the Weibull parameters derived through pooling of the experimental disinfection data on the basis of agent concentration are presented in Figures 6.40 and 6.41.

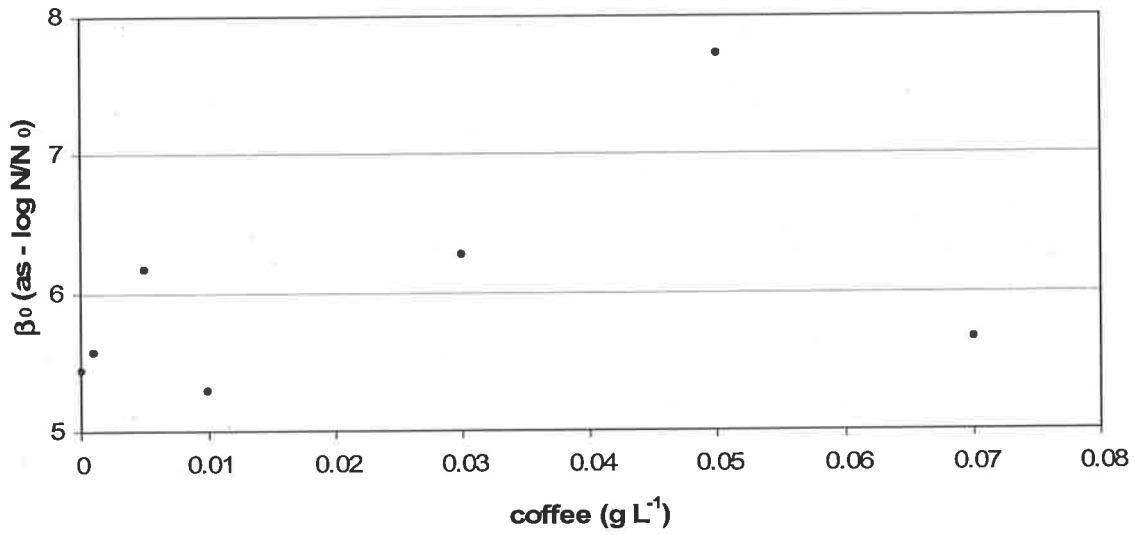

(b)

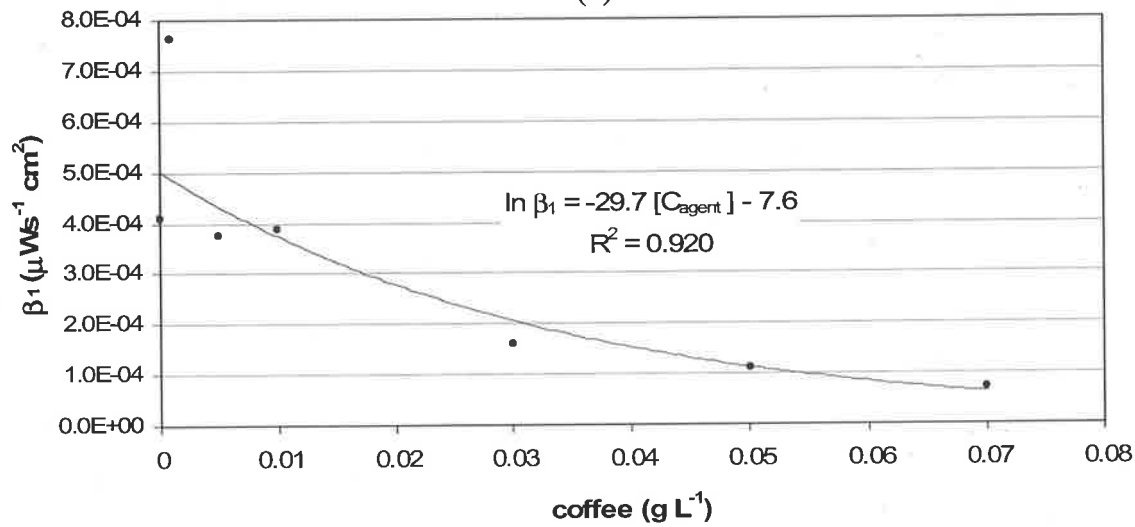

Figure 6.40. The Weibull parameters derived from pooled data against concentration of absorbing agent (a) β_0 (b) β_1

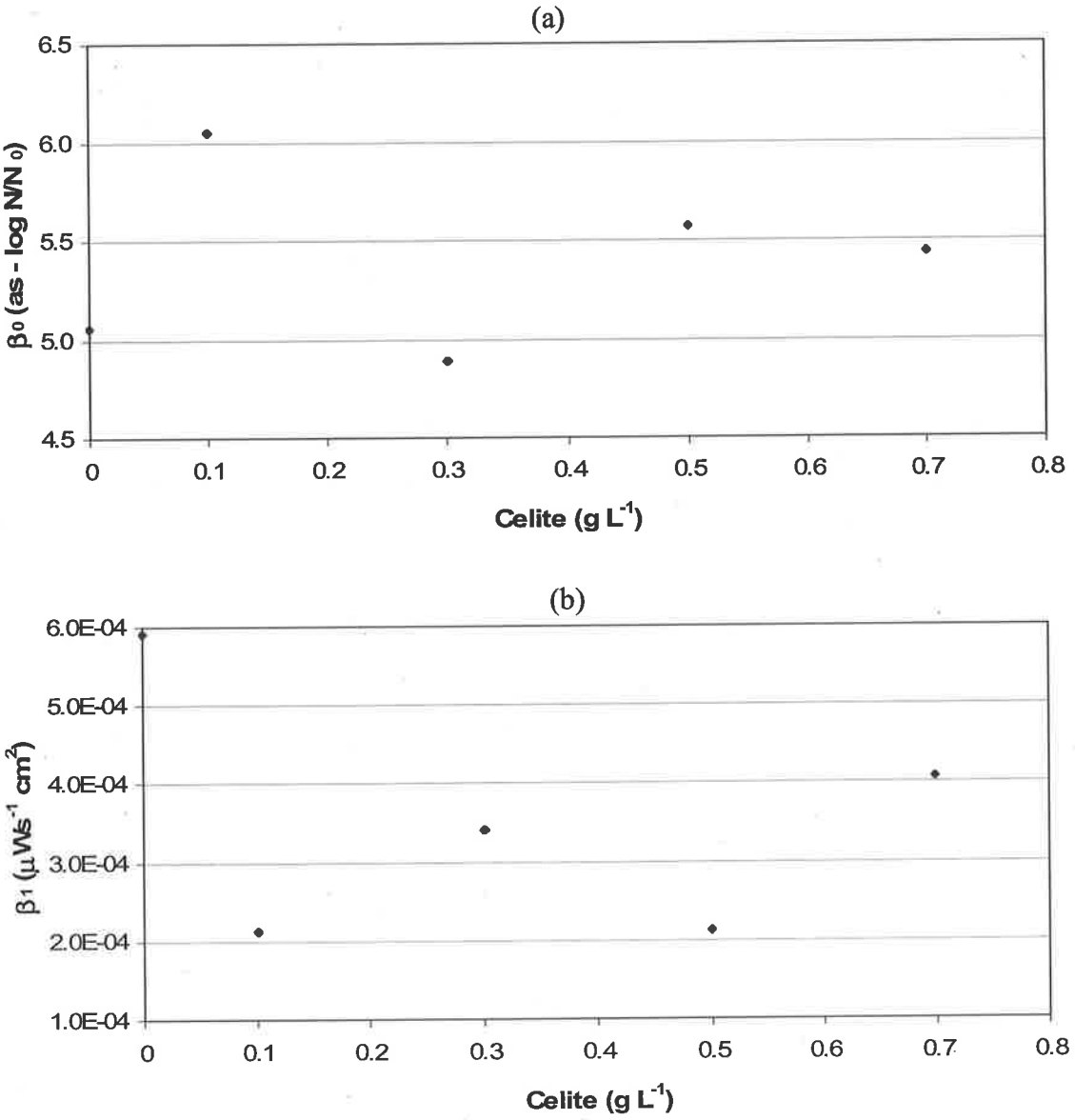

Figure 6.41. The Weibull parameters derived from pooled data against concentration of shielding agent (a) β_0 (b) β_1

As was the case for fits of the Weibull model to the unpooled disinfection data (*see.* Figures 6.33 and 6.34), the effect of either absorbing or shielding agent concentration on the Weibull model parameters is generally unclear. However, a notable exception is the effect of absorbing agent concentration on the Weibull shape parameter (β_1), as shown by Figure 6.40b. The shape parameter, β_1, again appears to decrease in a near exponential manner with respect to absorbing agent concentration (as for the unpooled data – Figure 6.33b), and may be well described by the relationship given below by Equation (6.8):

$$\ln \beta_1 = -29.7\,[C_{agent}] - 7.6 \qquad (6.8)$$

The correlation described by Equation (6.8) is strong, with a value of 0.920 for the coefficient of determination (R^2) quantifying the fit. However, the correlation could be strengthened by omission of the outlier corresponding to an absorbing agent concentration of 0.001 g L^{-1}, which appears to skew the response.

The initial rates of disinfection as predicted by the Weibull model at zero UV dose ($k_0 = \beta_0.\beta_1$) when fitted to the pooled disinfection data are presented against the concentration of both absorbing and shielding agent in Figure 6.42. The predicted initial rates of disinfection appear to exhibit log-linear dependence on the concentration of both the absorbing (coffee) and shielding (Celite 503^{TM}) agents. The correlations established for both absorbing and shielding agent appear parallel; suggesting the initial rate of disinfection is equally sensitive to changes in concentration of either agent (i.e. same slope in each case). This has important implications for further analysis of UV disinfection kinetics. Pooling of the disinfection data also appears to have minimised the confounding effect of variations in the initial concentration of viable bacteria present prior to UV disinfection, particularly when shielding agent is present. When the disinfection data remained unpooled, the effect of shielding agent concentration on the initial rate of disinfection (UV dose = 0) predicted by the Weibull model remained unclear. However, when the disinfection data are pooled, the initial rate of disinfection predicted by the Weibull model decreases log-linearly with increasing shielding agent concentration.

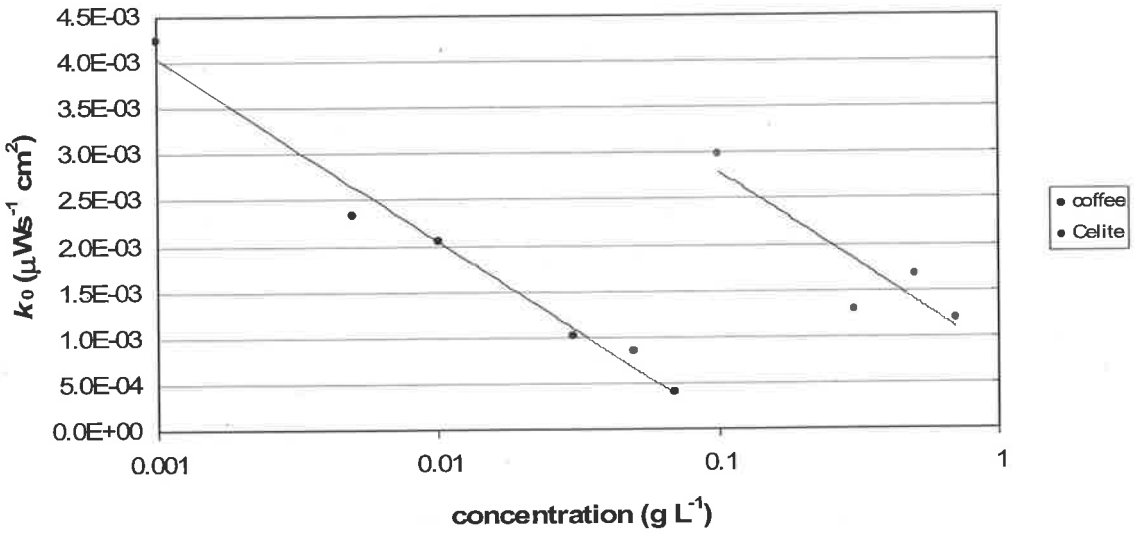

Figure 6.42. Rate of disinfection predicted by the Weibull model at zero UV dose (k_0) against additive concentration when fitted to the pooled disinfection data

The effects of absorbing agent and shielding agent concentration respectively on the initial rates of disinfection (k_0) predicted by the Weibull model when fitted to the pooled disinfection data may be summarised by Equations (6.9) and (6.10) below:

$$k_0 = -9\times10^{-4} \ln [C_{agent}] - 1.9\times10^{-3} \quad (6.9)$$

$$k_0 = -9\times10^{-4} \ln [C_{agent}] + 8.0\times10^{-4} \quad (6.10)$$

The fits of Equations (6.9) and (6.10) correspond to respective values of 0.980 and 0.797 for the coefficient of determination, R^2. The correlation is not as strong in the case of the shielding agent (Equation 6.10), owing to fewer data defining the correlation in this case (4 *cf.* 6 data). An interesting point of note is the equality of slopes defining the correlations, suggesting that the initial rates of disinfection as predicted by the Weibull model are equally sensitive to changes in concentration of both shielding and absorbing agent. Similarly, for a fixed initial rate of disinfection as predicted by the Weibull model, Equations (6.9) and (6.10) reveal the required concentration of absorbing agent to be 20 times lower than the corresponding shielding agent concentration to have the same inhibitory effect.

The correlation summarising the effect of the absorbing agent (Equation 6.9), however, can be seen to predict a negative rate of disinfection as the absorbing agent concentration

exceeds approximately 0.12 g L^{-1}. Consequently these correlations should be used with caution, and not generally extended to use beyond the range of observed concentrations without further experimental validation against independent disinfection data.

In summary, generally no clear systematic trends in either of the Weibull model parameters, β_0 or β_1, are evident with respect to absorbing agent or shielding agent concentration when the UV disinfection data remain unpooled. The notable exception however was the effect of absorbing agent concentration on the shape parameter, β_1, which appeared to decay exponentially with increasing absorbing agent concentration. This trend was apparent despite significant variation in values for the shape parameter, from 3×10^{-4} to 8×10^{-4} μWs^{-1} cm^2, at absorbing agent concentrations of 0.005 g L^{-1} and lower.

The Weibull model over-predicted the delivered level of disinfection when less than 4 $\log_{10}$ reductions were observed experimentally; and when in excess of 4-$\log_{10}$ reductions were observed, variability between the disinfection data and model predictions increased. This reduced accuracy of prediction at higher levels of disinfection (> 4-$\log_{10}$ reductions), is attributable to the inability of the Weibull model to account for ongoing disinfection observed in the tailed data.

Generally the effect of absorbing and shielding agent concentrations on the Weibull parameters were confounded by variation in the concentration of viable bacteria initially present prior to UV disinfection. For fixed concentrations of both absorbing and shielding agents, the effect of the initial concentration of viable bacteria on the Weibull parameters was generally not known. However, the notable exception was the effect on the shape parameter, β_1, for fixed concentrations of absorbing agent. When the absorbing agent concentration is constant, the shape parameter (β_1) is reduced for increases in the concentration of viable bacteria initially present prior to UV treatment. As the concentration of absorbing agent is increased (to a maximum of 0.03 g L^{-1}), the shape parameter becomes increasingly insensitive to changes in the initial concentration of viable bacteria present prior to UV exposure.

No obvious correlation between the scale and shape parameters of the Weibull model is apparent, despite higher values of the scale parameter corresponding to low values of the shape parameter, and vice-versa, suggesting some form of dependence.

The initial rate of disinfection predicted by the Weibull model at zero UV dose (k_0) appears to be log-linearly dependent on absorbing agent concentration, decreasing with increasing concentration of absorbing agent. When fitted to the unpooled disinfection data, dependence of the predicted initial (i.e. UV dose = 0) rate of disinfection on shielding agent concentration was unclear. However, when the disinfection data was pooled on the basis of agent concentration, a log-linear dependence on shielding agent concentration became apparent. Analyses showed when fitted to the pooled disinfection data, the predicted rate of disinfection at zero- UV dose was equally sensitive to changes in absorbing and shielding agent concentrations – an interesting finding which requires further investigation.

6.3.3 A comparison of the synthesised model forms

Analyses have shown that both the modified exponentially damped polynomial (EDP_m) and Weibull models are of a form suited to simulate tailing often observed in experimentally obtained UV disinfection data.

The EDP_m is a piecewise-continuous model consisting of three parameters (k, λ and $[dose]_B$), which has the flexibility to account for ongoing disinfection in the tail. By imposing a constraint on the rate of disinfection in the tail of the data ($k' \geq 0$), the model can be used for further optimisation.

The Weibull model is monotonic and is defined by only two parameters, namely the scale parameter (β_0) and the shape parameter (β_1). The Weibull model has the advantage of predicting a limiting extent of disinfection in the tail which is quantified as the scale parameter, β_0, and presents an intuitive limiting case.

Each of the two model forms assessed exhibit both advantages and drawbacks. Herein each of the two (2) forms are further assessed and compared.

On the basis of residual sums of squares (RSS), fits of the EDP_m and Weibull models to the experimental disinfection data may be considered to be comparable. The respective values to range from 0.03 to 2.13 for the EDP_m model, and from 0.16 to 4.37 for the Weibull model, as shown by Tables 6.4 and 6.11 respectively. The effect of one fewer terms in definition of the Weibull model as opposed to the EDP_m model is also reflected in the respective values of the residual sums of squares. The EDP_m model was shown in Table 6.4 not to converge to a solution for each of the parameter estimates for data sets 15 through 18 inclusive. When only sets of data for which the EDP_m model converged are considered, the maximum value of the residual sum of squares is reduced to 1.57. The lack of convergence of the EDP_m model derives from the piecewise nature of the model, which is particularly problematic when few disinfection data are available for analysis, and also, when insufficient disinfection data is distributed about the breakpoint dose $[dose]_B$.

The *P-values* associated with the Weibull shape parameter β_1, are typically comparable to those of the respective EDP_m parameters (k, λ and $[dose]_B$), indicating that they are of

similar statistical significance in the definition of the respective Weibull and EDP_m model forms. In the case of the Weibull model, *P-values* range from 1.50×10^{-1} to 8.00×10^{-7}, and from 3.48×10^{-1} to 8.48×10^{-4} for the scale (β_0) and shape (β_1) parameters respectively. For the EDP_m model, *P-values* range from 1.52×10^{-1} to 2.56×10^{-4}, from 1.97×10^{-1} to 4.94×10^{-4}, and from 7.51×10^{-1} to 5.48×10^{-4} for the disinfection rate coefficient (k), damping coefficient (λ) and breakpoint dose ($[dose]_B$) respectively. The *P-values* associated with the scale parameter (β_0) of the Weibull model typically take values lower than for the shape parameter (β_1), or for any of the parameters defining the EDP_m model. This may arise from the Weibull model comprising of one fewer model terms (2 *cf.* 3). As a result, the standard error associated with each of the Weibull parameters will be comparatively lower owing to an extra available degree of freedom during regression analysis. For example, the values of the test-statistic (ratio of parameter estimate to its standard error) associated with the scale parameter, β_0, ranges from 2.3 to as high as 52.3 (*see.* Table 6.11). By comparison, values of the test-statistic associated with the disinfection rate constant (k) of the EDP_m model vary from 1.9 to 20.4, with the majority of values less than 10 (*see.* Table 6.4).

Arguably, on the basis of *P-values*, the scale parameter is much more important than the shape parameter in using the Weibull model to adequately describe practical UV disinfection kinetics. In contrast, *P-values* of each of the EDP_m model parameters are of comparable orders of magnitude for fits of the model to each experimental disinfection data-set, further highlighting that they are strongly dependent and equally important in adequately describing these experimentally observed UV disinfection data.

Table 6.14 presents a comparison of rates of disinfection predicted by the Weibull model at UV doses of zero (k_0), and at the maximum experimentally observed dose of 44,200 $\mu Ws\ cm^{-2}$ (k_T), with the disinfection rate coefficient (k) and the disinfection rate coefficient in the tailing region (k') predicted by the constrained EDP_m model fit against the experimental UV disinfection data.

Table 6.14. Kinetic rate constant data for both the Weibull and EDP_m models

	Weibull		EDP_m	
Data Set	k_0 ($\mu Ws^{-1}cm^2$)	k_T ($\mu Ws^{-1}cm^2$) (at 44,200 $\mu Ws\ cm^{-2}$)	k ($\mu Ws^{-1}cm^2$)	k' ($\mu Ws^{-1}cm^2$)
1	1.70×10^{-3}	2.94×10^{-9}	1.60×10^{-3}	1.68×10^{-5}
2	2.71×10^{-3}	5.50×10^{-13}	2.34×10^{-3}	1.31×10^{-5}
3	3.58×10^{-3}	8.68×10^{-17}	3.46×10^{-3}	2.60×10^{-5}
4	4.25×10^{-3}	9.39×10^{-18}	3.03×10^{-3}	zero #
5	2.78×10^{-3}	1.45×10^{-11}	2.38×10^{-3}	1.05×10^{-5}
6	2.06×10^{-3}	7.04×10^{-11}	1.85×10^{-3}	1.49×10^{-5}
7	2.77×10^{-3}	2.03×10^{-12}	2.46×10^{-3}	1.93×10^{-5}
8	1.20×10^{-3}	1.08×10^{-7}	1.13×10^{-3}	1.10×10^{-5}
9	2.99×10^{-3}	1.34×10^{-14}	2.71×10^{-3}	1.94×10^{-5}
10	2.00×10^{-3}	4.31×10^{-13}	1.44×10^{-3}	zero #
11	1.84×10^{-3}	6.77×10^{-10}	1.57×10^{-3}	zero #
12	1.48×10^{-3}	5.35×10^{-9}	1.35×10^{-3}	4.58×10^{-6}
13	2.05×10^{-3}	1.08×10^{-10}	1.65×10^{-3}	zero #
14	1.04×10^{-3}	5.95×10^{-7}	7.63×10^{-4}	zero #
15	1.09×10^{-3}	1.32×10^{-6}	1.20×10^{-3}	3.91×10^{-5}
16	1.78×10^{-3}	6.19×10^{-9}	1.58×10^{-3}	zero #
17	9.18×10^{-4}	2.30×10^{-6}	7.17×10^{-4}	zero #
18	8.58×10^{-4}	6.32×10^{-6}	7.34×10^{-4}	zero #
19	4.02×10^{-4}	1.75×10^{-5}	3.70×10^{-4}	zero #
20	9.72×10^{-4}	8.03×10^{-7}	9.73×10^{-4}	2.49×10^{-5}
21	1.30×10^{-3}	1.25×10^{-7}	1.29×10^{-3}	1.99×10^{-5}
22	1.87×10^{-3}	9.14×10^{-10}	1.67×10^{-3}	4.62×10^{-6}
23	9.43×10^{-4}	5.21×10^{-6}	1.05×10^{-3}	1.04×10^{-4}

zero denotes the disinfection rate coefficient has been constrained (= 0)

The initial rate of disinfection predicted by the Weibull model is seen to compare well with the disinfection rate coefficient of the EDP_m model, with a range of between 4.02×10^{-4} and 4.25×10^{-3} μWs^{-1} cm^2 observed for the initial rate of disinfection predicted by the Weibull model, compared to a range of between 3.70×10^{-4} and 3.46×10^{-3} μWs^{-1} cm^2 predicted for the disinfection rate coefficient of the EDP_m model. That is, the Weibull model generally predicts a higher range of values representative of the disinfection rates in the early stages of disinfection. It should be noted however, the disinfection rate coefficient of the EDP_m model is not a rate of disinfection evaluated at a UV dose of zero, but is representative of the rate of disinfection prior to the onset of tailing.

The disinfection rates representative of the tailing region compare less favourably. A range of between 9.39×10^{-18} and 1.75×10^{-5} μWs^{-1} cm^2 was predicted by the Weibull model for rates of disinfection at a UV dose of 44,200 μWs cm^{-2}. This is symptomatic of the inherent property of the Weibull model in prediction of a limiting extent of disinfection, whereby the rate of disinfection becomes negligible. The rates of disinfection predicted by the EDP_m model in the tailing region (neglecting those cases where the rate was constrained to zero) were substantially higher than comparable rates of disinfection in the tail predicted by the Weibull model, ranging from 4.58×10^{-6} to 1.04×10^{-4} μWs^{-1} cm^2. It is worthy to note, that the rate of disinfection in the tail (k') predicted by the EDP_m model is based on the observed rate of disinfection at the onset of tailing, which typically occurs at a UV dose substantially less than the 44,200 μWs cm^{-2} used with the Weibull model to predict the rate of disinfection in the tail.

The limiting levels of disinfection predicted by the Weibull and constrained EDP_m models compare well when fit to the experimental UV disinfection data. The scale parameter of the Weibull model, β_0, is seen to vary from 3.98 to 8.02 (as $\log_{10} N/N_0$) $\log_{10}$ reductions as shown in Table 6.11, and is a measure of the limiting observed level of disinfection in the tail. This compares to predictions of the constrained EDP_m model of between 3.97 and 7.51-$\log_{10}$ reductions at the breakpoint dose (-c), indicative of the onset of tailing (*see.* Table 6.6). The shape parameter, β_1, is also seen to vary from 7.09×10^{-5} to 7.64×10^{-4} μWs^{-1} cm^2, an order of magnitude difference, for fits of the Weibull model to the experimental disinfection data (*see.* Table 6.11). This is comparable to the range of values taken for the damping coefficient (λ) of the EDP_m model, ranging from 2.50×10^{-5} to 2.81×10^{-4} μWs^{-1} cm^2 (*see.* Table 6.4).

The level of disinfection predicted by the EDP_m model at the breakpoint dose (c), is presented against the scale parameter predicted by the Weibull model (β_0) in Figure 6.43, when each model is fitted to the experimental disinfection data. The scale parameter consistently over-predicts the level of disinfection predicted at the breakpoint dose by the EDP_m model over the entire range of data.

The Weibull model is of a form which predicts a negligible of rate disinfection in the tailing region, tending towards zero, whereas the constrained EDP_m model is limited to

prediction of non-negative rates of disinfection in the tail ($k' \geq 0$). Consequently, the level of disinfection indicated by the scale parameter (β_0) of the Weibull model is greater than that predicted by the EDP_m model at the onset of tailing ($-c$), since it is a measure of the average level of disinfection observed in the tail. By comparison, the EDP_m parameter ($-c$) is a measure of level of disinfection at the commencement of tailing only. This is due to the increased flexibility of the EDP_m model over the Weibull form in that it can account for increasing levels of disinfection over the range of UV doses spanning the tailed data. This is in contrast to the Weibull form which cannot account for such a continuing level of disinfection.

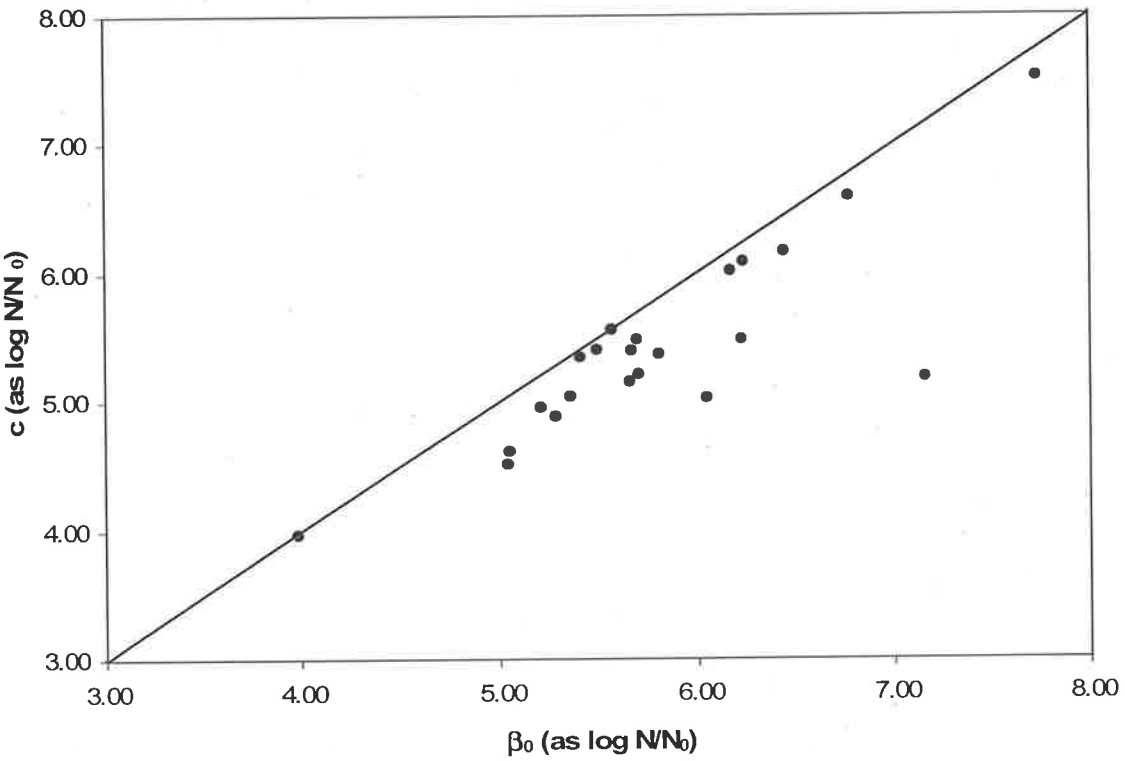

Figure 6.43. Predicted level of disinfection at the breakpoint dose (c) by the EDP_m model *versus* the Weibull scale parameter (β_0) for fits to the experimental UV disinfection data

The predicted *versus* observed levels of disinfection (as $\log_{10} N/N_0$) for the fits of Weibull and EDP_m models to the experimental disinfection data is presented in Figure 6.44. Importantly, predictions of both models are randomly and evenly distributed over the entire range of data.

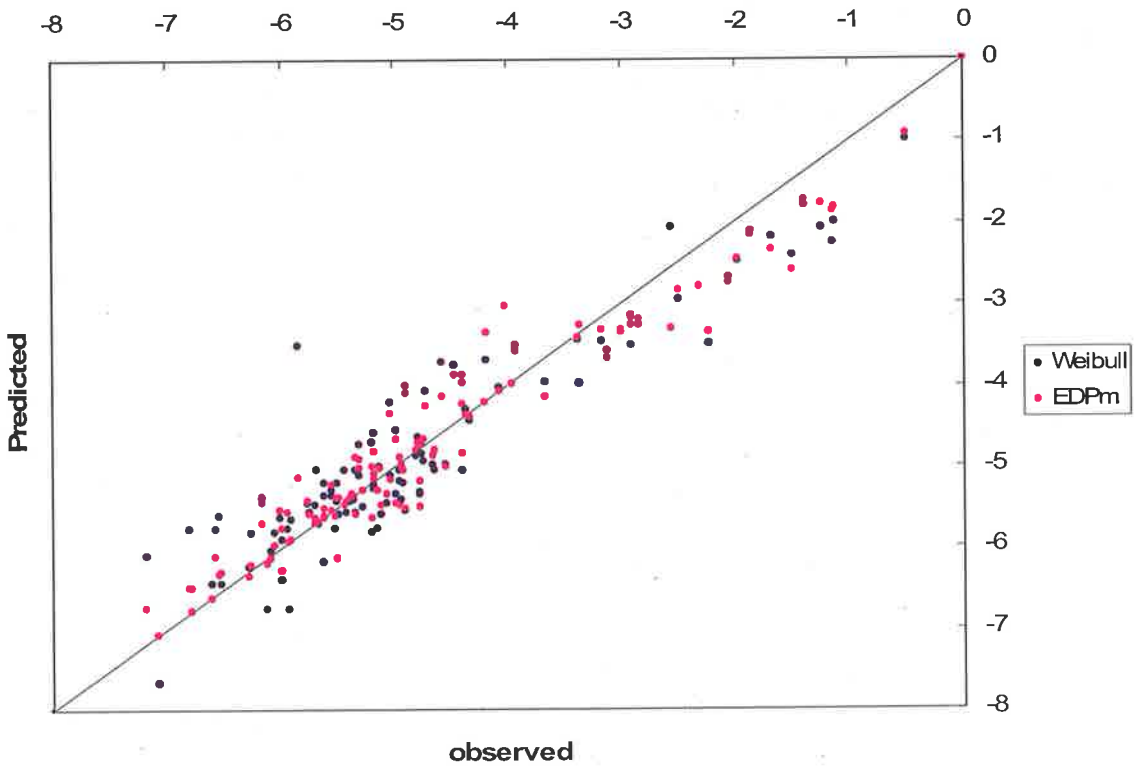

Figure 6.44. Predicted *versus* observed level of disinfection (as $\log_{10} N/N_0$) for fits of the Weibull and EDP_m models to the experimental UV disinfection data

Both the EDP_m and Weibull model are seen to over-predict the extent of disinfection when the observed level is less than 99.99% (4-$\log_{10}$ reductions). The Weibull model also exhibits a greater difference between the predicted and observed levels of disinfection than the EDP_m model when the observed disinfection of viable bacteria exceeds 6-$\log_{10}$ reductions. This is a result of the flexibility afforded by the EDP_m model in that it has the capacity to account for increases in disinfection observed in the tailing region. The Weibull model does not have this ability, and simply imposes an averaged constant predicted level of reduction to represent the tailed data.

A comparison between the levels of disinfection predicted by the Weibull and EDP_m models when fitted to the experimental disinfection data is presented more clearly in Figure 6.45. It is observed that when the expected (i.e. predicted) level of disinfection is less than 5-$\log_{10}$ reductions, the predictions of the Weibull and EDP_m models compare well. As the expected level of disinfection increases (corresponding to increased UV dose) beyond 5-$\log_{10}$ reductions, the variation between the predictions of the models becomes increasingly large. This is again symptomatic of the inability of the Weibull model to account for 'non-zero' rates of disinfection in the tailing region. As a result, the level of disinfection predicted by the EDP_m model may be expected to exceed that predicted by the Weibull model when each model is fitted to tailed disinfection data. Through inspection of Figure 6.44 however, in this instance, this notion remains unclear.

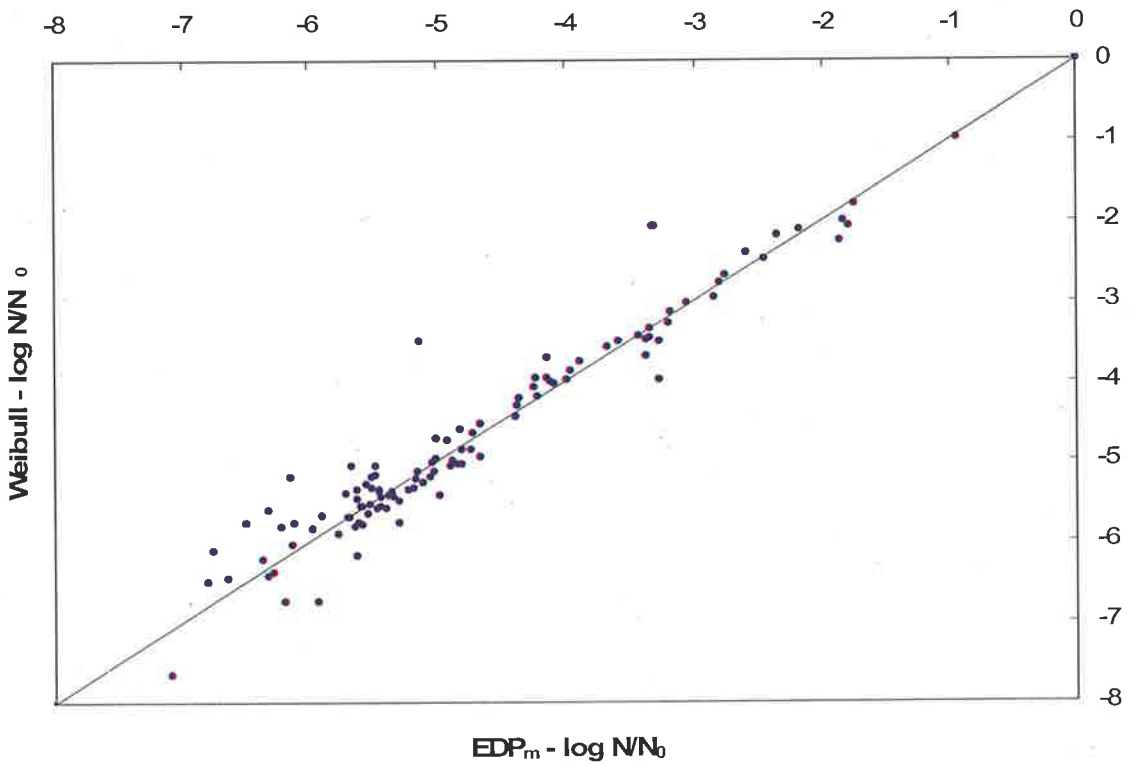

Figure 6.45. A comparison of the predicted level of disinfection of the Weibull and EDP_m models (as $\log_{10} N/N_0$) fitted to the experimental disinfection data

A comparison between the rate of disinfection predicted by the Weibull model at zero UV dose (k_0), and the disinfection rate coefficient of the EDP_m model (k) is presented in Figure 6.46, for fits of each model to the experimental disinfection data. Despite the favourable comparison, the initial rate of disinfection predicted by the Weibull model (UV dose = 0) is seen to consistently over-estimate the initial rate of disinfection predicted by the EDP_m model, represented as the disinfection rate coefficient, k, across the range of experimental data. The disinfection rate coefficient of the EDP_m model is representative of the rate of disinfection prior to the onset of tailing, whereas the rate of disinfection predicted by the Weibull model, is seen through inspection to be maximum for a UV dose of zero.

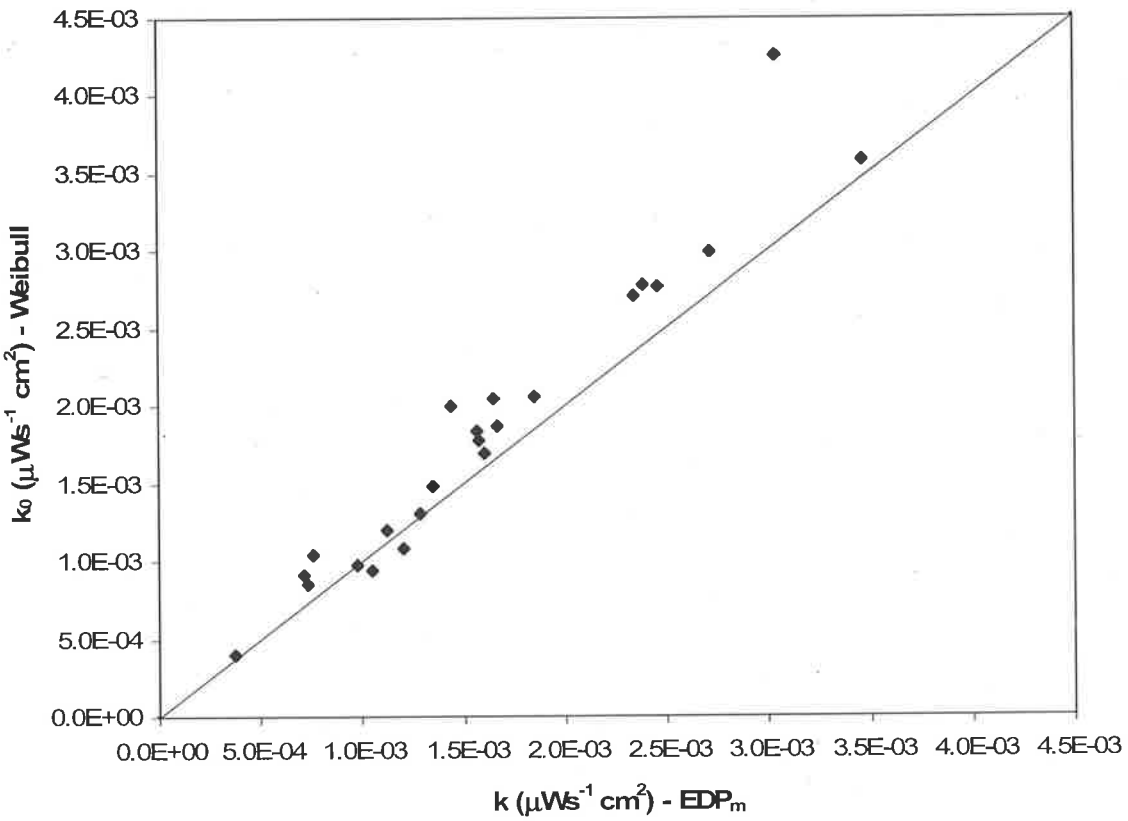

Figure 6.46. A comparison of the rate of disinfection predicted by the Weibull model at zero UV dose (k_0) to the disinfection rate coefficient of the EDP_m model (k)

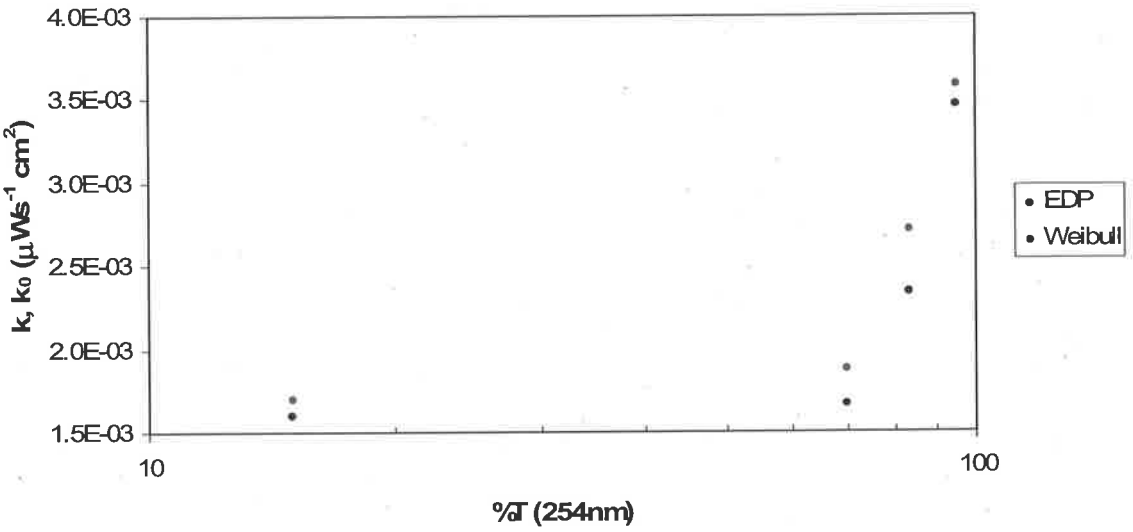

Figure 6.47. Rates of disinfection defined by the Weibull and EDP_m models as affected by transmission in the absence of absorbing or shielding agent

The predicted rate of disinfection at zero dose of the Weibull model (k_0), and the disinfection rate coefficient of the EDP_m model (k) are presented against water transmission (at 254 nm) in Figure 6.47 when only bacteria and neither absorbing nor shielding agent are present. It is noted that as the water transmission reaches a value of 70 %, the rates of disinfection increase log-linearly with increases in water transmission (corresponding to a reduced initial concentration of bacteria in the water). When the concentration of bacteria initially present is elevated (i.e. transmission reduced), the rate of disinfection appears to tend towards a limiting value. It is also clear that for a fixed water transmission, the rate of disinfection predicted by the Weibull model at zero UV dose exceeds the disinfection rate coefficient of the EDP_m model. This is not unexpected, as the disinfection rate coefficient of the EDP_m model is representative of the rate of disinfection prior to the onset of tailing, not just at zero UV dose.

6.4 Some comparisons with the data of Nguyen (1999)

Nguyen (1999) performed an experimental study to assess the effects of UV absorbance (i.e. absorbing agent concentration), suspended solids (i.e. shielding agent) concentration, and dose on the UV disinfection of *Escherichia coli* (ATCC 25922), with the aim of obtaining data for model development. However the model failed to adequately account for the effect of either agent on the extent of UV disinfection.

The absorbing and shielding agents used by Nguyen (1999) were those used throughout the current study respectively (i.e. International Roast^{TM} – instant coffee powder and diatomaceous earth as Celite 503^{TM}). The concentrations ranges investigated were from 0.001 to 0.03 g L^{-1} for the absorbing agent and from 0.01 to 0.3 g L^{-1} for the shielding agent. The UV doses employed ranged from 10,800 to 44,200 μWs cm^{-2}.

The UV survivor data of Nguyen (1999) obtained for disinfection of *E coli* in an LC5^{TM} UV disinfection unit, are presented against UV dose for a range of absorbing agent (0.001 to 0.03 g L^{-1}) and shielding agent (0.01 to 0.3 g L^{-1}) concentrations in Figure 6.48. The data of Nguyen (1999) display systematic behaviour with respect to both the absorbing agent and shielding agent concentrations; in that reduced disinfection efficacy is generally observed with increasing concentrations of either agent. This trend however was not readily observed in the UV disinfection data generated during the current study (*see.* Figure 6.1). The predicted level of disinfection when no agent is present ranges from approximately 4.5 to 5-$\log_{10}$ reductions for UV doses between 10,800 and 44,200 μWs cm^{-2}. This compares to between 5 and 6-$\log_{10}$ reductions obtained for the current study over the same dose range when no agents are present (*see.* Figure 6.1).

The survivor data of Nguyen (1999) presented in Figure 6.48 are characteristic of the tail often observed in practical UV disinfection kinetics, with only minor additional disinfection generally observed as the UV dose is increased from 10,800 to 44,200 μWs cm^{-2} irrespective of both the type and concentration of agent present. The level of disinfection described by the tail ranges from 3 to 5-$\log_{10}$ reductions, compared with 5 to 7-$\log_{10}$ reductions observed in the current study (*see.* Figure 6.1). The current study also investigated a broader range of both absorbing agent (0.001 to 0.07 g L^{-1}) and shielding agent (0.01 to 0.7 g L^{-1}) concentrations than Nguyen (1999).

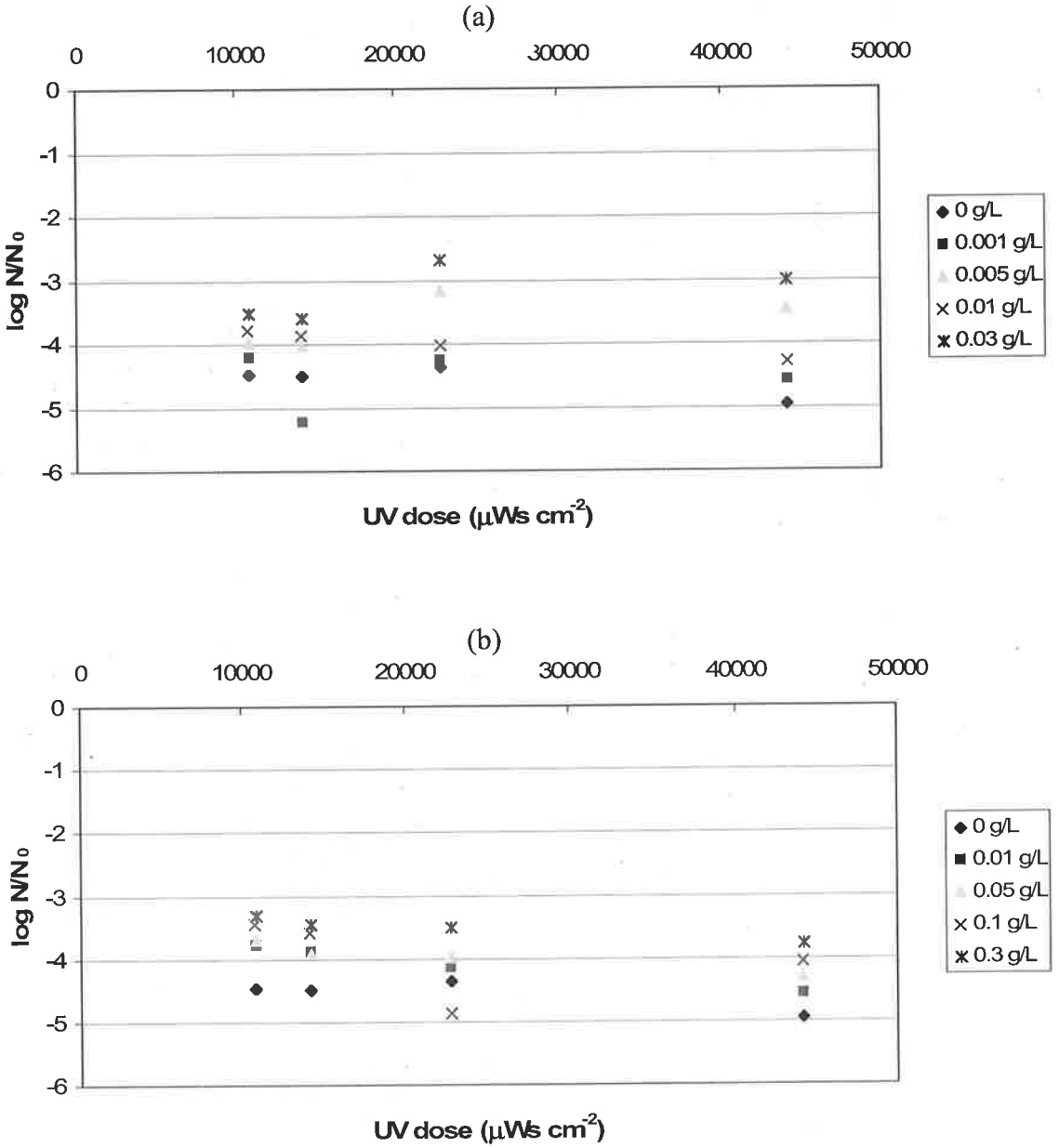

Figure 6.48. UV survivor data of Nguyen (1999) for *Escherichia coli* in RO water (presented as $\log_{10} N/N_0$) in the presence of (a) absorbing agent (instant coffee powder), and (b) shielding agent (Celite 503)

The absence of any disinfection data obtained at low UV doses (< 10,000 μWs cm^{-2}) is also apparent in the disinfection data of Nguyen (1999), as presented in Figure 6.48. The lack of such data at low UV dose makes it difficult to accurately predict the onset of tailing. Generation of disinfection data at low UV dose (< 10,000 μWs cm^{-2}) was therefore identified as a necessary step towards robust model development.

The model developed by Nguyen (1999) accounted for the effect of UV dose only on disinfection, and did not account for the influence of absorbing or shielding agent concentrations on disinfection kinetics. Analyses of these data for *E. coli* disinfection however highlights that the extent of disinfection exhibits dependence on both UV dose and shielding agent concentration in particular. The model form of Nguyen (1999) is therefore inadequate. Both because it is not capable of predicting the onset of experimentally observed tailing and because it does not account for the combined effect of UV dose and either absorbing or shielding agent concentration on disinfection.

The study of Nguyen (1999) failed to adequately account for the influence of the concentration of viable bacteria present prior to disinfection on the UV transmission of the feed-water. Nguyen (1999) reported a constant UV transmission of 78 % for disinfection of *E. coli* in the absence of either absorbing or shielding agents. This is despite the replicate data of Nguyen (1999) indicating that the initial concentration of viable bacteria ranged from 86×10^5 to 68×10^7 cells mL^{-1} in this instance. No reflection of the respective change in transmission of the seeded water has been made over these values by Nguyen (1999). Findings of the present study, presented in Figure 6.5, suggest such a change in the concentration of viable bacteria initially present would have a marked effect on the UV transmission of the feed-water, and potentially on the capacity for disinfection.

The current study sought to make a number of improvements on that of Nguyen (1999). The foremost was acquisition of robust disinfection data at low values of UV dose (<10,000 $\mu Ws\ cm^{-2}$). As such, disinfection data was generated for UV doses of 2,700 and 5,400 $\mu Ws\ cm^{-2}$ during the current study. The data generated at these low doses made it possible to accurately predict both the initial rate of disinfection, and the onset of tailing. The present investigation also considered a larger number of UV doses than investigated by Nguyen (1999), generating more data, allowing for more robust model development.

Both the modified exponentially damped polynomial (EDP_m) and Weibull model forms developed in the current study are capable of accounting for variation in the initial rates of disinfection, and are good predictors of the onset of tailing and the limiting disinfection efficacy. These forms also allowed for assessment of the combined effect of UV dose and either absorbing or shielding agent concentration on the efficacy of disinfection in contrast to the model of Nguyen (1999).

6.5 Concluding remarks

The results of this UV disinfection study have shown that both the modified exponentially damped polynomial model (EDP_m) and the Weibull model are of a suitable form to adequately describe the nature of UV disinfection kinetics exhibiting tailing in the survivor data. The EDP_m model afforded a better fit to the data than did the Weibull model, and has the added advantage of accounting for increasing levels of disinfection observed over the range of doses describing the tailing region. This is in contrast to the Weibull form, which imposes a limiting extent of disinfection with no rate of disinfection in the tail. The EDP_m model can also be constrained such that the minimum level of disinfection observed in the tailing region is zero – an intuitive limiting case. The Weibull model is advantageous over the EDP_m form, when there are few disinfection data available, and the observed level of additional disinfection in the tail is negligible.

The piecewise nature of the EDP_m model can present difficulties for convergence of model parameter estimates, particularly when there are few disinfection data available. However the model parameter which governs the piecewise nature of the EDP_m model, the breakpoint dose, is arguably an important design criterion in that it delineates between the initially observed kinetics, and those observed in the tailing region. It remains to be seen whether this threshold for the onset of tailing is characteristic of the bacterial species under investigation or the dose distribution within the specified UV disinfection unit.

The maximum extents of disinfection achieved observed during the study seemed to be independent of the type or concentration of additive present. The effect of suspended solids (shielding agent) in particular was difficult to quantify, and may have been susceptible to adsorption of bacteria – leading to an over estimate of the extent of disinfection. Pooling of the data on the basis of concentration of suspended matter, led to the conclusion than increases in suspended solids concentration led to decreases in the initially observed rates of disinfection. The effect of the UV absorbing agent was found to afford a greater reduction in transmittance than suspended matter when present in equal concentrations. The initial rates of disinfection exhibited strong exponential dependence (decreasing) on the concentration of absorbing agent present.

There was also limited evidence to suggest the initial rates of disinfection were dependent upon the initial level of viable bacteria when no additive is present, with an increase in

viable bacteria levels leading to a decrease in the observed rate of disinfection when the bacterial concentration ranges between approximately 10^6 and 10^8 cells mL^{-1}. Beyond these concentrations of bacteria, transmission levels become insensitive to change. This is in contradiction to the work of Nguyen (1999), which suggested the extent of disinfection (as $\log_{10} N/N_0$) was in dependent of the initial concentration of bacteria. This work proves this to be untrue at low UV doses, further highlighting the importance of disinfection data at low doses (<10,000 $\mu Ws\ cm^{-2}$) in defining the kinetics of UV disinfection.

6.6 Shortcomings

This study failed to identify a general trend in the effect of either shielding or absorbing agent concentrations on the maximum observed levels of disinfection. Whilst initial rates of disinfection are clearly important in defining the kinetics of UV disinfection, a limiting extent of disinfection is arguably more important from a design point of view. This is particularly true when treating wastewater, where typically elevated levels of suspended matter (shielding agents) and colour (absorbing agents) are observed. Further work is required to investigate the effects of these process variables on the maximum possible extents of UV disinfection.

CHAPTER 7: CONCLUSIONS

1. Neither a UV absorbing agent (International Roast^{TM} – instant coffee powder: 0.001 to 0.07 g L^{-1}) nor a UV shielding agent (Celite 503^{TM} – diatomaceous earth: 0.1 to 0.7 g L^{-1}) displayed any systematic reduction in the observed extent of UV disinfection with increasing concentration.

2. Initial rates of disinfection appear to be dependent upon both absorbing agent and shielding agent concentration (over the ranges studied), with increased levels of additive leading to a reduced initial rate of disinfection.

3. UV disinfection kinetics observed for *E. coli* (in RO water) in the presence of UV absorbing and shielding agents exhibit significant tailing in the survivor data.

4. The EDP_m and Weibull models are both of a form suited to represent the tailing in UV disinfection data of *E. coli* as affected by either UV absorbing or UV shielding agents.

5. In the absence of either UV shielding or absorbing agents, the initial rates of disinfection of *E. coli* are dependent upon the initial level of viable bacteria over the range of 6.6×10^6 to 3×10^8 cfu/ml; with increased concentrations of bacteria exhibiting lower initial rates of disinfection. Beyond this range, water transmittance is insensitive to changes in concentration of viable bacteria.

6. In equivalent concentrations, UV absorbing agent affords a greater reduction in transmittance than the UV shielding agent, and also exhibits a lower initial rate of disinfection.

7. The EDP_m model form gives an explicit measure of the minimum UV dose required for the onset of tailing. ie. the breakpoint dose $[dose]_B$.

8. The Weibull model form is advantageous (over the EDP_m form) when few UV disinfection data are observed and it can be reasonably implied that there is no additional disinfection in the tailing region.

9. The independence of the observed extent of UV disinfection upon either absorbing or shielding agent concentration may be due to laminar flow effects at high UV doses (viz. at 44,200 $\mu Ws\ cm^{-2}$).

10. The absorbing agent may have a toxic effect on the viable bacteria.

11. The shielding agent may adsorb significant levels of viable bacteria, and protect against the effects of UV irradiation – leading to an over estimate of the extent of disinfection.

12. These studies highlight the importance of survivor data obtained at low UV doses (<10,000 $\mu Ws\ cm^{-2}$) in defining the kinetics of UV disinfection.

13. Transmittance and suspended solids concentration alone are not good measures by which to predict the maximum extent of disinfection by UV irradiation.

RECOMMENDATIONS FOR FURTHER STUDY:

- More independent UV disinfection data should be generated for a range of contaminants (offering varying resistance to UV), such that the suitability of the EDP_m and Weibull model forms may be further validated. The models may be shown to be of a universal form with the possibility of physiological insights to follow. The result may extend to a mixed culture, where the kinetic parameters may be represented as a weighted average of the individual components.

- The disinfection kinetics of a selected bacterial contaminant should be determined under static test conditions. Dynamic tests can then follow and be standardised against the static disinfection data. As such, the effects (and nature) of the liquid hydrodynamics may be more easily understood.

- Future dynamic disinfection studies should be conducted in a straight length of tube (as a PFR), equally irradiated from each side of the disinfection control volume. This eliminates the need to quantify the effects of bends, for example, on the residence time distribution within the disinfection unit.

- The effects of dispersion inherent in laminar or transitional flow upon UV disinfection kinetics should be quantified, and compared against kinetics derived from turbulent (plug-flow) conditions.

- Future studies should attempt to correlate kinetic parameters with not only transmission and suspended solids concentration, but with a wider variety of common measures of wastewater quality. These include: biochemical oxygen demand (BOD); chemical oxygen demand (COD); total organic carbon (TOC), dissolved organic carbon (DOC); turbidity (as NTU); and colour (as HU). This study has shown transmission and suspended solids concentration alone to be ineffective as indicators for predicting the extent of UV disinfection.

- The effect of the particle size distribution (as opposed to mass concentration) of suspended matter on UV disinfection kinetics needs to be better understood. Investigation may shed light on dominant modes of protection during disinfection such as adsorption to particulate matter, and shielding effects.

- The mechanism of shielding, or protection of viable bacteria by suspended solids, should be further studied. Clay with the capacity to absorb bacteria should be investigated with the aim of determining if there is any significant correlation between the number of bacteria remaining viable after UV treatment and the concentration of the suspended solid. A series of adsorption isotherms may then be generated to determine the proportion of survivors that are adsorbed to the solid, and thus those survivors remaining dispersed in solution. The significance of the extent of turbulence should be investigated with regard to the numbers of the survivors remaining dispersed in solution – giving a quantitative measure of the shielding effect arising from clumping of viable bacteria.

- Future research is required to investigate cell reactivation following UV treatment. Since many organisms possess the ability to repair damage to DNA by either light-dependent (photo reactivation) or light-independent (dark repair) mechanisms following exposure to UV light, a practical limitation in disinfection efficacy may become apparent.

- Re-growth kinetics of post-irradiated bacteria need to be better understood. Rates of repair should be quantified against treatment (ie. exposure) and storage conditions (ie. post exposure).

Appendix A: A definition of some important terms used in this study

The definition of some important terms in relation to this study as they are used throughout this thesis is discussed in this appendix.

absorbance	the degree to which the water to be treated absorbs UV irradiation – absorption of incident energy per unit depth of the water (i.e. reduction in transmission in one dimension)
absorbing agent	water soluble material capable of increasing UV absorbance of water
additive	Of a model, factors having an independent cumulative effect
bacteriophage	a virus parasitic to a bacterium, reproducing inside it
breakpoint dose	UV dose that denotes the onset of tailing predicted by the EDP_m model
coliform	non-pathogenic bacteria present in the digestive tract of warm-blooded animals, water and wastewater, whose presence is an indicator of contamination
coliphage	a virus parasitic to a coliform
clumping	aggregation of micro-organisms, to particulate matter or each other
disinfect	a unit operation used to cleanse of infection
disinfection	rendering harmless contaminating and pathogenic micro-organisms
enteric	of or pertaining to the intestines (of infection - usually by means of ingestion)
Escherichia coli	A bacterium found in water contaminated with faecal material – used as an indicator for enteric pathogens
exposure time	time for which an element of water is exposed to UV light in the disinfection unit
faecal coliform	a coliform found in, or associated with, animal or human faeces or waste
facultative	the ability to live either with or without oxygen
Gram-stain	a method of differentiating bacteria by staining with a dye, then removing the dye for identification

intensity	energy of UV radiation per unit area over which it is received
irradiate	to shine UV light upon
macromolecule	molecules containing a very large number of atoms – the main chemical components of cells such as proteins, polysaccharides and enzymes
micro-organism	any of variety microscopic organisms including bacteria, protozoa, fungi, algae and viruses
multiplicative	having an interactive effect i.e. two-factors combining to have an effect which is different from the sum of the two single-effects
MPN	Most probable number, a statistical measure of the concentration of viable cells
nutrient broth	a solution containing the necessary components to facilitate in which growth of micro-organisms
occlusion	adsorption of micro-organisms to the surface of, and pores within, particulate matter
pathogen	a micro-organism capable of causing disease in humans
pathogenic	capable of causing disease
potable	drinkable, or fit for human consumption
photo-reactivation	recovery from the effects of UV radiation following exposure to visible or near-UV light
P-Value	a measure of statistical significance – probability based on distribution of a known test-statistic. Of model parameters, small values (usually <0.05) indicate statistical significance
re-growth	recovery from the effects of UV radiation, including regaining cell activity
repair	enzymatic excision of thymine dimers from damaged DNA followed by reinsertion
residual	chemical disinfectant retained in treated water after the initial application of the disinfectant
Reverse Osmosis	
septic	contaminated with bacteria
shielding	offering protection to micro-organisms by providing a physical barrier to UV irradiation

shielding agent	An additive capable of shielding micro-organisms from UV induced damage
sterilise	destruction of all forms of microbial life
sterilisation	reduction in viable numbers of contaminant micro-organisms to a pre-determined acceptable level
tailing	reduction in the rate of disinfection, to near zero, for increasing UV dose
transmittance	indicates absorption of energy per unit depth of the water
turbidity	measure of lack of clarity – a measure of the concentration of colloidal particles determined by transmission of light through a sample
ultraviolet	invisible rays of the electromagnetic spectrum beyond the violet rays, ranging from 100 to 400 nm in wavelength
viable	capable of maintaining life and functioning as a living cell
viable counts	a measure of the density of active micro-organisms

Appendix B: Refereed publications from this research

Amos S A, Davey K R and Thomas C J 2001. A comparison of predictive models for the combined effect of UV dose and solids concentration on disinfection kinetics of *Escherichia coli* for potable water production. *Transactions of the Institution of Chemical Engineers* **79**, Part B, 174-182.

Amos S A, Davey K R and Thomas C J 2001. Predicting the combined effect of UV dose and suspended solids concentration on UV disinfection kinetics of *Escherichia coli*. In: *Proc. 6th World Congress of Chemical Engineering*, Melbourne, 23-27 September, Health and Safety (Session 3110), p.107.

Davey K R and Amos S A 2002. Letter to the Editor. *Journal of Applied Microbiology* **92** (3), 583-587.

Amos, S. A., Davey, K. R. and Thomas, C. J. 2003. A new EDP model for predicting UV disinfection kinetics of coliforms as effected by dose and suspended solids. In: *Proc. 31st Australasian Chemical Engineering Conference (Products and Processes for the 21st Century)*, CHEMECA 2003, Stamford Plaza, Adelaide, South Australia, Australia, September 28 – October 1, paper 185. (ISBN 0 8639 6829 5).

Amos, S. A., Davey, K. R. and Thomas, C. J. 2004. A new Weibull model for prediction of tailing in UV disinfection survivor data. In *Proc. 32nd Australasian Chemical Engineering Conference (Sustainable Processes)*, CHEMECA 2004, Australian Technology Park, Sydney, NSW, Australia, September 26 – 29, paper 106. (ISBN 1 8770 4012 6).

Amos S A, Davey K R and Thomas C J 2004. A new model for predicting the combined effect of UV dose and suspended solids concentration on disinfection kinetics of vegetative bacteria. *Transactions of the Institution of Chemical Engineers*, Part B, Process Safety and Environmental Protection – in preparation.

Appendix C: Particle size analysis

Particle size analysis was performed using a Malvern Mastersizer.

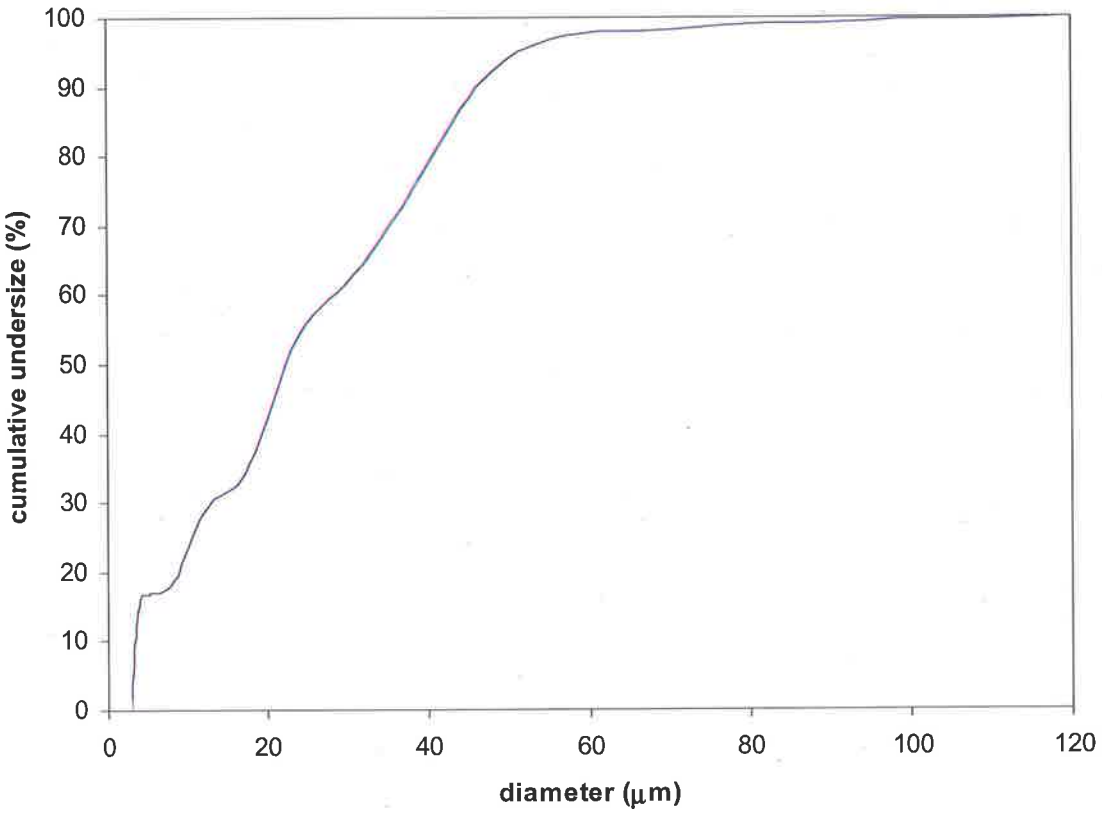

Figure C1. Cumulative undersize distribution of Celite 503™

Some properties of the particle size distribution are presented in Table C1.

Table C1. Volume-mean (d_v) and surface-mean (d_s) diameters obtained for Celite 503™ at a volume concentration of 0.02 %

d_v (mean)	25.2 μm
d_s (mean)	11.4 μm
d_v (90% undersize)	46.1 μm
d_v (50% undersize)	22.2 μm
d_v (10% undersize)	3.5 μm

The nominal specific surface area of the sample distribution is 262.5 m^2/g.

Appendix D: Test for cumulative damage

The following test is aimed at determining whether disinfection kinetics between two blocks of experiments are different. In the first experiment, data was pooled for UV disinfection trials where there was no additive present in the water (no coffee powder or Celite present). This pooled data set consisted of 3 subsets of data; each with a different initial concentration of bacteria (as seen in Tables D1 – D3).

Table D1. Survivor data for seeded water with no additive

UV dose (μWs cm^{-2})	N (cfu/ml)	$\log_{10}(N/N_0)$
0	2.99×10^8	0.00
2700	3.65×10^5	-2.91
5400	3.13×10^3	-4.98
10800	2.56×10^3	-5.07
14100	9.79×10^2	-5.48
44200	3.65×10^2	-5.91

Table D2. Survivor data for seeded water with no additive

UV dose (μWs cm^{-2})	N (cfu/ml)	$\log_{10}(N/N_0)$
0	1.27×10^7	0.00
2700	1.38×10^3	-3.96
5400	9.38×10^1	-5.13
10800	2.10×10^2	-4.78
14100	3.50×10^1	-5.56
44200	3.00×10^1	-5.63

Table D3. Survivor data for seeded water with no additive

UV dose (μWs cm^{-2})	N (cfu/ml)	$\log_{10}(N/N_0)$
0	6.64×10^6	0.00
2700	2.84×10^2	-4.37
5400	1.19×10^2	-4.75
10800	1.49×10^2	-4.65
14100	7.38×10^1	-4.95
44200	1.38×10^1	-5.68

The remaining set displays response data using bacteria cultured from a survivor colony that was exposed at 44,200 μWs cm^{-2} (*see.* Table D4). It is hypothesized that there is no accumulated damage to the exposed survivor, and hence; the cultured population will exhibit an unchanged kinetic response. As a result, there should be no change between model parameters across the two data sets. The two data sets are plotted in Figure D1.

Table D4. Survivor data for water seeded with bacteria cultured from a survivor exposed at 44,200 μWs cm^{-2}

UV dose (μWs cm^{-2})	N (cfu/ml)	$\log_{10}(N/N_0)$
0	7.58×10^7	0.00
2700	7.41×10^4	-3.01
5400	3.73×10^2	-5.31
10800	9.35×10^2	-4.91
14100	7.50×10^1	-6.00
44200	1.61×10^2	-5.67

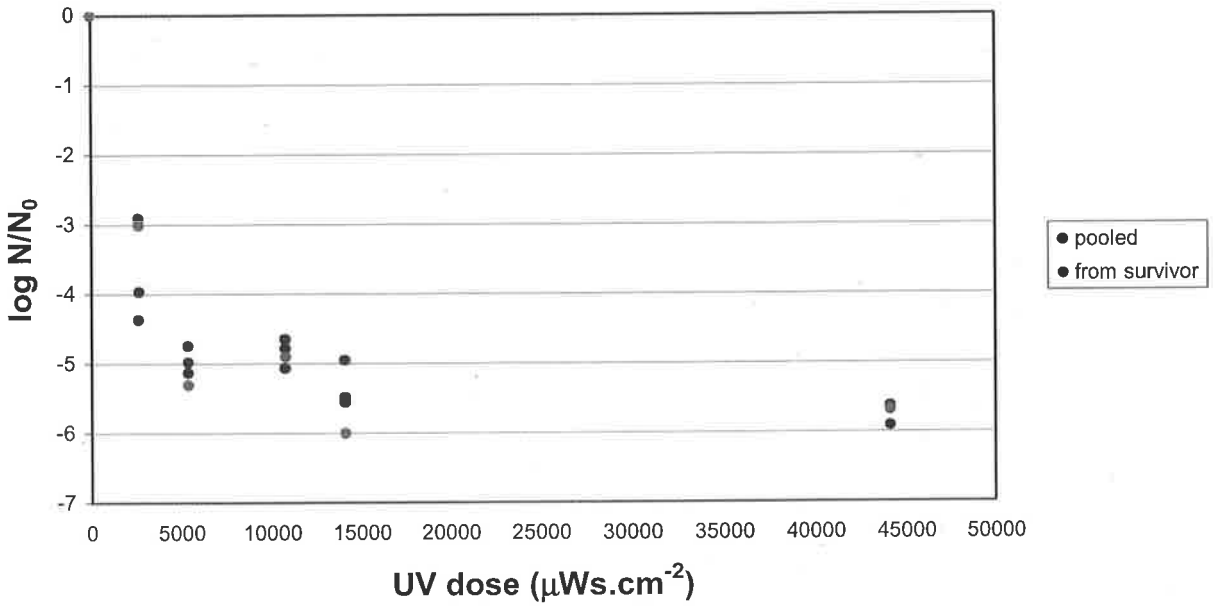

Figure D1. Reduction in viable numbers of bacteria following UV exposure. The pooled data are displayed as ●, with the data from the cultured survivor shown as ●

A good starting point in the analysis is to fit the model in question separately to each data set. Parameter values and their associated standard errors may then be compared across data sets. A summary of the regression output is presented in Table D5.

Table D5. Parameter summary for the EDP_m model fitted to each data set

Parameter	Estimate	Std. Error	t - value	P - value
k	2.18×10^{-3}	2.25×10^{-4}	9.675	7.71×10^{-8}
λ	1.64×10^{-4}	1.99×10^{-5}	8.209	6.26×10^{-7}
$[dose]_B$	5.97×10^{3}	7.38×10^{2}	8.083	7.58×10^{-7}
SSR*	1.889			
k	1.67×10^{-3}	3.27×10^{-4}	5.106	0.0145
λ	1.12×10^{-4}	2.86×10^{-5}	3.928	0.0294
$[dose]_B$	8.85×10^{3}	2.42×10^{3}	3.655	0.0354
SSR*	0.849			

*SSR denotes sum of square of residuals

The values for each of the model parameters do not appear to change appreciably between data sets. Similarly, the standard errors for each of the parameters are of the same order of magnitude, with exception of the damping coefficient, λ. The higher P-values associated with the second data set may be attributed to the fewer available degrees of freedom owing to the smaller amount of data comprising the set (three times fewer data). All model parameters are seen to be significant for each data set ($P<0.05$). The purpose of this test is to illustrate that we do not have a mixed population of UV sensitive and UV resistant bacteria.

For these UV disinfection data, it is desired to test whether using sub-lethally exposed bacteria as a source culture changes the parameter values obtained through regressing the data to the modified exponentially damped polynomial model (EDP_m). The EDP_m model form is given by equation D1 below:

$$\log_{10}\frac{N}{N_0} = -\delta_1 k[dose]\exp(-\lambda[dose]) - \delta_2(k'[dose]+c) \qquad \text{(D1)}$$

$$\text{if } [dose] \le [dose]_B \;\; \delta_1 = 1;\; \delta_2 = 0 \qquad k' = k.\exp(-\lambda[dose]_B)(1-\lambda[dose]_B)$$

$$\text{if } [dose] > [dose]_B \;\; \delta_1 = 0;\; \delta_2 = 1 \qquad c = k.\exp(-\lambda[dose]_B)[dose]_B$$

This EDP_m model has three coefficients, namely: the rate coefficient for UV inactivation, k, the damping coefficient, λ, and the breakpoint dose, $[dose]_B$.

Introduction of incremental parameters is useful when testing whether parameter values for a particular model change across sets of data to be fitted. This incremental parameter accounts for a change in parameter value between blocks of data, and is associated with an indicator variable (Bates and Watts 1998).

Three incremental parameters: ϕ_1, ϕ_2 and ϕ_3 are introduced, which are associated with the disinfection rate coefficient, the damping coefficient, and the breakpoint dose respectively. An indicator variable, ψ, is also required with the introduction of the incremental parameters, and can take values of 0 and 1 following:

$\Psi = 0$ pooled data

$= 1$ from sub-lethally exposed bacteria

The disinfection rate coefficient is now replaced with: $k + \Psi.\phi_1$

The damping coefficient is replaced with: $\lambda + \Psi.\phi_2$

And, the breakpoint dose is replaced with: $[dose]_B + \Psi.\phi_3$

These modified parameters now replace their respective parameters in the EDP_m model (equation D1). To determine if any of the incremental parameters are unchanged, we test the significance of one at a time using an extra sum of squares analysis, which requires fitting a full and a partial model. The full model corresponds to completely different sets of parameters for each of the data sets, while the partial model corresponds to setting (at least 1) the value of an incremental variable to zero. For the fits of the model to be the same across the data sets, we are interested in testing whether each of the incremental parameters are zero; one parameter at a time. The first step is to fit the full model. The full model (equation D1) was fitted with all incremental parameters included and the results of this fit are displayed in Table D6.

Table D6. Parameter summary for the 6-parameter EDP_m model fitted to the combined data set

Parameter	Estimate	Std. Error	t - value	P - value
k	2.18×10^{-3}	2.47×10^{-4}	8.804	6.10×10^{-8}
λ	1.64×10^{-4}	2.19×10^{-5}	7.470	6.42×10^{-7}
$[dose]_B$	5.97×10^{3}	8.11×10^{2}	7.356	7.93×10^{-7}
ϕ_1	-5.05×10^{-4}	3.44×10^{-4}	-1.466	0.160
ϕ_2	-5.15×10^{-5}	3.03×10^{-5}	-1.701	0.106
ϕ_3	2.89×10^{3}	1.95×10^{3}	1.479	0.156
SSR	2.738			

Table D6 suggests that each of the incremental parameters (ϕ_1, ϕ_2 and ϕ_3) could be zero, since they each have a P–value > 0.05. Hence we fit the partial model with $\phi_3 = 0$. That is, the breakpoint dose is the same across data sets. The fit of the partial model (with $\phi_3 = 0$) is shown in Table D7.

Table D7. Parameter summary for the 5-parameter EDP_m model fitted to the combined data set

Parameter	Estimate	Std. Error	t - value	P - value
k	1.98×10^{-3}	1.92×10^{-4}	10.317	3.18×10^{-9}
λ	1.46×10^{-4}	1.71×10^{-5}	8.541	6.25×10^{-8}
$[dose]_B$	6.72×10^{3}	8.11×10^{2}	8.289	9.85×10^{-8}
ϕ_1	3.19×10^{-5}	1.44×10^{-4}	0.222	0.827
ϕ_2	-2.22×10^{-7}	2.70×10^{-6}	-0.082	0.935
ϕ_3	-	-	-	-
SSR	3.200			

Table D7 suggests that each of the remaining incremental variables could be zero. We proceed by retaining ϕ_3 to be zero, and setting ϕ_2 to be zero also. The resulting fit of the further partial model is summarised in Table D8.

Table D8. Parameter summary for the 4-parameter EDP_m model fitted to the combined data set

Parameter	Estimate	Std. Error	t - value	P - value
k	1.98×10^{-3}	1.85×10^{-4}	10.71	9.87×10^{-10}
λ	1.46×10^{-4}	1.66×10^{-5}	8.768	2.75×10^{-8}
$[dose]_B$	6.73×10^{3}	7.91×10^{2}	8.504	4.48×10^{-8}
ϕ_1	4.15×10^{-5}	8.25×10^{-5}	0.503	0.621
ϕ_2	-	-	-	-
ϕ_3	-	-	-	-
SSR	3.201			

Expectedly, it is observed that ϕ_1 may also be zero. The remaining step is to fit the EDP_m model to both data sets, with no incremental variables, viz. the parameters remain unchanged across the sets. The parameter values are shown in Table D9 below.

Table D9. Parameter summary for the 3-parameter EDP_m model fitted to the combined data set

Parameter	Estimate	Std. Error	t - value	P - value
k	1.99×10^{-3}	1.82×10^{-4}	10.961	3.79×10^{-10}
λ	1.46×10^{-4}	1.64×10^{-5}	8.921	1.38×10^{-8}
$[dose]_B$	6.71×10^{3}	7.76×10^{2}	8.654	2.28×10^{-8}
ϕ_1	-	-	-	-
ϕ_2	-	-	-	-
ϕ_3	-	-	-	-
SSR	3.241			

The P–values seen in Table D9 suggest that all parameters of the EDP_m model are highly significant ($P << 0.05$) when we fit the model to the combined data set. The sum of squares analyses are presented in Tables D10 – D12, which are used to progressively eliminate incremental variables from the model, thus showing the fits to each of the data sets to be the same.

Table D10. Extra sum of squares analysis for the 5- and 6- parameter EDP_m model fitted to the combined data set

Source	Sum of Squares	Degrees of Freedom	Mean Square	F ratio	P - value
Extra	0.4620	1	0.4620	3.0375	0.0984
6-parameter	2.7378	18	0.1521		
5-parameter	3.1998	19			

Table D11. Extra sum of squares analysis for the 4- and 5- parameter EDP_m model fitted to the combined data set

Source	Sum of Squares	Degrees of Freedom	Mean Square	F ratio	P - value
Extra	0.0011	1	0.0011	0.0068	0.9353
5-parameter	3.1998	19	0.1684		
4-parameter	3.2009	20			

Table D12. Extra sum of squares analysis for the 3- and 4- parameter EDP_m model fitted to the combined data set

Source	Sum of Squares	Degrees of Freedom	Mean Square	F ratio	P - value
Extra	0.0405	1	0.0405	0.2528	0.6206
4-parameter	3.2009	20	0.1600		
3-parameter	3.2414	21			

Tables D10 shows the sum of squares analysis used to test the significance of the incremental parameter, ϕ_3, associated with the breakpoint dose. Since the P–value exceeds 0.05 in this case, the assertion that ϕ_3 may be regarded as zero holds true. Similarly, the incremental parameters ϕ_2 and ϕ_1 have been shown to be insignificant by the sum of squares analyses given in Tables D11 and D12 respectively. Consequently, we may conclude that prior UV exposure has no cumulative effect on UV sensitivity of daughter cells.

This is in agreement with the findings of Blatchley *et al.* (2001), who found there to be no discernable difference in the dose-response behaviour of the parent or daughter cultures over the dose range of 0 to 100 mWs cm^{-2}. The dose-response behaviour of the parent and daughter cultures are summarized in Figure D2.

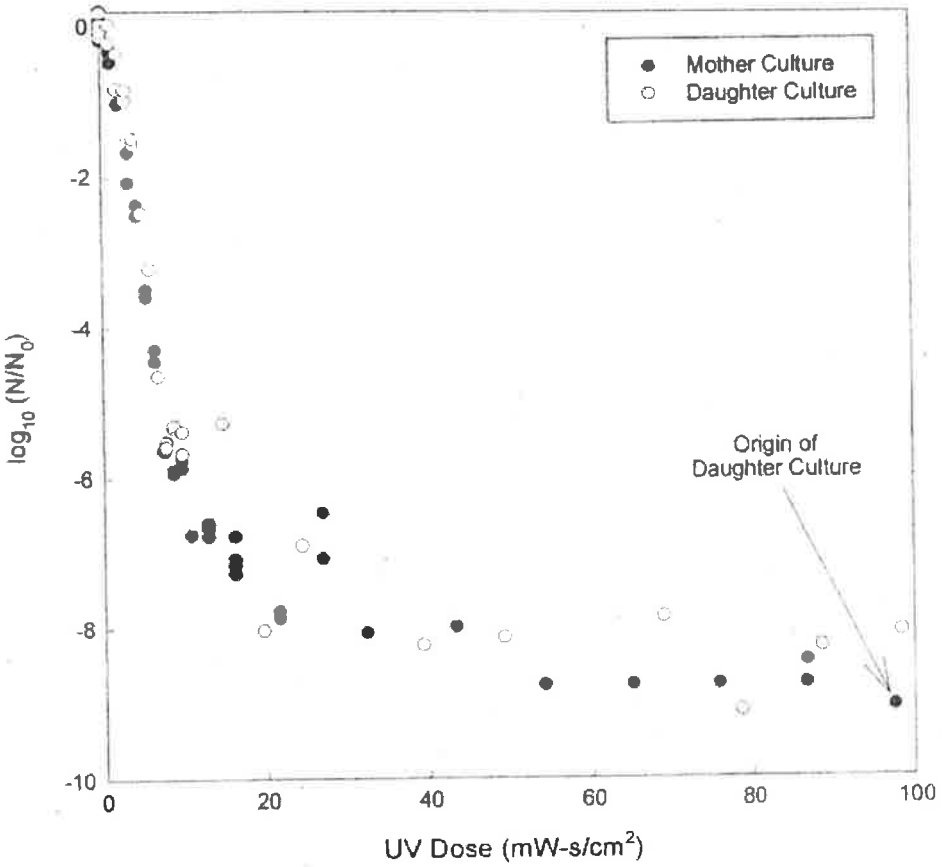

Figure D2. Viability as dose-response relationship for mother and daughter cultures of *E. coli* (CIP 5530) (from Blatchley *et al* 2001)

Blatchley *et al.* (2001) found that although the mechanism of bacterial inactivation by UV irradiation is dimerization within cellular nucleic acids, the ability to resist this damage is evidently not passed on to successive generations. This has important implications with regard to regrowth which may occur within distribution systems.

Appendix E: Reynolds' number calculation

The differences between laminar and turbulent pipe flows were first clarified by Osborne Reynolds in 1883 (Gerhart, Gross and Hochstein 1993). Reynolds found that variables characteristing the transition from laminar to turbulent may be combined to form a single dimensionless group, the Reynolds' Number (Re), defined as:

$$\mathrm{Re} = \frac{dv\rho}{\mu} \qquad \text{(E1)}$$

Where the variables are: pipe diameter (d), fluid velocity (v), fluid density (ρ), and fluid viscosity (μ).

Generally, the nature of pipe flow may be described by the following ranges for Reynolds' number (Nguyen 1999):

$\mathrm{Re} < 2{,}100$	– laminar flow
$2{,}100 < \mathrm{Re} < 10{,}000$	– transitional flow
$\mathrm{Re} > 10{,}000$	– turbulent flow

Gerhart, Gross and Hochstein (1993) suggest a maximum Reynolds' number of 2,300 for laminar flow in a pipe, and a minimum of 4,000 for stable turbulent pipe flow. If the Reynolds' number exceeds 4,000, flow is usually turbulent (Gerhart, Gross and Hochstein 1993).

For water at 25°C (Nguyen 1999):

$\rho = 1000 \text{ kg m}^{-3}$

$\mu = 1 \times 10^{-3} \text{ Pa s}$

For the LC5^{TM} UV disinfection unit:

$d = 11.11 \text{ mm} = 1.11 \times 10^{-2} \text{ m}$

Table E1 summarises the Reynolds' number for each of the water flow rates through the LC5^{TM} UV disinfection unit.

Table E1. Reynolds' number for each of the examined flow rates

Flow rate		Velocity	Reynolds' number
L/min	m^3/s	m/s	
4	6.67×10^{-5}	0.688	7.64×10^3
3	5.00×10^{-5}	0.516	5.73×10^3
1	1.67×10^{-5}	0.172	1.91×10^3

The flow may be considered turbulent for flow rates of 3 and 4 L min^{-1}, whereas when the flow rate is 1L min^{-1} we have laminar flow.

These values are contrary to the findings of Nguyen (1999), who suggested flow in the LC5™ disinfection unit was highly turbulent for flow ranging from 1 to 4 L min^{-1}. This is clearly not the case.

Appendix F: Calculation of UV dose

The LC5™ UV disinfection unit u-tube has the following dimensions:

- axial length (L) = 636.6 mm
- internal diameter (d) = 11.11 mm

And a nominal lamp intensity (I) of 11,940 μW cm^{-2} (Nguyen 1999).

The exposure time (t) of the water in the LC5™ UV disinfection unit is calculated by division of the exposed length (L), by the water velocity (v). For a water flow rate of 4 L min^{-1}, the water velocity is 0.688 m s^{-1} (*see.* Appendix E).

$$t = \frac{L}{v} = \frac{636.3 \times 10^{-3}}{0.688} = 0.9\,\text{s} \qquad \text{(F1)}$$

UV dose [*dose*] is the product of the exposure time (t) and the UV intensity (I), as follows:

$$[dose] = I \times t = 11940 \times 0.9 = 10{,}800\ \mu\text{Ws cm}^{-2} \qquad \text{(F2)}$$

Table F1 presents the flow rates and exposure times for each of the experimentally observed UV doses.

Table F1. UV dose data

Flow rate (L min^{-1})	Exposure length (mm)	Exposure time (s)	UV dose (μWs cm^{-2})
4	159.2	0.23	2,700
4	318.3	0.45	5,400
4	636.3	0.90	10,800
3	636.6	1.18	14,100
1	636.6	3.70	44,200

Appendix G: Microbiological data

Disinfection trial	number (cfu ml^{-1})	Disinfection trial	number (cfu ml^{-1})	Disinfection trial	number (cfu ml^{-1})	Disinfection trial	number (cfu ml^{-1})	Disinfection trial	number (cfu ml^{-1})
1	1.98×10^{8}	5	1.06×10^{3}	9	1.15×10^{2}	13	5.45×10^{6}	17	3.50×10^{1}
	3.36×10^{8}		2.02×10^{3}		7.00×10^{1}		8.00×10^{6}		4.00×10^{1}
	2.54×10^{8}		5.05×10^{2}		9.00×10^{1}		5.45×10^{6}		1.50×10^{1}
	4.10×10^{8}		3.40×10^{2}		1.00×10^{2}		7.65×10^{6}		2.05×10^{2}
2	3.75×10^{5}	6	4.45×10^{2}	10	2.60×10^{2}	14	2.40×10^{2}	18	1.50×10^{1}
	3.40×10^{5}		3.10×10^{2}		1.60×10^{2}		3.50×10^{2}		5.00×10^{0}
	4.55×10^{5}		2.50×10^{2}		1.35×10^{2}		2.25×10^{2}		1.50×10^{1}
	2.90×10^{5}		4.55×10^{2}		2.85×10^{2}		3.20×10^{2}		2.00×10^{1}
3	4.50×10^{3}	7	8.25×10^{6}	11	5.50×10^{1}	15	1.00×10^{2}	19	1.50×10^{6}
	3.50×10^{3}		1.45×10^{7}		2.00×10^{1}		1.25×10^{2}		3.60×10^{6}
	2.50×10^{3}		1.88×10^{7}		3.00×10^{1}		1.60×10^{2}		6.40×10^{6}
	2.00×10^{3}		9.35×10^{6}		3.50×10^{1}		9.00×10^{1}		2.45×10^{6}
4	2.81×10^{3}	8	1.50×10^{3}	12	5.50×10^{1}	16	1.20×10^{2}	20	2.50×10^{1}
	1.31×10^{3}		5.00×10^{2}		3.00×10^{1}		1.05×10^{2}		1.00×10^{2}
	2.83×10^{3}		3.00×10^{3}		2.00×10^{1}		1.35×10^{2}		2.00×10^{1}
	3.29×10^{3}		5.00×10^{2}		1.50×10^{1}		2.35×10^{2}		7.50×10^{1}

Microbiological data (continued)

Disinfection trial	number (cfu ml^{-1})	Disinfection trial	number (cfu ml^{-1})	Disinfection trial	number (cfu ml^{-1})	Disinfection trial	number (cfu ml^{-1})	Disinfection trial	number (cfu ml^{-1})
21	8.00×10^{0}	25	7.85×10^{6}	29	3.50×10^{0}	33	5.50×10^{1}	37	9.50×10^{5}
	7.50×10^{0}		1.13×10^{7}		6.00×10^{0}		4.50×10^{1}		4.20×10^{6}
	6.50×10^{0}		9.20×10^{6}		1.50×10^{0}		6.50×10^{1}		2.00×10^{6}
	5.50×10^{0}		1.05×10^{7}		5.00×10^{-1}		1.55×10^{2}		1.10×10^{6}
22	1.30×10^{1}	26	3.80×10^{2}	30	2.00×10^{0}	34	3.50×10^{1}	38	8.00×10^{1}
	1.10×10^{1}		9.05×10^{2}		5.00×10^{-1}		7.00×10^{1}		1.85×10^{2}
	1.85×10^{1}		1.55×10^{2}		4.00×10^{0}		5.00×10^{1}		1.20×10^{2}
	2.05×10^{1}		3.50×10^{2}		3.00×10^{0}		8.50×10^{1}		1.30×10^{2}
23	3.00×10^{0}	27	1.50×10^{1}	31	4.15×10^{6}	35	5.50×10^{1}	39	1.15×10^{1}
	5.50×10^{0}		1.50×10^{0}		5.70×10^{6}		3.00×10^{1}		7.50×10^{0}
	5.00×10^{0}		8.50×10^{0}		4.75×10^{6}		2.50×10^{1}		1.30×10^{1}
	1.10×10^{1}		8.50×10^{0}		5.25×10^{6}		2.00×10^{1}		1.40×10^{1}
24	1.95×10^{1}	28	1.25×10^{1}	32	5.20×10^{2}	36	1.50×10^{1}	40	1.00×10^{0}
	1.55×10^{1}		1.65×10^{1}		1.06×10^{3}		5.00×10^{0}		3.00×10^{0}
	1.15×10^{1}		5.50×10^{0}		1.51×10^{3}		1.50×10^{1}		3.00×10^{0}
	6.00×10^{0}		4.50×10^{0}		1.58×10^{3}		2.00×10^{1}		2.50×10^{0}

Microbiological data (continued)

Disinfection trial	number (cfu ml^{-1})	Disinfection trial	number (cfu ml^{-1})	Disinfection trial	number (cfu ml^{-1})	Disinfection trial	number (cfu ml^{-1})	Disinfection trial	number (cfu ml^{-1})
41	3.00×10^{1}	45	9.85×10^{2}	49	4.00×10^{6}	53	5.00×10^{0}	57	5.75×10^{2}
	2.00×10^{1}		1.61×10^{3}		7.50×10^{6}		1.00×10^{1}		2.20×10^{2}
	1.50×10^{1}		7.25×10^{2}		2.80×10^{6}		2.00×10^{1}		3.50×10^{2}
	5.00×10^{0}		1.02×10^{3}		3.55×10^{6}		1.50×10^{1}		1.05×10^{3}
42	1.00×10^{0}	46	2.50×10^{2}	50	3.15×10^{2}	54	1.00×10^{1}	58	1.15×10^{3}
	1.00×10^{0}		2.90×10^{2}		2.70×10^{2}		1.50×10^{1}		6.35×10^{2}
	1.50×10^{0}		2.20×10^{2}		1.05×10^{2}		5.00×10^{0}		6.75×10^{2}
	1.00×10^{0}		2.40×10^{2}		2.20×10^{2}		1.00×10^{1}		7.90×10^{2}
43	2.88×10^{7}	47	1.45×10^{2}	51	5.00×10^{1}	55	1.98×10^{7}	59	4.48×10^{3}
	2.74×10^{7}		8.50×10^{1}		3.00×10^{1}		1.89×10^{7}		3.98×10^{3}
	2.42×10^{7}		1.55×10^{2}		6.00×10^{1}		2.04×10^{7}		4.28×10^{3}
	2.94×10^{7}		8.50×10^{1}		5.50×10^{1}		2.37×10^{7}		4.51×10^{3}
44	3.63×10^{5}	48	7.00×10^{1}	52	1.60×10^{2}	56	7.70×10^{4}	60	1.76×10^{4}
	3.00×10^{5}		2.00×10^{1}		1.30×10^{2}		5.35×10^{4}		6.35×10^{3}
	2.85×10^{5}		6.00×10^{1}		1.25×10^{2}		7.10×10^{4}		5.50×10^{3}
	2.19×10^{5}		7.00×10^{1}		2.50×10^{1}		6.50×10^{4}		5.40×10^{3}

Microbiological data (continued)

Disinfection trial	number (cfu ml^{-1})	Disinfection trial	number (cfu ml^{-1})	Disinfection trial	number (cfu ml^{-1})	Disinfection trial	number (cfu ml^{-1})	Disinfection trial	number (cfu ml^{-1})
61	5.50×10^{7}	65	1.70×10^{2}	69	2.40×10^{3}	73	1.17×10^{8}	77	2.00×10^{1}
	1.13×10^{8}		1.60×10^{2}		1.89×10^{3}		1.06×10^{8}		1.10×10^{2}
	1.01×10^{8}		1.90×10^{2}		2.14×10^{3}		1.09×10^{8}		6.00×10^{1}
	1.10×10^{8}		1.35×10^{2}		2.42×10^{3}		8.65×10^{7}		9.00×10^{1}
62	1.17×10^{5}	66	5.50×10^{2}	70	2.90×10^{3}	74	8.65×10^{4}	78	9.55×10^{2}
	1.39×10^{5}		4.35×10^{2}		3.34×10^{3}		6.75×10^{4}		1.02×10^{3}
	1.35×10^{5}		5.20×10^{2}		3.42×10^{3}		6.70×10^{4}		1.29×10^{3}
	1.35×10^{5}		4.45×10^{2}		3.74×10^{3}		6.00×10^{4}		1.49×10^{3}
63	6.15×10^{2}	67	1.30×10^{8}	71	4.45×10^{2}	75	5.40×10^{2}	79	1.70×10^{7}
	7.00×10^{2}		1.19×10^{8}		6.55×10^{2}		5.55×10^{2}		7.10×10^{7}
	5.95×10^{2}		1.18×10^{8}		6.60×10^{2}		7.00×10^{2}		1.10×10^{7}
	5.95×10^{2}		1.09×10^{8}		5.85×10^{2}		8.90×10^{2}		5.00×10^{6}
64	8.35×10^{2}	68	4.44×10^{5}	72	7.40×10^{2}	76	1.74×10^{3}	80	2.06×10^{6}
	8.70×10^{2}		5.52×10^{5}		8.10×10^{2}		1.65×10^{3}		2.09×10^{6}
	1.16×10^{3}		6.53×10^{5}		8.35×10^{2}		1.63×10^{3}		1.15×10^{6}
	9.70×10^{2}		6.13×10^{5}		7.70×10^{2}		1.97×10^{3}		1.94×10^{6}

Microbiological data (continued)

Disinfection trial	number (cfu ml^{-1})	Disinfection trial	number (cfu ml^{-1})	Disinfection trial	number (cfu ml^{-1})	Disinfection trial	number (cfu ml^{-1})	Disinfection trial	number (cfu ml^{-1})
81	1.14×10^{3}	85	3.05×10^{7}	89	-	93	1.05×10^{2}	97	1.46×10^{8}
	2.79×10^{3}		2.30×10^{7}		-		6.50×10^{1}		2.60×10^{8}
	1.43×10^{3}		8.70×10^{7}		-		5.00×10^{1}		1.25×10^{8}
	1.29×10^{3}		9.15×10^{7}		-		1.00×10^{2}		1.09×10^{8}
82	5.50×10^{1}	86	1.47×10^{6}	90	-	94	1.55×10^{2}	98	8.77×10^{6}
	6.00×10^{1}		7.95×10^{5}		-		3.35×10^{2}		9.30×10^{6}
	4.80×10^{2}		2.57×10^{6}		-		1.05×10^{2}		9.71×10^{6}
	5.45×10^{2}		2.49×10^{6}		-		1.00×10^{2}		8.48×10^{6}
83	5.00×10^{0}	87	5.30×10^{2}	91	5.00×10^{7}	95	5.00×10^{0}	99	1.63×10^{5}
	1.50×10^{1}		1.48×10^{3}		5.50×10^{7}		1.00×10^{1}		2.15×10^{5}
	1.00×10^{1}		4.95×10^{2}		6.00×10^{7}		3.00×10^{1}		1.97×10^{5}
	-		3.45×10^{2}		5.80×10^{7}		1.50×10^{1}		2.13×10^{5}
84	6.50×10^{1}	88	6.00×10^{1}	92	1.65×10^{5}	96	2.00×10^{1}	100	2.65×10^{2}
	1.10×10^{1}		8.50×10^{1}		1.36×10^{5}		4.50×10^{1}		4.10×10^{2}
	1.50×10^{1}		4.05×10^{2}		1.51×10^{5}		2.50×10^{1}		3.95×10^{2}
	6.00×10^{1}		1.40×10^{1}		1.59×10^{5}		5.50×10^{1}		4.85×10^{2}

Microbiological data (continued)

Disinfection trial	number (cfu ml^{-1})	Disinfection trial	number (cfu ml^{-1})	Disinfection trial	number (cfu ml^{-1})	Disinfection trial	number (cfu ml^{-1})	Disinfection trial	number (cfu ml^{-1})
101	2.00×10^{1}	105	6.04×10^{6}	109	1.11×10^{8}	113	7.60×10^{4}	117	9.10×10^{3}
	2.00×10^{1}		4.20×10^{6}		1.80×10^{8}		5.00×10^{4}		1.28×10^{4}
	2.50×10^{1}		5.30×10^{6}		1.39×10^{8}		1.57×10^{5}		9.40×10^{3}
	3.50×10^{1}		8.86×10^{6}		1.34×10^{8}		1.40×10^{5}		1.06×10^{4}
102	2.25×10^{2}	106	7.15×10^{2}	110	3.40×10^{7}	114	6.85×10^{2}	118	2.19×10^{3}
	1.00×10^{2}		7.20×10^{2}		3.23×10^{7}		4.60×10^{2}		2.21×10^{3}
	7.50×10^{1}		6.80×10^{2}		3.29×10^{7}		6.75×10^{2}		2.04×10^{3}
	8.50×10^{1}		6.80×10^{2}		7.77×10^{7}		4.75×10^{2}		1.33×10^{3}
103	1.13×10^{9}	107	5.50×10^{1}	111	4.75×10^{6}	115	7.60×10^{7}	119	3.90×10^{2}
	1.20×10^{9}		9.50×10^{1}		4.32×10^{6}		1.29×10^{8}		2.45×10^{2}
	1.03×10^{9}		6.50×10^{1}		8.00×10^{6}		8.40×10^{7}		3.40×10^{2}
	7.85×10^{8}		6.50×10^{1}		8.00×10^{6}		4.40×10^{7}		2.05×10^{2}
104	7.60×10^{7}	108	1.05×10^{2}	112	1.53×10^{4}	116	1.17×10^{6}	120	2.50×10^{1}
	7.02×10^{7}		9.50×10^{1}		1.39×10^{4}		1.26×10^{6}		1.45×10^{2}
	7.78×10^{7}		9.00×10^{1}		1.09×10^{4}		1.40×10^{6}		7.00×10^{1}
	7.47×10^{7}		5.50×10^{1}		1.20×10^{4}		1.04×10^{6}		5.00×10^{1}

Microbiological data (continued)

Disinfection trial	number (cfu ml^{-1})	Disinfection trial	number (cfu ml^{-1})	Disinfection trial	number (cfu ml^{-1})	Disinfection trial	number (cfu ml^{-1})	Disinfection trial	number (cfu ml^{-1})
121	7.55×10^{7}	125	5.50×10^{1}	129	3.70×10^{2}	133	1.06×10^{8}	137	5.00×10^{0}
	7.15×10^{7}		1.05×10^{2}		3.85×10^{2}		9.60×10^{7}		5.00×10^{0}
	6.35×10^{7}		8.00×10^{1}		2.90×10^{2}		8.90×10^{7}		2.00×10^{1}
	-		5.00×10^{1}		4.45×10^{2}		5.00×10^{7}		2.50×10^{1}
122	6.55×10^{5}	126	7.50×10^{1}	130	1.31×10^{3}	134	2.20×10^{6}	138	-
	7.55×10^{5}		2.00×10^{1}		6.05×10^{2}		2.47×10^{6}		-
	4.10×10^{5}		3.00×10^{1}		8.65×10^{2}		1.24×10^{6}		-
	-		2.00×10^{1}		9.60×10^{2}		1.08×10^{6}		-
123	4.55×10^{2}	127	7.30×10^{7}	131	1.15×10^{2}	135	2.05×10^{3}		
	7.95×10^{2}		6.00×10^{7}		7.00×10^{1}		4.15×10^{3}		
	4.60×10^{2}		8.45×10^{7}		7.50×10^{1}		2.55×10^{3}		
	8.80×10^{2}		8.55×10^{7}		4.00×10^{1}		2.60×10^{3}		
124	7.55×10^{2}	128	6.80×10^{4}	132	1.25×10^{2}	136	1.01×10^{3}		
	5.15×10^{2}		9.50×10^{4}		2.55×10^{2}		6.90×10^{2}		
	4.70×10^{2}		5.95×10^{4}		9.00×10^{1}		4.30×10^{2}		
	3.75×10^{2}		7.40×10^{4}		1.75×10^{2}		2.90×10^{2}		

Appendix H: UV disinfection data of Nelson (2000)

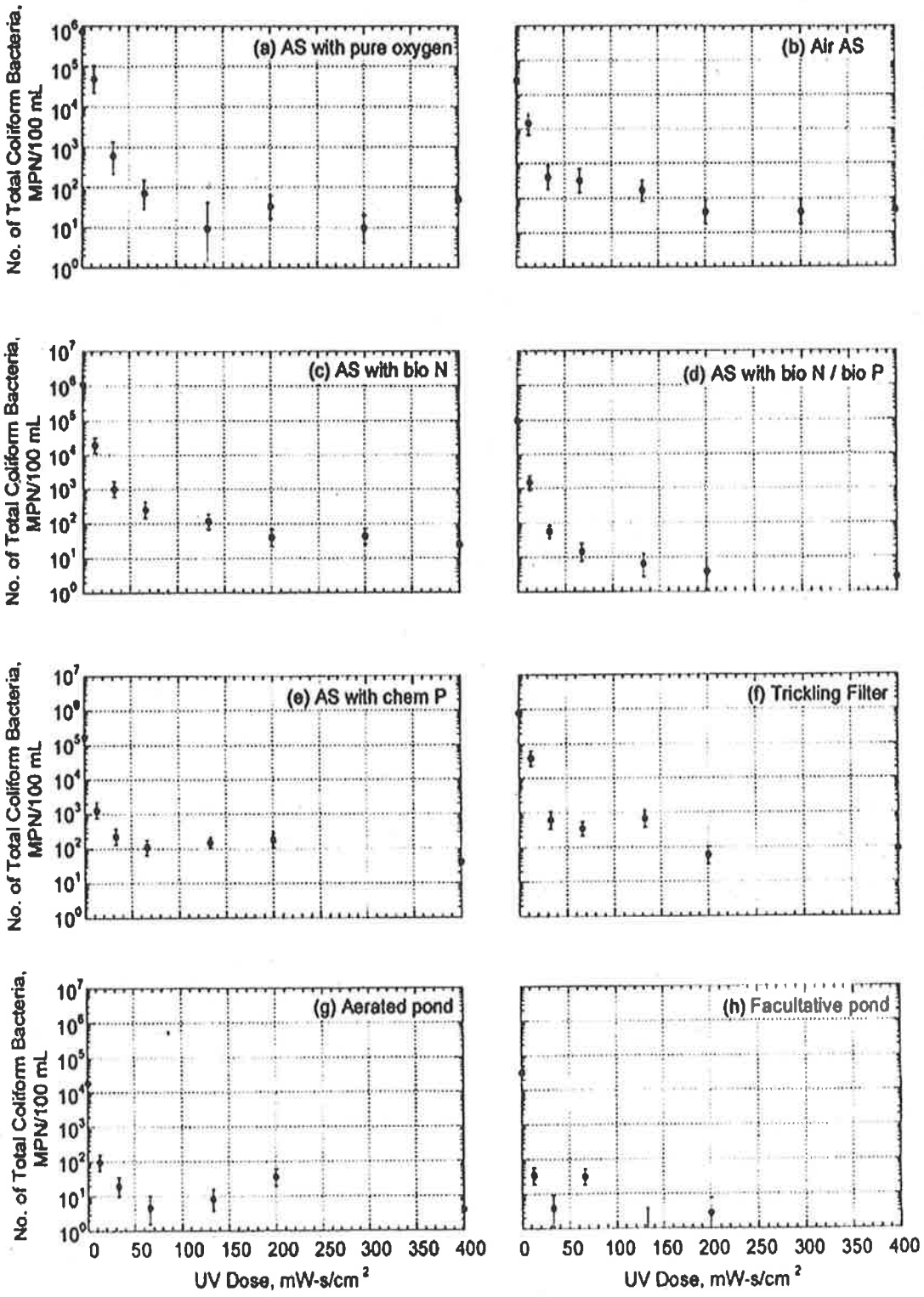

Figure H1. UV disinfection data of Nelson (2000) presented as survival of total coliform bacteria as a function of UV dose for eight different treatment effluents

Table H1. Digitised UV disinfection data for each of the treatment options employed by Nelson (2000)

(a) AS with pure O_2

N (MPN 100ml^{-1})	UV dose (mWs cm^{-2})
7.00×10^{5}	0
5.00×10^{4}	12.5
6.00×10^{2}	33.3
7.00×10^{1}	66.7
1.00×10^{1}	133.3
3.50×10^{1}	200
1.00×10^{1}	300
5.00×10^{1}	400

(b) Air AS

N (MPN 100ml^{-1})	UV dose (mWs cm^{-2})
2.50×10^{5}	0
1.50×10^{4}	12.5
4.00×10^{2}	33.3
3.00×10^{2}	66.7
1.50×10^{2}	133.3
4.00×10^{1}	200
4.00×10^{1}	300
4.50×10^{1}	400

(c) AS with bio N

N (MPN 100ml^{-1})	UV dose (mWs cm^{-2})
1.00×10^{6}	0
2.00×10^{4}	12.5
1.00×10^{3}	33.3
2.50×10^{2}	66.7
1.00×10^{2}	133.3
4.00×10^{1}	200
5.00×10^{1}	300
2.00×10^{1}	400

(d) AS with bio N/bio P

N (MPN 100ml^{-1})	UV dose (mWs cm^{-2})
1.00×10^{5}	0
1.50×10^{3}	12.5
5.50×10^{1}	33.3
1.50×10^{1}	66.7
6.00×10^{0}	133.3
4.00×10^{0}	200
2.50×10^{0}	400

(e) AS with chem P

N (MPN 100ml^{-1})	UV dose (mWs cm^{-2})
1.50×10^{5}	0
1.00×10^{3}	12.5
2.00×10^{2}	33.3
1.00×10^{2}	66.7
1.50×10^{2}	133.3
2.00×10^{2}	200
4.00×10^{1}	400

(f) Trickling filter

N (MPN 100ml^{-1})	UV dose (mWs cm^{-2})
7.00×10^{5}	0
4.00×10^{4}	12.5
6.00×10^{2}	33.3
3.50×10^{2}	66.7
7.00×10^{2}	133.3
6.00×10^{1}	200
9.00×10^{1}	400

(g) Aerated pond

N (MPN 100ml^{-1})	UV dose (mWs cm^{-2})
2.00×10^{4}	0
1.00×10^{2}	12.5
2.00×10^{1}	33.3
5.00×10^{0}	66.7
9.00×10^{0}	133.3
4.00×10^{1}	200
4.00×10^{0}	400

(h) Facultative pond

N (MPN 100ml^{-1})	UV dose (mWs cm^{-2})
3.00×10^{4}	0
3.50×10^{1}	12.5
4.00×10^{0}	33.3
3.00×10^{1}	66.7
3.00×10^{0}	200

Appendix I: UV disinfection data of Nguyen (1999)

Table I.1 UV inactivation and microbiological results

UV dose = 10,800 μWs cm^{-2}, t = 0.9 s, flow = 4 L min^{-1}

Disinfection trial	1	2	3	4	5	6
Test micro-organism	*E. coli*	*E. coli*	*E. coli*	*E. coli*	*E. coli*	*E. coli*
Coffee or Celite added (g L^{-1})	0 coffee	0.001 coffee	0.005 coffee	0.01 coffee	0.03 coffee	0.01 Celite
UV transmittance (%)	78	69	65	60	52	70
pH	5.95	5.76	5.85	5.44	5.62	6.13
Initial number, N_0 (No mL^{-1})	88 x 10^6	16 x 10^7	22 x 10^7	20 x 10^6	40 x 10^6	79 x 10^6
Survival number, N (No mL^{-1})	30 x 10^2	10 x 10^3	23 x 10^3	33 x 10^2	122 x 10^2	132 x 10^2
% Survival (100 x N/N_0)	0.003	0.0065	0.0103	0.0165	0.0304	0.017
$\ln(N/N_0)$	-10.29	-9.64	-9.18	-8.71	-8.1	-8.69
$\log_{10}(N/N_0)$	-4.47	-4.19	-3.99	-3.78	-3.52	-3.77

Disinfection trials	7	8	9	10	11	12
Test micro-organism	*E. coli*	*E. coli*	*E. coli*	*P. aeruginosa*	*P. aeruginosa*	*P. aeruginosa*
Coffee or Celite added (g L^{-1})	0.05 Celite	0.1 Celite	0.3 Celite	0 coffee	0.001 coffee	0.005 coffee
UV transmittance (%)	66	61	55	80	71	66
pH	6.06	6.03	5.90	5.38	5.51	5.93
Initial number, N_0 (No mL^{-1})	31 x 10^7	80 x 10^7	24 x 10^7	98 x 10^6	90 x 10^6	80 x 10^6
Survival number, N (No mL^{-1})	64 x 10^3	280 x 10^3	116 x 10^3	130 x 10^2	260 x 10^2	270 x 10^2
% Survival (100 x N/N_0)	0.0207	0.0352	0.0482	0.0126	0.0285	0.0336
$\ln(N/N_0)$	-8.48	-7.95	-7.64	-8.98	-8.16	-7.99
$\log_{10}(N/N_0)$	-3.68	-3.45	-3.32	-3.90	-3.54	-3.47

Disinfection trials	13	14	15	16	17	18
Test micro-organism	*P. aeruginosa*	*P. aeruginosa*	*P. aeruginosa*	*P. aeruginosa*	*P. aeruginosa*	*P. aeruginosa*
Coffee or Celite added (g L^{-1})	0.01 coffee	0.03 coffee	0.01 Celite	0.05 Celite	0.1 Celite	0.3 Celite
UV transmittance (%)	62	55	72	65	61	53
pH	5.58	5.98	6.23	6.26	6.17	6.02
Initial number, N_0 (No mL^{-1})	36 x 10^6	38 x 10^6	900 x 10^6	70 x 10^6	106 x 10^6	34 x 10^6
Survival number, N (No mL^{-1})	150 x 10^2	210 x 10^2	34 x 10^2	300 x 10^2	53 x 10^2	250 x 10^2
% Survival (100 x N/N_0)	0.0416	0.0564	0.038	0.0429	0.0503	0.0721
$\ln(N/N_0)$	-7.78	-7.48	-7.88	-7.75	-7.59	-7.24
$\log_{10}(N/N_0)$	-3.38	-3.25	-3.42	-3.36	-3.30	-3.14

Table I.2 UV inactivation and microbiological results

UV dose = 14,100 μWs cm^{-2}, t = 1.2 s, flow = 3 L min^{-1}

Disinfection trial	19	20	21	22	23	24
Test micro-organism	*E. coli*	*E. coli*	*E. coli*	*E. coli*	*E. coli*	*E. coli*
Coffee or Celite added (g L^{-1})	0 coffee	0.001 coffee	0.005 coffee	0.01 coffee	0.03 coffee	0.01 Celite
UV transmittance (%)	78	69	65	60	52	70
pH	5.95	5.76	5.85	5.44	5.62	6.13
Initial number, N_0 (No.mL^{-1})	64 x 10^6	170 x 10^6	130 x 10^6	50 x 10^6	40 x 10^6	90 x 10^6
Survival number, N (No mL^{-1})	20 x 10^2	10 x 10^2	124 x 10^2	69 x 10^2	100 x 10^2	122 x 10^2
% Survival (100 x N/N_0)	0.0029	0.0057	0.0095	0.0138	0.025	0.0136
$\ln(N/N_0)$	-10.45	-9.77	-9.26	-8.89	-8.29	-8.90
$\log_{10}(N/N_0)$	-4.54	-4.24	-4.02	-3.86	-3.60	-3.86

Disinfection trial	25	26	27	28	29	30
Test micro-organism	*E. coli*	*E. coli*	*E. coli*	*P. aeruginosa*	*P. aeruginosa*	*P. aeruginosa*
Coffee or Celite added (g L^{-1})	0.05 Celite	0.1 Celite	0.3 Celite	0 coffee	0.001 coffee	0.005 coffee
UV transmittance (%)	66	61	55	80	71	66
pH	6.06	6.03	5.90	5.38	5.51	5.93
Initial number, N_0 (No mL^{-1})	120 x 10^7	160 x 10^7	31 x 10^7	112 x 10^5	70 x 10^6	50 x 10^6
Survival number, N (No mL^{-1})	150 x 10^3	42 x 10^4	113 x 10^3	15 x 10^2	170 x 10^2	140 x 10^2
% Survival (100 x N/N_0)	0.0126	0.0263	0.0365	0.0130	0.0225	0.0279
$\ln(N/N_0)$	-8.98	-8.24	-7.92	-8.95	-8.40	-8.18
$\log_{10}(N/N_0)$	-3.90	-3.58	-3.44	-3.89	-3.65	-3.55

Disinfection trial	31	32	33	34	35	36
Test micro-organism	*P. aeruginosa*	*P. aeruginosa*	*P. aeruginosa*	*P. aeruginosa*	*P. aeruginosa*	*P. aeruginosa*
Coffee or Celite added (g.L^{-1})	0.01 coffee	0.03 coffee	0.01 Celite	0.05 Celite	0.1 Celite	0.3 Celite
UV transmittance (%)	62	55	72	65	61	53
pH	5.58	5.98	6.23	6.26	6.17	6.02
Initial number, N_0 (No mL^{-1})	35 x 10^6	54 x 10^6	70 x 10^5	90 x 10^6	86 x 10^6	44 x 10^6
Survival number, N (No mL^{-1})	120 x 10^2	270 x 10^2	15 x 10^2	280 x 10^2	33 x 10^3	270 x 10^2
% Survival (100 x N/N_0)	0.0341	0.0504	0.0214	0.031	0.038	0.0601
$\ln(N/N_0)$	-7.98	-7.59	-8.45	-8.08	-7.88	-7.42
$\log_{10}(N/N_0)$	-3.46	-3.30	-3.67	-3.51	-3.42	-3.22

Table I.3 UV inactivation and microbiological results

UV dose = 22,700 μWs cm^{-2}, t = 1.9 s, flow = 2 L min^{-1}

Disinfection trial	37	38	39	40	41	42
Test micro-organism	*E. coli*	*E. coli*	*E. coli*	*E. coli*	*E. coli*	*E. coli*
Coffee or Celite added (g L^{-1})	0 coffee	0.001 coffee	0.005 coffee	0.01 coffee	0.03 coffee	0.01 Celite
UV transmittance (%)	78	69	65	60	52	70
pH	5.95	5.76	5.85	5.44	5.62	6.13
Initial number, N_0 (No mL^{-1})	46×10^6	180×10^6	130×10^5	50×10^6	30×10^6	100×10^6
Survival number, N (No $.mL^{-1}$)	20×10^2	100×10^2	87×10^2	48×10^2	61×10^3	74×10^2
% Survival (100 x N/N_0)	0.0021	0.0056	0.0067	0.0096	0.0203	0.0074
$\ln(N/N_0)$	-10.77	-9.79	-9.61	-9.25	-8.50	-9.51
$\log_{10}(N/N_0)$	-4.68	-4.25	-4.17	-4.02	-3.69	-4.13

Disinfection trial	43	44	45	46	47	48
Test micro-organism	*E. coli*	*E. coli*	*E. coli*	*P. aeruginosa*	*P. aeruginosa*	*P. aeruginosa*
Coffee or Celite added (g L^{-1})	0.05 Celite	0.1 Celite	0.3 Celite	0 coffee	0.001 coffee	0.005 coffee
UV transmittance (%)	66	61	55	80	71	66
pH	6.06	6.03	5.90	5.38	5.51	5.93
Initial number, N_0 (No mL^{-1})	55×10^7	700×10^7	50×10^7	81×10^6	80×10^6	90×10^6
Survival number, N (No mL^{-1})	56×10^3	96×10^3	162×10^3	69×10^2	11×10^3	160×10^2
% Survival (100 x N/N_0)	0.0101	0.0137	0.0284	0.0085	0.0135	0.0175
$\ln(N/N_0)$	-9.20	-8.89	-8.17	-9.37	-8.91	-8.65
$\log_{10}(N/N_0)$	-3.99	-3.86	-3.55	-4.07	-3.87	-3.76

Disinfection trial	49	50	51	52	53	54
Test micro-organism	*P. aeruginosa*	*P. aeruginosa*	*P. aeruginosa*	*P. aeruginosa*	*P. aeruginosa*	*P. aeruginosa*
Coffee or Celite added (g L^{-1})	0.01 coffee	0.03 coffee	0.01 Celite	0.05 Celite	0.1 Celite	0.3 Celite
UV transmittance (%)	62	55	72	65	61	53
pH	5.58	5.98	6.23	6.26	6.17	6.02
Initial number, N_0 (No mL^{-1})	80×10^6	45×10^6	110×10^5	104×10^6	80×10^6	56×10^6
Survival number, N (No mL^{-1})	240×10^2	150×10^2	154×10^2	200×10^2	23×10^3	260×10^2
% Survival (100 x N/N_0)	0.0295	0.0341	0.014	0.0186	0.029	0.0458
$\ln(N/N_0)$	-8.13	-7.98	-8.87	-8.59	-8.15	-7.69
$\log_{10}(N/N_0)$	-3.53	-3.46	-3.85	-3.73	-3.54	-3.34

Table I.4 UV inactivation and microbiological results

UV dose = 44,200 μWs cm^{-2}, t = 3.7 s, flow = 1 L min^{-1}

Disinfection trial	55	56	57	58	59	60
Test micro-organism	*E. coli*	*E. coli*	*E. coli*	*E. coli*	*E. coli*	*E. coli*
Coffee or Celite added (g L^{-1})	0 coffee	0.001 coffee	0.005 coffee	0.01 coffee	0.03 coffee	0.01 Celite
UV transmittance (%)	78	69	65	60	52	70
pH	5.95	5.76	5.85	5.44	5.62	6.13
Initial number, N_0 (No mL^{-1})	64 x 10^6	140 x 10^6	250 x 10^5	30 x 10^6	20 x 10^6	110 x 10^6
Survival number, N (No mL^{-1})	7 x 10^2	37 x 10^2	88 x 10^2	15 x 10^2	20 x 10^3	30 x 10^2
% Survival (100 x N/N_0)	0.0011	0.0026	0.0035	0.0050	0.0100	0.0027
$\ln(N/N_0)$	-11.42	-10.56	-10.26	-9.9	-9.21	-10.52
$\log_{10}(N/N_0)$	-4.96	-4.58	-4.45	-4.30	-4.00	-4.57

Disinfection trial	61	62	63	64	65	66
Test micro-organism	*E. coli*	*E. coli*	*E. coli*	*P. aeruginosa*	*P. aeruginosa*	*P. aeruginosa*
Coffee or Celite added (g L^{-1})	0.05 Celite	0.1 Celite	0.3 Celite	0 coffee	0.001 coffee	0.005 coffee
UV transmittance (%)	66	61	55	80	71	66
pH	6.06	6.03	5.90	5.38	5.51	5.93
Initial number, N_0 (No mL^{-1})	130 x 10^7	90 x 10^7	48 x 10^7	63 x 10^6	90 x 10^6	30 x 10^6
Survival number, N (No mL^{-1})	66 x 10^3	80 x 10^3	82 x 10^3	10 x 10^2	40 x 10^2	19 x 10^2
% Survival (100 x N/N_0)	0.0051	0.0089	0.0171	0.0016	0.0044	0.0064
$\ln(N/N_0)$	-9.88	-9.33	-8.67	-11.04	-10.03	-9.66
$\log_{10}(N/N_0)$	-4.29	-4.05	-3.76	-4.79	-4.35	-4.19

Disinfection trial	67	68	69	70	71	72
Test micro-organism	*P. aeruginosa*	*P. aeruginosa*	*P. aeruginosa*	*P. aeruginosa*	*P. aeruginosa*	*P. aeruginosa*
Coffee or Celite added (g L^{-1})	0.01 coffee	0.03 coffee	0.01 Celite	0.05 Celite	0.1 Celite	0.3 Celite
UV transmittance (%)	62	55	72	65	61	53
pH	5.58	5.98	6.23	6.26	6.17	6.02
Initial number, N_0 (No mL^{-1})	39 x 10^6	61 x 10^6	90 x 10^5	104 x 10^6	124 x 10^6	58 x 10^6
Survival number, N (No mL^{-1})	37 x 10^2	73 x 10^2	67 x 10^2	94 x 10^2	24 x 10^3	160 x 10^2
% Survival (100 x N/N_0)	0.0095	0.0120	0.0074	0.0090	0.0189	0.0275
$\ln(N/N_0)$	-9.26	-9.03	-9.51	-9.32	-8.57	-8.20
$\log_{10}(N/N_0)$	-4.02	-3.92	-4.13	-4.05	-3.72	-3.56

Appendix J: Development of the EDP_m model form

Here the development of the modified exponentially damped polynomial model (EDP_m) is outlined based of the general EDP form. A method for constraining the breakpoint dose estimate is also presented to ensure non-negative rates of disinfection are predicted for the tailing region.

For UV disinfection kinetics, the general exponentially damped polynomial (EDP) form is given by equation J1:

$$\log_{10}\frac{N}{N_0} = -k[dose]\exp(-\lambda[dose]) \tag{J1}$$

Differentiation of equation J1 with respect to UV dose [dose], gives a measure of the rate of disinfection, as outlined below:

$$\begin{aligned}\frac{d\left[\log_{10}\frac{N}{N_0}\right]}{d[dose]} &= -k[\exp(-\lambda[dose])(-\lambda)[dose]+\exp(-\lambda[dose])] \\ &= -k.\exp(-\lambda[dose])(1-\lambda[dose])\end{aligned} \tag{J2}$$

In development of the EDP_m model, the region of tailing may be considered as those doses exceeding the breakpoint dose $[dose]_B$. This region is to be represented by log-linear disinfection kinetics. This piecewise model requires continuity at the breakpoint dose, and hence the rate of disinfection for the tailing region (k') may be evaluated by substitution of the breakpoint dose in equation J2, and is given by equation J3:

$$k' = k.\exp(-\lambda[dose]_B)(1-\lambda[dose]_B) \tag{J3}$$

Similarly, the predicted level of disinfection at the onset of tailing ($-c$) may be calculated by substitution of breakpoint dose in equation J1, and is given by equation J4:

$$-c = -k.\exp(-\lambda[dose]_B).[dose]_B \tag{J4}$$

These properties predicted at the breakpoint dose may be used to define the log-linear disinfection kinetics in the tailing region. Coupling of these kinetics of the tailing region with those of the initial region ($[dose] < [dose]_B$) of disinfection yields the modified EDP_m form of equation J5.

$$\log_{10}\frac{N}{N_0} = -\delta_1 k[dose]\exp(-\lambda[dose]) - \delta_2(k'[dose]+c) \qquad \text{(J5)}$$

Where δ_1 and δ_2 are dummy variables for the respective regions of disinfection.

- if $[dose] \leq [dose]_B$ then $\delta_1 = 1$; $\delta_2 = 0$ – initial region of disinfection.
- if $[dose] > [dose]_B$ then $\delta_1 = 0$; $\delta_2 = 1$ – tailed region of disinfection.

The EDP_m form (equation J5) may be constrained to prevent the prediction of negative rates of disinfection in the tail. This may arise due to data at high doses ($> [dose]_B$) forcing the fit of the model. An intuitive limiting case would be when the predicted rate of disinfection (k') in the tail is zero. Hence the rate of disinfection as defined by equation J2 may be set to zero.

$$-k.\exp(-\lambda[dose])(1-\lambda[dose]) = 0 \qquad \text{(J2)}$$

$$1-\lambda[dose] = 0$$

$$[dose] = \lambda^{-1} \qquad \text{(J6)}$$

The limiting case arises when the dose is equal in value to the reciprocal of the damping coefficient λ. The rate of disinfection can now be determined to be positive for doses less than this limiting value; and negative when it is exceeded.

$$\frac{d\left[\log_{10}\frac{N}{N_0}\right]}{d[dose]}$$

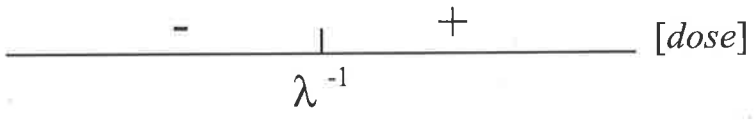

The breakpoint dose is now constrained to take values no greater than the reciprocal of the damping coefficient. When the reciprocal of the damping coefficient and the breakpoint dose are equal, the rate of disinfection in the tailing region (k') is zero.

Appendix K: Fits of the EDP_m model to the disinfection data of Nelson (2000)

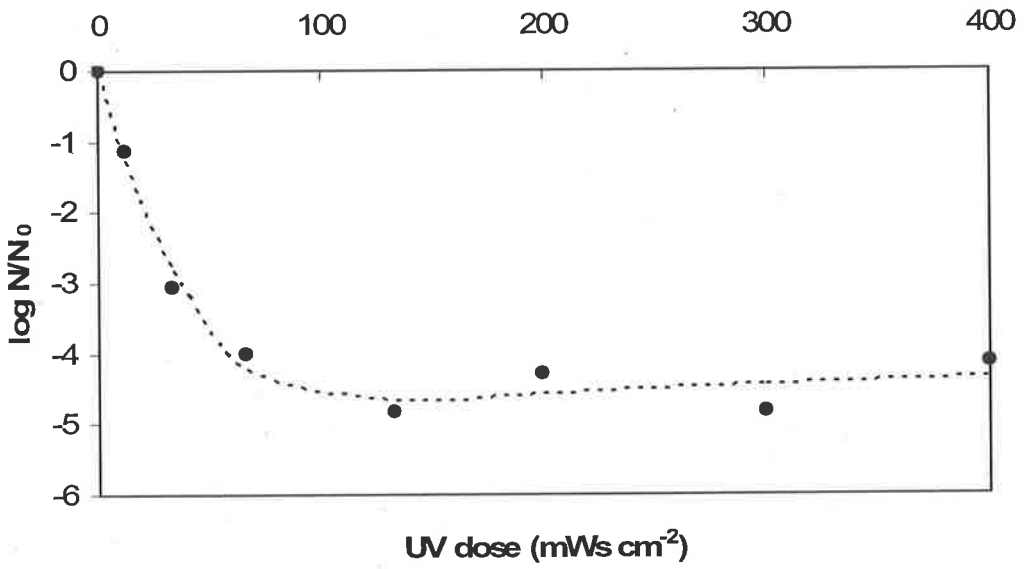

Figure K1. EDP_m model predictions for UV disinfection of activated sludge effluent where pure oxygen was utilized

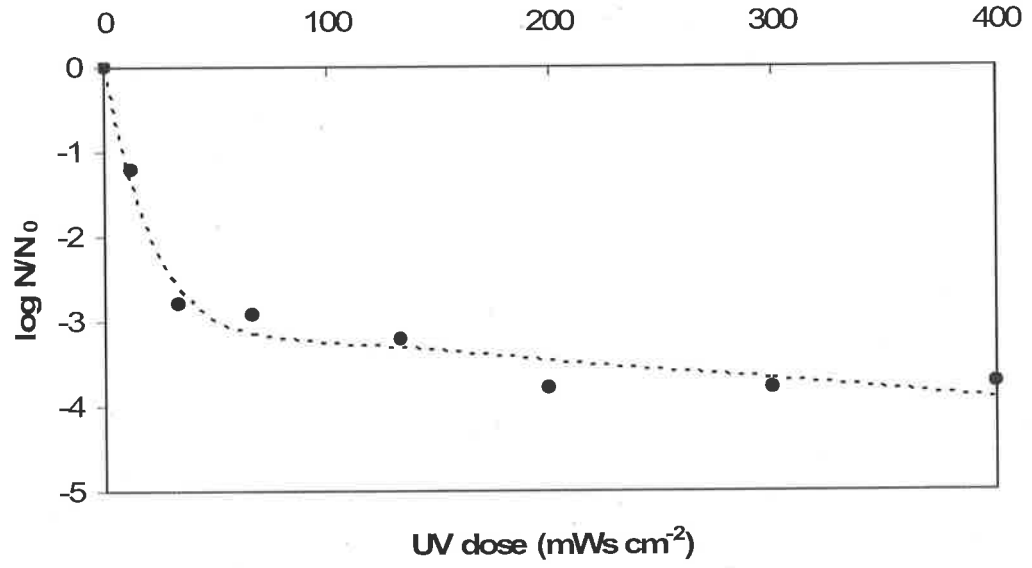

Figure K2. EDP_m model predictions for UV disinfection of activated sludge effluent where air was utilized

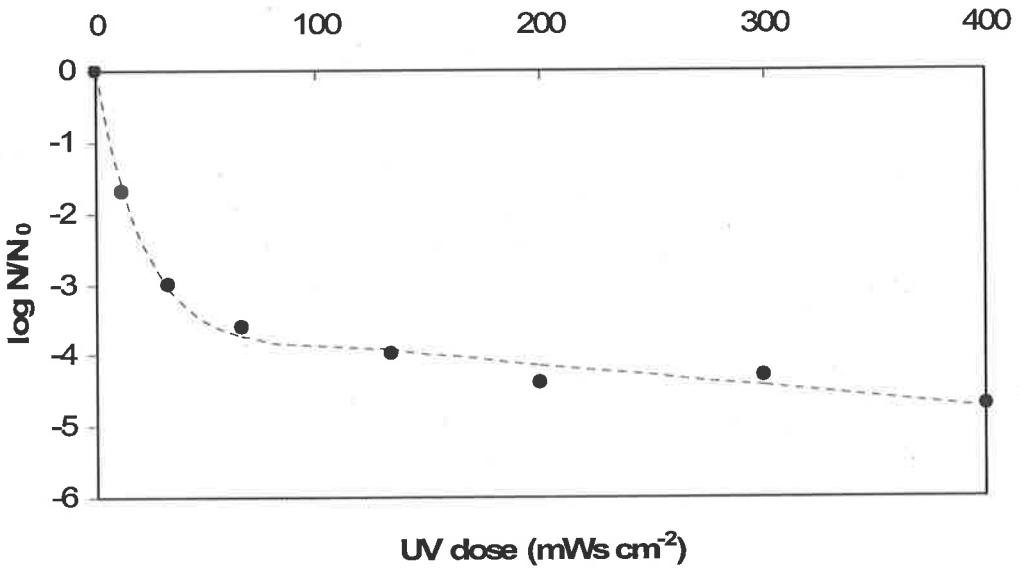

Figure K3. EDP_m model predictions for UV disinfection of activated sludge effluent with biological nitrogen removal

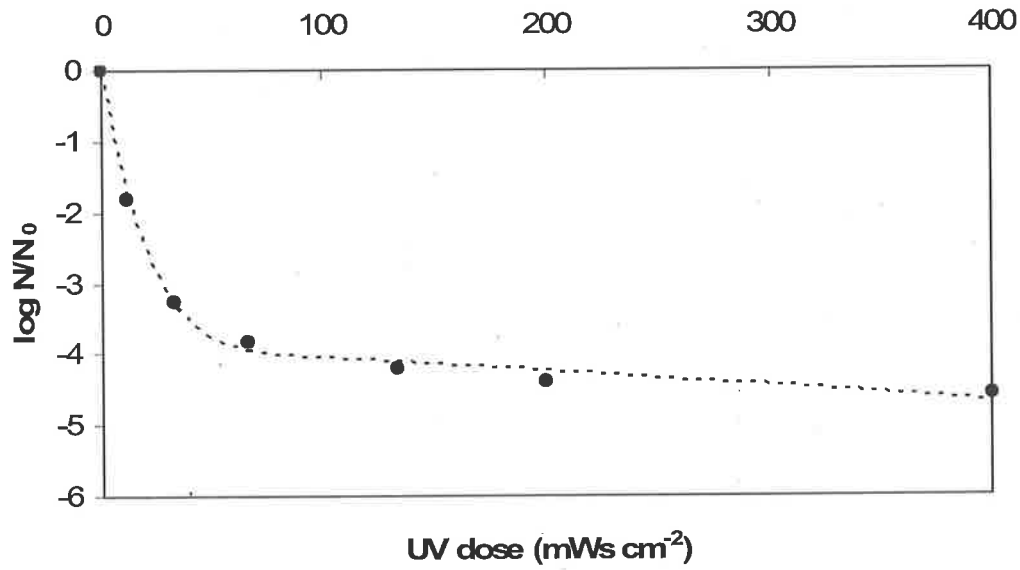

Figure K4. EDP_m model predictions for UV disinfection of activated sludge effluent with biological nitrogen and phosphorous removal

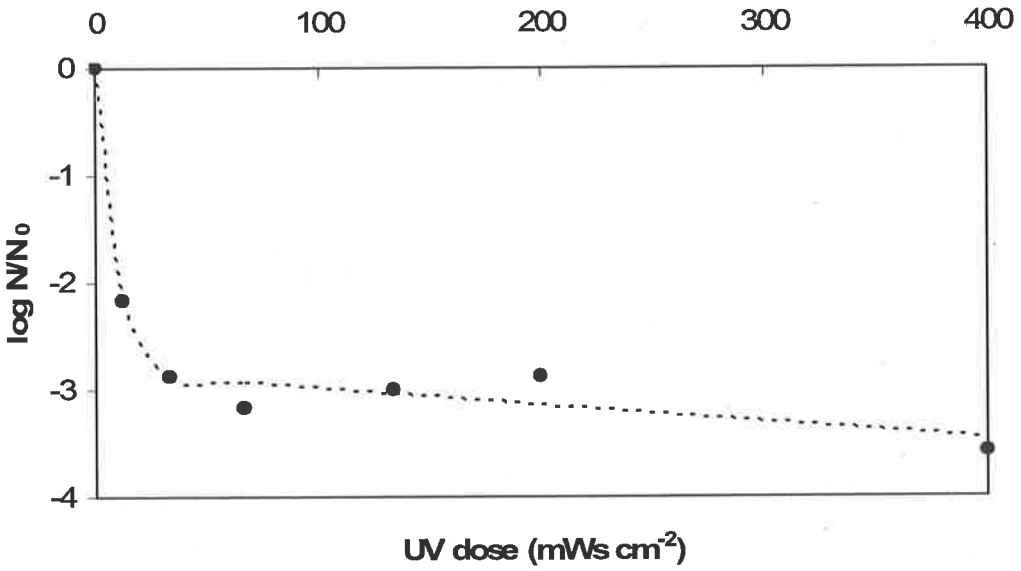

Figure K5. EDP_m model predictions for UV disinfection of activated sludge effluent with chemical phosphorous removal

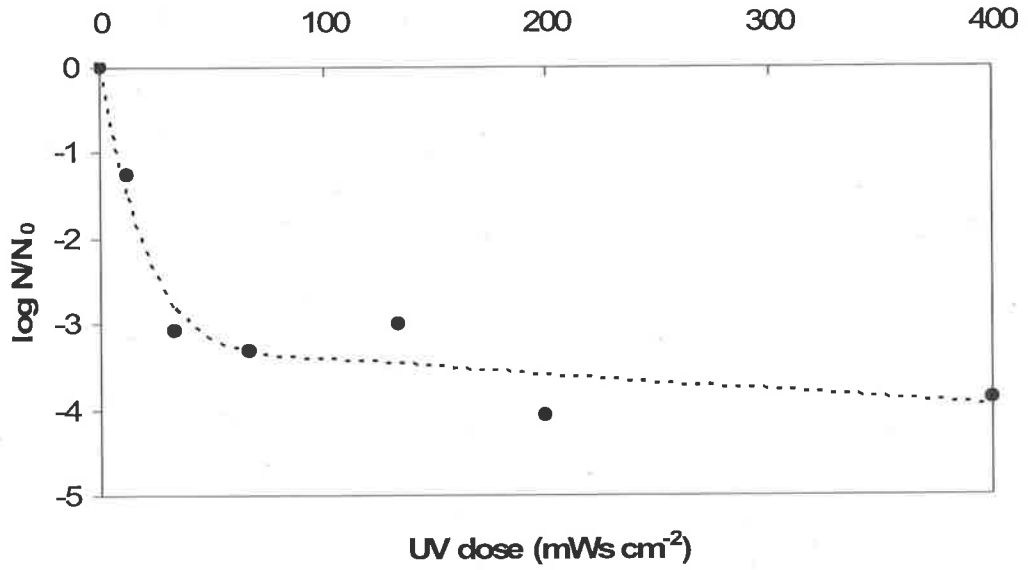

Figure K6. EDP_m model predictions for UV disinfection of trickling filter effluent

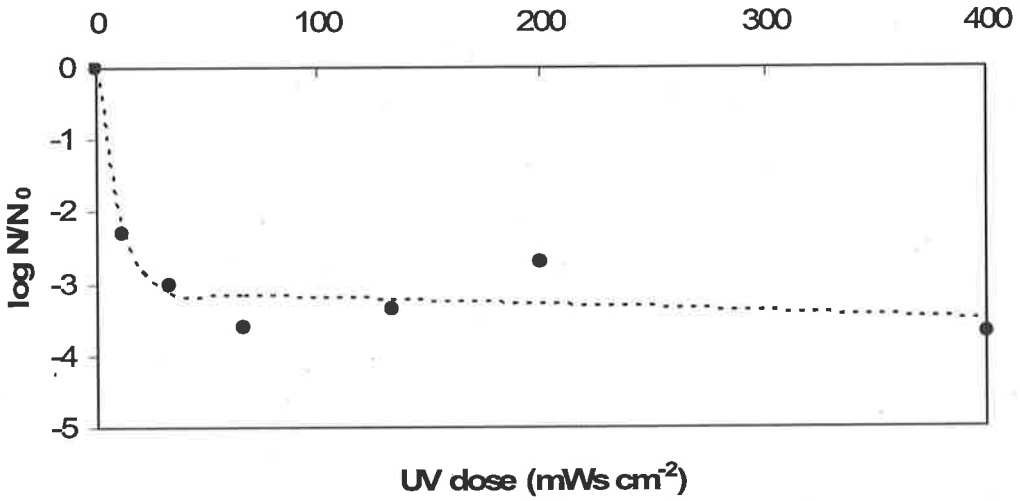

Figure K7. EDP_m model predictions for UV disinfection of aerated pond effluent

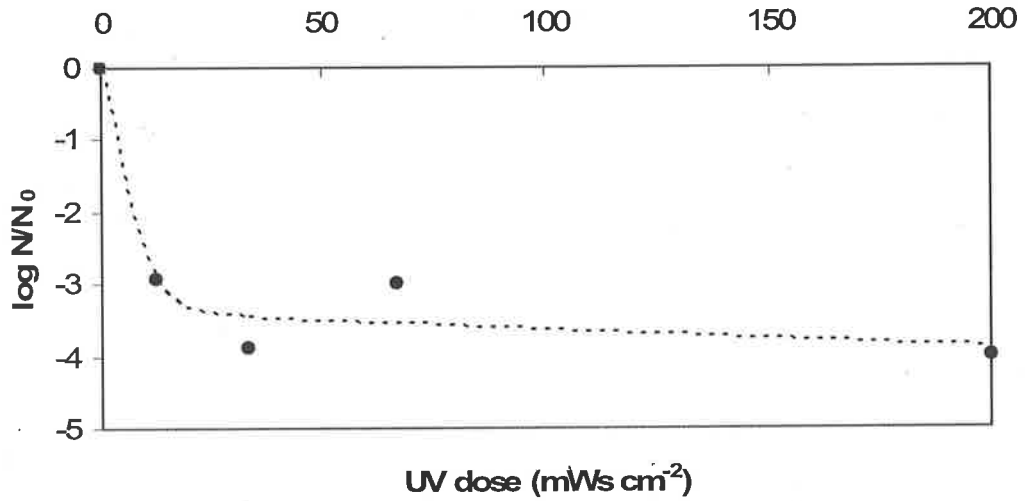

Figure K8. EDP_m model predictions for UV disinfection of facultative pond effluent

Appendix L: Fits of the Weibull model to the disinfection data of Nelson (2000)

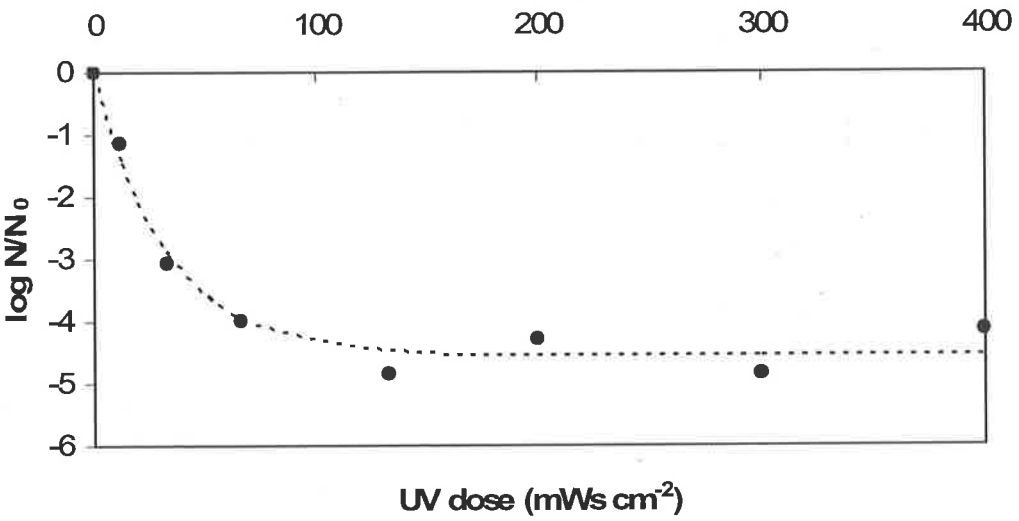

Figure L1. Weibull model predictions for UV disinfection of activated sludge effluent where pure oxygen was utilized

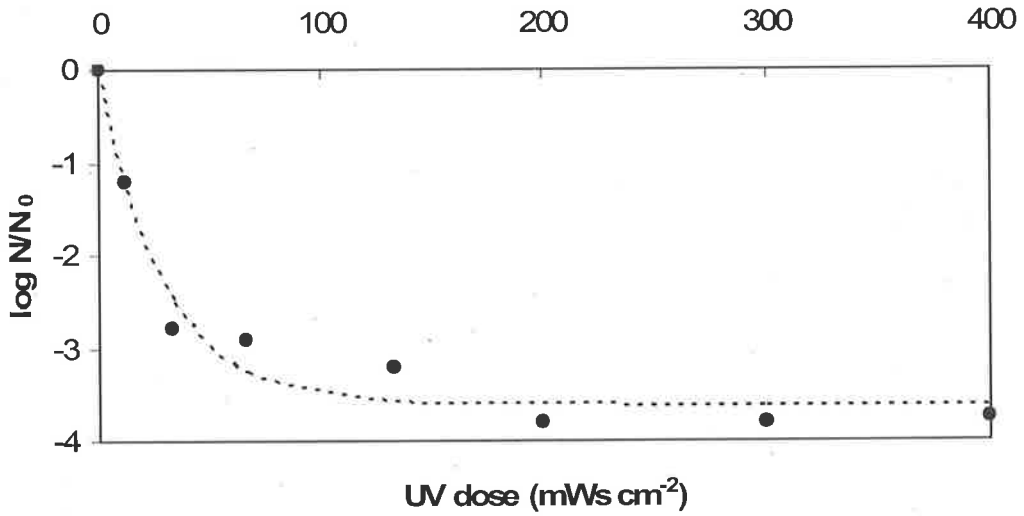

Figure L2. Weibull model predictions for UV disinfection of activated sludge effluent where air was utilized

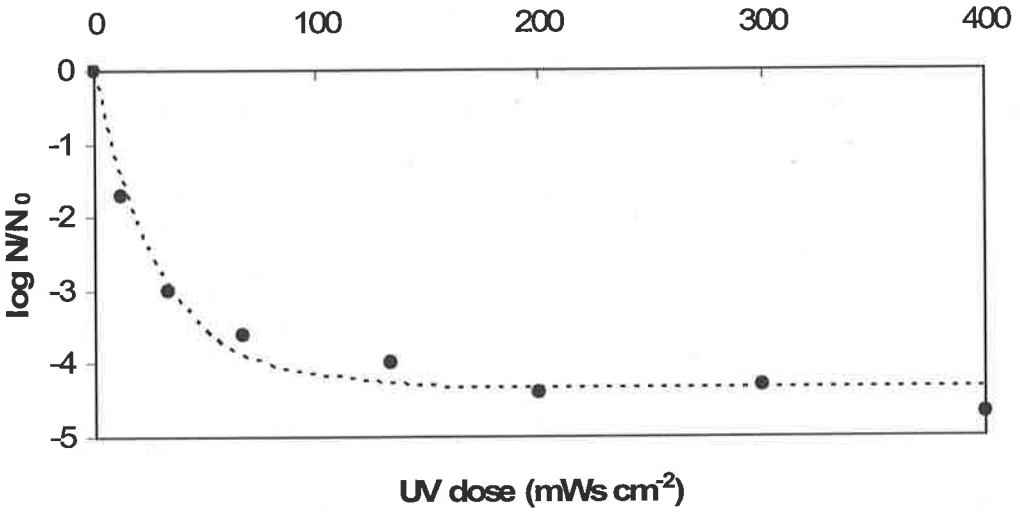

Figure L3. Weibull model predictions for UV disinfection of activated sludge effluent with biological nitrogen removal

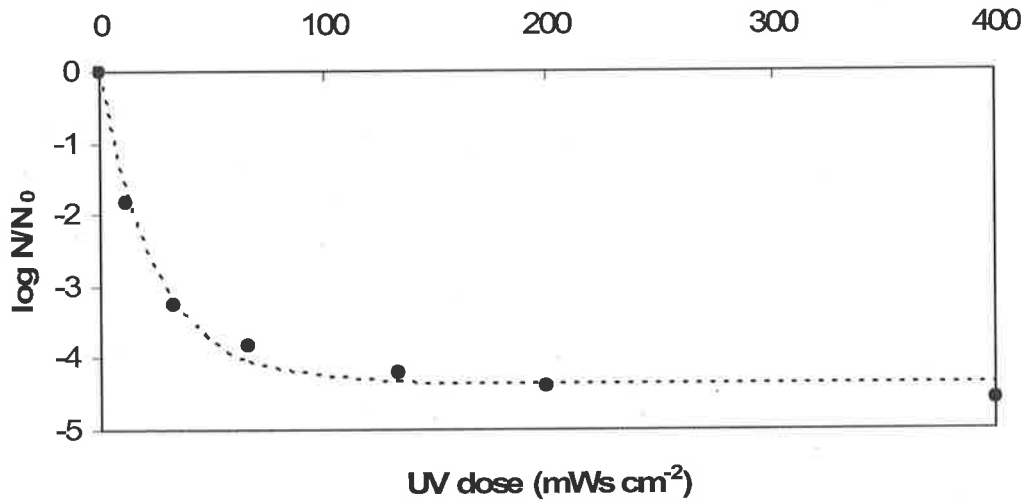

Figure L4. Weibull model predictions for UV disinfection of activated sludge effluent with biological nitrogen and phosphorous removal

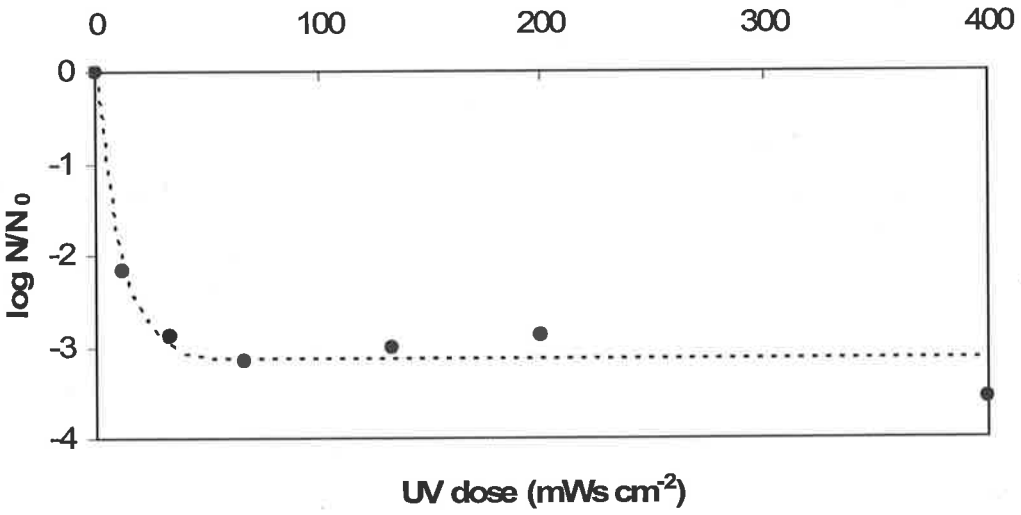

Figure L5. Weibull model predictions for UV disinfection of activated sludge effluent with chemical phosphorous removal

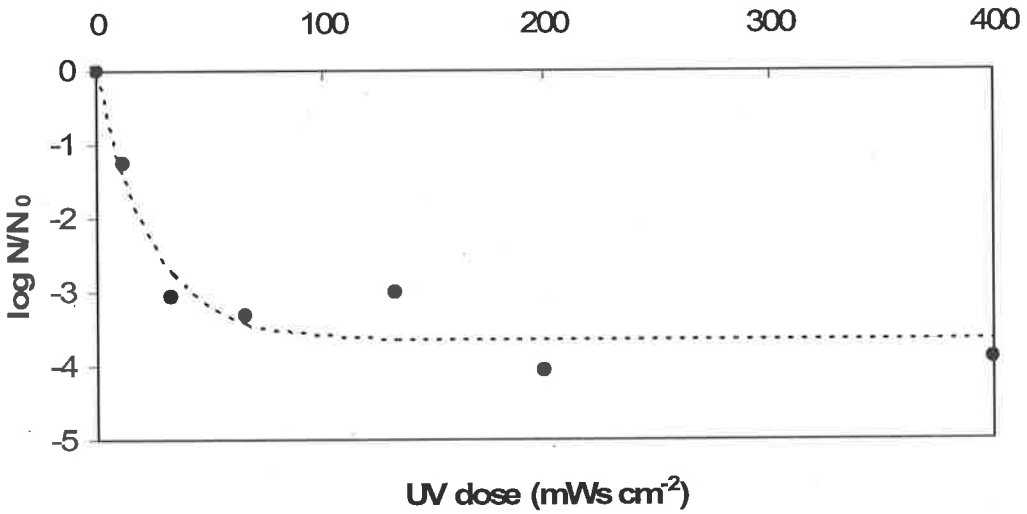

Figure L6. Weibull model predictions for UV disinfection of trickling filter effluent

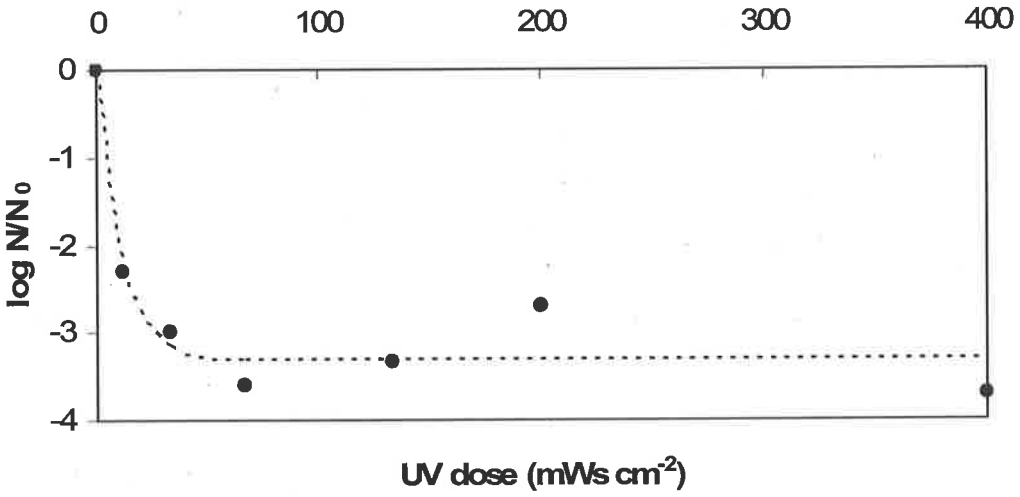

Figure L7. Weibull model predictions for UV disinfection of aerated pond effluent

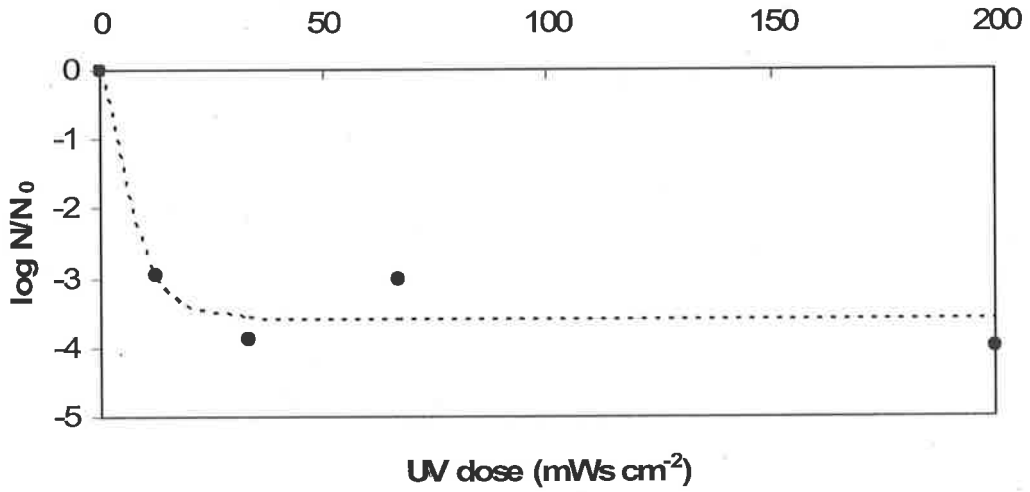

Figure L8. Weibull model predictions for UV disinfection of facultative pond effluent

Appendix M: Fits of the EDP_m model to the experimental disinfection data

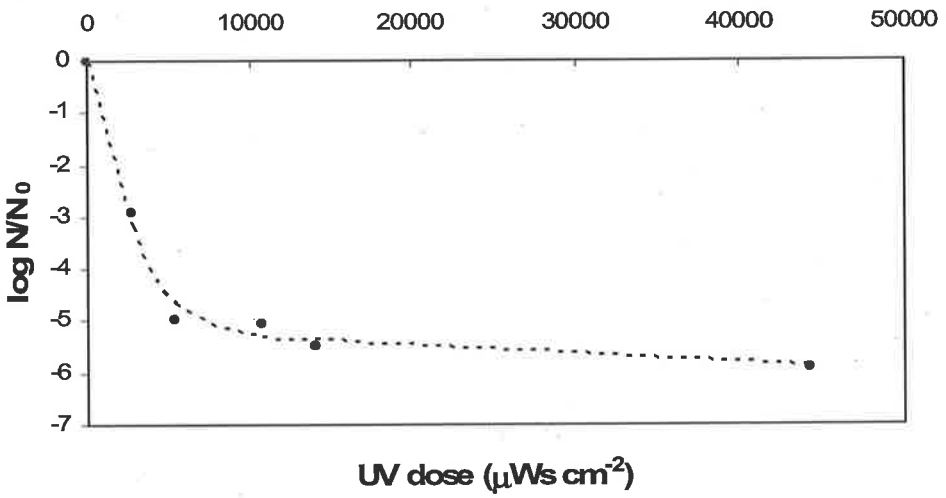

Figure M1. EDP_m model predictions for data set 1

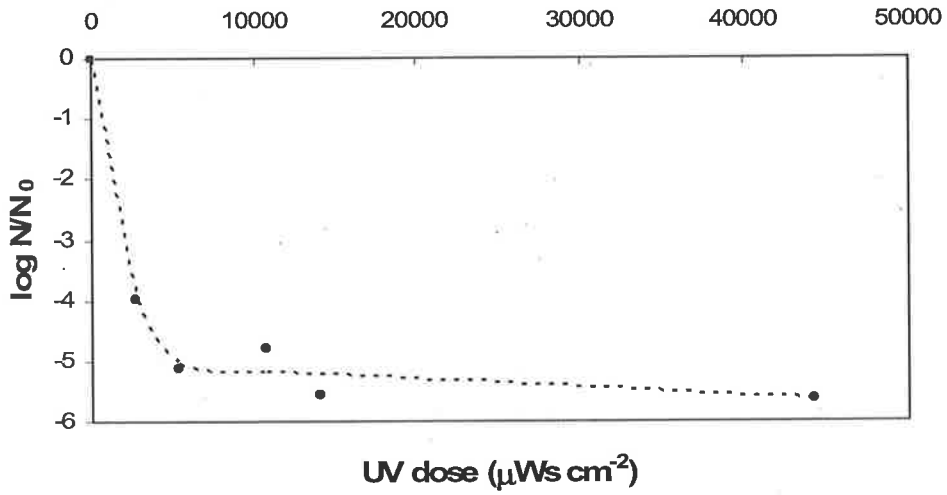

Figure M2. EDP_m model predictions for data set 2

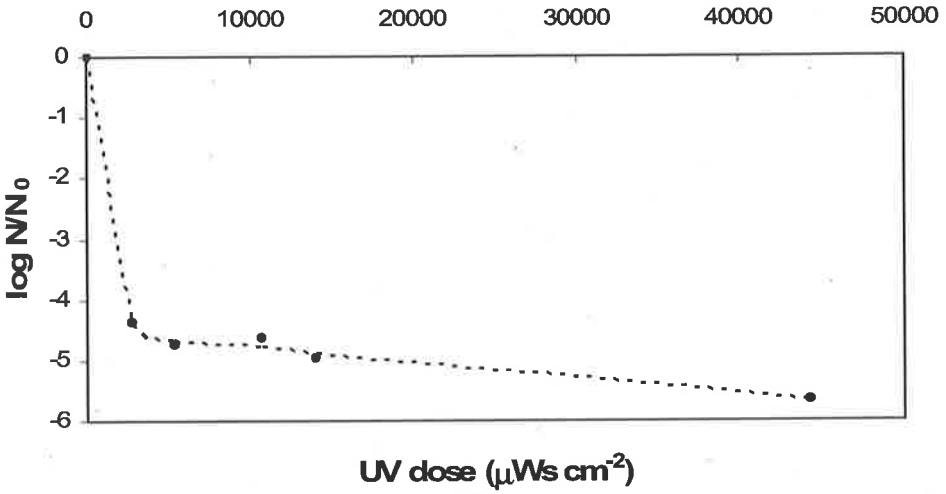

Figure M3. EDP_m model predictions for data set 3

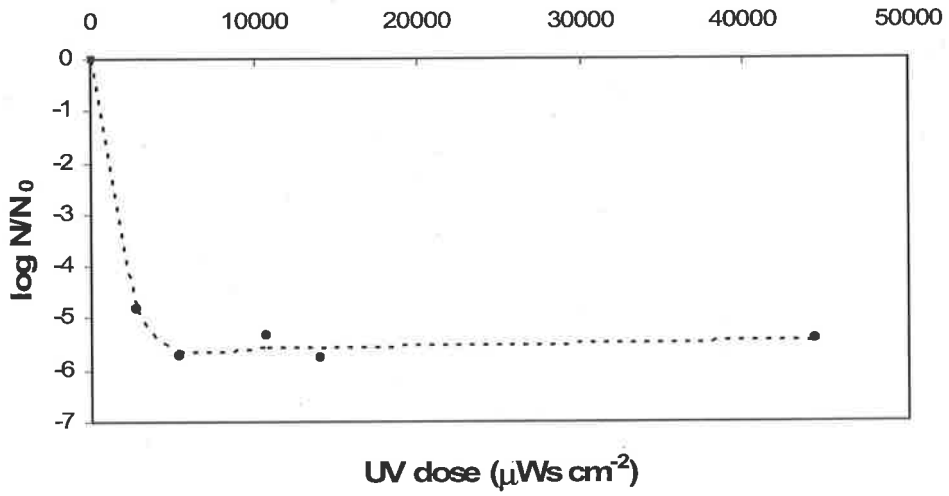

Figure M4. EDP_m model predictions for data set 4

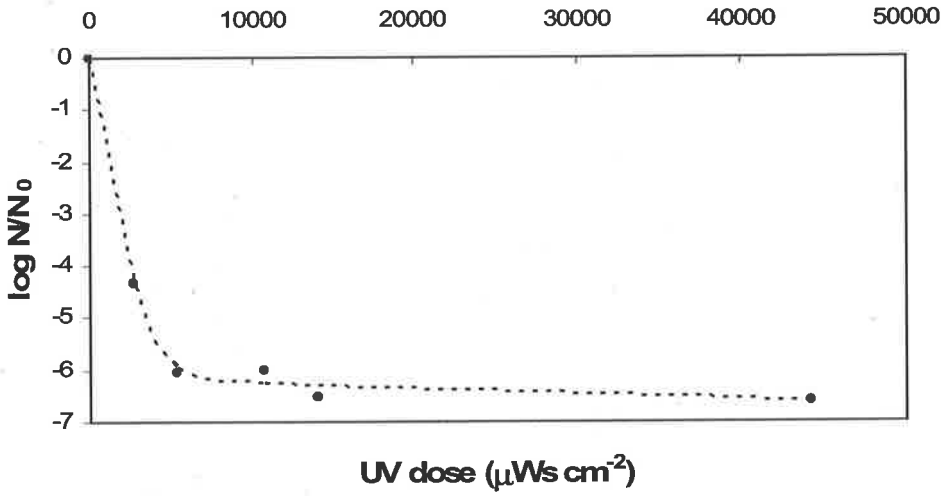

Figure M5. EDP_m model predictions for data set 5

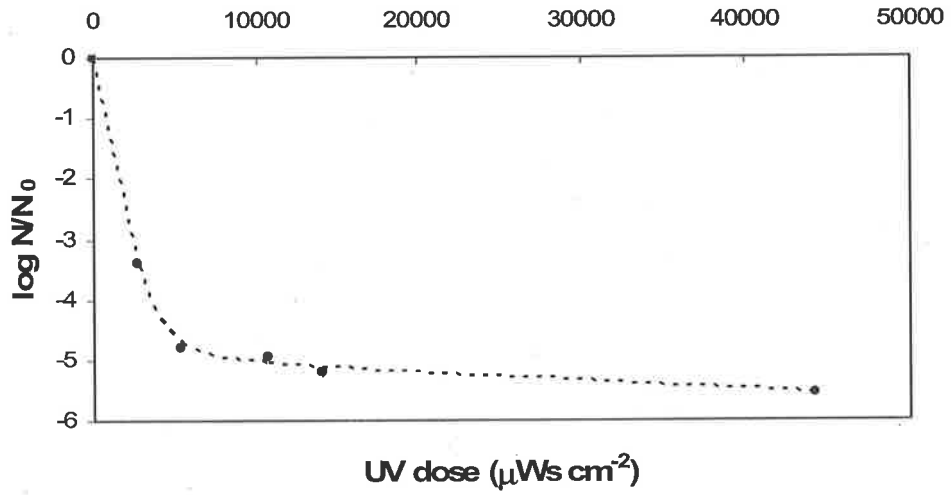

Figure M6. EDP_m model predictions for data set 6

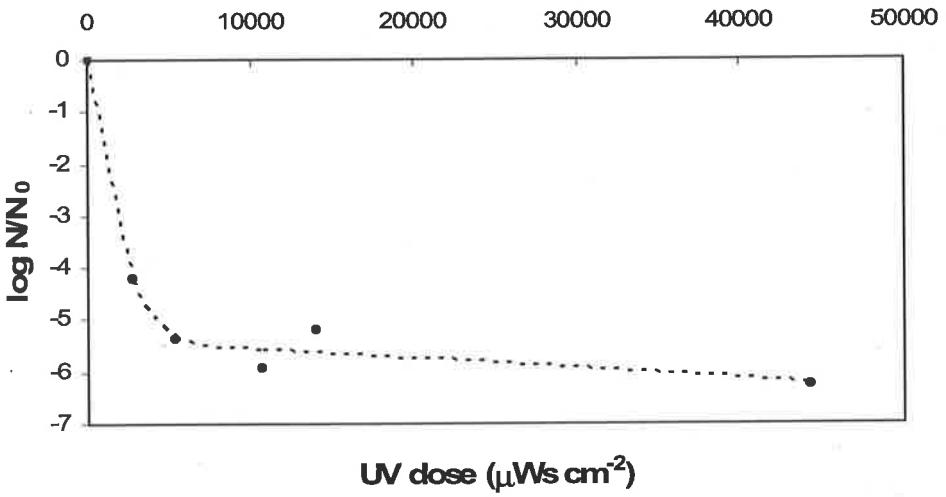

Figure M7. EDP_m model predictions for data set 7

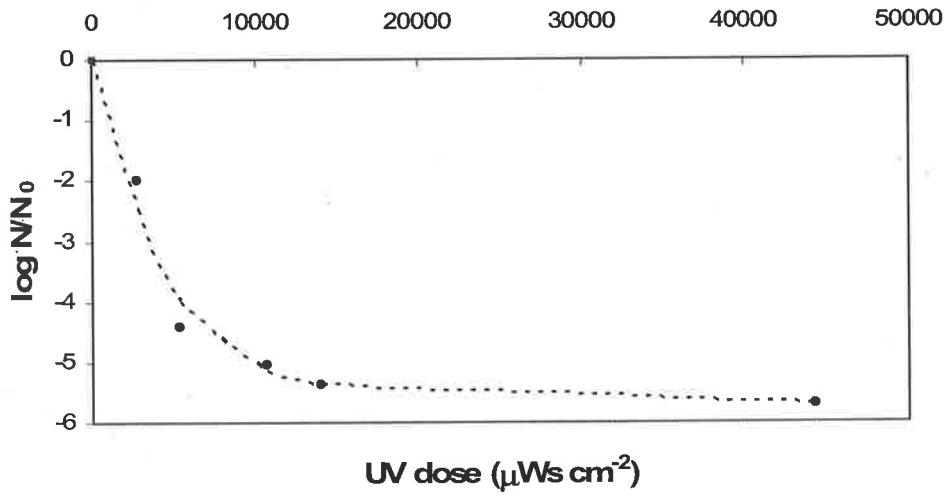

Figure M8. EDP_m model predictions for data set 8

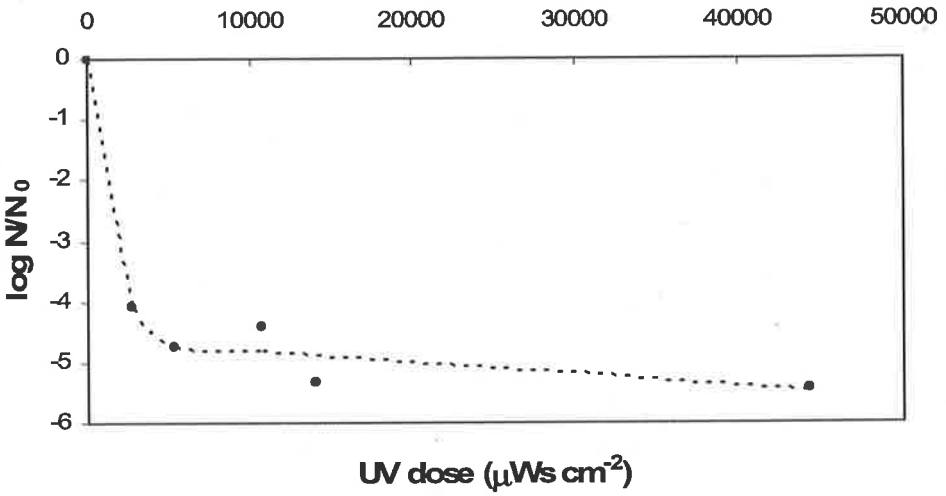

Figure M9. EDP_m model predictions for data set 9

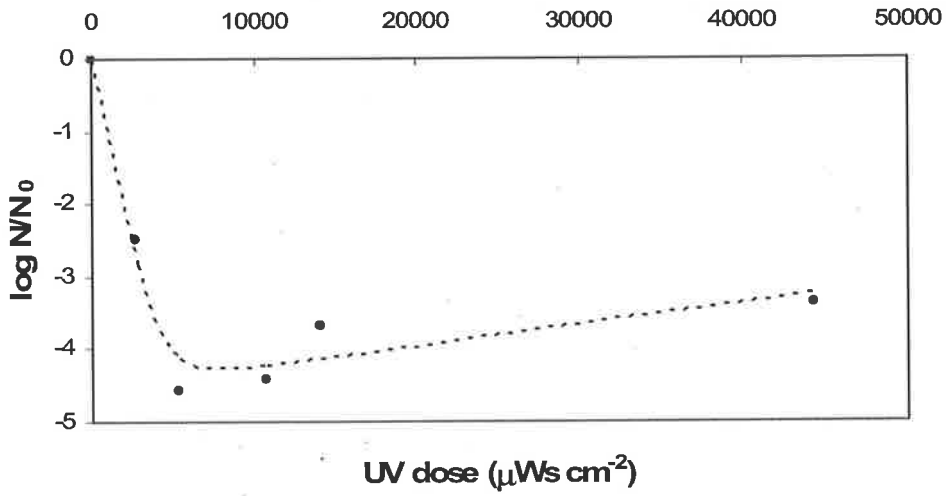

Figure M10. EDP_m model predictions for data set 10

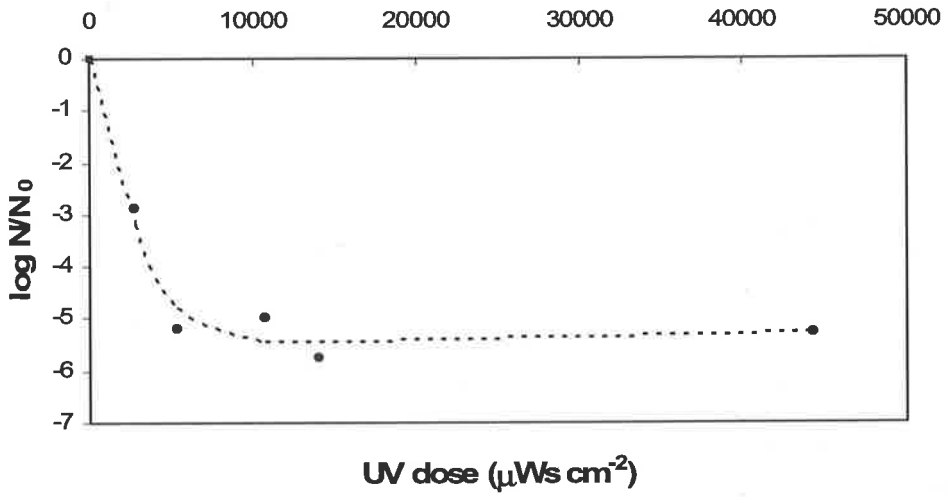

Figure M11. EDP_m model predictions for data set 11

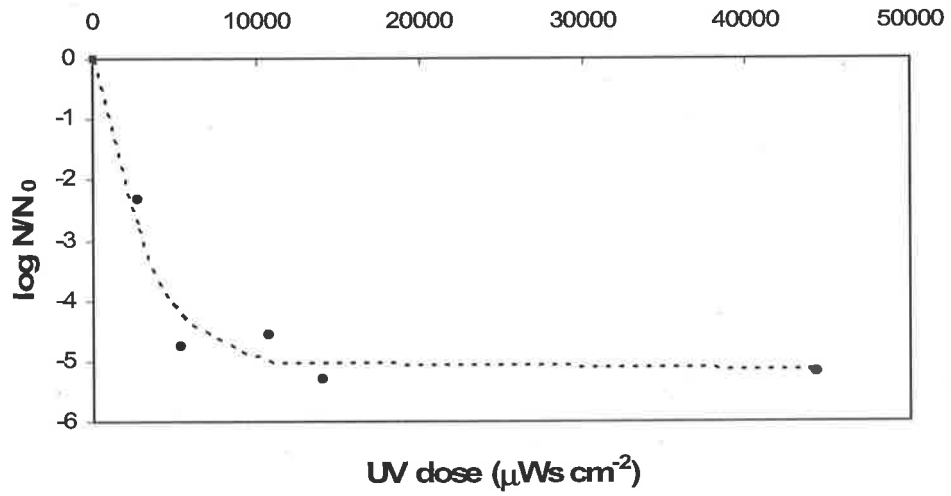

Figure M12. EDP_m model predictions for data set 12

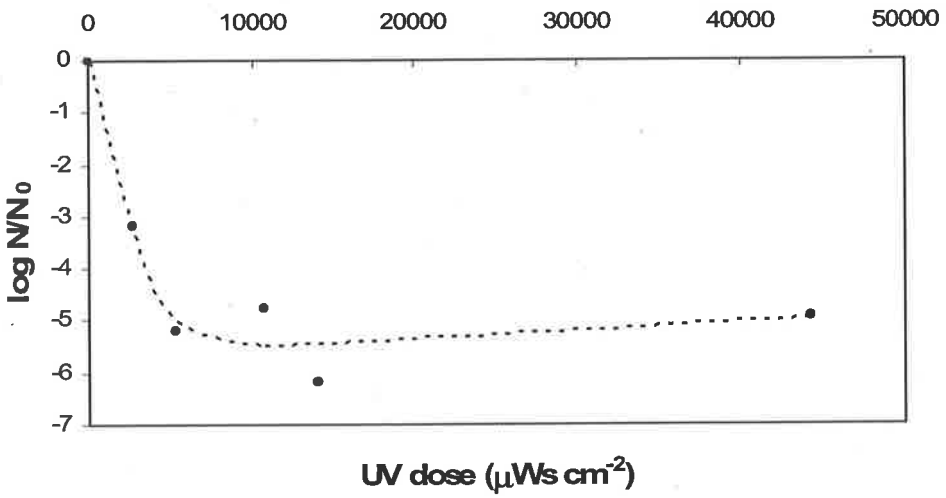

Figure M13. EDP_m model predictions for data set 13

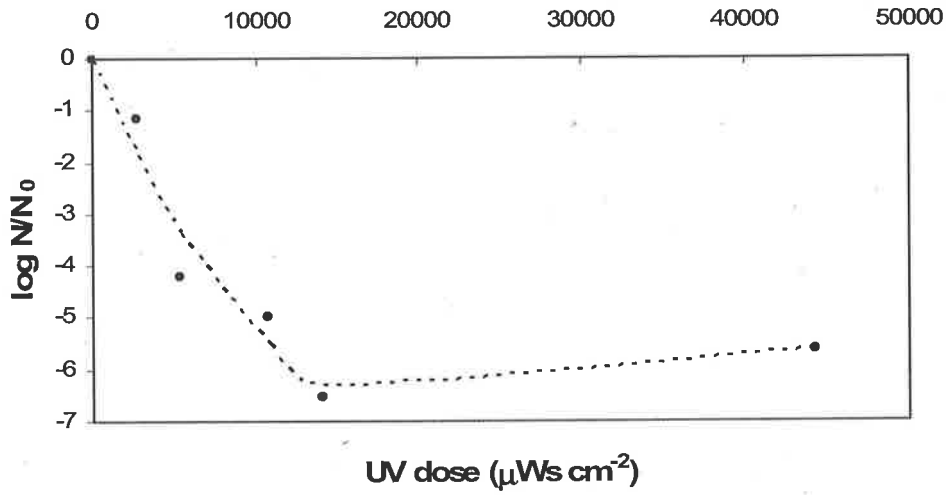

Figure M14. EDP_m model predictions for data set 14

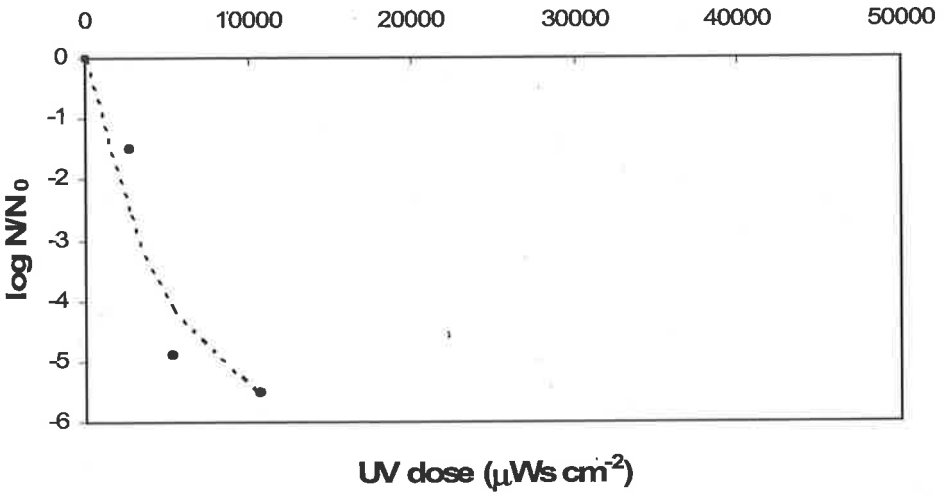

Figure M15. EDP_m model predictions for data set 15

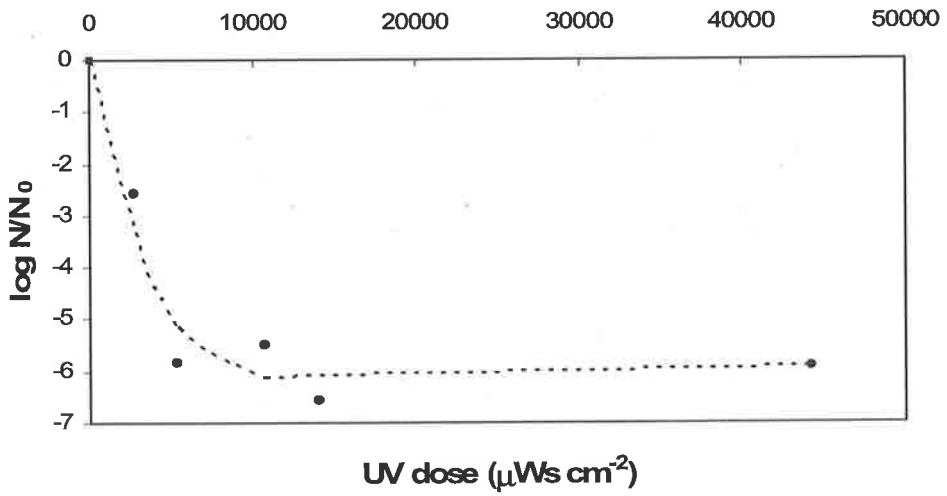

Figure M16. EDP_m model predictions for data set 16

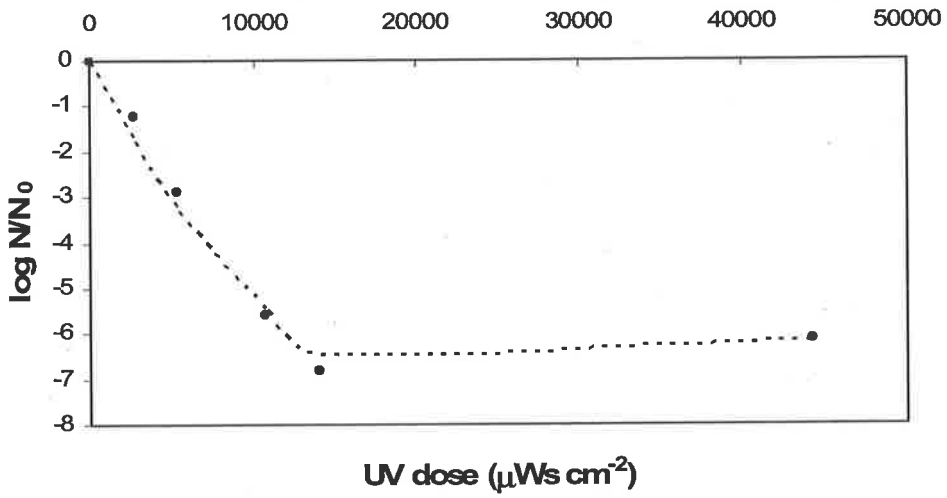

Figure M17. EDP_m model predictions for data set 17

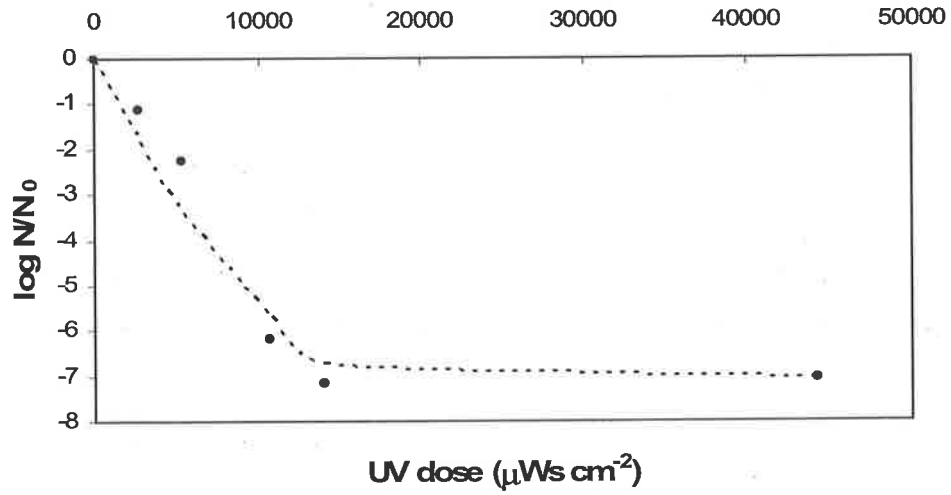

Figure M18. EDP_m model predictions for data set 18

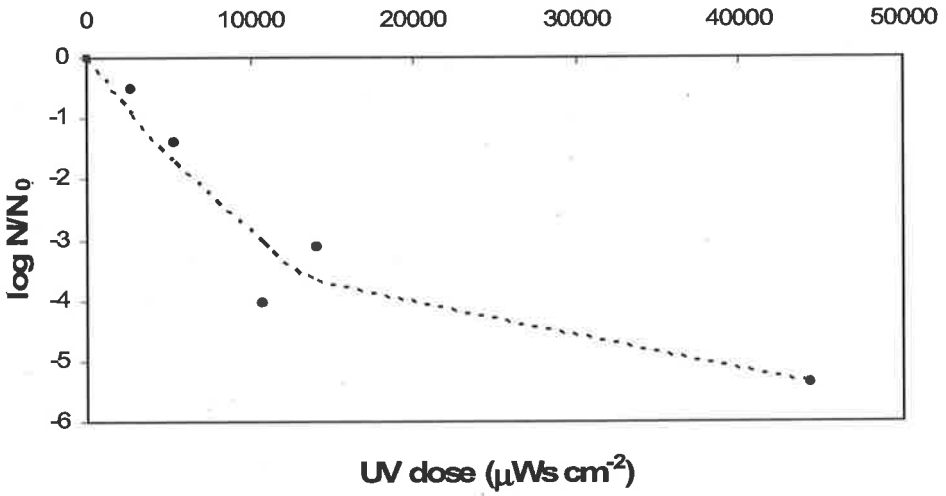

Figure M19. EDP_m model predictions for data set 19

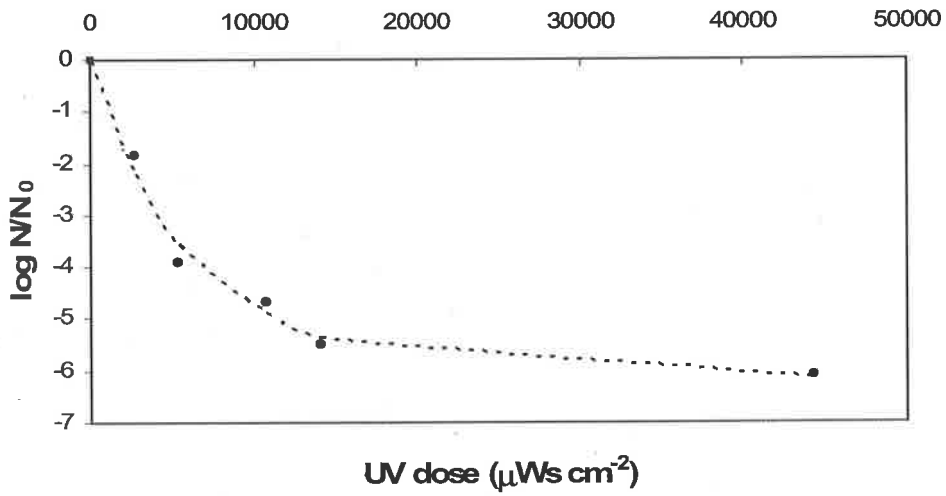

Figure M20. EDP_m model predictions for data set 20

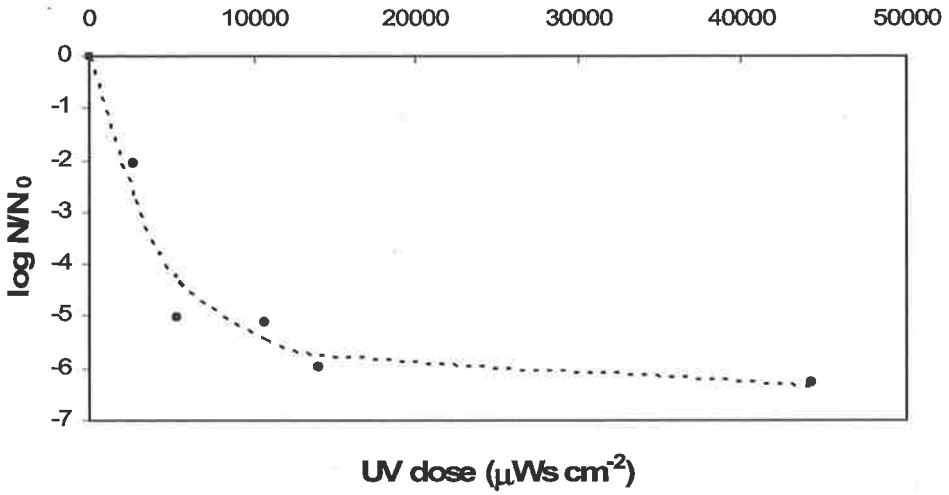

Figure M21. EDP_m model predictions for data set 21

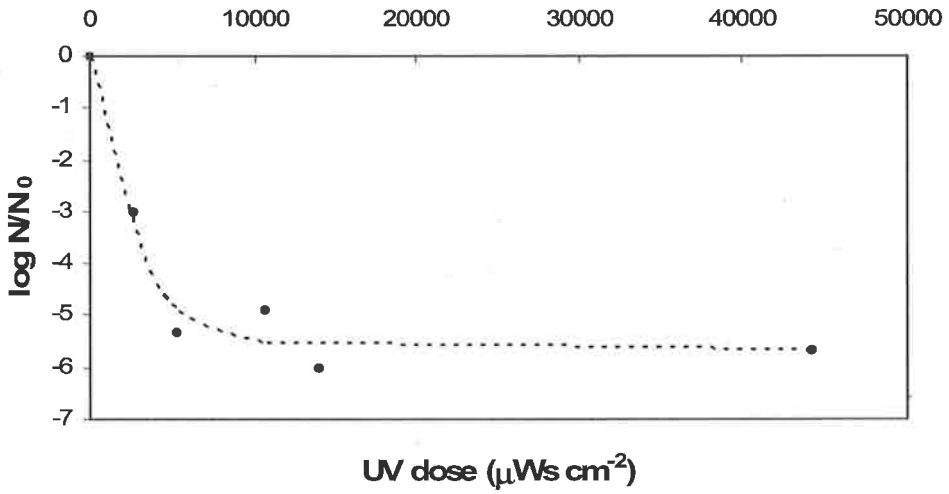

Figure M22. EDP_m model predictions for data set 22

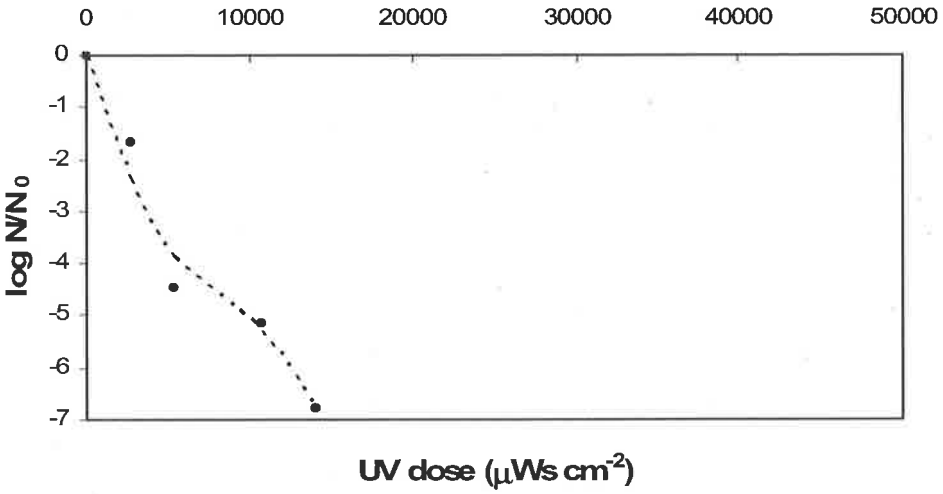

Figure M23. EDP_m model predictions for data set 23

Appendix N: Fits of the Weibull model to the experimental disinfection data

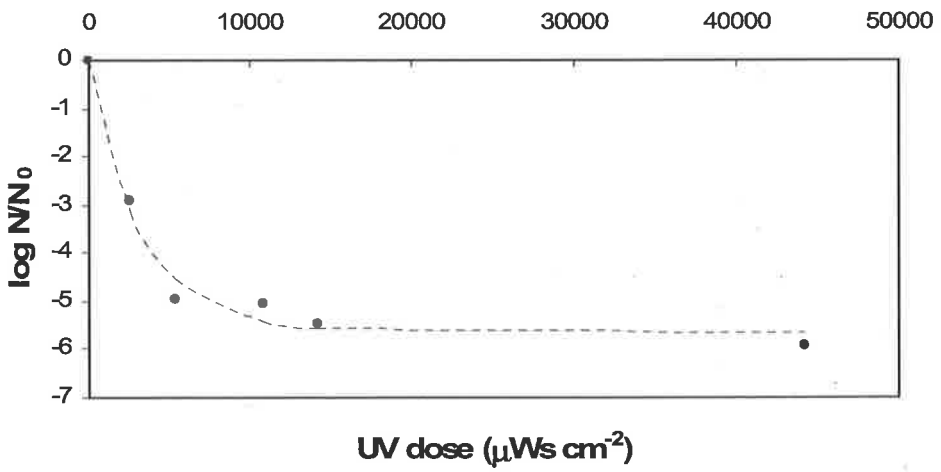

Figure N1. Weibull model predictions for data set 1

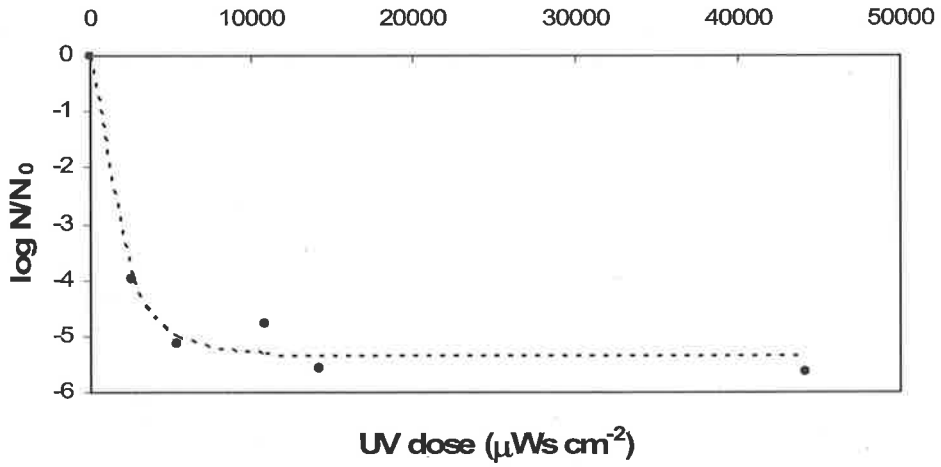

Figure N2. Weibull model predictions for data set 2

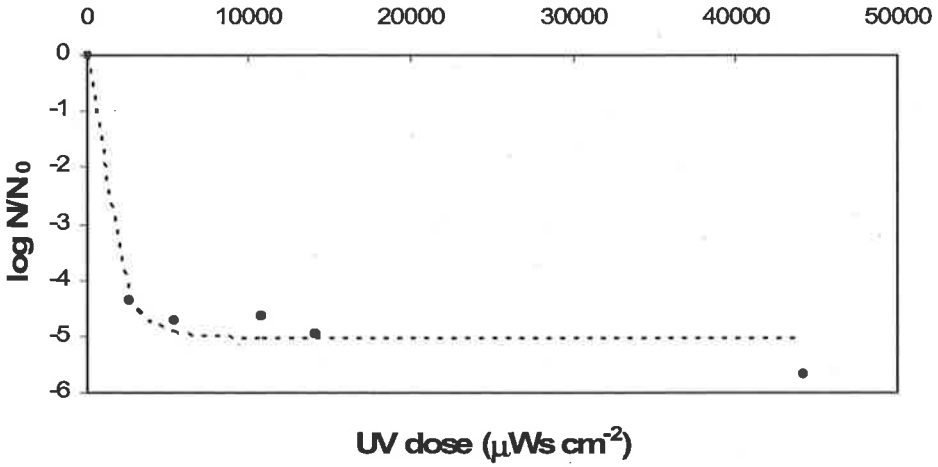

Figure N3. Weibull model predictions for data set 3

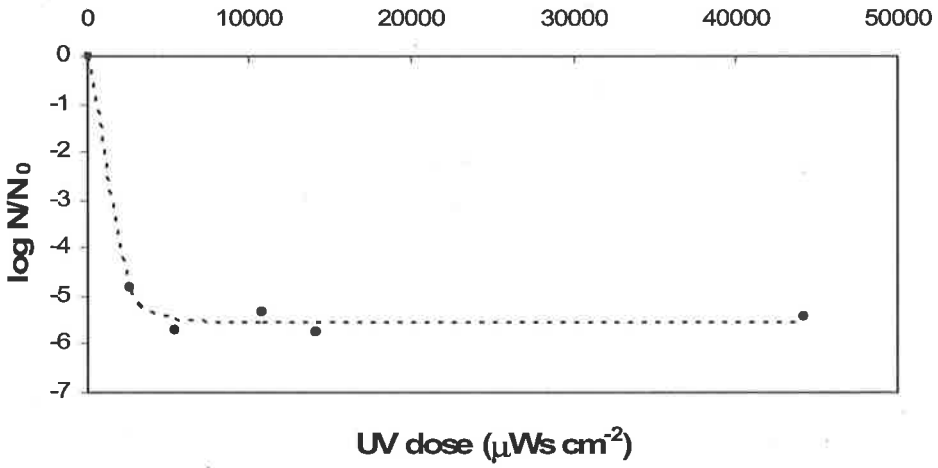

Figure N4. Weibull model predictions for data set 4

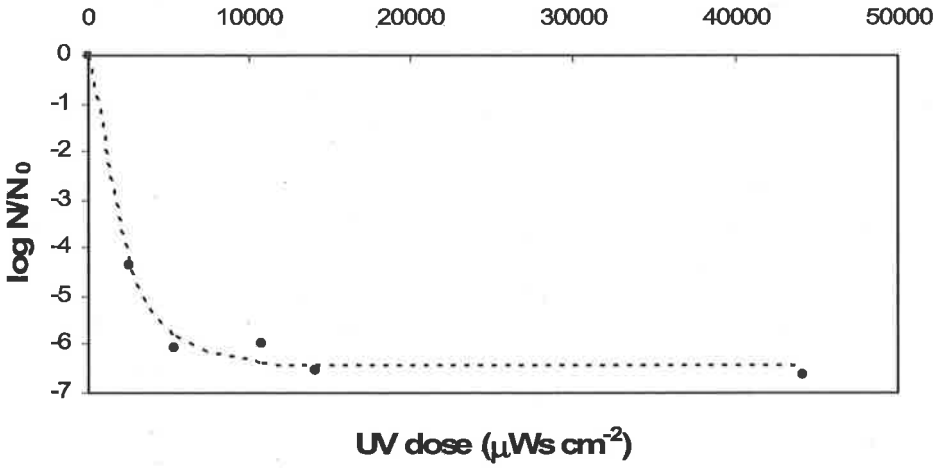

Figure N5. Weibull model predictions for data set 5

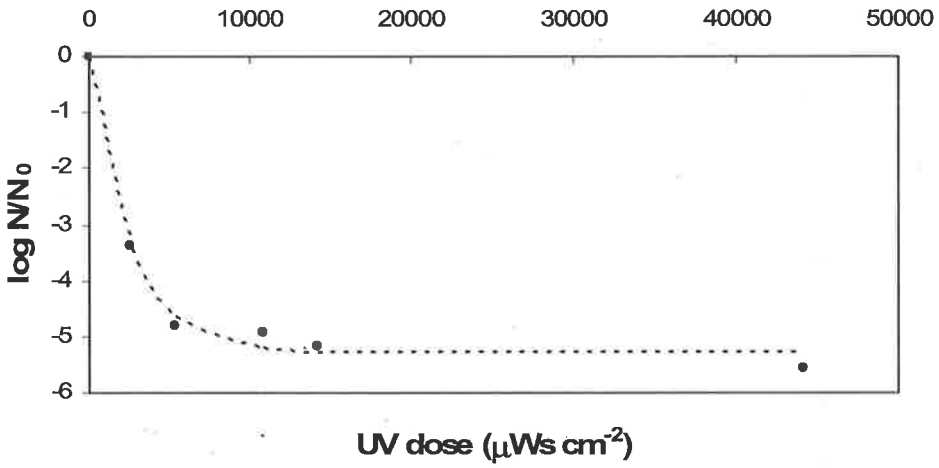

Figure N6. Weibull model predictions for data set 6

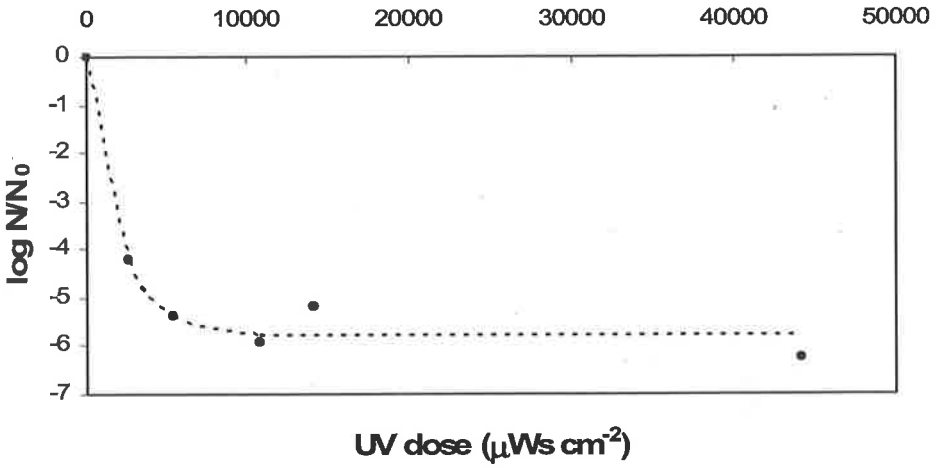

Figure N7. Weibull model predictions for data set 7

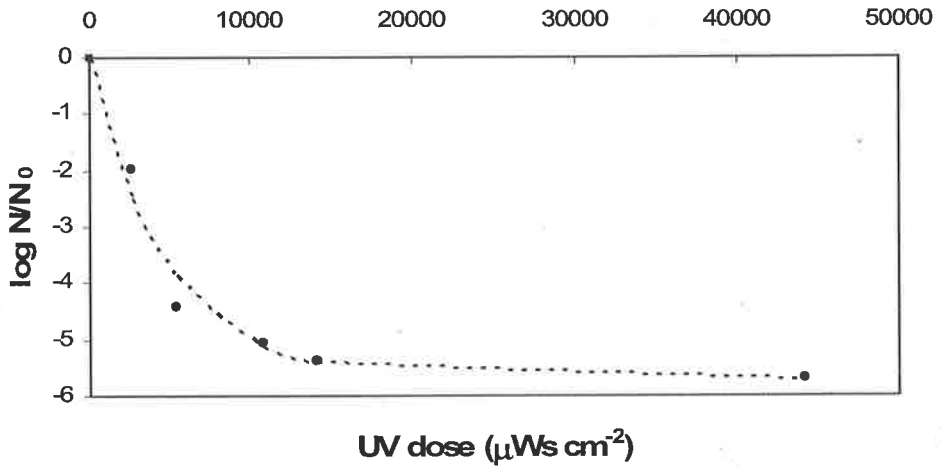

Figure N8. Weibull model predictions for data set 8

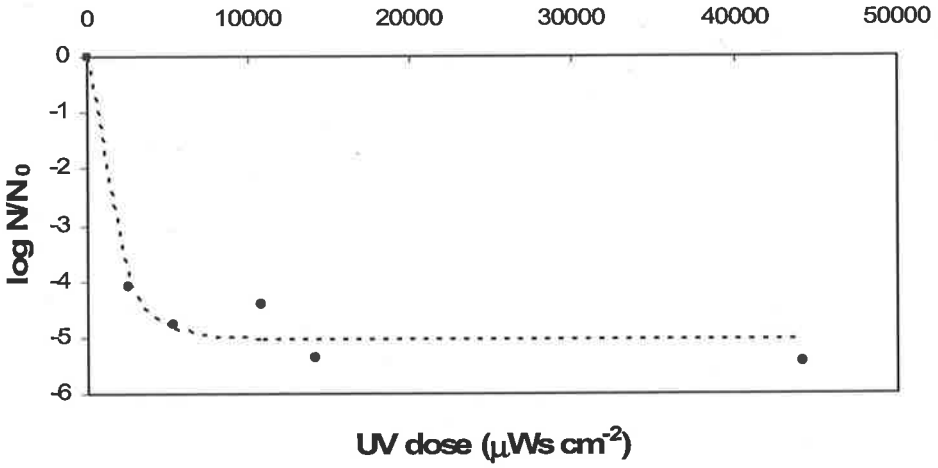

Figure N9. Weibull model predictions for data set 9

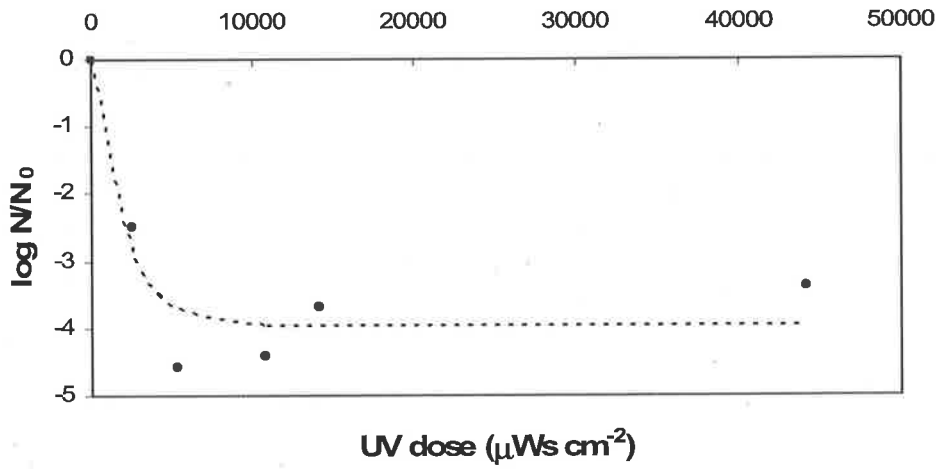

Figure N10. Weibull model predictions for data set 10

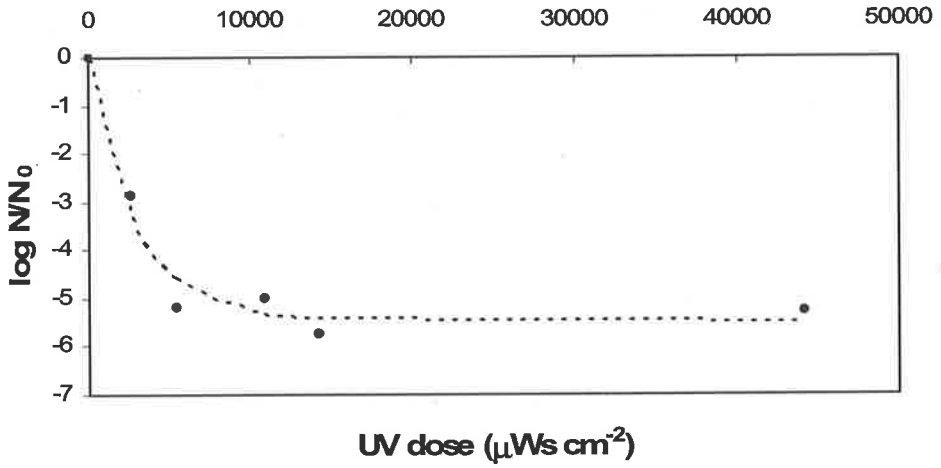

Figure N11. Weibull model predictions for data set 11

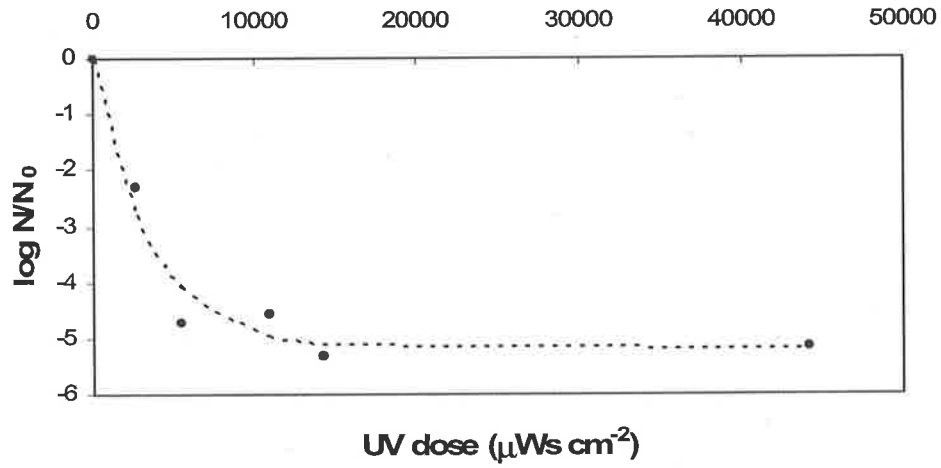

Figure N12. Weibull model predictions for data set 12

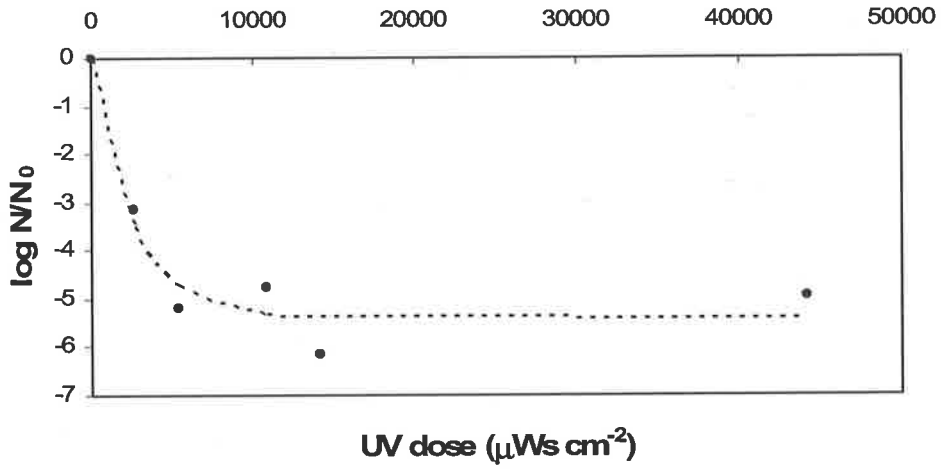

Figure N13. Weibull model predictions for data set 13

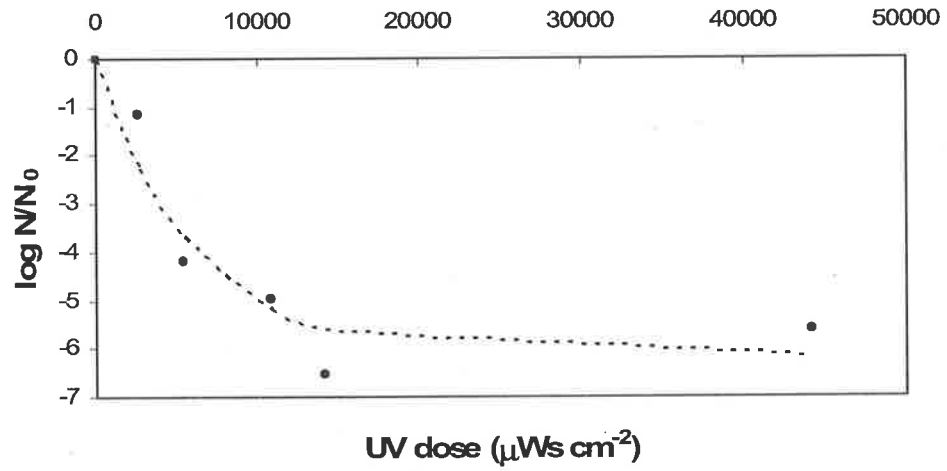

Figure N14. Weibull model predictions for data set 14

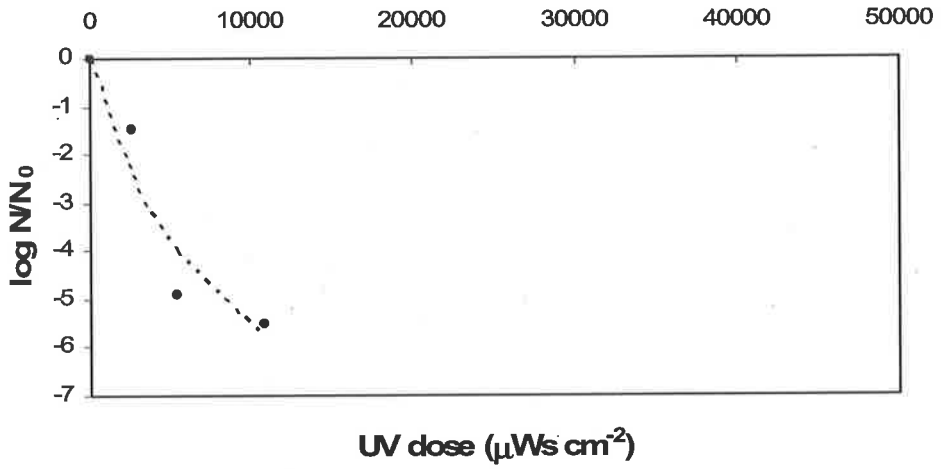

Figure N15. Weibull model predictions for data set 15

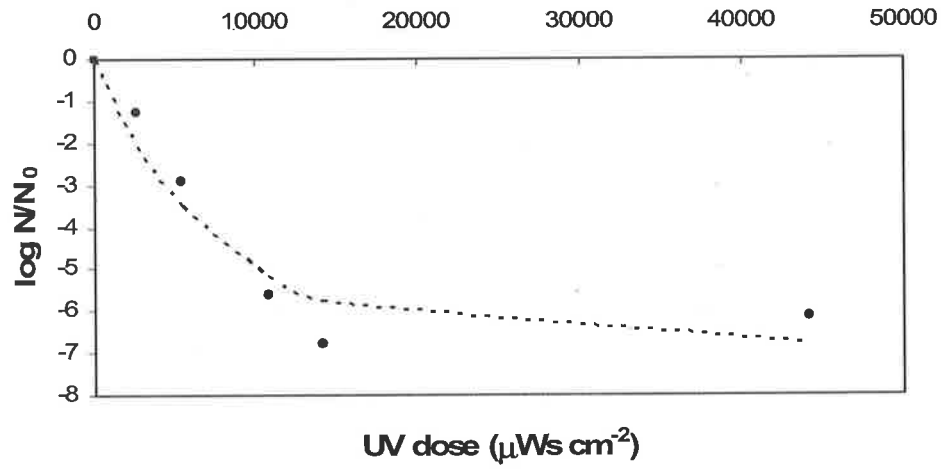

Figure N16. Weibull model predictions for data set 16

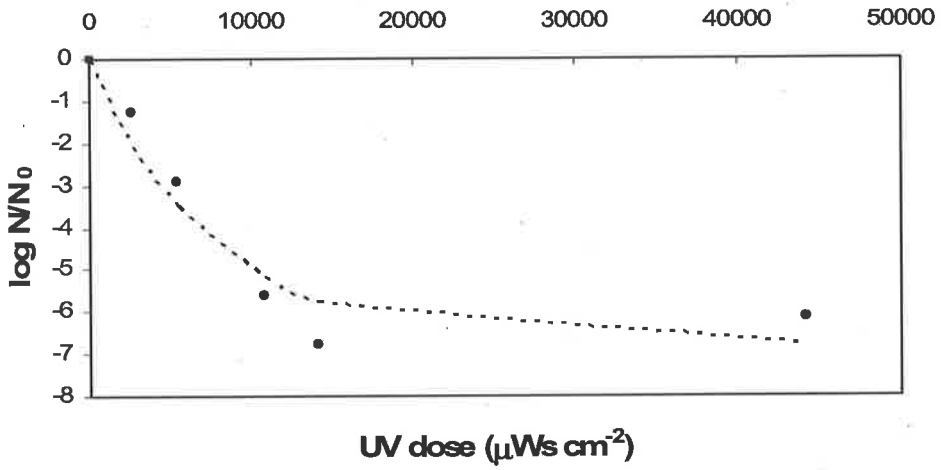

Figure N17. Weibull model predictions for data set 17

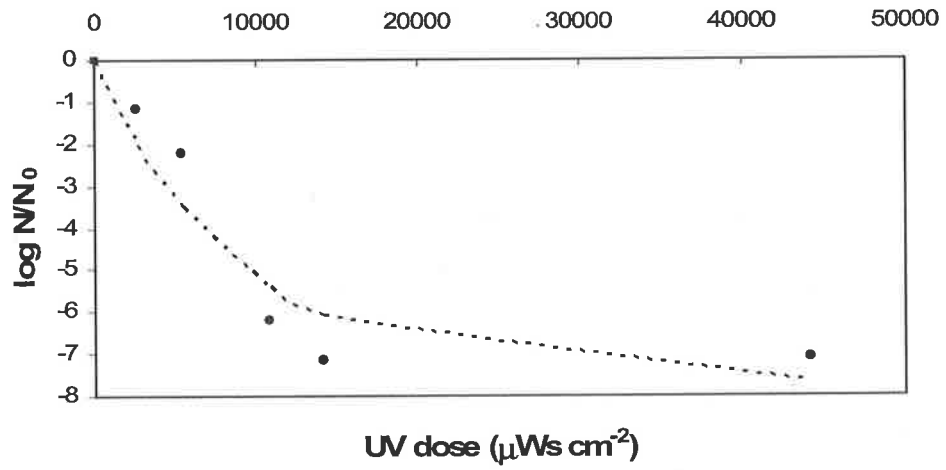

Figure N18. Weibull model predictions for data set 18

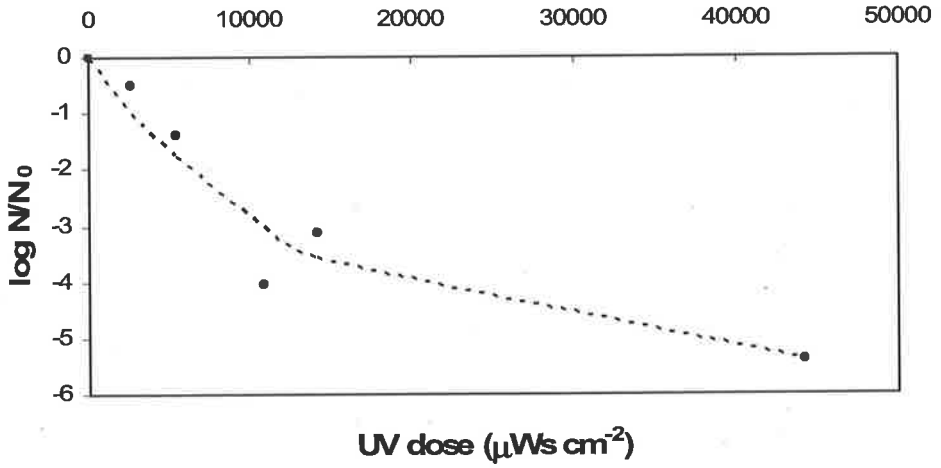

Figure N19. Weibull model predictions for data set 19

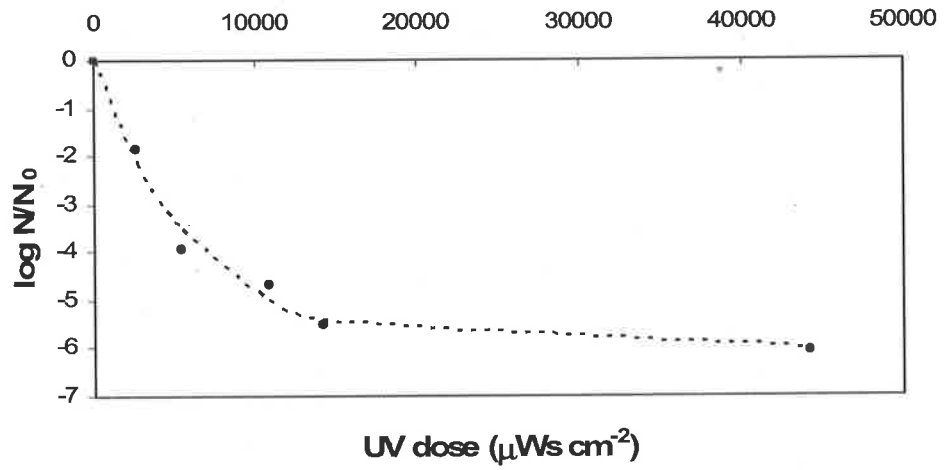

Figure N20. Weibull model predictions for data set 20

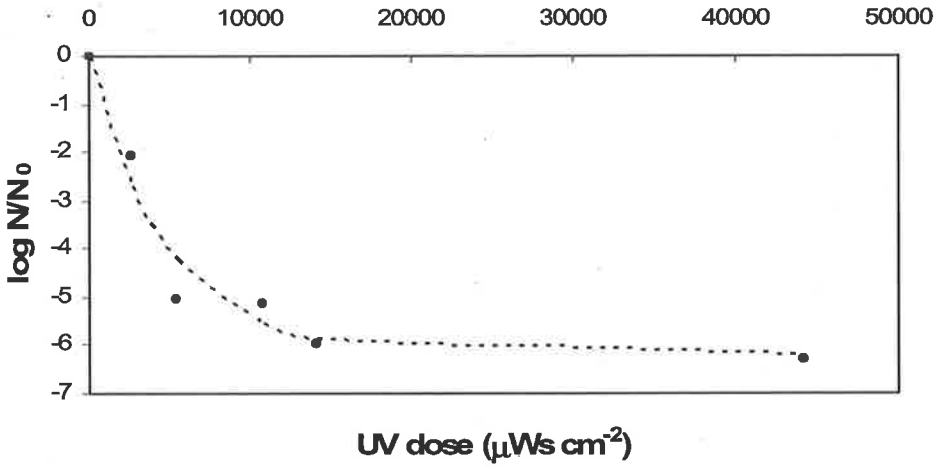

Figure N21. Weibull model predictions for data set 21

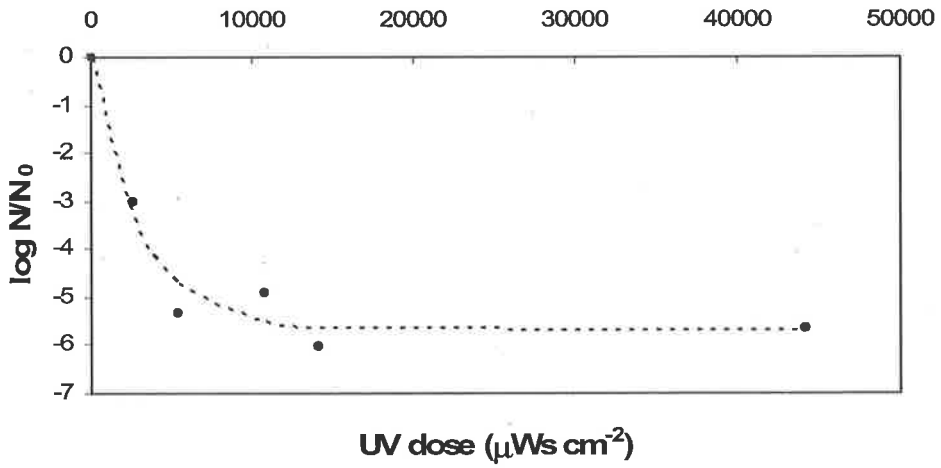

Figure N22. Weibull model predictions for data set 22

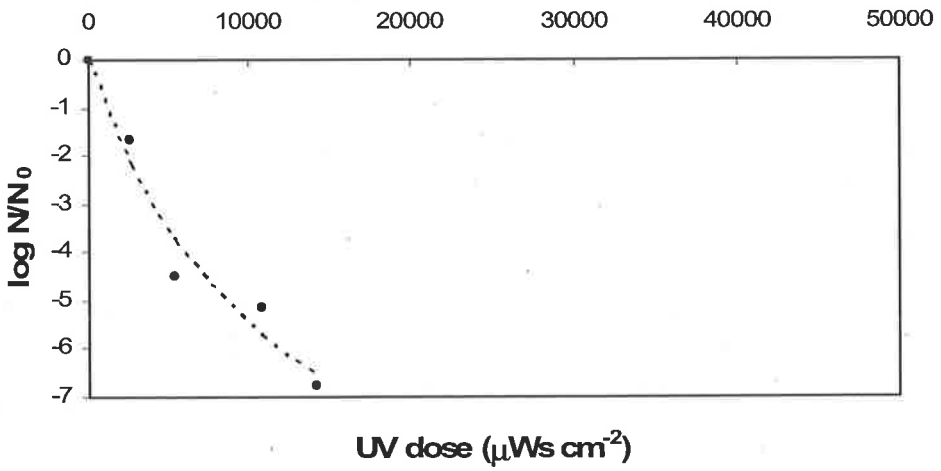

Figure N23. Weibull model predictions for data set 23

Appendix O: Experimental disinfection data

Table O.1. UV disinfection data and microbiological results

(a): data set 1

Disinfection trial	1	2	3	4	5	6
UV dose (μWs cm^{-2})	0	2700	5400	10800	14100	44200
additive	-	-	-	-	-	-
additive conc (g L^{-1})	0	0	0	0	0	0
UV trans - pre additive (%)	15	15	15	15	15	15
UV trans - post additive (%)	15	15	15	15	15	15
Temperature (^{o}C)	23	23	23	23	23	23
pH	7.03	7.03	7.03	7.03	7.03	7.03
Initial number, N_0 (mL^{-1})	2.99×10^{8}	2.99×10^{8}	2.99×10^{8}	2.99×10^{8}	2.99×10^{8}	2.99×10^{8}
Survival number, N (mL^{-1})	2.99×10^{8}	3.65×10^{5}	3.13×10^{3}	2.56×10^{3}	9.79×10^{2}	3.65×10^{2}
$\log_{10}$ (N/N_0)	0.00	-2.91	-4.98	-5.07	-5.48	-5.91

(b): data set 2

Disinfection trial	7	8	9	10	11	12
UV dose (μWs cm^{-2})	0	2700	5400	10800	14100	44200
additive	-	-	-	-	-	-
additive conc (g L^{-1})	0	0	0	0	0	0
UV trans - pre additive (%)	83	83	83	83	83	83
UV trans - post additive (%)	83	83	83	83	83	83
Temperature (^{o}C)	23	23	23	23	23	23
pH	6.91	6.91	6.91	6.91	6.91	6.91
Initial number, N_0 (mL^{-1})	1.27×10^{7}	1.27×10^{7}	1.27×10^{7}	1.27×10^{7}	1.27×10^{7}	1.27×10^{7}
Survival number, N (mL^{-1})	1.27×10^{7}	1.38×10^{3}	9.38×10^{1}	2.10×10^{2}	3.50×10^{1}	3.00×10^{1}
$\log_{10}$ (N/N_0)	0.00	-3.96	-5.13	-4.78	-5.56	-5.53

(c): data set 3

Disinfection trial	13	14	15	16	17	18
UV dose (μWs cm^{-2})	0	2700	5400	10800	14100	44200
additive	-	-	-	-	-	-
additive conc (g L^{-1})	0	0	0	0	0	0
UV trans - pre additive (%)	95	95	95	95	95	95
UV trans - post additive (%)	95	95	95	95	95	95
Temperature (^{o}C)	24	24	24	24	24	24
pH	7.26	7.26	7.26	7.26	7.26	7.26
Initial number, N_0 (mL^{-1})	6.64×10^{6}	6.64×10^{6}	6.64×10^{6}	6.64×10^{6}	6.64×10^{6}	6.64×10^{6}
Survival number, N (mL^{-1})	6.64×10^{6}	2.84×10^{2}	1.19×10^{2}	1.49×10^{2}	7.38×10^{1}	1.38×10^{1}
$\log_{10}$ (N/N_0)	0.00	-4.37	-4.75	-4.65	-4.95	-5.68

Table O.1. *continued*

(d): data set 4

Disinfection trial	19	20	21	22	23	24
UV dose (μWs cm^{-2})	0	2700	5400	10800	14100	44200
additive	coffee	coffee	coffee	coffee	coffee	coffee
additive conc (g L^{-1})	0.001	0.001	0.001	0.001	0.001	0.001
UV trans - pre bacteria (%)	98	98	98	98	98	98
UV trans - post bacteria (%)	91	91	91	91	91	91
Temperature (°C)	24	24	24	24	24	24
pH	6.84	6.84	6.84	6.84	6.84	6.84
Initial number, N_0 (mL^{-1})	3.49×10^{6}	3.49×10^{6}	3.49×10^{6}	3.49×10^{6}	3.49×10^{6}	3.49×10^{6}
Survival number, N (mL^{-1})	3.49×10^{6}	5.50×10^{1}	6.88×10^{0}	1.58×10^{1}	6.13×10^{0}	1.31×10^{1}
$\log_{10}$ (N/N_0)	0.00	-4.80	-5.71	-5.34	-5.76	-5.43

(e): data set 5

Disinfection trial	25	26	27	28	29	30
UV dose (μWs cm^{-2})	0	2700	5400	10800	14100	44200
additive	coffee	coffee	coffee	coffee	coffee	coffee
additive conc (g L^{-1})	0.005	0.005	0.005	0.005	0.005	0.005
UV trans - pre bacteria (%)	92	92	92	92	92	92
UV trans - post bacteria (%)	75	75	75	75	75	75
Temperature (°C)	25	25	25	25	25	25
pH	6.85	6.85	6.85	6.85	6.85	6.85
Initial number, N_0 (mL^{-1})	9.70×10^{6}	9.70×10^{6}	9.70×10^{6}	9.70×10^{6}	9.70×10^{6}	9.70×10^{6}
Survival number, N (mL^{-1})	9.70×10^{6}	4.48×10^{2}	8.38×10^{0}	9.75×10^{0}	2.88×10^{0}	2.38×10^{0}
$\log_{10}$ (N/N_0)	0.00	-4.34	-6.06	-6.00	-6.53	-6.61

(f): data set 6

Disinfection trial	31	32	33	34	35	36
UV dose (μWs cm^{-2})	0	2700	5400	10800	14100	44200
additive	coffee	coffee	coffee	coffee	coffee	coffee
additive conc (g L^{-1})	0.01	0.01	0.01	0.01	0.01	0.01
UV trans - pre bacteria (%)	86	86	86	86	86	86
UV trans - post bacteria (%)	65	65	65	65	65	65
Temperature (°C)	25	25	25	25	25	25
pH	6.84	6.84	6.84	6.84	6.84	6.84
Initial number, N_0 (mL^{-1})	4.96×10^{6}	4.96×10^{6}	4.96×10^{6}	4.96×10^{6}	4.96×10^{6}	4.96×10^{6}
Survival number, N (mL^{-1})	4.96×10^{6}	2.04×10^{3}	8.00×10^{1}	6.00×10^{1}	3.25×10^{1}	1.38×10^{1}
$\log_{10}$ (N/N_0)	0.00	-3.39	-4.79	-4.92	-5.18	-5.56

Table O.1. *continued*

(g): data set 7

Disinfection trial	37	38	39	40	41	42
UV dose (μWs cm^{-2})	0	2700	5400	10800	14100	44200
additive	coffee	coffee	coffee	coffee	coffee	coffee
additive conc (g L^{-1})	0.005	0.005	0.005	0.005	0.005	0.005
UV trans - pre bacteria (%)	92	92	92	92	92	92
UV trans - post bacteria (%)	74	74	74	74	74	74
Temperature (°C)	25	25	25	25	25	25
pH	6.87	6.87	6.87	6.87	6.87	6.87
Initial number, N_0 (mL^{-1})	2.06×10^6	2.06×10^6	2.06×10^6	2.06×10^6	2.06×10^6	2.06×10^6
Survival number, N (mL^{-1})	2.06×10^6	1.29×10^2	8.75×10^0	2.38×10^0	1.30×10^1	1.13×10^0
$\log_{10}$ (N/N_0)	0.00	-4.20	-5.37	-5.94	-5.20	-6.26

(h): data set 8

Disinfection trial	43	44	45	46	47	48
UV dose (μWs cm^{-2})	0	2700	5400	10800	14100	44200
additive	coffee	coffee	coffee	coffee	coffee	coffee
additive conc (g L^{-1})	0.03	0.03	0.03	0.03	0.03	0.03
UV trans - pre bacteria (%)	69	69	69	69	69	69
UV trans - post bacteria (%)	50	50	50	50	50	50
Temperature (°C)	25	25	25	25	25	25
pH	7.07	7.07	7.07	7.07	7.07	7.07
Initial number, N_0 (mL^{-1})	2.74×10^7	2.74×10^7	2.74×10^7	2.74×10^7	2.74×10^7	2.74×10^7
Survival number, N (mL^{-1})	2.74×10^7	2.92×10^5	1.08×10^3	2.50×10^2	1.18×10^2	5.50×10^1
$\log_{10}$ (N/N_0)	0.00	-1.97	-4.40	-5.04	-5.37	-5.70

(i): data set 9

Disinfection trial	49	50	51	52	53	54
UV dose (μWs cm^{-2})	0	2700	5400	10800	14100	44200
additive	Celite	Celite	Celite	Celite	Celite	Celite
additive conc (g L^{-1})	0.1	0.1	0.1	0.1	0.1	0.1
UV trans - pre additive (%)	-	-	-	-	-	-
UV trans - both (%)	63	63	63	63	63	63
Temperature (°C)	25	25	25	25	25	25
pH	7.81	7.81	7.81	7.81	7.81	7.81
Initial number, N_0 (mL^{-1})	2.78×10^6	2.78×10^6	2.78×10^6	2.78×10^6	2.78×10^6	2.78×10^6
Survival number, N (mL^{-1})	2.78×10^6	2.28×10^2	4.88×10^1	1.10×10^2	1.25×10^1	1.00×10^1
$\log_{10}$ (N/N_0)	0.00	-4.09	-4.76	-4.4	-5.35	-5.44

Table O.1. *continued*

(j): data set 10

Disinfection trial	55	56	57	58	59	60
UV dose (μWs cm^{-2})	0	2700	5400	10800	14100	44200
additive	Celite	Celite	Celite	Celite	Celite	Celite
additive conc (g L^{-1})	0.5	0.5	0.5	0.5	0.5	0.5
UV trans - pre additive (%)	58	58	58	58	58	58
UV trans - post additive (%)	42	42	42	42	42	42
Temperature (°C)	25	25	25	25	25	25
pH	7.82	7.82	7.82	7.82	7.82	7.82
Initial number, N_0 (mL^{-1})	2.07×10^7	2.07×10^7	2.07×10^7	2.07×10^7	2.07×10^7	2.07×10^7
Survival number, N (mL^{-1})	2.07×10^7	6.66×10^4	5.49×10^2	8.11×10^2	4.30×10^3	8.70×10^3
$\log_{10}$ (N/N_0)	0.00	-2.49	-4.58	-4.41	-3.68	-3.38

(k): data set 11

Disinfection trial	61	62	63	64	65	66
UV dose (μWs cm^{-2})	0	2700	5400	10800	14100	44200
additive	Celite	Celite	Celite	Celite	Celite	Celite
additive conc (g L^{-1})	0.5	0.5	0.5	0.5	0.5	0.5
UV trans - pre additive (%)	62	62	62	62	62	62
UV trans - post additive (%)	43	43	43	43	43	43
Temperature (°C)	26	26	26	26	26	26
pH	7.81	7.81	7.81	7.81	7.81	7.81
Initial number, N_0 (mL^{-1})	9.45×10^7	9.45×10^7	9.45×10^7	9.45×10^7	9.45×10^7	9.45×10^7
Survival number, N (mL^{-1})	9.45×10^7	1.31×10^5	6.26×10^2	9.58×10^2	1.64×10^2	4.88×10^2
$\log_{10}$ (N/N_0)	0.00	-2.86	-5.18	-4.99	-5.76	-5.29

(l): data set 12

Disinfection trial	67	68	69	70	71	72
UV dose (μWs cm^{-2})	0	2700	5400	10800	14100	44200
additive	Celite	Celite	Celite	Celite	Celite	Celite
additive conc (g L^{-1})	0.7	0.7	0.7	0.7	0.7	0.7
UV trans - pre additive (%)	53	53	53	53	53	53
UV trans - post additive (%)	27	27	27	27	27	27
Temperature (°C)	26	26	26	26	26	26
pH	7.46	7.46	7.46	7.46	7.46	7.46
Initial number, N_0 (mL^{-1})	1.19×10^8	1.19×10^8	1.19×10^8	1.19×10^8	1.19×10^8	1.19×10^8
Survival number, N (mL^{-1})	1.19×10^8	5.65×10^5	2.21×10^3	3.35×10^3	5.81×10^2	7.89×10^2
$\log_{10}$ (N/N_0)	0.00	-2.32	-4.73	-4.55	-5.31	-5.18

Table O.1. *continued*

(m): data set 13

Disinfection trial	73	74	75	76	77	78
UV dose (μWs cm^{-2})	0	2700	5400	10800	14100	44200
additive	Celite	Celite	Celite	Celite	Celite	Celite
additive conc (g L^{-1})	0.3	0.3	0.3	0.3	0.3	0.3
UV trans - pre additive (%)	60	60	60	60	60	60
UV trans - post additive (%)	47	47	47	47	47	47
Temperature (°C)	26	26	26	26	26	26
pH	7.42	7.42	7.42	7.42	7.42	7.42
Initial number, N_0 (mL^{-1})	1.05×10^8	1.05×10^8	1.05×10^8	1.05×10^8	1.05×10^8	1.05×10^8
Survival number, N (mL^{-1})	1.05×10^8	7.03×10^4	6.71×10^2	1.75×10^3	7.00×10^1	1.19×10^3
$\log_{10}$ (N/N_0)	0.00	-3.17	-5.19	-4.78	-6.18	-4.95

(n): data set 14

Disinfection trial	79	80	81	82	83	84
UV dose (μWs cm^{-2})	0	2700	5400	10800	14100	44200
additive	Celite	Celite	Celite	Celite	Celite	Celite
additive conc (g L^{-1})	0.3	0.3	0.3	0.3	0.3	0.3
UV trans - pre additive (%)	53	53	53	53	53	53
UV trans - post additive (%)	42	42	42	42	42	42
Temperature (°C)	24	24	24	24	24	24
pH	6.74	6.74	6.74	6.74	6.74	6.74
Initial number, N_0 (mL^{-1})	2.60×10^7	2.60×10^7	2.60×10^7	2.60×10^7	2.60×10^7	2.60×10^7
Survival number, N (mL^{-1})	2.60×10^7	1.81×10^6	1.66×10^3	2.85×10^2	7.50×10^0	6.25×10^1
$\log_{10}$ (N/N_0)	0.00	-1.16	-4.19	-4.96	-6.54	-5.62

(o): data set 15

Disinfection trial	85	86	87	88	89	90
UV dose (μWs cm^{-2})	0	2700	5400	10800	14100	44200
additive	Celite	Celite	Celite	Celite	Celite	Celite
additive conc (g L^{-1})	0.5	0.5	0.5	0.5	0.5	0.5
UV trans - pre additive (%)	54	54	54	54	54	54
UV trans - post additive (%)	36	36	36	36	36	36
Temperature (°C)	24	24	24	24	24	24
pH	6.88	6.88	6.88	6.88	6.88	6.88
Initial number, N_0 (mL^{-1})	5.80×10^7	5.80×10^7	5.80×10^7	5.80×10^7	5.80×10^7	5.80×10^7
Survival number, N (mL^{-1})	5.80×10^7	1.83×10^6	7.13×10^2	1.73×10^2	-	-
$\log_{10}$ (N/N_0)	0.00	-1.5	-4.91	-5.53	-	-

Table O.1. *continued*

(p): data set 16

Disinfection trial	91	92	93	94	95	96
UV dose (μWs cm^{-2})	0	2700	5400	10800	14100	44200
additive	coffee	coffee	coffee	coffee	coffee	coffee
additive conc (g L^{-1})	0.005	0.005	0.005	0.005	0.005	0.005
UV trans - pre additive (%)	76	76	76	76	76	76
UV trans - post additive (%)	71	71	71	71	71	71
Temperature (°C)	23	23	23	23	23	23
pH	5.77	5.77	5.77	5.77	5.77	5.77
Initial number, N_0 (mL^{-1})	5.58×10^{7}	5.58×10^{7}	5.58×10^{7}	5.58×10^{7}	5.58×10^{7}	5.58×10^{7}
Survival number, N (mL^{-1})	5.58×10^{7}	1.53×10^{5}	8.00×10^{1}	1.74×10^{2}	1.50×10^{1}	6.63×10^{1}
$\log_{10}$ (N/N_0)	0.00	-2.56	-5.84	-5.51	-6.57	-5.93

(q): data set 17

Disinfection trial	97	98	99	100	101	102
UV dose (μWs cm^{-2})	0	2700	5400	10800	14100	44200
additive	coffee	coffee	coffee	coffee	coffee	coffee
additive conc (g L^{-1})	0.03	0.03	0.03	0.03	0.03	0.03
UV trans - pre additive (%)	59	59	59	59	59	59
UV trans - post additive (%)	47	47	47	47	47	47
Temperature (°C)	23	23	23	23	23	23
pH	5.71	5.71	5.71	5.71	5.71	5.71
Initial number, N_0 (mL^{-1})	1.60×10^{8}	1.60×10^{8}	1.60×10^{8}	1.60×10^{8}	1.60×10^{8}	1.60×10^{8}
Survival number, N (mL^{-1})	1.60×10^{8}	9.07×10^{6}	1.97×10^{5}	3.89×10^{2}	2.50×10^{1}	1.21×10^{2}
$\log_{10}$ (N/N_0)	0.00	-1.25	-2.91	-5.61	-6.81	-6.12

(r): data set 18

Disinfection trial	103	104	105	106	107	108
UV dose (μWs cm^{-2})	0	2700	5400	10800	14100	44200
additive	coffee	coffee	coffee	coffee	coffee	coffee
additive conc (g L^{-1})	0.05	0.05	0.05	0.05	0.05	0.05
UV trans - pre additive (%)	77	77	77	77	77	77
UV trans - post additive (%)	37	37	37	37	37	37
Temperature (°C)	26	26	26	26	26	26
pH	4.83	4.83	4.83	4.83	4.83	4.83
Initial number, N_0 (mL^{-1})	1.03×10^{9}	1.03×10^{9}	1.03×10^{9}	1.03×10^{9}	1.03×10^{9}	1.03×10^{9}
Survival number, N (mL^{-1})	1.03×10^{9}	7.47×10^{7}	5.96×10^{6}	6.90×10^{2}	7.00×10^{1}	8.63×10^{1}
$\log_{10}$ (N/N_0)	0.00	-1.14	-2.24	-6.17	-7.17	-7.08

Table O.1. *continued*

(s): data set 19

Disinfection trial	109	110	111	112	113	114
UV dose (μWs cm^{-2})	0	2700	5400	10800	14100	44200
additive	coffee	coffee	coffee	coffee	coffee	coffee
additive conc (g L^{-1})	0.07	0.07	0.07	0.07	0.07	0.07
UV trans - pre additive (%)	78	78	78	78	78	78
UV trans - post additive (%)	28	28	28	28	28	28
Temperature (°C)	26	26	26	26	26	26
pH	4.61	4.61	4.61	4.61	4.61	4.61
Initial number, N_0 (mL^{-1})	1.41×10^8	1.41×10^8	1.41×10^8	1.41×10^8	1.41×10^8	1.41×10^8
Survival number, N (mL^{-1})	1.41×10^8	4.42×10^7	5.69×10^6	1.30×10^4	1.06×10^5	5.74×10^2
$\log_{10}$ (N/N_0)	0.00	-0.50	-1.39	-4.04	-3.12	-5.39

(t): data set 20

Disinfection trial	115	116	117	118	119	120
UV dose (μWs cm^{-2})	0	2700	5400	10800	14100	44200
additive	Celite	Celite	Celite	Celite	Celite	Celite
additive conc (g L^{-1})	0.7	0.7	0.7	0.7	0.7	0.7
UV trans - pre additive (%)	75	75	75	75	75	75
UV trans - post additive (%)	42	42	42	42	42	42
Temperature (°C)	23	23	23	23	23	23
pH	6.02	6.02	6.02	6.02	6.02	6.02
Initial number, N_0 (mL^{-1})	8.89×10^7	8.89×10^7	8.89×10^7	8.89×10^7	8.89×10^7	8.89×10^7
Survival number, N (mL^{-1})	8.89×10^7	1.21×10^6	1.05×10^4	1.90×10^3	2.81×10^2	7.25×10^1
$\log_{10}$ (N/N_0)	0.00	-1.87	-3.93	-4.67	-5.50	-6.09

(u): data set 21

Disinfection trial	121	122	123	124	125	126
UV dose (μWs cm^{-2})	0	2700	5400	10800	14100	44200
additive	Celite	Celite	Celite	Celite	Celite	Celite
additive conc (g L^{-1})	0.3	0.3	0.3	0.3	0.3	0.3
UV trans - pre additive (%)	76	76	76	76	76	76
UV trans - post additive (%)	57	57	57	57	57	57
Temperature (°C)	23	23	23	23	23	23
pH	5.96	5.96	5.96	5.96	5.96	5.96
Initial number, N_0 (mL^{-1})	7.02×10^7	7.02×10^7	7.02×10^7	7.02×10^7	7.02×10^7	7.02×10^7
Survival number, N (mL^{-1})	7.02×10^7	6.07×10^5	6.48×10^2	5.29×10^2	7.25×10^1	3.63×10^1
$\log_{10}$ (N/N_0)	0.00	-2.06	-5.03	-5.12	-5.99	-6.29

Table O.1. *continued*

(v): data set 22

Disinfection trial	127	128	129	130	131	132
UV dose (μWs cm^{-2})	0	2700	5400	10800	14100	44200
additive	-	-	-	-	-	-o
additive conc (g L^{-1})	0	0	0	0	0	0
UV trans - pre additive (%)	70	70	70	70	70	70
UV trans - post additive (%)	70	70	70	70	70	70
Temperature (^{o}C)	23	23	23	23	23	23
pH	6.81	6.81	6.81	6.81	6.81	6.81
Initial number, N_0 (mL^{-1})	7.58×10^{7}	7.58×10^{7}	7.58×10^{7}	7.58×10^{7}	7.58×10^{7}	7.58×10^{7}
Survival number, N (mL^{-1})	7.58×10^{7}	7.41×10^{4}	3.73×10^{2}	9.35×10^{2}	7.50×10^{1}	1.61×10^{2}
$\log_{10}$ (N/N_0)	0.00	-3.01	-5.31	-4.91	-6.00	-5.67

(w): data set 23

Disinfection trial	133	134	135	136	137	138
UV dose (μWs cm^{-2})	0	2700	5400	10800	14100	44200
additive	Celite	Celite	Celite	Celite	Celite	Celite
additive conc (g L^{-1})	0.3	0.3	0.3	0.3	0.3	0.3
UV trans - pre additive (%)	56	56	56	56	56	56
UV trans - post additive (%)	42	42	42	42	42	42
Temperature (^{o}C)	24	24	24	24	24	24
pH	6.49	6.49	6.49	6.49	6.49	6.49
Initial number, N_0 (mL^{-1})	8.51×10^{7}	8.51×10^{7}	8.51×10^{7}	8.51×10^{7}	8.51×10^{7}	8.51×10^{7}
Survival number, N (mL^{-1})	8.51×10^{7}	1.75×10^{6}	2.84×10^{3}	6.04×10^{2}	1.38×10^{1}	-
$\log_{10}$ (N/N_0)	0.00	-1.69	-4.48	-5.15	-6.79	-

NOTATION:

C_i	model coefficients (*see* Equations 3.1 and 3.4)
c_i	coefficients for expanded Square-Root model (*see* Equations 3.2a through 3.2e)
a,b	empirical constants (*see* Equation 2.16)
c,m	empirical constants (*see* Equations 2.14 and 2.15)
k	rate coefficient for disinfection (μWs^{-1} cm^2 or mWs^{-1} cm^2)
k'	rate coefficient for disinfection in the tail of survivor data predicted by the EDP_m model (μWs^{-1} cm^2 or mWs^{-1} cm^2)
k_0	rate of disinfection at zero dose (μWs^{-1} cm^2 or mWs^{-1} cm^2)
k_T	rate of disinfection at UV dose of 44,200 μWs cm^{-2} predicted by Weibull model (μWs^{-1} cm^2 or mWs^{-1} cm^2)
EDP	exponentially damped polynomial
EDP_m	modified exponentially damped polynomial
c	predicted disinfection at breakpoint dose (as $\log_{10}$ reductions)
n	number of data
N	number of viable cells following UV (cells mL^{-1} or MPN per 100mL)
N_0	number of viable cells present prior to UV (cells mL^{-1} or MPN per 100mL)
N_p	Particle associated viable cell concentration following UV (cells mL^{-1} or MPN per 100mL)
N_D	number of disperse viable cells present prior to UV (cells mL^{-1} or MPN per 100mL)
$\overline{N_P}$	number of particles containing at least one viable cell prior to UV

N_T	number of terms in a model
N_L	number of point source elements in UV lamp
T	threshold number in series event and multi-target kinetics
$[C_{agent}]$	shielding of absorbing agent concentration (g L^{-1})
$[dose]$	UV dose = $I\,t$ (μWs cm^{-2} or mWs cm^{-2})
$[dose]_B$	breakpoint (UV) dose (μWs cm^{-2} or mWs cm^{-2})
I	UV intensity (μW cm^{-2})
I_0	UV intensity at lamp surface (μW cm^{-2})
$\bar{I}$	Average UV intensity (μW cm^{-2})
R	distance from UV lamp (cm)
S	lamp output (W)
u	water velocity (cm s^{-1})
x	average distance travelled by UV exposed water element (cm)
L	length of UV lamp (cm)
E	dispersion coefficient (cm^2 s^{-1})
d	tube diameter (cm)
SS	suspended solids concentration (mg L^{-1})
$\%T$	water transmittance (% at 254 nm)
t	exposure time to UV (s)
$\%V$	*percent variance accounted for*
R^2	coefficient of determination
Re	Reynolds' Number
MSE	Mean Square Error
RSS	residual sum of squares

Greek Symbols

γ_i	coefficients for *n*OP model (*see* equation 5) for i = 1 to 6
δ	absorbance coefficient (cm^{-1})
λ	damping coefficient (μWs^{-1} cm^2 or mWs^{-1} cm^2)
α	projected level of disinfection (as $\log_{10}$ reductions)
β_0	Weibull scale parameter (as $\log_{10}$ reductions)
β_1	Weibull shape parameter (μWs^{-1} cm^2 or mWs^{-1} cm^2)
ρ	fluid density ($g\ cm^{-3}$)
μ	fluid viscosity ($g\ cm^{-1}\ s^{-1}$)

REFERENCES

Alvarez I, Pagan R, Condon S and Raso J 2003 The influence of process parameters for the inactivation of *Listeria monocytogenes* by pulsed electric fields. *International Journal of Food Microbiology* **77** (1-2): 147-153.

Baron J and Bourbigot M-M 1996 Repair of Escherichia coli and enterococci in sea water after ultraviolet disinfection quantification using diffusion chambers. *Water Research* **30** (11): 2817-2821.

Bates D M and Watts D G 1988 *Nonlinear Regression Analysis and its Applications*, John Wiley & Sons, Inc. pp 104 ff.

Bayliss C E and Waites W M 1979 The combined effect of hydrogen peroxide and ultraviolet irradiation on bacterial spores. *Journal of Applied Bacteriology* **47** (2): 263-269.

Belehradek J 1926 Influence of temperature on biological processes. *Nature* **118**: 117-118.

Blatchley III E R, Dumoutier N, Halaby T N, Levi Y and Laîne J M 2001 Bacterial responses to ultraviolet irradiation. *Water Science and Technology* **43** (10): 179-186.

Block S S 1983 *Disinfection, Sterilization and Preservation*, 3rd edn., Lea and Febiger, London. pp. 3-153.

Bohrerova Z and Linden K G 2007 Standardizing photoreactivation: Comparison of DNA photorepair rate in *Escherichia* coli using four different fluorescent lamps. *Water Research* **41** (12): 2832-2838.

Brock T D and Madigan M T 1991 *Biology of Microorganisms*, 6th edn., Prentice-Hall, New Jersey. pp. 235 ff.

Cabaj A, Sommer R and Schoenen D 1996 Biodosimetry: Model calculations for UV water disinfection devices with regard to dose distributions. *Water Research* **30** (4): 1003-1009.

Cairns W L 1995 UV technology for water supply treatment. *Water Supply* **13** (3/4): 211-214.

Cano R T and Colome J S 1986 *Microbiology*, West Publishing Company, New York. pp. 214-218.

Cantwell RE and Hofmann R 2008 Inactivation of indigenous coliform bacteria in unfiltered surface water by ultraviolet light. *Water Research* **42** (10-11): 2729-2735.

Carnimeo D, di Marino R, Donadio F, Liberti L, Ranieri E, Pizurra M and Savino A 1995 Comparison between H_2O_2/UV and ClO_2 disinfection of drinking water. *Water Supply* **13** (2): 159-169.

Cerf O 1977 Tailing of survival curves of bacterial spores. *Journal of Applied Bacteriology* **42** (1):1-19.

Chang J C H, Ossoff S F, Lobe D C, Dorfman D H, Dumais C M, Qualls R G and Johnson J D 1985 UV inactivation of pathogenic and indicator microorganisms. *Applied and Environmental Microbiology* **49** (6): 1361 – 1365.

Christensen E R 1984 Dose-response functions in aquatic toxicity testing and the Weibull model. *Water Research* **18** (2): 213-221.

Chiruta J 2000 Thermal Sterilisation Kinetics. *PhD Thesis*. University of Adelaide.

Cortelyou J R, Mc Whinnie M A, Riddiford M S and Semrad J E 1954 Effects of ultraviolet irradiation on large populations of certain water-borne bacteria in motion: The development of adequate agitation to provide an effective exposure period. *Applied Microbiology* **2** (4): 227-235.

Crandall R A 1986 The use of ultraviolet light in the treatment of water in public spas and hot tubs. *Journal of Environmental Health* **49** (1): 16-23.

Crowder M 1983 A Growth curve analysis for EDP curves. *Applied Statistics* **31** (1): 15-18.

Crowder M J and Tredger J A 1981 The use of exponentially damped polynomials for biological recovery data. *Applied Statistics* **30** (2): 147-152.

Darby J, Heath M, Jacangelo J, Loge F, Swaim P and Tchobanoglous G 1995 Comparative efficiencies of Chlorination/Dechlorination and Ultraviolet Irradiation. Project 91-WWD-1. Water Environment Research Foundation, USA.

Darby J, Emerick R, Loge F and Tchobanoglous G 1999 The Effect of Upstream Treatment Processes on UV Disinfection Performance. Project 96-CTS-3. Water Environment Research Foundation, USA.

Darby J L, Snider K E and Tchobanoglous G 1993 Ultraviolet disinfection for wastewater reclamation and reuse subject to restrictive standards. *Water Environment Research* **65** (2): 169-180.

D'Agostino R B and Stephens M A 1986 *Goodness-of-fit Techniques*, Marcel Dekker, Inc., New York. pp. 54 ff.

Daughtry B J, Davey K R, Thomas C J and Verbyla A P 1997 *Food processing - A new model for the thermal destruction of contaminating bacteria*. In: Jowitt, R. (Ed.), *Engineering and Food at ICEF* 7, Sheffield Academic Press, England. pp. A113-A116.

Davey K R 1999 Belehradek models - Application to chilled foods preservation. Symposium International, *La Microbiologie Previsionnelle Appliquee a la Conservation des Aliments Refrigeres* (Predictive Microbiology Applied to Chilled Food Preservation), *Commission on Food Science and Technology (C2) of the International Institute of Refrigeration* (IIR), Quimper, France, 16 - 18 June 1997. pp. 37-47.

Davey K R, Hall R F and Thomas C J 1995 Experimental and model studies of the combined effect of temperature and pH on the thermal sterilisation of vegetative bacteria in liquid. *Transactions of the Institution of Chemical Engineers, Part C, Food and Bio products Processing* **73** (3): 127-132.

Davey K R, Gardner T, Thomas C J and Manning V K 1995 Potable water production using UV irradiation. In: *Proc. 23rd Australasian Chemical Engineering Conference* - CHEMECA '95, Adelaide, Australia, September 24-27. **3**: 104-109.

Davey K R 1993 Linear-Arrhenius models for bacterial growth and death and vitamin denaturations. *Journal of Industrial Microbiology* **12** (3-5): 172-179.

Dizer H, Bartocha W, Bartel H, Seidel K, Lopez-Pila J M and Grohmann A 1993 Use of ultraviolet radiation for inactivation of bacteria and coliphages on pre-treated wastewater. *Water Research* **27** (3): 397-403.

Downes A and Blount T 1877 Research on the effect of light upon bacteria and other organisms. *Proceedings of the Royal Society* (London) **26**: 488-500.

Emerick R W, Loge F J, Thompson D and Darby J L 1999 Factors influencing ultraviolet disinfection performance. Part II: Association of coliform bacteria with wastewater particles. *Water Environment Research* **71** (6): 1178-1187.

Emerick R W, Loge F J, Ginn T and Darby J L 2000 Modeling the inactivation of particle-associated coliform bacteria. *Water Environment Research* **72** (4): 432-438.

Fernández A, Collado J, Cunha L M, Ocio M J and Martínez A 2002 Empirical model building based on Weibull distribution to describe the joint effect of pH and temperature on the thermal resistance of *Bacillus cereus* in vegetable substrate. *International Journal of Food Microbiology* **77** (1-2): 147-153.

Gerhart P M, Gross R J and Hochstein J I 1992 *Fundamentals of Fluid Mechanics*, 2nd edn., Addison-Wesley Publishing Company Inc., USA. pp. 462 ff.

Giese N and Darby J 2000 Sensitivity of microorganisms to different wavelengths of UV light: Implications on modelling of medium pressure UV systems. *Water Research* **34** (16): 4007-4013.

Harm W 1980 *Biological Effects of Ultraviolet Radiation*, IUPAB Biophysics Series, Murray Printing Company, Westford, Massachusetts, USA.

Heinonen-Tanski H, Juntunen P, Rajala R, Haume E and Niemelä A 2003 Costs of tertiary treatment of municipal wastewater by rapid sand filter with coagulants and UV. *Water Science and Technology: Water Supply* **3** (4): 145-152.

Hengesbach B, Schoenen D, Hoyer O, Bernhardt H, Mark G, Schuchmann H-P and van Sonntag C 1993 UV disinfection of drinking water – the question of bacterial regrowth and the photolytic degredation of biogenic high-molecular-weight substances. *Journal of Water Supply Research and Technology – Aqua* **42** (1): 13-22.

Ho L W A and Bohm P 1981 UV Disinfection of tertiary and secondary effluents. *Water Pollution Research Journal (Canada)* **16**: 33-44.

Holdsworth S D 1997 *Thermal Processing of Packaged Foods*, Blackie Academic & Professional, Chapman & Hall, London. pp. 86 ff.

Hu J Y, Chu X N, Quek P H, Feng Y Y and Tan X L 2007 Inactivation of particle-associated viruses by UV. *Journal of Water Supply Research and Technology – AQUA* **56** (6-7): 393-397.

Janex M L, Savoye P, Do-Quang Z, Blatchley III E and Laîne J M 1998 Impact of water quality and reactor hydrodynamics on wastewater disinfection by UV, use of CFD modeling for performance optimization. *Water Science & Technology* **38** (6): 71-78.

Jacob S M and Dranoff J S 1970 Light Intensity profiles in a perfectly mixed photoreactor. *American Institute of Chemical Engineers Journal* **16** (3): 359-363.

Jones B M, Langlois G W, Sakaji R H and Daughton C G 1985 Effect of ozonation and UV irradiation on biorefractory organic solutes in oil shale retort water. *Environmental Progress* **4** (4): 252-258.

Jungfer C, Schwartz T and Obst U 2007 UV-induced dark repair mechanisms in bacteria associated with drinking water. *Water Research* **41** (1): 188-196.

Jung J Y, Oh B S and Kang J-W 2008 Synergistic effect of sequential or combined use of ozone and UV radiation for the disinfection of *Bacillus subtilis* spores. *Water Research* **42** (6-7): 1613-1621.

Kelly C B 1961. Disinfection of sea water by ultraviolet radiation. *American Journal of Public Health* **51** (11): 1670-1680.

Kiely G 1998 *Environmental Engineering*, Chemical and Petroleum Engineering Series, International Editions, McGraw-Hill, New York. pp. 474 ff.

Kohler L R 1965 *Ultraviolet Radiation*, John Wiley & Son Inc., New York. pp. 236-257.

Koivunen J and Heinonen-Tanski H 2005 Inactivation of enteric microorganisms with chemical disinfectants, UV irradiation and combined chemical/UV treatments. *Water Research* **39** (8): 1519-1526.

Kühne C and Walter A 1975a Numerical evaluation of experimental data using a damped exponential function polynomial. I. Solution method. *Zeitschrift fuer Physikalische Chemie (Leipzig)* **256** (3): 487-496.

Kühne C and Walter A 1975b Numerical evaluation of experimental data using a damped exponential function polynomial. II. Use in a special case of chemical kinetics. *Zeitschrift fuer Physikalische Chemie (Leipzig)* **256** (4): 689-697.

Labas M D, Brandi R J, Martín C A and Cassano A E 2006 Kinetics of bacteria inactivation employing UV radiation under clear water conditions. *Chemical Engineering Journal* **121** (2-3): 135-145.

Lebovka N I and Vorobiev E 2004 On the origin of the deviation from first-order kinetics in inactivation of microbial cells by pulsed electric fields. *International Journal of Food Microbiology* **91** (1): 83-89.

Leuker G 1999 Description and application of biodosimetry – a testing procedure for UV systems. *Journal of Water Supply Research and Technology – Aqua* **48** (4): 154-160.

Lin L S and Blatchley III E R 2001 UV dose distribution characterisation using fractal concepts for system performance evaluation. *Water Science and Technology* **43** (11): 181-188.

Lin L S, Johnston C T and Blatchley E R 1999 Inorganic fouling at quartz: water interfaces in ultraviolet photoreactors - I. Chemical Characterization. *Water Research* **33** (15): 3321-3329.

Loge F J, Emerick R W, Heath M, Jacangelo J, Tchobanoglous G and Darby J L 1996 Ultraviolet disinfection of secondary wastewater effluents: prediction of performance and design. *Water Environment Research* **68** (5): 900-916.

Mafart P, Couvert O, Gaillard S and Leguérinel I 2002 On calculating sterility in thermal preservation methods: Application of the Weibull frequency distribution model. *International Journal of Food Microbiology* **72** (1-2): 107-113.

Mafart P, Couvert O and Leguérinel I 2001 Effect of pH on the heat resistance of spores: Comparison of two models. *International Journal of Food Microbiology* **63** (1-2): 51-56.

Manning V 1994 *Potable water production using UV irradiation*. Honours Research Report, Department of Chemical Engineering, The University of Adelaide. pp. 58.

Meulemans C C E 1987 The basic principles of UV-disinfection of water. *Ozone: Science and Engineering* **9** (4): 299-314.

Meynell G G and Meynell E 1970 *Theory and Practice in Experimental Bacteriology*, University Press, Cambridge, UK. pp. 23 ff.

McMeekin T A, Olley J N, Ross T and Ratkowsky D A 1993 *Predictive Microbiology: Theory and Application*, Research Studies Press Ltd., Taunton, England. pp. 11 ff.

Montgomery D C 2001 *Design and Analysis of Experiments*, 5^{th} *edn.*, Hamilton Printing Company, John Wiley & Sons, Inc. USA. pp. 392 ff.

Murphy H M, Payne S J and Gagnon G A 2008 Sequential UV- and chlorine-based disinfection to mitigate *Escherichia coli* in drinking water biofilms. *Water Research* **42** (8-9): 2083-2092.

Nebot Sanz E, Salcedo Dávila I, Andrade Balao J A and Quiroga Alonso J M 2007 Modelling of reactivation after UV disinfection: Effect of UV-C dose on subsequent photoreactivation and dark repair. *Water Research* **41** (14): 3141-3151.

Nelson K L 2000 Ultraviolet light disinfection of wastewater stabilization pond effluents. *Water Science and Technology* **42** (10-11): 165-170.

Nguyen H T 1999 Effects of transmittance and suspended solids on the efficacy of UV disinfection of bacterial contaminants in water. *MApplSc Thesis*. University of Adelaide.

Nguyen H T, Davey K R, Gardner T and Thomas C J 1998 Effect of transmittance and suspended solids on the efficacy of UV disinfection of water. In: *Proc. 26th Australasian and New Zealand Chemical Engineering Conference* - CHEMECA '98, Port Douglas, Queensland, Australia, September 28-30, paper 91.

Oliver B G and Carey J H 1976 Ultraviolet disinfection: An alternative to chlorination. *Journal of the Water Pollution Control Federation* **48** (11): 2619-2624.

Oliver B G and Cosgrove E G 1975 The disinfection of sewage treatment plant effluents using UV light. *Canadian Journal of Chemical Engineering* **53:** 170-174.

Parker J A and Darby J L 1995 Particle-associated coliform in secondary effluents: shielding from ultraviolet light disinfection. *Water Environment Research* **67** (7): 1065-1075.

Peleg M and Cole M B 1998 Reinterpretation of microbial survival curves. *Critical Reviews in Food Science* **38** (5): 353-380.

Petrasek A C, Wolf H W, Esmond S E and Andrews D C 1980 *Ultraviolet disinfection of municipal wastewater effluents*. U.S. Environment Protection Agency, Publication EPA-600/2-80-102. Municipal Environmental Research Laboratory, Cincinnati, USA.

Qasim S R 1999 *Waste Water Treatment Plants; Planning, Design and Operation.* 2nd edn., Technomic Publishing Company Inc., Lancaster, Pennsylvania. pp. 545 – 619.

Qualls R G, Dorfman D C and Johnson J D 1989 Evaluation of the efficiency of UV disinfection systems. *Water Research* **23** (3): 317-325.

Qualls R G and Johnson J D 1985 Modeling and efficiency of ultraviolet disinfection systems. *Water Research* **19** (8): 1039-1046.

Qualls R G and Johnson J D 1983 Bioassay and dose measurement in UV disinfection. *Applied and Environmental Microbiology* **45** (3): 872-877.

Qualls R G, Flynn M P and Johnson J D 1983 The role of suspended particles in ultraviolet disinfection. *Journal of the Water Pollution Control Federation* **55** (10): 1280-1285.

Ratkowsky D A 1990 *Handbook of Nonlinear Regression Models*, Marcel Dekker, New York. pp. 19 ff.

Savolainen R 1991 Ultraviolet disinfection of secondary effluents. *Aqua Fennica* **21** (2): 211-218.

Scheible O K 1986 *Pilot Studies of UV Disinfection at Several Wastewater Treatment Plants. Summary Report.* U.S. Environment Protection Agency, Cincinnati, USA.

Schoolfield R M, Sharpe J P H and Magnuson C E 1981 Non-linear regression of biological temperature-dependent rate models based on absolute reaction-rate theory. *Journal of Theoretical Biology* **88** (4): 719-731.

Severin B F 1980 Disinfection of municipal wastewater effluents with ultraviolet light. *Journal of Water Pollution Control Federation* **52** (7): 2007-2018.

Severin B F and Suidan M T 1985 Ultraviolet disinfection for municipal wastewater. *Chemical Engineering Progress* **81** (4): 37-44.

Severin B F, Suidan M T and Engelbrecht R S 1983 Kinetic modeling of UV disinfection of water. *Water Research* **17** (11): 1669-1678.

Singer M and Nash N 1977 *Ultraviolet Disinfection of a Step Aeration Effluent*. Presented at: Winter Meeting of the New York Water Pollution Control Association. New York.

Snedecor G W and Cochran W G 1969 *Statistical Methods*, University Press, Iowa. pp. 403 ff.

Sobotka J 1993 The efficiency of water treatment and disinfection by means of ultraviolet radiation. *Water Science and Technology* **27** (3-4): 343-346.

Sobotka J 1992 Application of ultraviolet radiation for water disinfection and purification in Poland. *Water Science and Technology* **26** (9-11): 2313-2316.

Sommer R and Cabaj A 1993 Evaluation of the efficiency of a UV plant for drinking water disinfection. *Water Science and Technology* **27** (3-4): 357-362.

Stanier R Y, Doudoroff M and Adelberg EA 1971 *General Microbiology*. 3rd edn., Macmillan Press Ltd., London.

Suidan M T and Severin B F 1986 Light intensity models for annular UV disinfection reactors. *American Institute of Chemical Engineers Journal* **32** (11): 1902-1909.

Taghipour F 2004 Ultraviolet and ionizing radiation for microorganism inactivation. *Water Research* **38** (18): 3940-3948.

Tchobanoglous G, Emerick R, Loge F, Darby J and Soroushian F 1999 Recent developments in ultraviolet (UV) disinfection. In: *Proc. 6th National Drinking Water and Wastewater Treatment Technology Transfer Workshop, USEPA*, Kansas City, MO.

Tchobanoglous G, Loge F, Darby J and Devries M 1996 UV Design: Comparison of probabilistic and deterministic design approaches. *Water Science & Technology* **33** (10-11): 251-260.

Templeton M R, Andrews R C and Hofmann R 2005 Inactivation of particle associated viral surrogates by ultraviolet light. *Water Research* **39** (15): 3487-3500.

Thampi M V and Sorber C A 1987 A method for evaluating the mixing characteristics of UV reactors with short detention times. *Water Research* **21** (7): 765-771.

Trugo L C, Macrae R and Dick J 1983 Determination of purine alkaloids and trigonelline in instant coffee and other beverages using high performance liquid chromatography. *Journal of Science of Food and Agriculture* **34**: 300-306.

Ultraviolet Technology of Australasia (UVTA) Pty. Ltd., (For Export March 1998) *Product Specifications – Model LC Series*. Glynde, South Australia.

USEPA 1981 *Ultraviolet Disinfection of a Secondary Wastewater Treatment Plant Effluent*. U.S. Environment Protection Agency, Publication EPA 600/2-81/152. Municipal Environmental Research Laboratory, Cincinnati, USA.

USEPA 1986 *Design Manual: Municipal Wastewater Disinfection*. U.S. *Environment Protection Agency,* Publication EPA 625/1-86/021. Office of Research and Development, Cincinnati, USA.

USEPA 1990 *Ultrox International Ultraviolet Radiation/Oxidation Technology: Applications Analysis Report.* U.S. *Environment Protection Agency,* Publication EPA 540/A5-89/012. Risk Reduction Engineering Laboratory, Office of Research and Development, Cincinnati, USA.

USEPA 1992 *Ultraviolet Disinfection Technology Assessment.* U.S. *Environment Protection Agency,* Publication EPA 832/R-92/004. Office of Wastewater Enforcement and Compliance, Washington DC, USA.

USEPA 1996 *Ultraviolet Light Disinfection Technology in Drinking. Water Application - An Overview.* U.S. *Environment Protection Agency,* Publication EPA 811/R-96/002. Office of Ground Water and Drinking Water, Washington DC, USA.

van Boekel M A J S 2002 On the use of the Weibull model to describe thermal inactivation of microbial vegetative cells. *International Journal of Food Microbiology* **74** (1-2): 139-159.

Venosa A D 1983 Current state-of-the-art of wastewater disinfection. *Journal of Water Pollution Control Federation* **55** (5): 457-466.

Venosa A D, Petrasek A C, Brown D, Sparks H L and D M Allen H L 1984 Disinfection of secondary effluent with ozone/UV. *Journal of Water Pollution Control Federation* **56** (2): 137-142.

Wang T, MacGregor S J, Anderson J G and Woolsey G A 2005 Pulsed ultraviolet inactivation spectrum of *Escherichia coli. Water Research* **39** (13): 2921-2925.

Wolfe R L 1990 Ultraviolet disinfection of potable water. *Environmental Science and Technology* **24** (6): 768-773.

Whitby G E and Palmateer G 1993 The effect of UV transmission, suspended solids and photo-reactivation on micro-organisms in wastewater treated with UV light. *Water Science and Technology* **27** (3-4): 379-386.

Yip R W and Konasewich D E 1972 Ultraviolet sterilization of water - Its potential and limitations. *Water Pollution Control (Canada)* **110** (6): 14-15.